

THE EFFECT OF BULBOUS BOWS ON THE
RESISTANCE AND POWERING PERFORMANCE
OF A FORTY-FIVE FOOT TRAWLER YACHT

STEPHEN EDWARD LANE



**THE EFFECT OF BULBOUS BOWS ON THE RESISTANCE AND POWERING
PERFORMANCE OF A FORTY-FIVE FOOT TRAWLER YACHT**

by

©STEPHEN EDWARD LANE

A thesis submitted to the School of Graduate Studies
in partial fulfillment of the requirements for the
degree of Master of Engineering

Faculty of Engineering and Applied Science
Memorial University of Newfoundland

May 2010

St. John's

Newfoundland

Canada

Abstract

Several Newfoundland boatbuilders are interested in the ability to switch over from building fishing vessels to building yachts and other pleasure craft for the North American and European market or starting up yacht building operations.

This project is intended to provide them with an optimized trawler type yacht hull design with thoroughly tested and well documented performance characteristics. This information can then be used in their marketing efforts to break into this market that is new to them.

To partially complete this objective a series of tests were completed in the MUN OERC towing tank as well as in the IOT Ice Tank facility. Testing consisted of both bare hull resistance and self-propulsion tests. These tests are able to determine the powering performance of the vessel in calm water.

This report details the set-up, test procedure, and analysis of results of all testing completed on the hull with each of the bows designed. Also provided are detailed conclusions of the results as well as recommendations for further study of this hull form.

Acknowledgements

I would like to express my gratitude to MUN and NRC-IRAP for their financial and other support.

Thanks to Moya Crocker and the secretarial staff for all of their help throughout the past couple of years.

A huge thanks to the Technical Services Department in the S. J. Carew building; particularly Dave Snook, Jerry Smith, and last but not least Robert Murphy for doing an amazing job of constructing the model and other parts. Without you guys this project would never have been completed.

Another huge thanks to MUN Engineering technical staff, specifically Trevor Clark, for the countless hours spent setting up for and testing the various model configurations. Testing is made so much easier when you are working with good people.

Thank you also to my co-supervisor Wei Qui, I appreciate all of the practical help you have given me throughout my program.

Enough good things could not be said about my supervisor Dag Friis. I appreciate all of the guidance you have provided me throughout this project; many problems would not have been solved without your seemingly limitless knowledge. You have given me the opportunity time and time again to expand my knowledge in the Naval Architectural Engineering field, and for that I am especially grateful.

Finally, I would like to thank all of my friends and family. It would be difficult to complete such a feat without having such good people to fall back on and help you relax when times get hectic.

To everyone, your generosity will not be forgotten.

Table of Contents

Abstract	ii
Acknowledgements	iii
List of Tables	vi
List of Figures	ix
List of Abbreviations and Symbols	xiv
List of Appendices	xviii
Chapter 1 - Introduction	1
1.1 Aim	1
1.2 Background	1
Chapter 2 - Literature Review of Bulbous Bows	3
2.1 Timeline of Work Completed	3
2.1.1 Design Methods	5
2.1.2 Relevant Experimental Work.....	6
Chapter 3 - Model and Bulbous Bows	13
3.1 Model	13
3.2 Bulbous Bows	15
Chapter 4 - Model Construction	22
Chapter 5 - IOT Bare Hull Resistance Tests	28
5.1 IOT Test Facility	28
5.2 Test Instrumentation	30
5.2.1 Instrumentation Calibrations.....	32
5.3 Model Set-up.....	33
5.4 Test Plan.....	34
5.5 Description of Experiment (ITTC-57 Method).....	36
5.6 Blockage Corrections.....	38
5.7 Description of Data Analysis	42
5.7.1 Online Data Analysis	42
5.7.2 Offline Data Analysis	43
5.8 Results and Discussions	44
5.8.1 Conventional Bow	45
5.8.2 Bulbous Bows	54
5.8.3 Bow Comparisons	63
5.8.4 Dynamic Trim Results	74
5.8.5 Sinkage Results	79
Chapter 6 - MUN Bare Hull Resistance Tests	82
6.1 MUN Test Facility	82
6.2 Test Instrumentation	83
6.2.1 Instrumentation Calibrations.....	85
6.3 Model Set-up.....	85
6.4 Test Plan.....	85
6.5 Description of Experiment (ITTC-57 Method).....	86
6.6 Blockage Corrections.....	86
6.7 Description of Data Analysis	86

6.7.1	Online Data Analysis	86
6.7.2	Offline Data Analysis	88
6.8	Results and Discussions.....	89
6.8.1	Conventional Bow	89
6.8.2	Bulbous Bows	91
6.8.3	Bow Comparisons.....	115
6.8.4	Dynamic Trim Results	127
6.8.5	Sinkage Results.....	139
Chapter 7 - MUN/IOT Comparisons		145
7.1	Conventional Bow	145
7.1.1	Effective Power Comparison	145
7.1.2	Trim Comparison.....	147
7.1.3	Sinkage Comparison	149
7.2	Bulbous Bows	150
7.2.1	Effective Power Comparisons.....	150
7.2.2	Trim Comparisons	153
7.2.3	Sinkage Comparisons.....	156
7.3	Overall Comparisons	158
Chapter 8 - Self-Propulsion Tests.....		165
8.1	MUN Test Facility	167
8.2	Test Instrumentation	168
8.2.1	Instrumentation Calibrations.....	171
8.3	Model Set-up.....	172
8.4	Test Plan.....	172
8.5	Description of Experiment.....	173
8.6	Description of Experimental Procedure.....	178
8.7	Results and Discussion	179
8.7.1	Conventional Bow	179
8.7.2	Bulbous Bows	182
8.7.3	Bow Comparisons.....	187
8.7.4	Installed Power Values	192
Chapter 9 - Uncertainty Analysis		197
9.1	Bare Hull Resistance Tests	197
9.1.1	Test Design	198
9.1.2	Measurement System and Procedure.....	199
9.1.3	Calculating the Total Uncertainties	199
9.1.4	Uncertainty Analysis Results for IOT Testing.....	201
9.1.5	Uncertainty Analysis Results from MUN Tests	207
9.1.6	MUN/IOT Comparisons	213
9.2	Self-Propulsion Tests	216
Chapter 10 - Conclusions and Recommendations		218
10.1	Bare Hull Resistance Tests	218
10.2	Self-Propulsion Tests	222
References.....		225

List of Tables

Table 1: Vessel Particulars.....	14
Table 2: Bulbous Bow Characteristics (Model Scale).....	16
Table 3: Comparison of Top Bulb Area and Bulb Submergence (Level Trim)	16
Table 4: Comparison of Top Bulb Area and Bulb Submergence (0.75° by Stern)	17
Table 5: Comparison of Top Bulb Area and Bulb Submergence (1.5° by Stern)	17
Table 6: Test Plan for Resistance Tests at IOT.....	35
Table 7: Effective Power with Alpha Bow (IOT Tests)	45
Table 8: Effective Power with Alpha2 Bow (Retests at IOT)	45
Table 9: Comparison of Alpha Bow Tests at Level Trim.....	50
Table 10: Comparison of Alpha Bow Tests at 1.5° by Stern Trim.....	51
Table 11: Effective Power for Vessel with Beta Bow	54
Table 12: Effective Power for Vessel with Gamma Bow.....	56
Table 13 Effective Power for Vessel with Epsilon Bow	59
Table 14: Effective Power Comparison as a Percentage of the Conventional Bow at Level Trim.....	65
Table 15: Effective Power Comparison as a Percentage of the Conventional Bow at Level Trim (All Other Bows at 0.75° by Stern).....	68
Table 16: Effective Power Comparison as a Percentage of the Conventional Bow at Level Trim (All Other Bows at 1.5° by Stern).....	70
Table 17: Effective Power Comparison as a Percentage of the Conventional Bow at Level Trim (All Other Bows at 3.0° by Stern).....	72
Table 18: Optimal Trim Conditions for Each Bow	72
Table 19: Effective Power Comparison at Optimal Trim Conditions as a Percentage of the Conventional Bow at Level Trim.....	73
Table 20: Test Plan for Resistance Tests at MUN.....	85
Table 21: Test Plan for MUN Resistance Retests.....	86
Table 22: Effective Power for Vessel with Alpha Bow.....	89
Table 23: Effective Power for Vessel with Beta Bow	92
Table 24: Effective Power for Vessel with Delta Bow.....	93
Table 25: Effective Power for Vessel with Gamma Bow.....	97
Table 26: Effective Power for Vessel with Epsilon Bow	99
Table 27: Effective Power for Vessel with Eta Bow	100
Table 28: Effective Power for Vessel with Iota Bow	104
Table 29: Effective Power for Vessel with Theta Bow	107
Table 30: Effective Power for Vessel with Zeta Bow	111
Table 31: Effective Power Comparison as a Percentage of the Conventional Bow	117
Table 32: Ranking of Bulbous Bows at Level Trim	118
Table 33: Effective Power Comparison as a Percentage of the Conventional Bow at Level Trim (All Other Bows at 0.75° by Stern).....	121
Table 34: Ranking of Bulbous Bows at 0.75° by Stern.....	122
Table 35: Effective Power Comparison as a Percentage of the Conventional Bow at Level Trim (All Other Bows at 1.5° by Stern).....	124
Table 36: Ranking of Bulbous Bows at 1.5° by Stern.....	125
Table 37: Optimal Trim Conditions for Each Bow	125

Table 38: Effective Power Comparison at Optimal Trim Conditions as a Percentage of the Conventional Bow at Level Trim.....	126
Table 39: Ranking of Bulbous Bows in Order of Speed at which Maximum Trim by the Head Occurs at Static Level Trim.....	129
Table 40: Ranking of Bulbous Bows in Order of the Magnitude of Maximum Trim by the Head at Static Level Trim.....	130
Table 41: Ranking of Bulbous Bows in Order of Speed at which Maximum Trim by the Head Occurs at 0.75° by Stern Trim Condition.....	133
Table 42: Ranking of Bulbous Bows in Order of the Magnitude of Maximum Trim by the Head at 0.75° by Stern Trim Condition.....	133
Table 43: Ranking of Bulbous Bows in Order of Speed at which Maximum Trim by the Head Occurs at 1.5° by Stern Trim Condition.....	134
Table 44: Ranking of Bulbous Bows in Order of the Magnitude of Maximum Trim by the Head at 1.5° by Stern Trim Condition.....	135
Table 45: Breakdown of Dynamic Trim for Zeta Bow.....	138
Table 46: Standardized Effective Power Comparison of Alpha Bow Tested at IOT and MUN.....	146
Table 47: Standardized Effective Power Comparison of Beta Bow Tested at IOT and MUN.....	151
Table 48: Standardized Effective Power Comparison of Gamma Bow Tested at IOT and MUN.....	152
Table 49: Standardized Effective Power Comparison of Epsilon Bow Tested at IOT and MUN.....	153
Table 50: Test Plan for Self-Propulsion Tests at MUN.....	173
Table 51: Thrust Deduction and Wake Fractions for Alpha Bow.....	180
Table 52: Hull Efficiencies for Alpha Bow.....	181
Table 53: Relative Rotative Efficiencies for Alpha Bow.....	182
Table 54: Wake Fractions for all Bulbous Bows.....	183
Table 55: Thrust Deduction Fractions for all Bulbous Bows.....	184
Table 56: Hull Efficiencies for all Bulbous Bows.....	185
Table 57: Relative Rotative Efficiencies for all Bulbous Bows.....	186
Table 58: Quasi Propulsive Efficiencies for All Bows.....	191
Table 59: Installed Power Comparison.....	195
Table 60: Installed Power Comparison the Difference from the Conventional Bow.....	195
Table 61: Installed Power Comparison as a Percentage of the Conventional Bow.....	195
Table 62: Ranking of Bulbous Bows based on Installed Power Requirements.....	196
Table 63: Bias Errors for Alpha Bow Test Carried out in the IOT Ice Tank at 10 knots Full Scale.....	202
Table 64: Max/Min Full Scale Effective Powers for Alpha Bow during IOT Tests.....	204
Table 65: Max/Min Full Scale Effective Powers for Beta Bow during IOT Tests.....	204
Table 66: Max/Min Full Scale Effective Powers for Gamma Bow during IOT Tests.....	205
Table 67: Max/Min Full Scale Effective Powers for Epsilon Bow during IOT Tests.....	205
Table 68: Maximum Effective Power as Percentage of Minimum Effective Power for Conventional Bow from IOT Tests.....	207
Table 69: Max/Min Full Scale Effective Powers for Alpha Bow during MUN Tests.....	208
Table 70: Max/Min Full Scale Effective Powers for Beta Bow during MUN Tests.....	208

Table 71: Max/Min Full Scale Effective Powers for Delta Bow during MUN Tests.....	209
Table 72: Max/Min Full Scale Effective Powers for Gamma Bow during MUN Tests.	209
Table 73: Max/Min Full Scale Effective Powers for Epsilon Bow during MUN Tests.	209
Table 74: Max/Min Full Scale Effective Powers for Eta Bow during MUN Tests.....	210
Table 75: Max/Min Full Scale Effective Powers for Iota Bow during MUN Tests.....	210
Table 76: Max/Min Full Scale Effective Powers for Theta Bow during MUN Tests	210
Table 77: Max/Min Full Scale Effective Powers for Zeta Bow during MUN Tests	211
Table 78: Maximum Effective Power as Percentage of Minimum Effective Power for Conventional Bow from MUN Tests.....	213

List of Figures

Figure 1: Rendering of Finished Hull Surface.....	13
Figure 2: Model Assembled with Instrumentation for Self-Propulsion Tests	14
Figure 3: Rendering of Model Showing Removable Bow.....	15
Figure 4: Four Views of Beta Bow	18
Figure 5: Four Views of Delta Bow.....	18
Figure 6: Four Views of Gamma Bow.....	19
Figure 7: Four Views of Epsilon Bow	19
Figure 8: Four Views of Eta Bow	20
Figure 9: Four Views of Iota Bow	20
Figure 10: Four Views of Theta Bow	21
Figure 11: Four Views of Zeta Bow	21
Figure 12: Beginning to Mill Stern Section in CNC Machine.....	23
Figure 13: Milling Almost Complete on Stern Section	23
Figure 14: Milled Conventional Bow	24
Figure 15: Fibreglassed Epsilon Bulb.....	24
Figure 16: Fibreglassed Stern Section with Glued in Stern Tube.....	25
Figure 17: Stern Section during Refinishing	25
Figure 18: Two Bulbs during Refinishing	26
Figure 19: Fairing Bulb with Stern Section	26
Figure 20: Finished Model with Conventional Bow.....	27
Figure 21: Three Finished Bulbous Bows Complete with Turbulence Stimulators	27
Figure 22: IOT Ice Tank Schematic 1.....	29
Figure 23: IOT Ice Tank Schematic 2.....	29
Figure 24: Gimbal used for Resistance Tests	30
Figure 25: Inclinomometer Installed in Model	31
Figure 26: LVDT used for Resistance Tests.....	32
Figure 27: Model with Trim Hooks Attached (Ballast Weights in Model).....	34
Figure 28: Variation of b with Reynolds Number and form factor	40
Figure 29: Variation of k with Froude Number	41
Figure 30: Variation of c with Froude Number	42
Figure 31: Effective Power with Alpha Bow (IOT Tests).....	46
Figure 32: Effective Power with Alpha2 Bow (Retests at IOT).....	46
Figure 33: Comparison of both Alpha Bow Tests at IOT.....	47
Figure 34: Alpha2 Bow Test at Level Trim – Speed of 10 knots	48
Figure 35: Alpha2 Bow Test at 0.75° by Stern Trim – Speed of 10 knots	48
Figure 36: Alpha2 Bow Test at 1.5° by Stern Trim – Speed of 10 knots	49
Figure 37: Comparison of Alpha and Alpha2 Tests at Level Trim and 1.5° by Stern	50
Figure 38: Dynamic Trim Comparison of Alpha and Alpha2 Tests at Level Trim and 1.5° by Stern	51
Figure 39: Sinkage Comparison of Alpha and Alpha2 Tests at Level Trim and 1.5° by Stern	52
Figure 40: Difference Comparison of Dynamic Trim Data for Alpha and Alpha2 Tests at Level Trim and 1.5° by Stern.....	53

Figure 41: Difference Comparison of Sinkage Data for Alpha and Alpha2 Tests at Level Trim and 1.5° by Stern.....	53
Figure 42: Effective Power with Beta Bow	55
Figure 43: Effective Power with Gamma Bow	56
Figure 44: Gamma Bow Test at Level Trim – Speed of 10 knots	58
Figure 45: Gamma Bow Test at 0.75° by Stern – Speed of 10 knots	58
Figure 46: Gamma Bow Test at 1.5° by Stern – Speed of 10 knots	59
Figure 47: Effective Power with Epsilon Bow	60
Figure 48: Epsilon Bow Test at Level Trim – Speed of 10 knots.....	61
Figure 49: Epsilon Bow Test at 0.75° by Stern – Speed of 10 knots.....	62
Figure 50: Epsilon Bow Test at 1.5° by Stern – Speed of 10 knots.....	62
Figure 51: Epsilon Bow Test at 3.0° by Stern – Speed of 10 knots.....	63
Figure 52: Effective Power Comparison at Level Trim.....	64
Figure 53: Effective Power Comparison as the Difference from the Conventional Bow at Level Trim	64
Figure 54: Effective Power Comparison as a Percentage of the Conventional Bow at Level Trim	65
Figure 55: Effective Power Comparison at 0.75° by Stern Trim.....	66
Figure 56: Effective Power Comparison as the Difference from the Conventional Bow at Level Trim (All Other Bows at 0.75° by Stern)	67
Figure 57: Effective Power Comparison as a Percentage of the Conventional Bow at Level Trim (All Other Bows at 0.75° by Stern)	67
Figure 58: Effective Power Comparison at 1.5° by Stern Trim.....	68
Figure 59: Effective Power Comparison as the Difference from the Conventional Bow at Level Trim (All Other Bows at 1.5° by Stern)	69
Figure 60: Effective Power Comparison as a Percentage of the Conventional Bow at Level Trim (All Other Bows at 1.5° by Stern)	69
Figure 61: Effective Power Comparison at 3.0° by Stern Trim.....	70
Figure 62: Effective Power Comparison as a Difference of the Conventional Bow at Level Trim (All Other Bows at 3.0° by Stern)	71
Figure 63: Effective Power Comparison as a Percentage of the Conventional Bow at Level Trim (All Other Bows at 3.0° by Stern)	71
Figure 64: Effective Power Comparison at Optimal Trim Conditions as a Percentage of the Conventional Bow at Level Trim.....	73
Figure 65: Dynamic Trim Comparison at Static Level Trim.....	74
Figure 66: Dynamic Trim Comparison at 0.75° by Stern Trim.....	77
Figure 67: Dynamic Trim Comparison at 1.5° by Stern Trim.....	78
Figure 68: Dynamic Trim Comparison at 3.0° by Stern Trim.....	78
Figure 69: Sinkage Comparison at Static Level Trim	79
Figure 70: Sinkage Comparison at 0.75° by Stern Trim.....	80
Figure 71: Sinkage Comparison at 1.5° by Stern Trim.....	81
Figure 72: Sinkage Comparison at 3.0° by Stern Trim.....	81
Figure 73: MUN Tank Schematic.....	83
Figure 74: Towing Dynamometer.....	84
Figure 75: Typical Plot of Carriage Speed for One Run during Resistance Tests	87
Figure 76: Effective Power with Alpha Bow.....	90

Figure 77: Alpha Bow Test at Level Trim – Speed of 10 knots	91
Figure 78: Effective Power with Beta Bow	92
Figure 79: Beta Bow Test at Level Trim – Speed of 10 knots	93
Figure 80: Effective Power with Delta Bow	94
Figure 81: Delta Bow Test at Level Trim – Speed of 10 knots	95
Figure 82: Delta Bow Test at 0.75° by Stern Trim – Speed of 10 knots	95
Figure 83: Delta Bow Test at 1.5° by Stern Trim – Speed of 10 knots	96
Figure 84: Effective Power with Gamma Bow	97
Figure 85: Gamma Bow Test at Level Trim – Speed of 10 knots	98
Figure 86: Effective Power with Epsilon Bow	99
Figure 87: Epsilon Bow Test at Level Trim – Speed of 10 knots.....	100
Figure 88: Effective Power with Eta Bow	101
Figure 89: Eta Bow Test at Level Trim – Speed of 10 knots	102
Figure 90: Eta Bow Test at 0.75° by Stern Trim – Speed of 10 knots.....	102
Figure 91: Eta Bow Test at 1.5° by Stern Trim – Speed of 10 knots	103
Figure 92: Effective Power with Iota Bow	104
Figure 93: Iota Bow Test at Level Trim – Speed of 10 knots.....	105
Figure 94: Iota Bow Test at 0.75° by Stern Trim – Speed of 10 knots.....	106
Figure 95: Iota Bow Test at 1.5° by Stern Trim – Speed of 10 knots.....	106
Figure 96: Effective Power with Theta Bow	108
Figure 97: Theta Bow Test at Level Trim – Speed of 10 knots.....	109
Figure 98: Theta Bow Test at 0.75° by Stern Trim – Speed of 10 knots.....	109
Figure 99: Theta Bow Test at 1.5° by Stern Trim – Speed of 10 knots.....	110
Figure 100: Effective Power with Zeta Bow	111
Figure 101: Zeta Bow Test at Level Trim – Speed of 10 knots.....	112
Figure 102: Zeta Bow Test at 0.75° by Stern Trim – Speed of 10 knots.....	113
Figure 103: Zeta Bow Test at 1.5° by Stern Trim – Speed of 10 knots.....	113
Figure 104: Effective Power Comparison at Level Trim.....	115
Figure 105: Effective Power Comparison as a Difference of the Conventional Bow at Level Trim	116
Figure 106: Effective Power Comparison as a Percentage of the Conventional Bow at Level Trim	116
Figure 107: Effective Power Comparison at 0.75° by Stern Trim.....	120
Figure 108: Effective Power Comparison as a Difference of the Conventional Bow at Level Trim (All Other Bows at 0.75° by Stern)	120
Figure 109: Effective Power Comparison as a Percentage of the Conventional Bow at Level Trim (All Other Bows at 0.75° by Stern)	121
Figure 110: Effective Power Comparison at 1.5° by Stern Trim.....	123
Figure 111: Effective Power Comparison as a Difference of the Conventional Bow at Level Trim (All Other Bows at 1.5° by Stern)	123
Figure 112: Effective Power Comparison as a Percentage of the Conventional Bow at Level Trim (All Other Bows at 1.5° by Stern)	124
Figure 113: Effective Power Comparison at Optimal Trim Conditions as a Percentage of the Conventional Bow at Level Trim.....	126
Figure 114: Dynamic Trim Comparison at Static Level Trim.....	128

Figure 115: Regression Lines through Comparisons of Speed of Maximum Trim by the Head vs. Top Bulb Area and Bulb Submergence	130
Figure 116: Regression Lines through Comparisons of Maximum Trim by the Head vs. Top Bulb Area and Bulb Submergence	131
Figure 117: Dynamic Trim Comparison at 0.75° by Stern Trim.....	132
Figure 118: Dynamic Trim Comparison at 1.5° by Stern Trim.....	134
Figure 119: Dynamic Trim Comparison for Delta Bow	135
Figure 120: Dynamic Trim Comparison for Eta Bow	136
Figure 121: Dynamic Trim Comparison for Iota Bow	136
Figure 122: Dynamic Trim Comparison for Theta Bow	137
Figure 123: Dynamic Trim Comparison for Zeta Bow	137
Figure 124: Sinkage Comparison at Static Level Trim	139
Figure 125: Sinkage Comparison at 0.75° by Stern Trim.....	140
Figure 126: Sinkage Comparison at 1.5° by Stern Trim.....	140
Figure 127: Sinkage Comparison for Delta Bow.....	141
Figure 128: Sinkage Comparison for Eta Bow	142
Figure 129: Sinkage Comparison for Iota Bow	142
Figure 130: Sinkage Comparison for Theta Bow	143
Figure 131: Sinkage Comparison for Zeta Bow	143
Figure 132: Effective Power Comparison of Alpha Bow Tested at IOT and MUN.....	146
Figure 133: Dynamic Trim Comparison of Alpha Bow Tested at IOT and MUN.....	147
Figure 134: Trimming Moment Comparison of Alpha Bow Tested at MUN	149
Figure 135: Sinkage Comparison of Alpha Bow Tested at IOT and MUN.....	149
Figure 136: Effective Power Comparison of Beta Bow Tested at IOT and MUN	150
Figure 137: Effective Power Comparison of Gamma Bow Tested at IOT and MUN....	151
Figure 138: Effective Power Comparison of Epsilon Bow Tested at IOT and MUN	152
Figure 139: Dynamic Trim Comparison of Beta Bow Tested at IOT and MUN	154
Figure 140: Dynamic Trim Comparison of Gamma Bow Tested at IOT and MUN.....	154
Figure 141: Dynamic Trim Comparison of Epsilon Bow Tested at IOT and MUN	155
Figure 142: Trimming Moment Comparison of Bulbous Bows Tested at MUN.....	155
Figure 143: Sinkage Comparison of Beta Bow Tested at IOT and MUN	156
Figure 144: Sinkage Comparison of Gamma Bow Tested at IOT and MUN.....	157
Figure 145: Sinkage Comparison of Epsilon Bow Tested at IOT and MUN.....	157
Figure 146: Effective Power Comparison as a Difference IOT Test Data vs. MUN Test Data	158
Figure 147: Effective Power Comparison as a Percentage IOT Test Data vs. MUN Test Data	159
Figure 148: Dynamic Trim Comparison as a Difference IOT Test Data vs. MUN Test Data	160
Figure 149: Dynamic Trim Comparison as a Percentage IOT Test Data vs. MUN Test Data	160
Figure 150: Model Sinkage Comparison as a Difference IOT Test Data vs. MUN Test Data	162
Figure 151: Model Sinkage Comparison as a Percentage IOT Test Data vs. MUN Test Data	162
Figure 152: Outline of Self-Propulsion Instrumentation	168

Figure 153: Motor used in Self-Propulsion Tests	169
Figure 154: Motor Controller used in Self-Propulsion Tests.....	169
Figure 155: Tachometer Encoder Installed in Model	170
Figure 156: Thrust and Torque Dynamometer Installed in Model	170
Figure 157: K&R Dyno Torque Calibration.....	172
Figure 158: Thrust Deduction and Wake Fractions for Alpha Bow	180
Figure 159: Hull Efficiencies for Alpha Bow.....	181
Figure 160: Relative Rotative Efficiencies for Alpha Bow	182
Figure 161: Comparison of Wake Fractions for Bulbous Bows.....	183
Figure 162: Comparison of Thrust Deduction Fractions for Bulbous Bows	185
Figure 163: Comparison of Hull Efficiencies for Bulbous Bows.....	186
Figure 164: Comparison of Relative Rotative Efficiencies for Bulbous Bows	187
Figure 165: Comparison of Wake Fractions for All Bows	188
Figure 166: Comparison of Thrust Deduction Fractions for All Bows	188
Figure 167: Comparison of Hull Efficiencies for All Bows	190
Figure 168: Comparison of Relative Rotative Efficiencies for All Bows	191
Figure 169: Comparison of Quasi Propulsive Efficiencies for All Bows.....	192
Figure 170: Installed Power Comparison	193
Figure 171: Installed Power Comparison as the Difference from Conventional Bow ...	194
Figure 172: Installed Power Comparison as a Percentage of the Conventional Bow	194
Figure 173: Effective Power Comparison with Error Bars at Level Trim for IOT Tests	206
Figure 174: Maximum Effective Power as Percentage of Minimum Effective Power for Conventional Bow from IOT Tests.....	207
Figure 175: Effective Power Comparison with Error Bars at Level Trim for MUN Tests	211
Figure 176: Maximum Effective Power as Percentage of Minimum Effective Power for Conventional Bow from MUN Tests.....	212
Figure 177: Effective Power Comparison with Error Bars of Alpha Bow Tested at IOT and MUN	214
Figure 178: Effective Power Comparison with Error Bars of Beta Bow Tested at IOT and MUN	214
Figure 179: Effective Power Comparison with Error Bars of Gamma Bow Tested at IOT and MUN	215
Figure 180: Effective Power Comparison with Error Bars of Epsilon Bow Tested at IOT and MUN	215

List of Abbreviations and Symbols

∇	volume of displacement, m ³
α	half angle of entrance, deg
Δ	displacement, tonnes
ΔC_T	reduction in total resistance coefficient due to blockage correction
η_H	hull efficiency
η_O	propeller efficiency in open water
η_{OP}	propeller efficiency in behind hull condition
η_R	relative rotative efficiency
θ_V	model dynamic trim, deg
λ	wave length, m
ρ	water density in fresh water, kg/m ³
ρ_M	fresh water density, kg/m ³
ρ_S	salt water density, kg/m ³
σ_w	non-dimensional added resistance in head seas
ν_M	kinematic viscosity for fresh water, m ² /s
ν_S	kinematic viscosity for salt water, m ² /s
A	cross-sectional area of towing tank, m ²
A_m	midship sectional area, m ²
A_T	submerged transom area, m ²
A_{TB}	top of bulb area, in ²
A_{TP}	top profile angle of bulb, deg
A_W	waterplane area, m ²
b	parameter used in total resistance coefficient correction
B_ρ	total bias limit for density
B_ν	total bias limit for water viscosity
B_{CF}	total bias limit for frictional resistance coefficient
B_{CR}	total bias limit for residual resistance coefficient
B_{CT}	total bias limit for total resistance coefficient
B_L	total bias limit for model length
B_M	model beam on waterline, m

B_{R_x}	total bias limit for model resistance
B_S	vessel beam on waterline, m
B_T	width of towing tank at water surface, m
B_V	total bias limit for model speed
B_{WS}	total bias limit for wetted surface area
c	Bernoulli parameter
C_A	correlation allowance
C_B	block coefficient
C_{FD}	skin friction correction coefficient in propulsion test
C_{FM}	frictional resistance coefficient for model
C_{FM15}	frictional resistance coefficient for model at 15°C (from resistance tests)
C_{FMP}	frictional resistance coefficient for model at propulsion test temperature
C_{FS}	frictional resistance coefficient for smooth ship
C_m	midship coefficient
C_P	prismatic coefficient
C_R	residuary resistance coefficient
C_{TM}	total resistance coefficient for model
C_{TM15}	total resistance coefficient for model at 15°C (from resistance tests)
C_{TMP}	total resistance coefficient for model at propulsion test temperature
C_{TS}	total resistance coefficient for smooth ship
C_V	viscous resistance coefficient
C_W	wavemaking resistance coefficient
C_{WP}	waterplane coefficient
D_M	model propeller diameter, m
D_S	full scale propeller diameter, m
ET	transmission efficiency
f	model - tank function
F_{DMP}	skin friction correction in self-propulsion test, N
F_h	Froude depth number
F_H	Froude number in terms of draft
F_n	Froude number

g	acceleration due to gravity, 9.81 m/s^2
h_T	water depth in towing tank, m
H_w	wave height, m
J_O	advance coefficient in open water
J_P	advance coefficient in behind hull condition
k	parameter used in wave making correction
K	coverage factor
K_{TO}	propeller thrust coefficient in open water
K_{TP}	propeller thrust coefficient in behind hull condition
K_{QO}	propeller torque coefficient in open water
K_{QP}	propeller torque coefficient in behind hull condition
LBP	length between perpendiculars, m
L_M	model length on waterline, m
L_S	vessel length on waterline, m
LCB	longitudinal centre of buoyancy, m
LCF	longitudinal centre of flotation, m
LOA	length overall, m
M	number of runs for which a precision limit is to be established
M_{Trim}	trimming moment, N-m
n_P	propeller rotational speed at self-propulsion point, rps
n_T	power to which speed is raised in blockage correction
NC	normal continuous rating
P_{CR}	precision limit for residual resistance coefficient
P_{CT}	precision limit for total resistance coefficient
P_E	effective power of ship, W
P_{ins}	installed power of ship, W
Q_P	propeller torque at self-propulsion point, N-m
QPE	quasi propulsive efficiency
R	resistance in clam water, N
R_F	fairing radius of bulb into stem, in
R_{nM}	model Reynolds number

R_{nS}	ship Reynolds number
R_{seas}	resistance in head seas, N
R_{TM}	total model resistance, N
R_{TS}	total ship resistance, N
S_M	wetted surface area of model, m^2
S_S	wetted surface area of ship, m^2
S_{DevCR}	standard deviation for residual resistance coefficient
S_{DevCT}	standard deviation for total resistance coefficient
t	thrust deduction fraction
T_M	model draft to baseline, m
T_P	propeller thrust at self-propulsion point, N
T_S	vessel draft to baseline, m
T_{Diff}	difference between tow point and centroid of underwater portion of hull, m
U_{CR}	total uncertainty for residual resistance coefficient
U_{CT}	total uncertainty for total resistance coefficient
V_A	speed of advance, m/s
V_M	model speed, m/s
V_S	ship speed, knots (sometimes m/s)
w	Taylor wake fraction
WA	weather allowance
Z_V	model sinkage, m

List of Appendices

APPENDIX A: Model Characteristics

APPENDIX B: Tabular Data for IOT Bare Hull Resistance Tests

B-1: Resistance and Powering Data

B-2: Sinkage and Dynamic Trim Data

APPENDIX C: Tabular Data for MUN Bare Hull Resistance Tests

C-1: Resistance and Powering Data

C-2: Sinkage and Dynamic Trim Data

APPENDIX D: Tabular Data for Self-Propulsion Tests

APPENDIX E: Uncertainty Analysis for Bare Hull Resistance Tests

E-1: IOT Test Program

E-2: MUN Test Program

Chapter 1 - Introduction

1.1 Aim

This report describes the design, construction, and testing of a 6 ft model of a 45 ft trawler yacht designed for a group of Newfoundland boatbuilders. The testing was completed on a 1:7.654 scale model which has a removable bow section. A conventional bow along with eight different bulbous bows was tested in this project.

Two types of tests were carried out for the yacht hull; these include bare hull resistance tests and self-propulsion tests. Each of these tests is discussed in full detail within the report and the results of each are contained within their respective sections. Conclusions and recommendations are also provided at the end of the report.

1.2 Background

In the previous phase of the project the hull form along with three alternative bulbous bows had been designed using Rhinoceros3D. The hull form was designed to have a good balance between energy efficiency and seakeeping performance. A 1:7.654 scale model was constructed by Memorial University of Newfoundland Technical Services Department.

During the current phase of the project an additional 5 bulbous bows were designed, milled and finished. The hull form and previously constructed bulbous bows were also refinished during this phase of the project.

The following list summarizes the activities completed during this phase of the project:

- The design and construction of five alternative bulbous bows for the model
- Refinishing of hull form and three alternative bulbous bows that have been previously finished
- Resistance tank testing in calm water of all hull configurations in order to establish a ranking of their powering performance in calm water

- Self-propulsion tank testing in calm water of all hull configurations in order to determine the hull and propeller interaction effects
- Using the results from the resistance and propulsion tests to determine the relative energy efficiency of each of the hull configurations

Chapter 2 - Literature Review of Bulbous Bows

The effect of a bulbous bow fitted on the stem of a vessel has been known for quite some time now. Bulb like protrusions were first recorded on the stem of war ships back in Roman times. Their main purpose back then was to use as a device for ramming and sinking enemy ships. D.W. Taylor was the first to produce a true bulbous bow and designed such a bow in 1907 for the USS *Delaware*; a vessel which was said to have excellent powering performance. Much research was completed in this area since that time and many advances have been made in understanding the effects of adding a bulbous bow on the powering performance of a vessel.

Little theoretical work has been completed in attempting to fully understand the seakeeping effects of a bulbous bow. Common practice is to design the bulb by concentrating on optimizing the calm water powering performance of the vessel. Model testing is then typically completed to ensure good seakeeping performance of the bulbous bow vessel.

This section will provide a brief overview of the work that has been completed on the resistance and powering performance of bulbous bows throughout the years. Two well known design methods of bulbous bows will be described within this section. Finally, a review of the experimental work that has been completed on bulbous bows which is relevant to this project will also be given in this section.

2.1 Timeline of Work Completed

The earliest studies completed on bulbous bows were done by Taylor (1923) and Bragg (1930). These tests were completed on methodical series hull forms with Taylor bulbs. Shortly after Weinblum (1935) and Wigley (1936) began to study the linearized theory of wave resistance. This theory begins to explain how a bulb works, but it doesn't allow one to actually design a bulb for a given hull form. Wigley (1936) also discussed the practical benefits of fitting a bulbous bow to a ship, and how a bulbous bow works by minimizing the wave resistance of a hull form. This early work led to further

experimental work on methodical series hull forms by Ferguson et al. (1956), Iuni et al. (1960), Ferguson (1967), and Muntjewerf (1967). It also led to further investigation of the linearized theory of wave resistance by Inui (1962) and Yim (1963).

Some of the other work completed in this time frame includes work by Inui et al. (1960) which resulted in the development of a bulbous bow form known as the 'Inui Bow' and also referred to as a 'waveless' hull and bow combination. It is known however that it is not a true bow wave canceling bulb. Baba (1969) discussed some of the other possible benefits of using a bulbous bow, such as the reduction of wave breaking resistance. Dillon and Lewis (1955) were the first to attempt to determine the performance of a vessel outfitted with a bulbous bow in waves. Through a series of model tests in calm water and head seas they found a large reduction in calm water resistance and a small reduction in motions in head seas. They were then the first to hypothesize that a bulbous bow can be designed for calm water performance alone.

There have been several attempts at providing design methods for bulbous bows. However, none of these provide a way of designing the size, location, and method of fairing into the hull waterlines all at once. Inui (1962) described a way of determining the bulb size by matching the amplitude functions of regular waves from both the ship bow and bulb. Sharma (1967) described a technique to design the size and location of the bulb. Van Lammeren and Wahab (1965) completed work on designing spherical bulbs where they used a simple approximation theory to determine the radius of the sphere which would reduce the bow wave system as much as possible.

In the 1970's two different design methods were developed by Yim (1974) and Kracht (1978) for designing a bulbous bow for a given hull form. These are the two most popular design methods used in the initial stages of a hull and bulbous bow design. These two design methods will be discussed in further detail in the following section.

2.1.1 Design Methods

Yim (1974) wrote a paper describing a simple theory and method for designing a bulbous bow for a given ship. The paper describes a procedure that can be used to determine how large a bulb should be for a given ship hull; as well as methods for determining where the bulb should be located and how it should be faired into the hull waterlines. In this method the main parameters used to describe the hull and bulb are the half entrance angle, bulb volume, and Froude Number in terms of draft, as given in below equation:

$$F_H = V_s / \sqrt{gT_s} \quad (1)$$

This method relies on the linear wave theory to describe the wave patterns as well as dividing the given ship form into elementary sine ship (similar to dividing the hull into wedges). It is supposed that each elementary sine ship has an optimum bulbous bow at its bow; superimposing all of these bulbs will give an optimum bulb for the given ship and is automatically faired into the hull waterlines. This method relies solely on theoretical research and no published test data could be found to support this design method. Therefore, this design procedure should be used with caution; and at most should only be used as an initial guideline for designing an appropriate bulbous bow for a given hull form.

Another method for designing bulbous bows for ships was presented by Kracht (1978). His method provides more generalized design guidelines for reducing the hull resistance and is based on a statistical analysis of previous test results. The vessel length, beam, draft, and displacement are the main characteristics describing the given vessel hull. The cross-sectional bulb area, maximum breadth of cross-sectional bulb area, protruding length of bulb, height of the foremost point of the bulb over the baseline of the vessel, area of the bulb in the longitudinal direction, as well as the volume of the bulb are the six main characteristics used to describe the bulbous bow. These six main bulb characteristics are then non-dimensionalized into three linear and three non-linear bulb parameters.

The paper then provides a residual power reduction coefficient for a given bulbous bow design; or alternatively, a desired reduction coefficient can be chosen and a bulbous bow designed based on this reduction coefficient. This method is based on experimental work and is therefore useful in providing initial guidelines for designing a bulbous bow for a given hull form.

2.1.2 Relevant Experimental Work

Many researchers and naval architects have completed experiments to determine the effects of a bulbous bow on a certain parent hull. Literature has been found for model scale experiments conducted on everything from small workboats to large commercial vessels to determine if a bulbous bow would be suitable for that particular hull type. However, only the relevant literature found will be presented in this review; that is the testing completed on trawler hull forms. Trawlers typically run at high Froude Numbers (in the range of 0.30 – 0.37) and typically have high wavemaking resistance. Therefore, this vessel type potentially stands to have significant savings in required effective power at its design speeds.

A paper written by Johnson (1958) describes a series of bare hull resistance as well as self-propulsion tests which were carried out on a set of hull forms. One of the hull forms was used as a basis hull and was fitted with a conventional bow; while three other hull forms were designed, each incorporating a slightly different bulbous bow (each bulb has a slightly different front cross-sectional area). The bulbous bows designs are implicit bulbs, meaning there is no increase in the displacement of the hull. This is done by shifting part of the displacement volume of the main hull forwards. By doing so the sectional area curve of the original hull is changed.

The bare hull resistance tests were carried out for three displacements at both level trim and 4% trim by the stern. The results from these tests show a decrease in resistance for speeds higher than about 8 – 9 knots ($F_n = 0.25 - 0.28$). For example, for the fully loaded condition where the models are trimmed 4% by the stern the 10% bulb reduces the

required effective power by approximately 20%. For this same condition the 7% bulb reduces the required effective power by about 15% and the 4% bulb by about 10%. From these tests it was concluded that a larger bulb generally provides a larger reduction in required effective power. These tests also concluded that there is a general increase in model sinkage at amidships with increasing speed. Also, the model will trim by the head up to a certain speed then begin to significantly trim by the stern. This change in trim direction generally occurred around 11 – 11.5 knots ($F_n = 0.35 - 0.37$) for all bows. Also, the magnitude of dynamic trim by the head as well as sinkage at amidships generally increases with increasing bulb size.

The self-propulsion tests were carried out for one displacement for each trim condition. During the initial set of tests the conventional bow was tested using a different propeller than was used for the three hull outfitted with bulbous bows. Therefore, the author can only make comparisons for the three models with bulbous bows. The results from these tests show a general trend of slightly decreasing hull efficiency with increasing bulb size. This set of tests also clearly shows that an increase in bulb size will significantly increase the thrust deduction fraction.

In the second set of tests the model with conventional bow was tested with the same propeller as each of the models with bulbous bows. This then allowed for direct comparison between any of the four models tested. From this set of tests it was found that a bulb with a smaller size (i.e. approximately 5%) generally provides the lowest thrust deduction fractions, which lead to higher hull efficiencies.

Doust (1960) wrote a report which summarized resistance and propulsion experiments that were carried out on two models in calm water and rough seas. One model was a conventional long distance trawler while the other was a trawler outfitted with a bulbous bow having the same overall dimensions and displacement. It was found from the bare hull resistance tests it was found that the bulbous bow form provided a reduction in required effective power of 5 – 7.5% in the operating speed range of 12 – 14 knots ($F_n = 0.27 - 0.32$).

Two different propellers were tested in the propulsion test program. One propeller provided a 3 – 5% increase in the Quasi Propulsive Efficiency (QPE) in the speed range of 13 – 14 knots ($F_n = 0.29 - 0.32$) using a bulbous bow. The other provided a 7.5 – 8.5% increase in the same speed range. This increase in propulsive efficiency, when combined with the reductions in resistance, provided an overall reduction in required power on the order of 10 – 15%.

A paper by Heliotis and Goudey (1985) describes the results of experiments conducted on models of a 76 ft and 119 ft New England Trawler hulls. In the study they tested 12 cylindrical type bulbous bows, with no fairing into the hull, for each hull form all at a common draft (i.e. model with bulb attached had a heavier displacement than original hull). It was found that up to a 25% reduction in resistance could be achieved with a bulb that has a cross-sectional area of approximately 20% of the amidships sectional area. Also, a bulb length that corresponded to 1.5 times the diameter of the 20% bulb (i.e. bulb diameter of 60 inches and length to front tip of bulb of 90 inches) was found to give the largest reduction in resistance at the design speeds (F_n around 0.32 – 0.35).

Goudey and Heliotis (1985) performed a very similar study on a 50 m Freshfish Stern Trawler with similar findings. It was found that a bulb with a cross-sectional area of approximately 20% of the amidships sectional area provided the greatest reduction in resistance at the design speed (corresponding to an F_n of approximately 0.32). A bulb length that corresponded to the diameter of the 20% bulb (i.e. bulb diameter of 10.4 ft and length to front tip of bulb of 11.1 ft full scale) was found to give the highest potential for reduction in resistance at the design speed. This is different than what was found in their previous report where a bulb length corresponding to 1.5 times the diameter of the 20% bulb was found to be the most beneficial from a resistance point of view. No possible reason for this was given in either report.

A paper published by Newfoundland Oceans Research and Development Corporation (NORDCO) (1990) details the testing completed on a 65 ft single chine Newfoundland type fishing vessel. A conventional bow as well as a cylindrical type bulbous bow with

no fairing into the hull was tested. No details were provided for the design parameters for the bulbous bow. The test plans consisted of bare hull resistance tests from 2 – 12 knots full scale, self-propulsion tests from 2 – 10 knots, and seakeeping tests at 0, 3 and 9 knots.

From the resistance testing it was found that the bulbous bow was disadvantageous up to a Froude Number of about 0.27. At the design speed of 9 knots ($F_n = 0.34$) the bulb provided a 14% decrease in resistance.

It was found from the self-propulsion tests that there were significant differences in the propeller performance behind the two models. The thrust deduction fractions for the model with bulb generally had a much higher thrust deduction fraction than the model with conventional bow. The wake fraction was also generally slightly higher for the model with bulbous bow attached. This resulted in lower hull efficiency, and hence lower propulsive efficiency, for the model with the bulbous bow attached. The author believes this is due to the disturbed flow around the aft end of the model with a bulbous bow.

Friis et al. (1998) completed a study on the resistance and seakeeping characteristics of a model of the F/V *Newfoundland Tradition*. This vessel was a typical Newfoundland type fishing vessel with a length of 65 ft overall. The model was tested with a conventional bow as well as with two different bulbous bows. Details are not given of the actual particulars of the hull or the bulbous bows. However, the report does say that the shorter bulb does not extend past the 65 ft length overall, and the longer bulb extends 5 ft past the 65 ft length. It is also noted that all testing was performed at a common draft.

From the resistance tests it was found that the longer bulb provided a 8 – 9% reduction in model resistance at speeds above 7 knots full scale (corresponding to $F_n = 0.27$). The smaller bulb would only provide about half of that reduction.

Friis et al. (2007) published a paper which detailed model resistance tests carried out on a 110 ft unrestricted Canadian fishing vessel (not restricted by the 65 ft length rule, enforced by the Department of Fisheries and Oceans (DFO) at the time of the study). The three main bulb parameters studied in this project were: the top profile slope (either 10 or 15°), front cross-sectional area (either 17.8 or 19.9% of the amidships sectional area), as well as the fairing method into the hull (either no fairing lines at all, straight line fairing into hull waterlines, or faired into the hull water lines using S-shaped curves). Using these parameter there were a total of six bulbous bows tested along with the conventional bow.

For the resistance tests the conventional bow was tested at three different draft conditions (design, lightly loaded, and heavily loaded) as well as three static trim conditions for each draft (level trim, 1.5° by the stern, and 3.0° by the stern). All bulbous bows were tested at all three trim conditions for the design draft only. It was found that the conventional bow performed the best from an energy efficiency point of view up to a Froude Number of approximately 0.27. After a Froude Number of about 0.31 all of the bulbous bows begin to outperform the conventional bow. In the design speed range of $F_n = 0.34 - 0.37$ the bulbs with the S-shaped fairing provide approximately a 30 – 35% reduction in resistance. The two bulbs with no fairing at all provide a reduction in the range of 17.5 – 30%, and the two bulbs with straight line fairing provide anywhere between 15 – 25%. It is also noted that there is little difference in resistance reduction between similar bulbs with different front cross-sectional area. This however may be due to the fact that there is only a 2.1% difference in the percentage of the amidships sectional area between the small and large front cross-sectional areas of the bulbs.

Several other interesting results can be concluded from the data presented in the report. Firstly, at high Froude Numbers (i.e. above the design speed range) the bulb with no fairing and a larger front cross-sectional area consistently provides the highest reduction in resistance from the conventional bow. Also, looking at only the two bulbs with straight line fairing it can be seen that the bulb with a slope at the top of the bulb of 15°

consistently provides a much larger decrease in resistance than the similar bulb with a slope at the top of the bulb of 10° .

Finally, Friis et al. (2008) completed a study on the design of a fishing vessel for operation in the Newfoundland and Labrador fishery that is restricted by the DFO vessel length restriction of 89'-11". The study included the following testing on a 6 ft model: bare hull resistance tests, self-propulsion tests, as well as soft-moored seakeeping tests and seakeeping tests in head seas. The model was tested with a conventional bow as well as three different bulbous bows. The bulbs had a common length and front cross-sectional area (corresponding to approximately 24.6% of the submerged amidships sectional area). The main difference in the bulbs was the method of fairing into the hull waterlines. One had no fairing into the hull, one was faired in with straight lines, and the other was faired in with S-shaped curves. Also, the bulb with the straight line fairing had a top profile slope of 17° , while the other two had top profile slopes of 10° .

For the resistance tests the conventional bow was tested at three different draft conditions (design, lightly loaded, and heavily loaded) as well as three static trim conditions for each draft (level trim, 1.5° by the stern, and 3.0° by the stern). All bulbous bows were tested at all three trim conditions for the design draft only (however, there were some discrepancies in the draft due to errors in ballast calculations).

From these tests it was determined that the bulb with an s-shape fairing is likely to be the best performer from a calm water resistance point of view, with the straight line fairing a close contender over the full range. At the static level trim condition in the speed range of 10 – 11 knots ($F_n = 0.31 - 0.35$) the bulb with an s-shaped fairing provides anywhere between a 26.4 – 30.4% reduction in required effective power. The bulb with a straight line fairing provides between a 21.3 – 27% reduction in the same speed range; and the bulb with no fairing into the hull provides between a 6.6 – 28.9% reduction in this speed range.

Two further conclusions came from these tests; one is that the amount of bulb submergence has an impact on the extent of dynamic trim angle of the vessel. It was found that higher bulb submergence leads to a higher amount of trim by the head. Also, a larger top surface area of a bulb provides a bigger trim by the head, up to approximately the design speed.

From the self-propulsion testing it was found that all of the bulbs provided lower wake fractions but significantly higher thrust deduction fractions. This in turn provided lower hull efficiencies, and in turn lower propulsive efficiencies, for all three bulbous bows. The required installed power was calculated for all bows, and it was shown that at the vessel design speed of 10 knots the bulb with S-shaped fairing provided a decrease of about 8% in required power. The bulb with straight line fairing provided a decrease of just over 2% while the bulb with no fairing had a required installed power approximately 13% higher than the conventional bow. It should be noted here that there were significant problems encountered during the self-propulsion tests, which in turn render the collected data less than reliable.

Chapter 3 - Model and Bulbous Bows

3.1 Model

The yacht hull form used in this study was designed in the earlier stages of the project using Rhinoceros 3D. The following figure shows an isometric view of the rendered hull surface of the final design. Also, the following table outlines the principal particulars of the vessel. Further details of the hull form can be found in Appendix A.

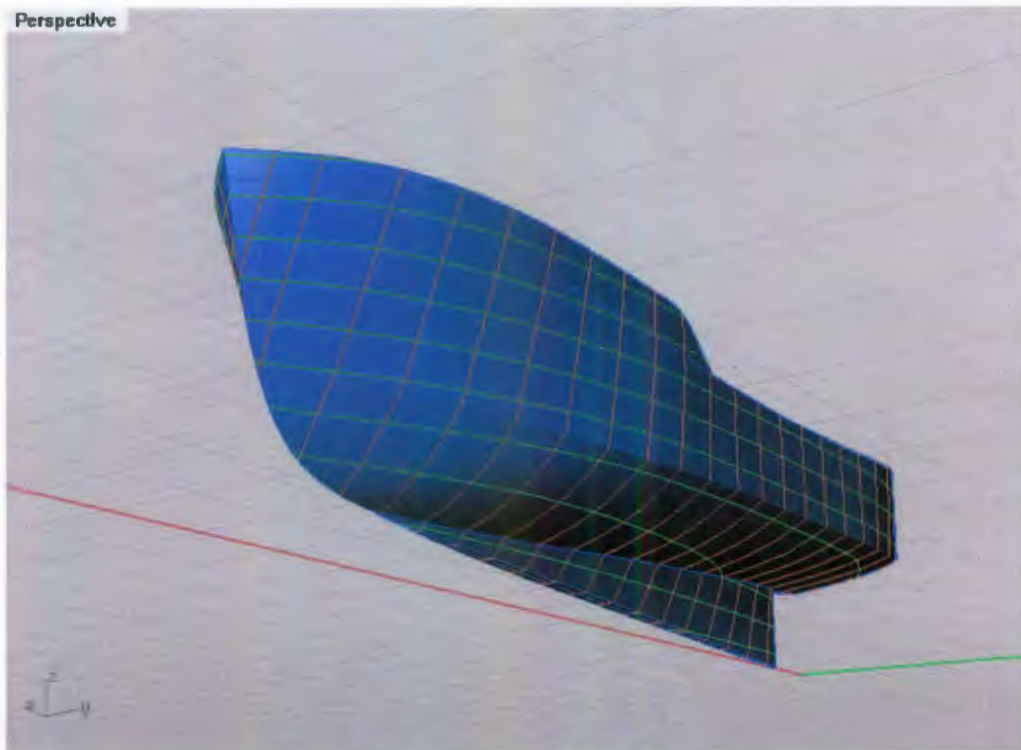


Figure 1: Rendering of Finished Hull Surface

Table 1: Vessel Particulars

Vessel (Full Scale)	(SI Units)	(Imperial Units)
Length Overall (LOA)	14 m	45.93 ft
Beam (B _S)	4.21 m	13.81 ft
Length on Waterline (L _S)	13.26 m	43.51 ft
Volume Displaced (∇)	30.45 m ³	1075.49 ft ³
Displacement (Δ)	30.45 tonnes	33.57 short tons
Draft from baseline (T _S) (at amidships)	1.44 m	4.72 ft
Longitudinal Centre of Buoyancy (LCB) (from transom)	6.15 m	20.18 ft
Wetted Surface Area (S _S)	66.77 m ²	718.78 ft ²
Waterplane Area (A _W)	47.29 m ²	509.08 ft ²
Submerged Transom Area (A _T)	1.11 m ²	11.95 ft ²
Block Coefficient (C _B)	0.377	
Waterplane Coefficient (C _{WP})	0.85	
Prismatic Coefficient (C _P)	0.717	
Midship Section Coefficient (C _m)	0.526	
1/2 Angle of Entrance (α)	30.5°	

The model was designed to have an overall length of 6 ft. This length is considered optimal for use in the MUN towing tank as it provides for easy handling around the lab area and it helps minimize blockage effects associated with tested in a confined tank.

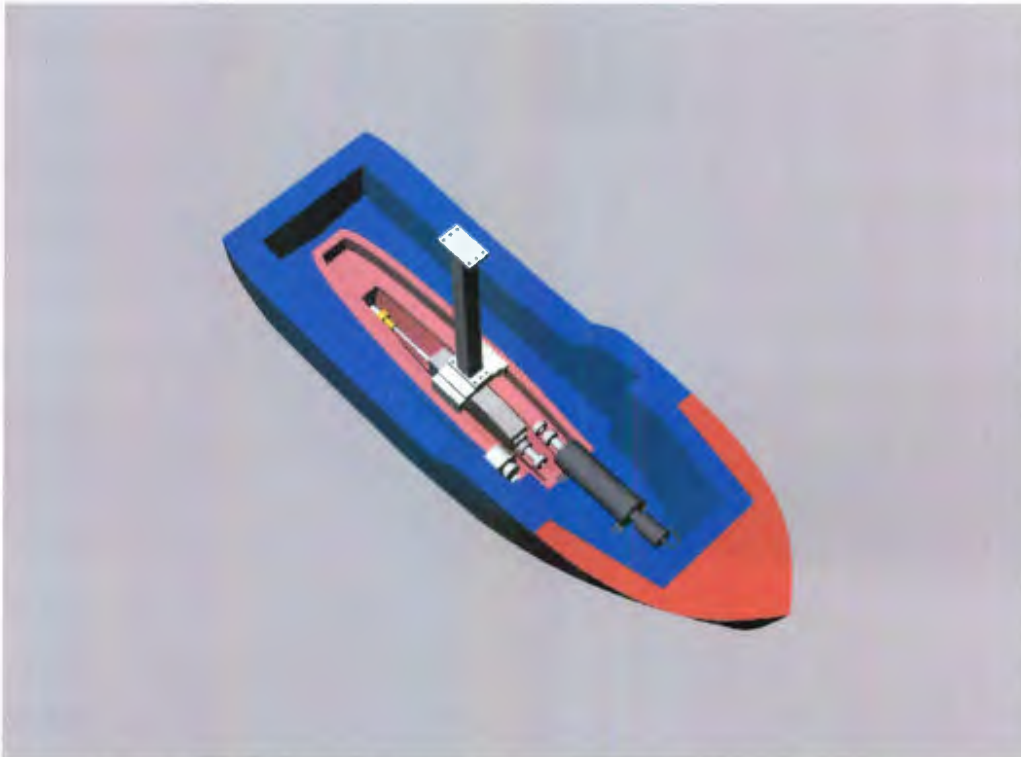


Figure 2: Model Assembled with Instrumentation for Self-Propulsion Tests

Since a smaller model was designed, the interior volume of the model used for testing had to be maximized in order to create as much room as possible for the instrumentation required in the self-propulsion tests, such as the K&R dynamometer and electric motor. This is shown in the previous figure.

In order to maximize the interior volume the model was design to have the different bulbs fit over an existing interior structure. This design gives sufficient interior space while allowing for quick bow changes. This is shown in the following figure.



Figure 3: Rendering of Model Showing Removable Bow

3.2 Bulbous Bows

A total of eight alternative bulbous bows were designed for tank testing. The methodology used to design these bulbs was based on previous design and testing completed by Friis et al. (2007 and 2008).

The main geometric characteristics of each of the eight bulbs are listed below. One of the main differences in the bulbs is the type of fairing into the hull waterlines. Three bulbs are faired using straight lines, three with no fairing, and two using s-shaped curves. The other differences are: the added length on the waterline (due to the presence of the bulb) from the front perpendicular, the front cross-sectional area, the fairing radius into the stem line, and the top profile slope.

Table 2: Bulbous Bow Characteristics (Model Scale)

Bow	Fairing Type	Added Length (ft)	Front Area (ft ²)	% of A _m (%)	R _F (ft)	A _{TP} (deg)
Beta	Straight Line	0.590	0.103	17.64	0.309	13.0
Delta	None	0.425	0.103	17.64	0.236	16.7
Gamma	None	0.590	0.103	17.64	0.309	13.0
Epsilon	S-Shaped	0.590	0.103	17.64	0.309	13.0
Eta	Straight Line	0.590	0.138	23.48	0.309	13.0
Iota	None	0.425	0.173	29.47	0.236	16.7
Theta	Straight Line	0.425	0.138	23.48	0.236	16.7
Zeta	S-Shaped	0.425	0.103	17.64	0.236	16.7

The following three tables list the top bulb area and bulb submergence of each of the bulbs at static level trim, 0.75° by the stern and 1.5° by the stern trim conditions. The top bulb area is the waterplane area that has been added due to the presence of the bulb. The bulb submergence is the underwater volume added due to the bulb presence.

Table 3: Comparison of Top Bulb Area and Bulb Submergence (Level Trim)

Level Trim		
Bow	Top Bulb Area (ft ²)	Bulb Submergence (ft ³)
Beta	0.4348	0.2390
Delta	0.1135	0.0843
Gamma	0.1458	0.1035
Epsilon	0.2745	0.1832
Eta	0.5215	0.2788
Iota	0.2194	0.1554
Theta	0.4315	0.2304
Zeta	0.2360	0.1599

Table 4: Comparison of Top Bulb Area and Bulb Submergence (0.75° by Stern)

0.75° by Stern		
Bow	Top Bulb Area (ft ²)	Bulb Submergence (ft ³)
Beta	0.5518	0.2188
Delta	0.1679	0.0783
Gamma	0.2108	0.0969
Epsilon	0.4022	0.1627
Eta	0.6754	0.2546
Iota	0.3196	0.1436
Theta	0.5550	0.1993
Zeta	0.3257	0.1420

Table 5: Comparison of Top Bulb Area and Bulb Submergence (1.5° by Stern)

1.5° by Stern		
Bow	Top Bulb Area (ft ²)	Bulb Submergence (ft ³)
Beta	0.6261	0.1946
Delta	0.2164	0.0717
Gamma	0.2679	0.0911
Epsilon	0.4807	0.1489
Eta	0.7643	0.2260
Iota	0.3906	0.1279
Theta	0.6210	0.1885
Zeta	0.4165	0.1344

The following series of figures shows each of the eight bulbous bows designed. There are four views in each figure in order to provide a good idea of the shape of each bulb.

Beta Bow

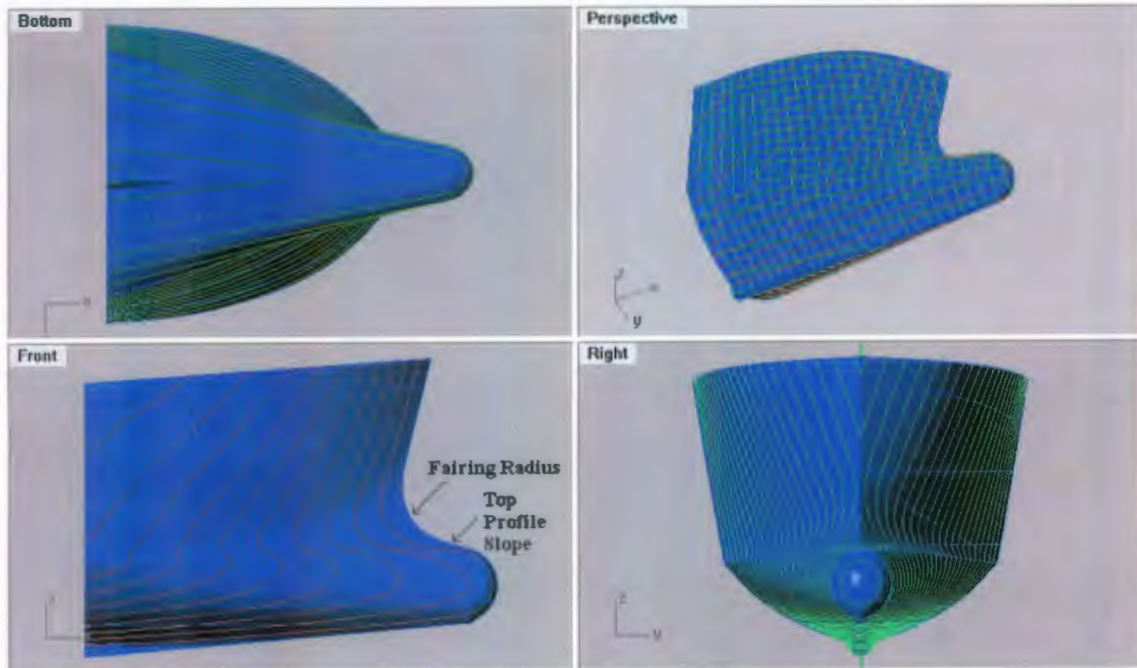


Figure 4: Four Views of Beta Bow

Delta Bow

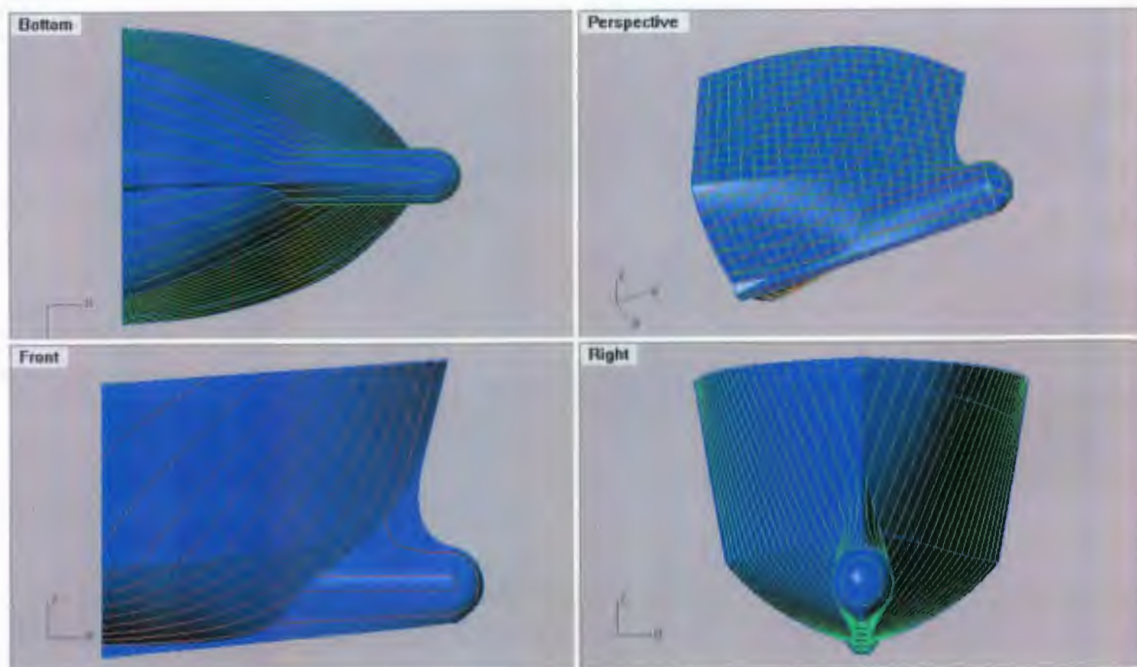


Figure 5: Four Views of Delta Bow

Gamma Bow

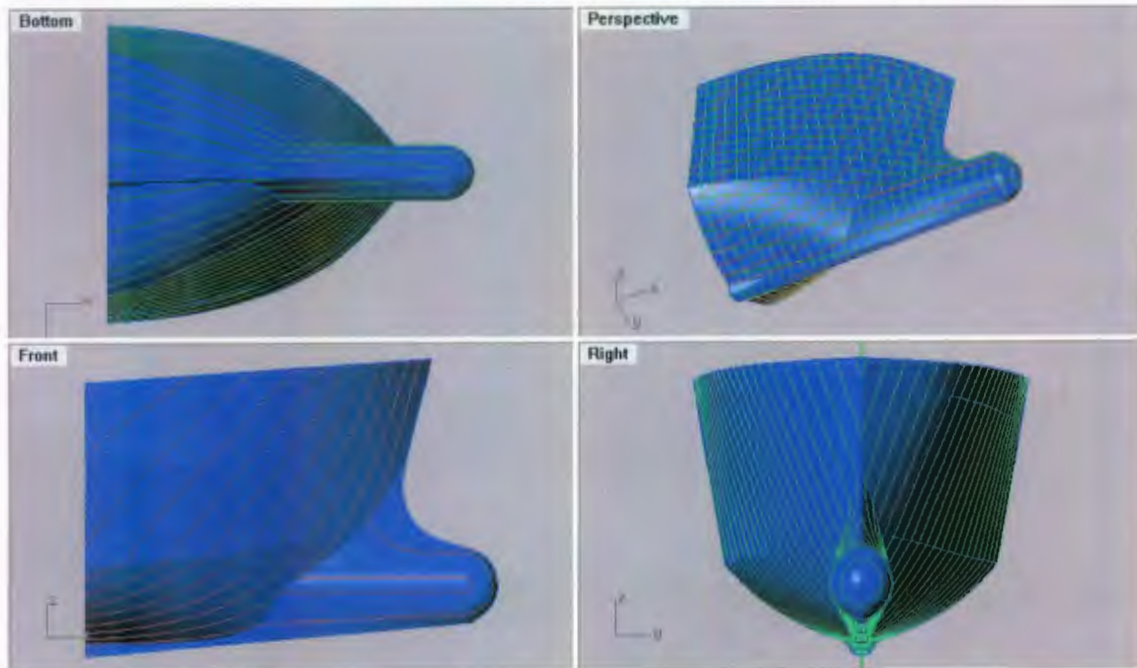


Figure 6: Four Views of Gamma Bow

Epsilon Bow

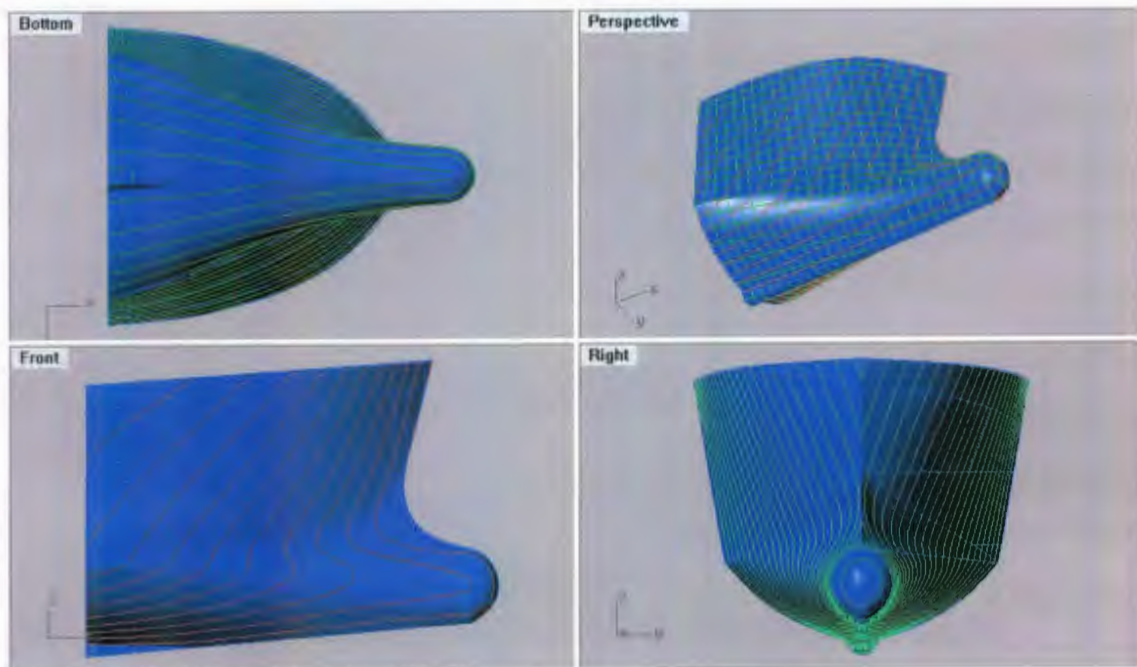


Figure 7: Four Views of Epsilon Bow

Eta Bow

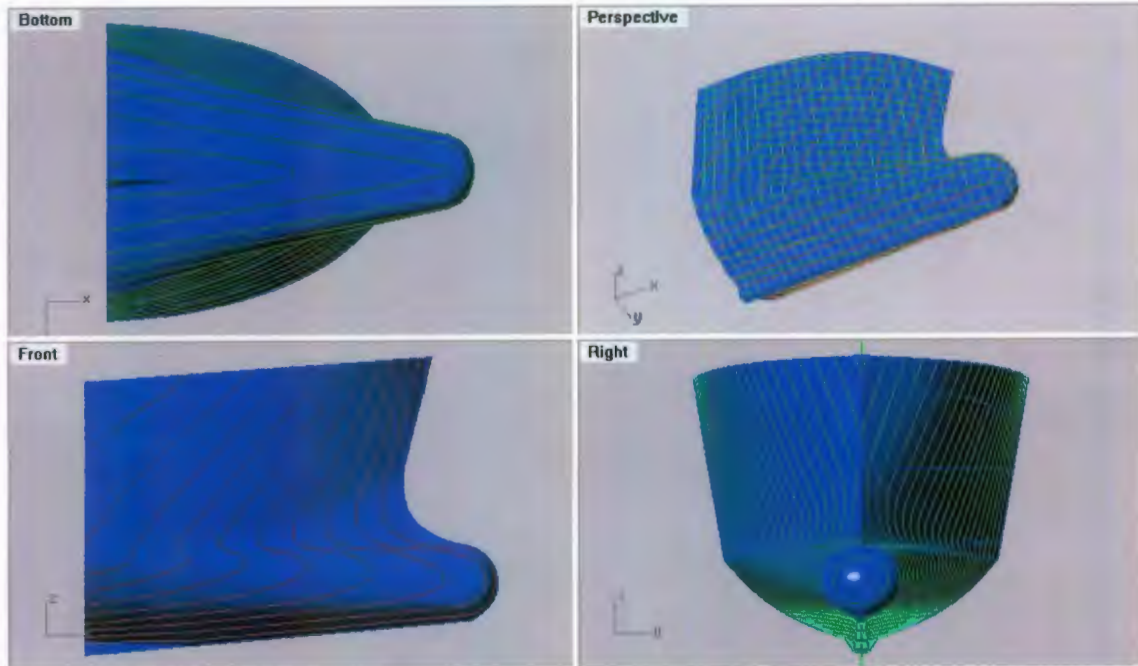


Figure 8: Four Views of Eta Bow

Iota Bow

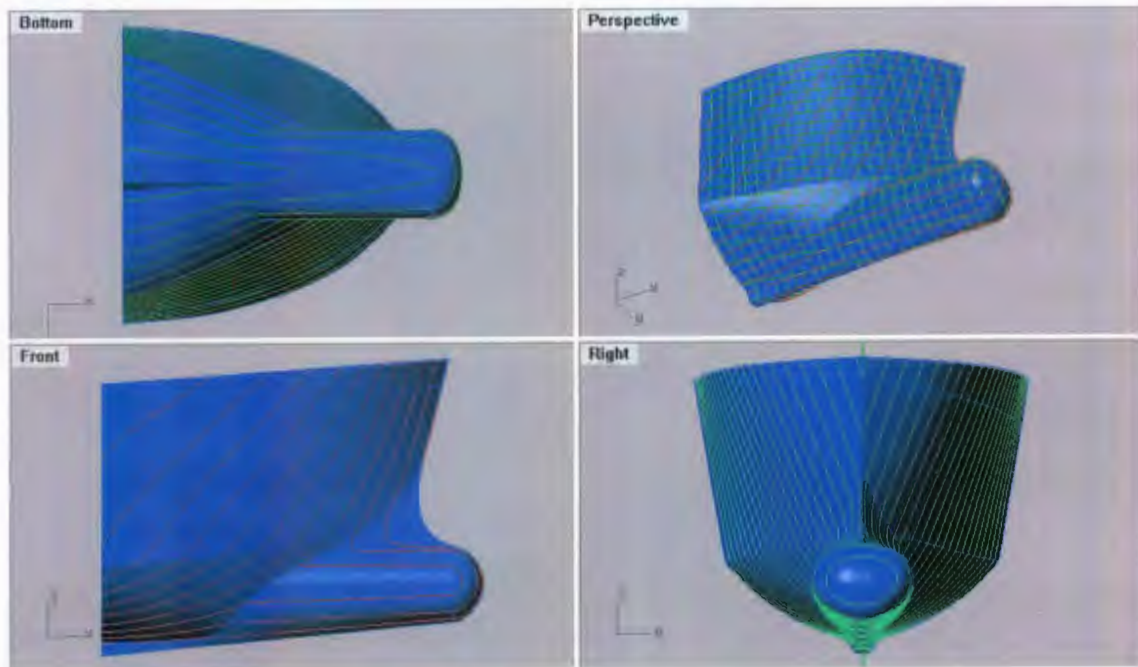


Figure 9: Four Views of Iota Bow

Theta Bow

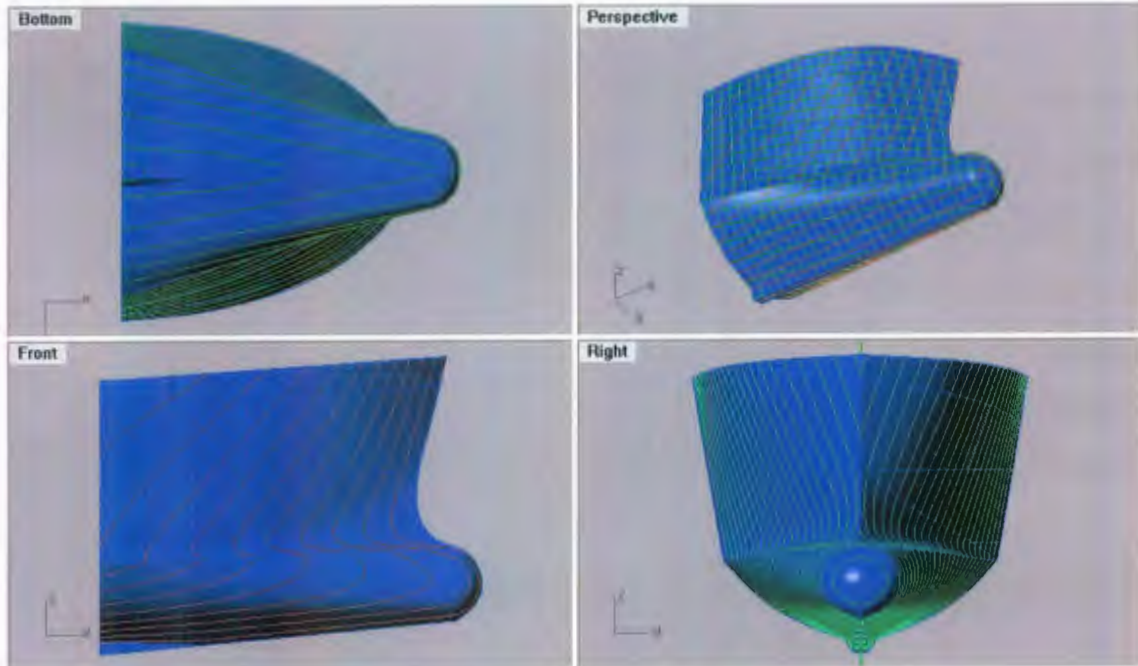


Figure 10: Four Views of Theta Bow

Zeta Bow

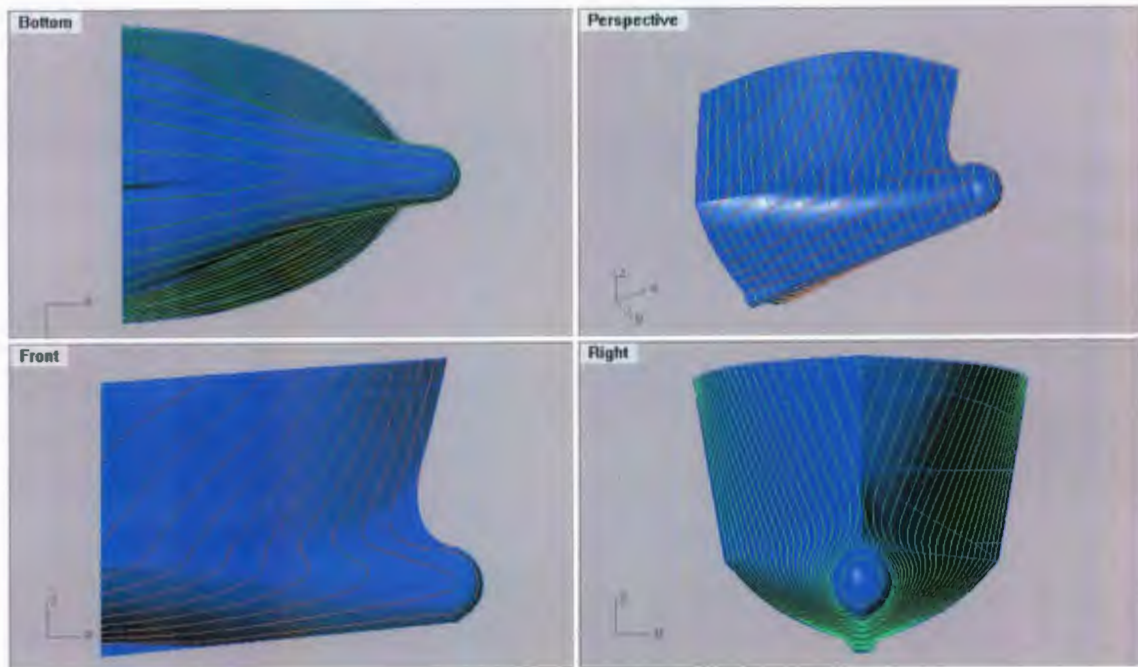


Figure 11: Four Views of Zeta Bow

Chapter 4 - Model Construction

The construction and finishing of the model was done by Memorial University of Newfoundland Technical Services Department. The following section gives a brief overview of the procedure involved in the construction of the model. The figures provided show the various stages of the model construction process up to completion. Note here that the model construction was completed using the IOT Standard Test Method for Model Construction (2007).

To begin, sheets of high density foam are glued together to create a foam layup from which the model will be milled. A material called Renshape® is placed in the layup in the appropriate positions. The keel is also milled out of Renshape®. After the glue is set the layup is placed in the CNC milling machine where it is milled to yield the model surface; an undercut of 80 thousandths of an inch is used to account for fiberglass. After Fiberglassing the surface is primed with Duratec® Primer Surface and sanded smooth after which it is painted with a high gloss Imron® Polyurethane paint.

The stern section of the model as well as three of the bulbous bows was finished in an earlier phase of the project, while the five remaining bulbous bows were finished during the present phase. Due to a low quality finishing job done during the previous phase of the project the stern section and three bulbous bows previously constructed had to be refinished during this phase. A 3D laser scanner, used for reverse engineering, was used to scan all exterior surfaces of the model stern section as well as all bows to ensure that the model was within acceptable tolerances. This was done by comparing the scanned surface to the original 3D surfaces. These were all found to be well within acceptable tolerances.



Figure 12: Beginning to Mill Stern Section in CNC Machine



Figure 13: Milling Almost Complete on Stern Section



Figure 14: Milled Conventional Bow



Figure 15: Fibreglassed Epsilon Bulb



Figure 16: Fibreglassed Stern Section with Glued in Stern Tube



Figure 17: Stern Section during Refinishing



Figure 18: Two Bulbs during Refinishing



Figure 19: Fairing Bulb with Stern Section



Figure 20: Finished Model with Conventional Bow



Figure 21: Three Finished Bulbous Bows Complete with Turbulence Stimulators

Chapter 5 - IOT Bare Hull Resistance Tests

Resistance tests were conducted to determine total hull resistance and effective power of the full scale vessel. The study is based on an experiment performed on the model in the IOT ice tank in the period of December 17, 2008 – December 23, 2008. This objective was completed by testing the model over speeds corresponding to 0 – 12 knots full scale. This analysis was done using the International Towing Tank Conference - 1957 (ITTC-57) procedures.

Note that the ice tank was used for this study as the IOT clear water towing tank was already booked during the available test time. Also, the MUN towing tank was out of operation for repairs and general maintenance. However, the IOT ice tank is routinely used for bare hull resistance tests when the IOT towing tank is not available.

5.1 IOT Test Facility

The IOT ice tank (http://iot-ito.nrc-cnrc.gc.ca/facilities/it_e.html) has a length of 90 m, is 12 m wide, and has a water depth of 3 m. The tank is used to carry out experiments in both open and ice covered waters. The 80 tonne tow carriage, capable of speeds from 0.0002 m/s to 4 m/s, can accommodate ship models up to 12 m in length and other test apparatuses for a wide range of test types. An ammonia based refrigeration system is used to reduce the ambient air temperature down as low as -30°C and freeze a chemical solution composed of Ethylene Glycol/Aliphatic Detergent/Sugar (EG/AD/S) to produce a uniform ice sheet with scaled properties of crystal size and flexural strength from 10 to 150 mm thick.

For open water resistance testing, the thermal barrier was open for complete access to the entire tank. The fluid temperature varied from 1 to 3°C . The service carriage was not required and was docked over the melt pit while the underwater carriage was disconnected from the tow carriage. The side beaches were deployed for bow wave absorption. Test runs were carried out with the carriage running towards the melt pit.

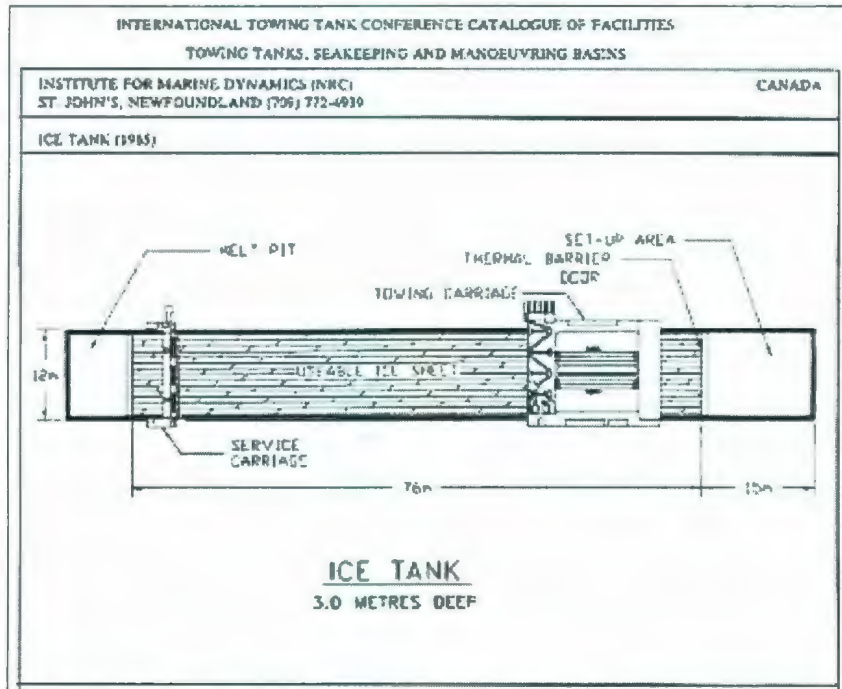


Figure 22: IOT Ice Tank Schematic 1

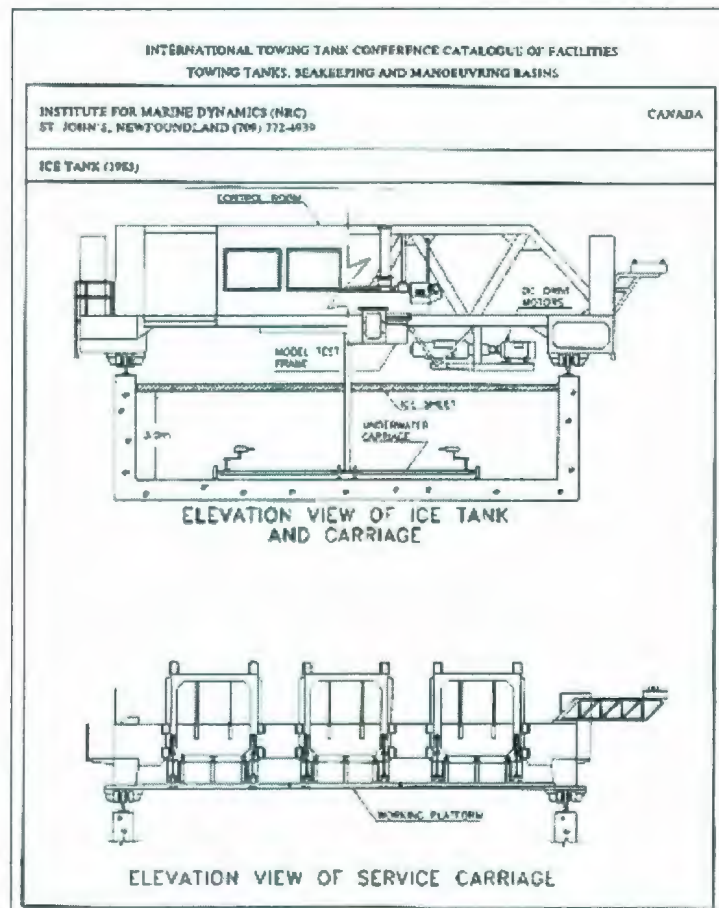


Figure 23: IOT Ice Tank Schematic 2

5.2 Test Instrumentation

There are several pieces of instrumentation that are involved in model resistance testing. The list includes: towing gimbal for measuring resistance, inclinometer for measuring pitch, as well as a Linear Variable Differential Transformer (LVDT) for measuring heave.

Towing Gimbal

The gimbal used for measuring resistance during testing is an in house design which was used for a previous project at IOT. The load cell mounted in the gimbal has a rating of ± 50 lbs (approximately ± 220 N). The load cell is protected from overloading by use of a set-screw which only allows the cell to deflect a safe amount. This gimbal allows the model to pitch, roll and heave. The model is confined from yawing, surging and swaying.

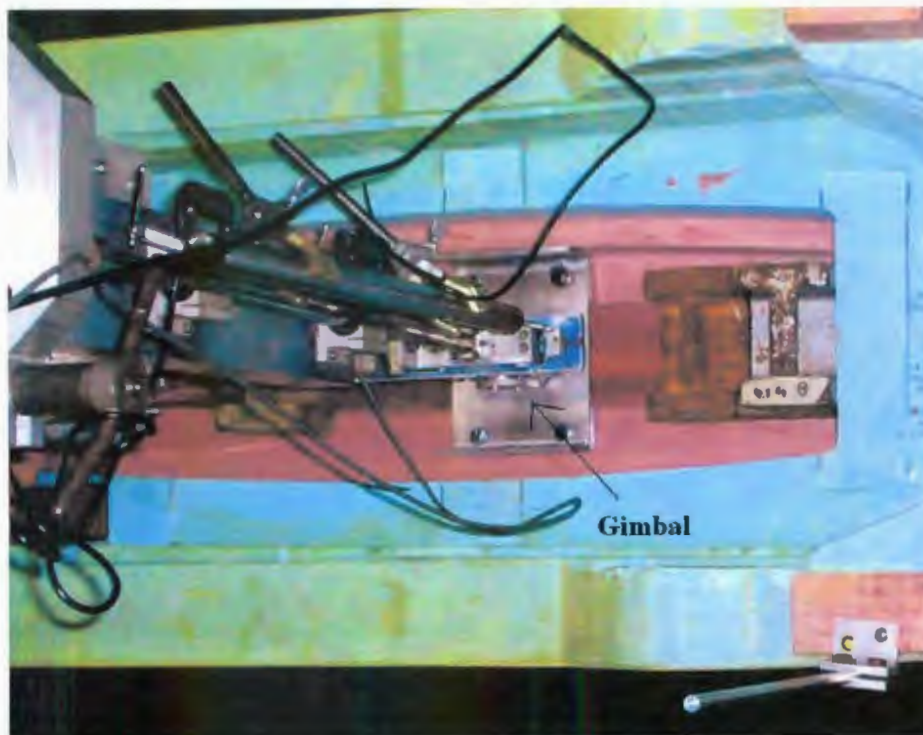


Figure 24: Gimbal used for Resistance Tests

Inclinometer

To measure pitch angles a Servo Inclinometer from *Jewell Instruments LLC* was used. The inclinometer is fully self-contained and designed to operate in hostile environments. It is designed to operate from a standard DC power source. The output is an analog DC signal which is directly proportional to the sine of the angle of tilt; in level (horizontal) position, the DC output is zero. In one direction the output is 0 to +5 V and in the other it is 0 to -5 V.



Figure 25: Inclinometer Installed in Model

LVDT

The LVDT measures the vertical movements of the model at the tow point. It was attached directly to the tow post via clamps and to the towing gimbal via a nut. The LVDT was positioned such that the model would be free to heave up to approximately 6 – 8 in.

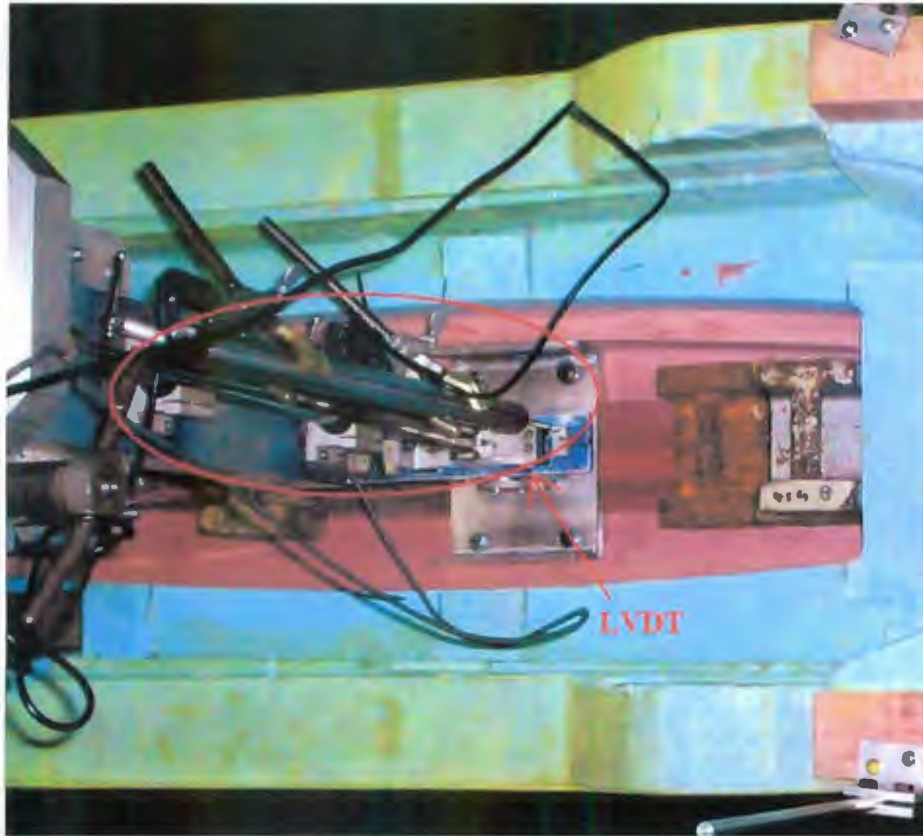


Figure 26: LVDT used for Resistance Tests

5.2.1 Instrumentation Calibrations

Before testing can commence all the instrumentation used has to be calibrated using proper procedures. This includes the calibration of the load cell contained in the towing gimbal for resistance, the inclinometer used for measuring dynamic trim, as well as the LVDT used for measuring model sinkage.

The calibration of the load cell is completed by placing a series of known masses (and hence forces) on the sensor up to a maximum of approximately 45 lbs. The voltage output from the load cell is then recorded on a computer. The voltage output is then plotted against the known forces applied and a linear relationship should be found. If a linear relationship is not found then it is known that the calibration was completed incorrectly or there is a physical problem with the instrument. A regression line is then fit through the plot and an equation of the line relating voltage to force is determined.

This equation is then used during testing to convert the voltage measured during each run into a force applied on the hull (which is the model's resistance at any given speed).

The calibration of the inclinometer is completed by placing the instrument on a series of known angles (usually -45° , -30° , -15° , 0° , 15° , 30° , and 45°). The measured voltage from each reading is then plotted against the known angle. A similar procedure as explained is then used to determine the equation used during testing.

The LVDT is calibrated by extending the tip out by known distances (i.e. 10 increments of 1 inch). These distances are then plotted against the measured voltage and an equation of the line is determined.

5.3 Model Set-up

Appropriate turbulence stimulation is used to ensure that the model is operating in turbulent flow. The turbulence stimulation used for this model is compliant with the IOT Standard Test Method for Model Construction (2007). For the original hull this consists of a single row of cylindrical brass studs that are 3 mm long and 3 mm in diameter. These studs are placed parallel to the stem line at a distance of approximately 35 mm, and are spaced 25 mm apart. There are two lines of studs for each of the bulbous bows. The first line follows the stem of the bow similarly to the conventional bow until it intersects with the top of the bulb, at which point the row extends vertically down the side of the bulb until it reaches the keel. The second is a vertical row placed 25% the length of the bulbous bow from the forward end of the bulb.

Before the model can be attached to the carriage it must be ballasted properly to the correct waterline. This is done using trim hooks attached to milled pads on the model. The distance from the top of the milled pad to the waterline is known, so the trim hooks can be set at this length. It is then known that the trim hooks should be just touching the surface of the water.

For the purpose of testing the displacement of the model with each bow was determined using the 3D Rhino drawings. When the model was placed in the tank the required

weight was distributed within the model until each of the trim hooks were just touching the water. At this point it is known that the model is sitting at the correct waterline.

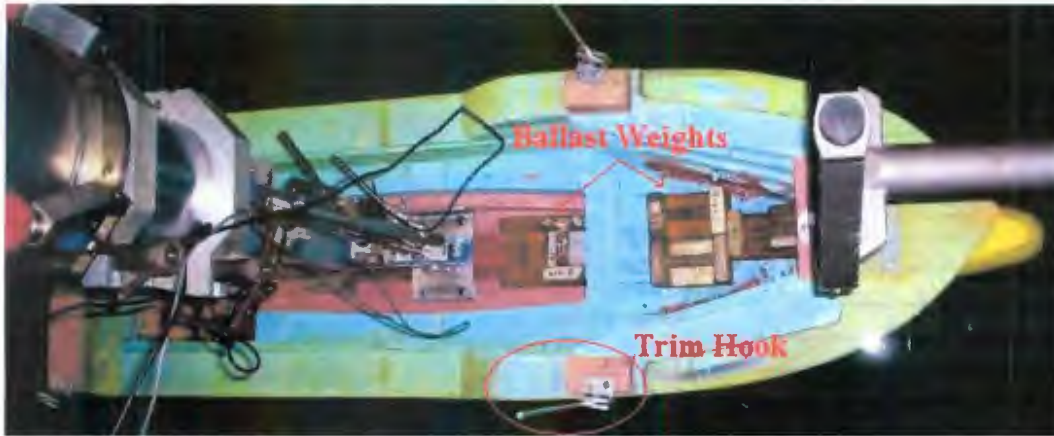


Figure 27: Model with Trim Hooks Attached (Ballast Weights in Model)

5.4 Test Plan

The original test plan included testing each of the bows at the design draft of 0.188 m model scale and three different trim angles (level trim, 1.5° by stern, and 3.0° by stern). The vessel speed was originally set to range from 1 – 12 knots full scale. The following table shows the original test plan for the following bows; Alpha, Beta, Gamma, and Epsilon.

**Table 6: Test Plan for Resistance Tests at IOT
For Each Trim Condition**

Run #	V _S (knots)	V _M (m/s)
Roughup	6	1.116
Roughup	6	1.116
1	1	0.186
2	2	0.372
3	3	0.558
4	4	0.744
5	6	1.116
6	8	1.487
7	9.5	1.766
8	10.5	1.952
9	11.5	2.138
10	12	2.231
11	11	2.045
12	10	1.859
13	9	1.673
14	7	1.301
15	5	0.930
16	3.5	0.651
17	2.5	0.465
18	1.5	0.279

Unfortunately, as with most testing, there were several unexpected results found during the testing procedure. It was found that when the first bulb (Beta Bulb) was tested the model tended to yaw to starboard and roll to port. It was determined the model was not correctly aligned with the centreline of the tank. Many hours were spent trying to mitigate this effect; but it could not be completely solved. It was therefore decided to test the remainder of the bows up to a full scale speed of only 10 knots.

Since it was determined that the model had not been centred with the test frame during the first model configuration (i.e. fitted with Alpha bow), it was decided to retest this configuration. For the retests the model was tested up to 10 knots for each of the following three trim conditions: level trim, 0.75° by stern, and 1.5° by stern.

It was also found that the model fitted with the different bulbous bows was not trimming by the head as was recorded with previous fishing boat models tested by Dag Friis. It

was therefore decided to test Epsilon bow at a total of four trim conditions, with 0.75° trim by stern being added in. For Gamma bow the trim condition of 3.0° by stern was replaced by 0.75° by stern. As stated above when Alpha bow was retested the condition of 3.0° by stern was replaced by 0.75° by stern.

5.5 Description of Experiment (ITTC-57 Method)

To determine the full scale ship resistance and effective power the ITTC-57 method is used. During testing the model is towed at a range of speeds from low to speeds corresponding to the maximum expected for full scale. The total model resistance is measured along with the water temperature at the beginning, middle, and end of each day of testing.

Another possible method that could be used is the ITTC-78 method, which uses a 'form factor' to account for the ship's shape. The advantage of using this method is that it provides a more accurate ship-model correlation than the ITTC-57 method. However, a disadvantage of the ITTC-78 method is that in order to determine the form factor further experimentation would be required. The form factor is usually determined by means of Prohaska's method; which requires that 8 to 10 runs be completed in the Froude Number range of 0.12 – 0.20 (i.e. the wave making resistance is negligible in this range). This would therefore add a further 5 to 8 extra runs for each bow tested.

It was decided that the ITTC-57 method would be better suited. This method still gives acceptable ship-model correlation results and can be done in fewer test runs. Also, one of the main aims of this project is to study the difference in effects of different bows on resistance and motions. The ITTC-57 method provides adequate results for this kind of study.

The ITTC-57 method is then completed using the following series of steps:

- 1) From the test results calculate C_{TM} at each speed using:

$$C_{TM} = \frac{R_{TM}}{\frac{1}{2} \rho_M V_M^2 S_M} \quad (2)$$

Where: R_{TM} = total model resistance measured

ρ_M = fresh water density (which is a function of water temperature)

V_M = model speed (i.e. carriage speed)

S_M = model wetted surface area

2) Calculate the model frictional resistance coefficient using the ITTC-57 Model-ship Correlation Line at each speed:

$$C_{FM} = \frac{0.075}{(\log_{10} R_{nM} - 2)^2} \quad (3)$$

Where R_{nM} is given as:

$$R_{nM} = \frac{V_M L_M}{\nu_M} \quad (4)$$

3) Calculate the residuary resistance coefficient, C_R , at each speed:

$$C_R = C_{TM} - C_{FM} \quad (5)$$

Note: The residuary resistance coefficient is the same at model and full scales.

4) Calculate the ship frictional resistance coefficient C_{FS} (for smooth hull) using ITTC-57 Model-Ship Correlation Line at each speed:

$$C_{FS} = \frac{0.075}{(\log_{10} R_{nS} - 2)^2} \quad (6)$$

Where R_{nS} is given as:

$$R_{nS} = \frac{V_S L_S}{\nu_S} \quad (7)$$

5) Calculate the total resistance coefficient for a smooth ship:

$$C_{TS} = C_{FS} + C_R + C_A \quad (8)$$

Where: C_A = correlation allowance (taken as 0.0004)

6) Calculate the total ship resistance for each speed:

$$R_{TS} = C_{TS} \frac{1}{2} \rho_S V_S^2 S_S \quad (9)$$

Note: This total resistance is for the naked hull only.

7) Calculate the effective power for each speed:

$$P_E = R_{TS} V_S \quad (10)$$

5.6 Blockage Corrections

A blockage correction is used in model resistance tests when the boundaries of the tank may influence the resistance of the model. There are two relations between the model and tank that can be used as preliminary checks to see if there is likely any blockage effects:

$$B_M = \frac{1}{10} B_T \quad (11)$$

$$T_M = \frac{1}{10} h_T \quad (12)$$

Where:

B_M = model beam on waterline

B_T = width of the tank at the water surface

T_M = model draft

h_T = water depth in the towing tank

The following relationships exist for the yacht model in the IOT Ice Tank:

$$B_M = 0.046B_T \quad (13)$$

$$T_M = 0.08h_T \quad (14)$$

Therefore, this shows that there probably isn't much in the way of blockage in this tank; and hence a blockage correction may not be required for these tests.

However, the following relationships exist for this model in the MUN Towing Tank:

$$B_M = 0.122B_T \quad (15)$$

$$T_M = 0.131h_T \quad (16)$$

This shows that there may be significant blockage effects in this tank and a blockage correction should be performed on any resistance data collected in this tank.

One method of calculating the blockage corrections is given by Scott (1976) and is given as:

$$\Delta C_T = \{n_T C_T b \nabla A^{-3/2} + kf(1 + kf)^{-1} C_w\} (1 - cF_h^2)^{-1} \quad (17)$$

In this equation ΔC_T is the reduction of total resistance coefficient, C_T , at a given speed. This then has to be calculated for each model speed tested, and the value of ΔC_T is subtracted from the corresponding value of C_T at that model speed.

In the above equation n_T is defined as the power to which the speed has to be raised to produce a quantity proportional to actual resistance in the vicinity of the speed concerned. It is given by the following equation:

$$n_T = 2 + \left(\frac{F_n}{C_T} \right) \left(\frac{dC_T}{dF_n} \right) \quad (18)$$

Where: F_n = Froude Number for a given speed.

C_T is the total resistance coefficient for a given speed.

b is a function of Reynolds Number, R_n , and the form factor $L\nabla^{-1/3} \delta^{-1}$, where δ is the block coefficient of the model. The following figure is then used to determine the value of b for each Reynolds Number corresponding to each speed tested.

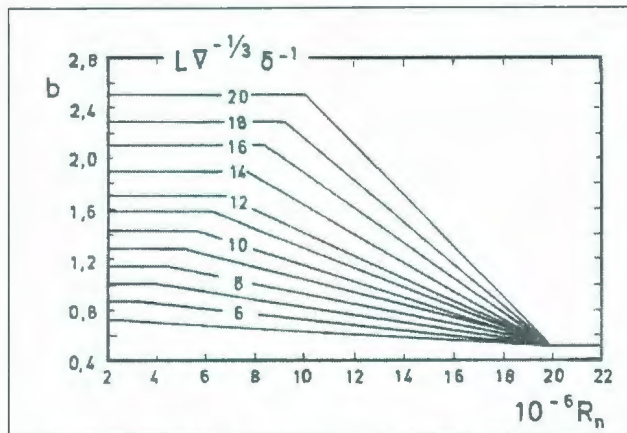


Figure 28: Variation of b with Reynolds Number and form factor

∇ is the volume of displacement of the model.

A is the cross-sectional area of the towing tank.

k is a parameter used in the wavemaking correction and is only a function of Froude Number. The following figure shows the variation of k with Froude Number.

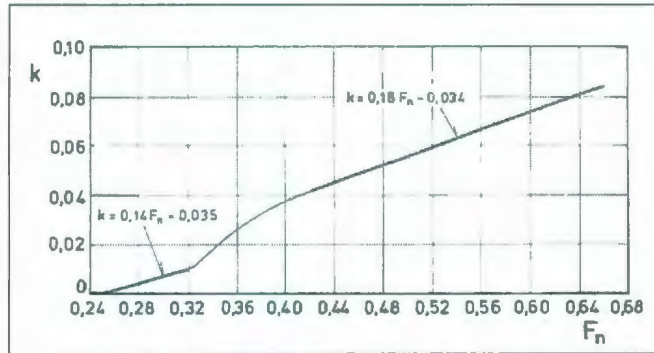


Figure 29: Variation of k with Froude Number

f is a model-tank function given by the following equation:

$$f = L_M^4 (BT)^{1/4} A^{-1.25} h^{-2} \quad (19)$$

Where: L_M = model length on the waterline

B = model beam on the waterline

T = model draft

h = water depth in the towing tank

C_W is a wavemaking resistance coefficient that is determined by the following equation:

$$C_W = C_T - C_v \quad (20)$$

Where C_v is a viscous resistance coefficient given by the following equation:

$$C_v = C_{T(F_n=0.1)} \frac{(\log R_{n(F_n=0.1)} - 2)^2}{(\log R_n - 2)^2} \quad (21)$$

In the above equation the subscript of $F_n = 0.1$ means the value of C_T and R_n at this Froude Number only.

c is used in the Bernoulli term and is a function of Froude Number only. The following figure shows the variation of c with Froude Number.

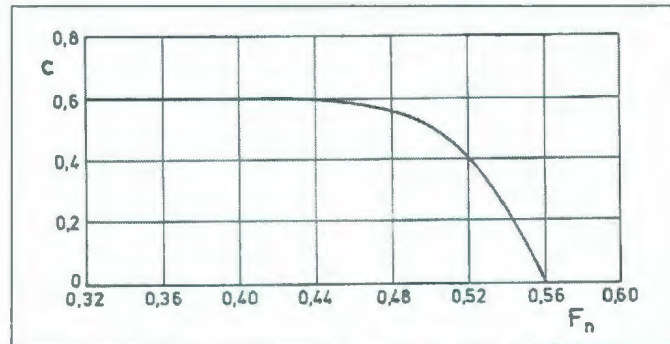


Figure 30: Variation of c with Froude Number

F_h is the Froude Depth Number defined as:

$$F_h = \frac{V}{\sqrt{gh}} \quad (22)$$

Where: V = model speed

g = acceleration due to gravity

5.7 Description of Data Analysis

5.7.1 Online Data Analysis

The data were acquired in GDAC format (*.DAC files) as outlined by Miles (1996 and 1996) and converted to GEDAP format, again as outlined by Miles (1990), prior to carrying out an online data analysis on the ice tank carriage workstation during the test to verify the integrity of the acquired data.

The resistance online data analysis is described as follows:

- The basic resistance channels (forward speed, tow force, sinkage, and trim) are plotted on the screen in the time domain. Start and end times (T1, T2) are interactively selected for the initial tare segment as well as for each steady state segment. There was more than one steady state segment if more than one forward speed was acquired during a single run up the tank – a common situation for low forward speeds.
- The following four plots are displayed on the same screen:
 - 1) Resistance (N) vs. Froude Number
 - 2) Trim (degrees) vs. Froude Number
 - 3) Sinkage (cm) vs. Froude Number
 - 4) $10^3 C_{TM}$ vs. Froude Number
- Run designation, acquire time, and mean values of carriage speed (m/s), resistance, $10^3 C_{TM}$, sinkage, and trim computed over each steady state time segment were output in tabular form for all runs completed up to the given run.

5.7.2 Offline Data Analysis

The following data analysis was carried out to assess the hull resistance using the IOT Standard Resistance Procedure (2006). Within this standard the effective power is estimated using the ITTC-57 Method (1957).

- Run designation, acquire time, carriage speed (m/s), resistance (N), sinkage (cm) and trim (degrees) values were output in tabular form for all runs carried out for the model.
- The model resistance coefficients were then plotted vs. Froude Number and $\log_{10} R_{eM}$. Coefficients plotted include C_{TM} , blockage corrected C_{TM} (ice tank blockage corrected using Scott's Method (1976)), and C_{FM} .

- A table of model resistance coefficients corrected to standard conditions (15 °C) was generated including F_n , $10^{-6}R_{nM}$, 10^3C_{TM15} , and 10^3C_{FM15} .
- A plot of effective power vs. ship speed (knots) using the ITTC-57 methodology was generated.
- A table of ship resistance and effective power using the ITTC-57 prediction method was provided for the ship in salt water and including the tank blockage correction using Scott's Method. The table includes: V_S (knots), P_E (kW), R_{TS} (kN), F_n , $10^{-8}R_{nS}$, 10^3C_{TS} , 10^3C_{FS} , and 10^3C_R .
- The user then executed an option to interactively fit a spline through the sinkage and trim data. Once the splines were fit, a plot of sinkage in the form of $10^2Z_V/L_M$ and dynamic trim (θ_V) were plotted vs. Froude Number (both the test data and smoothed lines fitted through the data).
- A table of sinkage and trim information was also generated and included: V_S (knots), F_n , $10^2Z_V/L_M$, and θ_V .

Additional data analysis including comparison of the effective power, sinkage and trim for the various model configurations (bow, static trim) could be carried out after exporting the data to EXCEL format files.

5.8 Results and Discussions

This section is intended to give an overview of the results obtained from the analysis of the testing. The effective power results shown in this report are scaled to a full scale boat of 45.93 ft in length. The detailed results are contained in Appendix B.

5.8.1 Conventional Bow

As stated above, this bow was tested twice as alignment issues were raised during testing. In this section the results will be provided for both set of tests and comparisons will be given. The first set of tests is given the name of 'Alpha' and the retests are named 'Alpha2'. The results shown are in terms of full scale effective power, which is defined as the power required to overcome the hull resistance at a given speed.

Table 7: Effective Power with Alpha Bow (IOT Tests)

Effective Power for Alpha Bow (W)			
Ship Speed (knots)	Level Trim	1.5° by Stern Trim	3.0° by Stern Trim
1	40	49	105
2	179	148	302
3	499	521	884
4	1252	1342	2022
5	2831	3362	4824
6	5807	6526	8352
7	13031	15041	18696
8	26274	28039	30165
9	47018	48261	52058
10	83649	82622	88649

Table 8: Effective Power with Alpha2 Bow (Retests at IOT)

Effective Power for Alpha2 Bow (W)			
Ship Speed (knots)	Level Trim	0.75° by Stern Trim	1.5° by Stern Trim
2	57	100	110
3	401	329	385
4	985	1011	1177
5	2058	2127	2599
6	4164	4885	5385
7	10201	11653	12242
8	22314	24487	24901
9	41631	41732	42639
10	76280	74843	75181

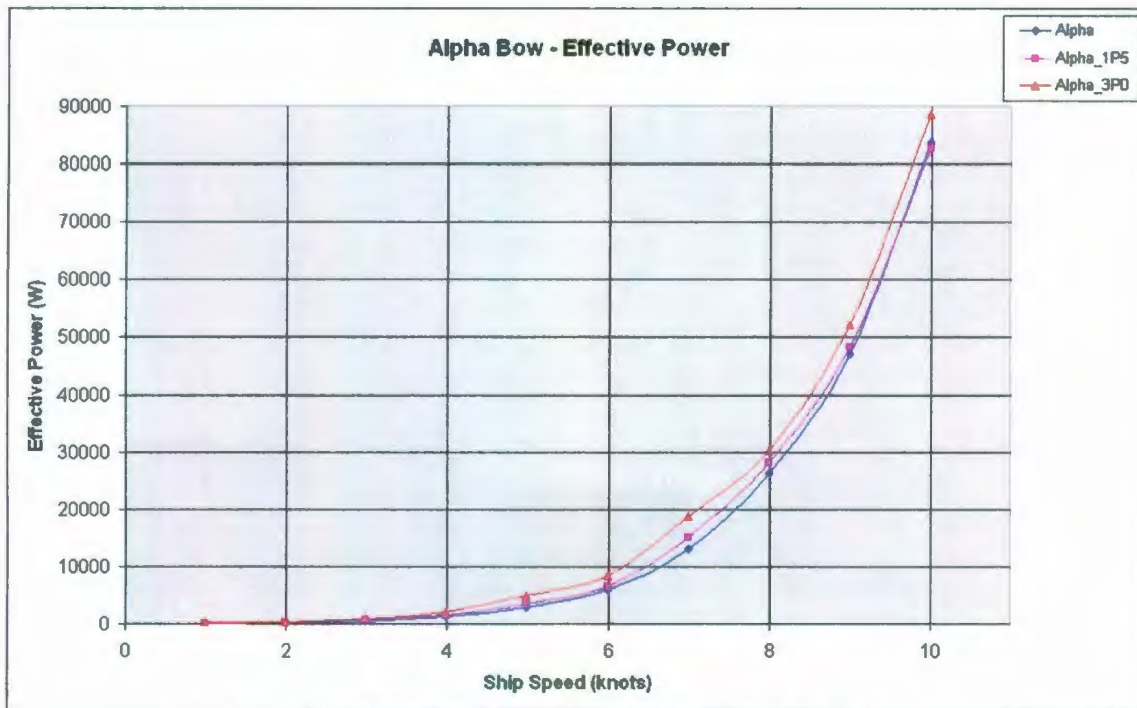


Figure 31: Effective Power with Alpha Bow (IOT Tests)

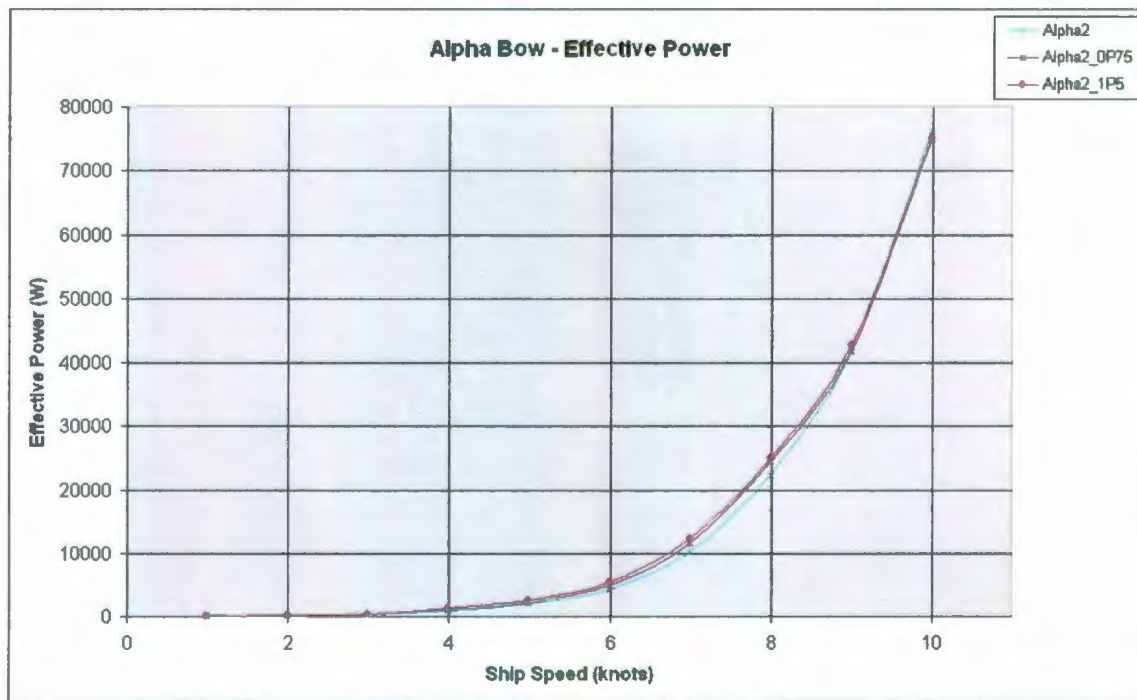


Figure 32: Effective Power with Alpha2 Bow (Retests at IOT)

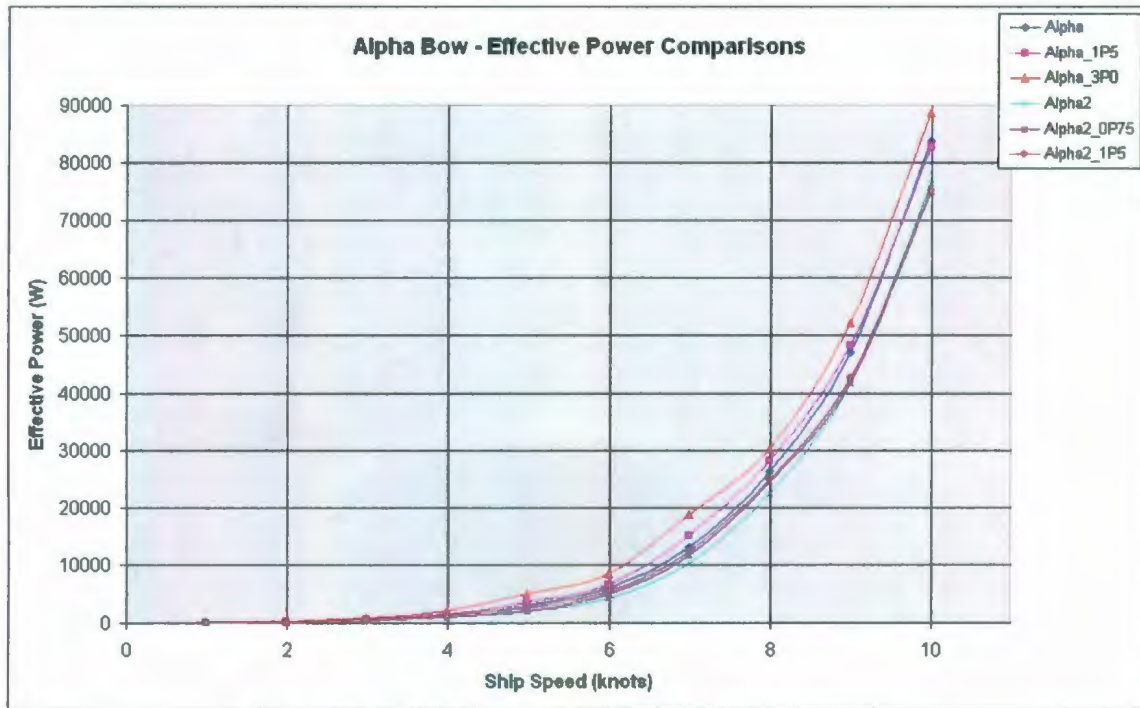


Figure 33: Comparison of both Alpha Bow Tests at IOT

From these three plots it can be seen that the effective power increases as the trim angle increases. This is to be expected as there is a larger area of transom submerged. This leads to a larger wake which in turn requires extra energy to pull along.

It can also be noted that the resistance, and hence effective power, starts to significantly increase at speeds of about 7 – 8 knots full scale. Therefore, significant amounts of extra power would be required to enable the boat to go an extra knot in calm water conditions.

The following figures are screen captures of video footage taken during the retests of Alpha bow. The pictures show the model for each of the trim conditions tested at a speed of 10 knots full scale. From these photos it can be seen that there is a large bow wave created regardless of the initial trim angle. It can also be seen that there is quite a bit of spray at the stem, which increases the overall resistance of the hull.



Figure 34: Alpha2 Bow Test at Level Trim – Speed of 10 knots



Figure 35: Alpha2 Bow Test at 0.75° by Stern Trim – Speed of 10 knots



Figure 36: Alpha2 Bow Test at 1.5° by Stern Trim – Speed of 10 knots

Tabular comparisons can also be made between the two sets of tests conducted on the conventional bow. The aim of the retests was to check if the resistance curve follows the same basic trend as the original tests when the model was misaligned. When the retests were completed it was shown that the resistance curve is slightly below that of the original tests, while following the same trend.

The following figure is a plot of the ‘difference’ between the ‘Alpha’ and ‘Alpha2’ effective power data at two different static trim conditions. From the plot it is observed that there is a general trend of increasing difference in required effective power between ‘Alpha’ and ‘Alpha2’ with speed. This is to be expected as when the model is misaligned the resistance is expected to increase more rapidly than if it is properly aligned as speed is increased. Also, the trend for both the level trim as well as the 1.5° by stern trim conditions are very similar; with the exception of a couple of points in the 1.5° by stern trim case.



Figure 37: Comparison of Alpha and Alpha2 Tests at Level Trim and 1.5° by Stern

The following two tables show the comparisons between ‘Alpha’ and ‘Alpha2’ for level trim and 1.5° by stern respectively. This numerically shows the trend of increasing difference of resistance between the two tests with increasing speed.

Table 9: Comparison of Alpha Bow Tests at Level Trim

Speed (knots)	Effective Power (W)		Difference
	Alpha	Alpha2	
3	499	401	98
4	1252	985	267
5	2831	2058	773
6	5807	4164	1642
7	13031	10201	2830
8	26274	22314	3960
9	47018	41631	5387
10	83649	76280	7370

Table 10: Comparison of Alpha Bow Tests at 1.5° by Stern Trim

Speed (knots)	Effective Power (W)		
	Alpha1P5	Alpha2_1P5	Difference
3	521	385	135
4	1342	1177	165
5	3362	2599	762
6	6526	5385	1141
7	15041	12242	2799
8	28039	24901	3138
9	48261	42639	5623
10	82622	75181	7441

The dynamic trim effects as well as the sinkage, or ‘squat’, of the hull into the water can also be compared for each of these tests. The following two figures show the dynamic trim and model sinkage comparisons of ‘Alpha’ and ‘Alpha2’ tests at both static level trim and 1.5° by the stern.

From the first plot it can be seen that the ‘Alpha’ tests tend to provide slightly less trim by the head than the ‘Alpha2’ tests throughout the speed range tested. The second plot shows that the ‘Alpha’ tests tend to provide slightly more sinkage than the ‘Alpha2’ tests throughout the speed range tested.

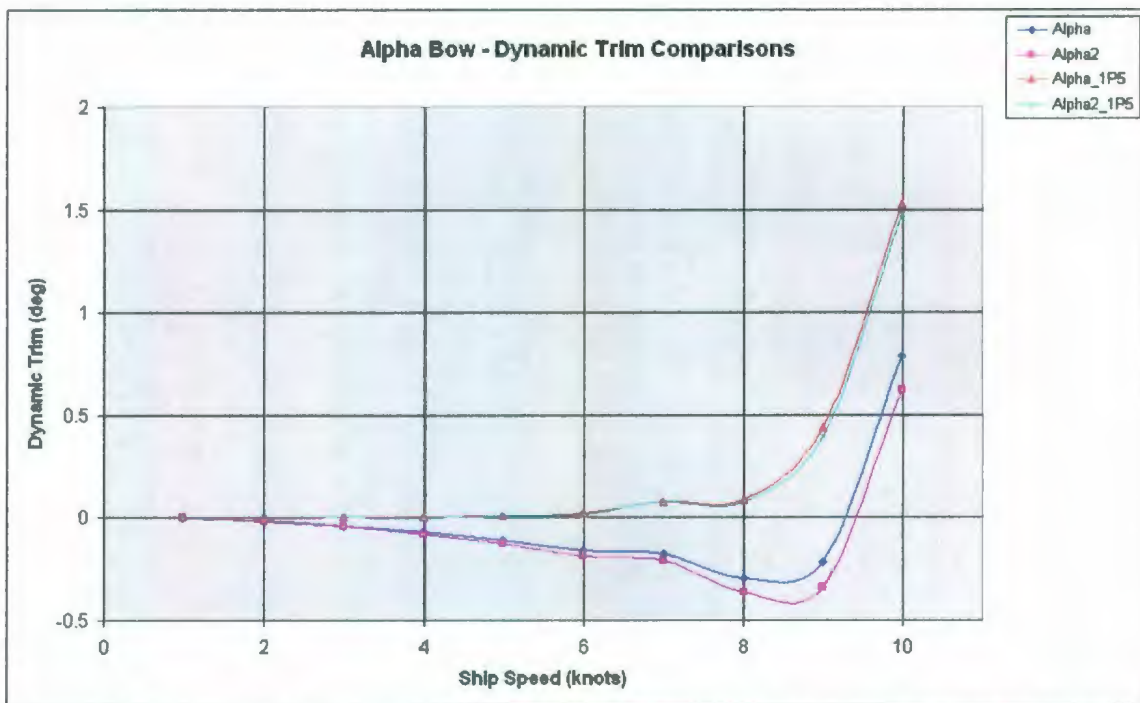


Figure 38: Dynamic Trim Comparison of Alpha and Alpha2 Tests at Level Trim and 1.5° by Stern

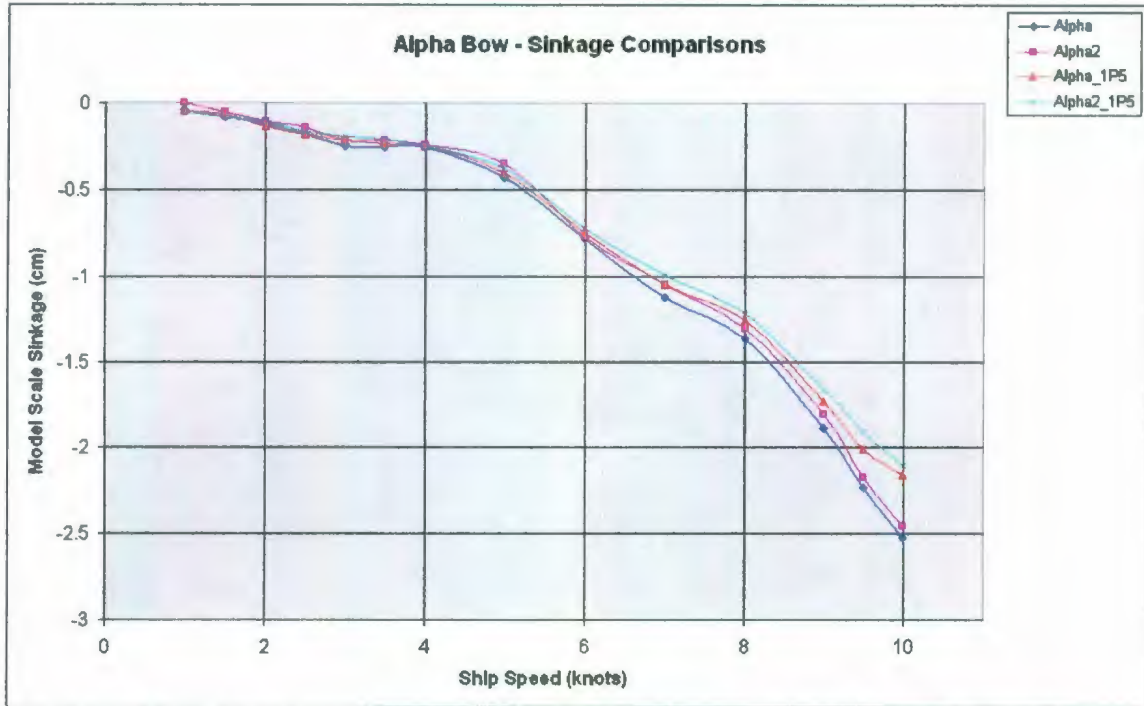


Figure 39: Sinkage Comparison of Alpha and Alpha2 Tests at Level Trim and 1.5° by Stern

It is useful to plot the dynamic trim and sinkage comparisons in terms of the difference between the 'Alpha' and 'Alpha2' tests. The following two figures show the difference between the dynamic trim and model sinkage data of 'Alpha' and 'Alpha2' tests at both static level trim and 1.5° by the stern.

The two plots show that there is an increasing difference in the dynamic trim as well as the model sinkage between 'Alpha' and 'Alpha2' with speed. This supports the conclusion drawn above, that is the model misalignment during the initial tests is likely responsible for the increasing differences in the measured data with increasing speed. However, it would be very difficult to actually pinpoint the actual mechanism causing the increasing differences between dynamic trim and sinkage with increasing speed.

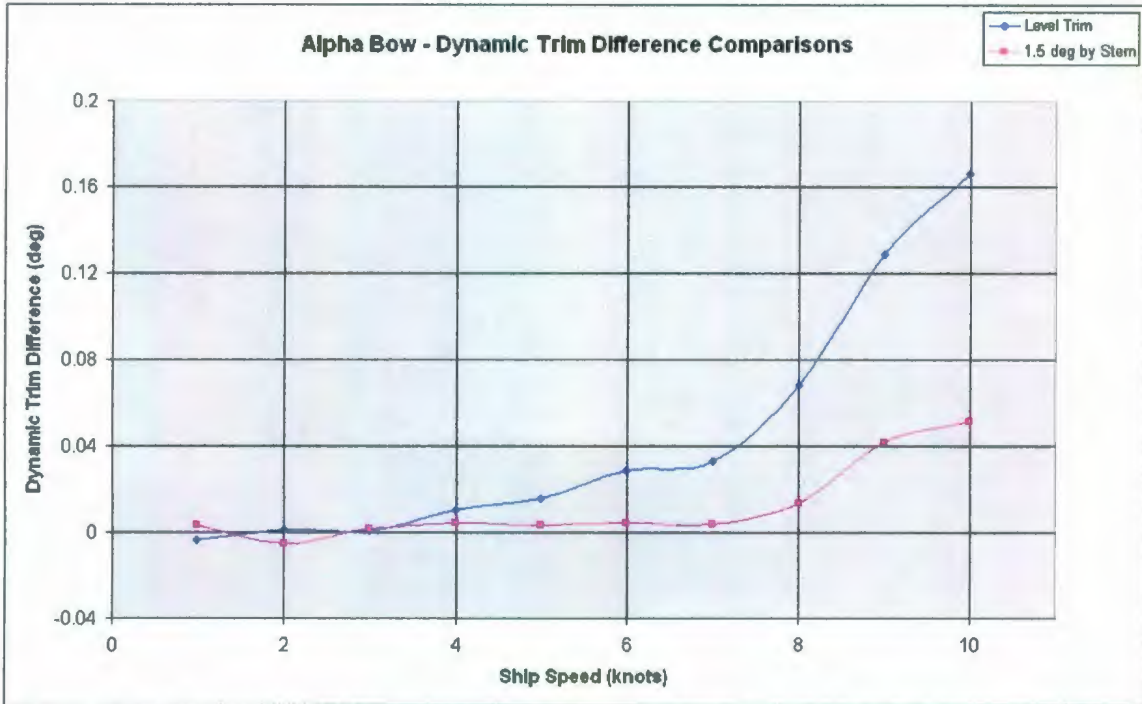


Figure 40: Difference Comparison of Dynamic Trim Data for Alpha and Alpha2 Tests at Level Trim and 1.5° by Stern

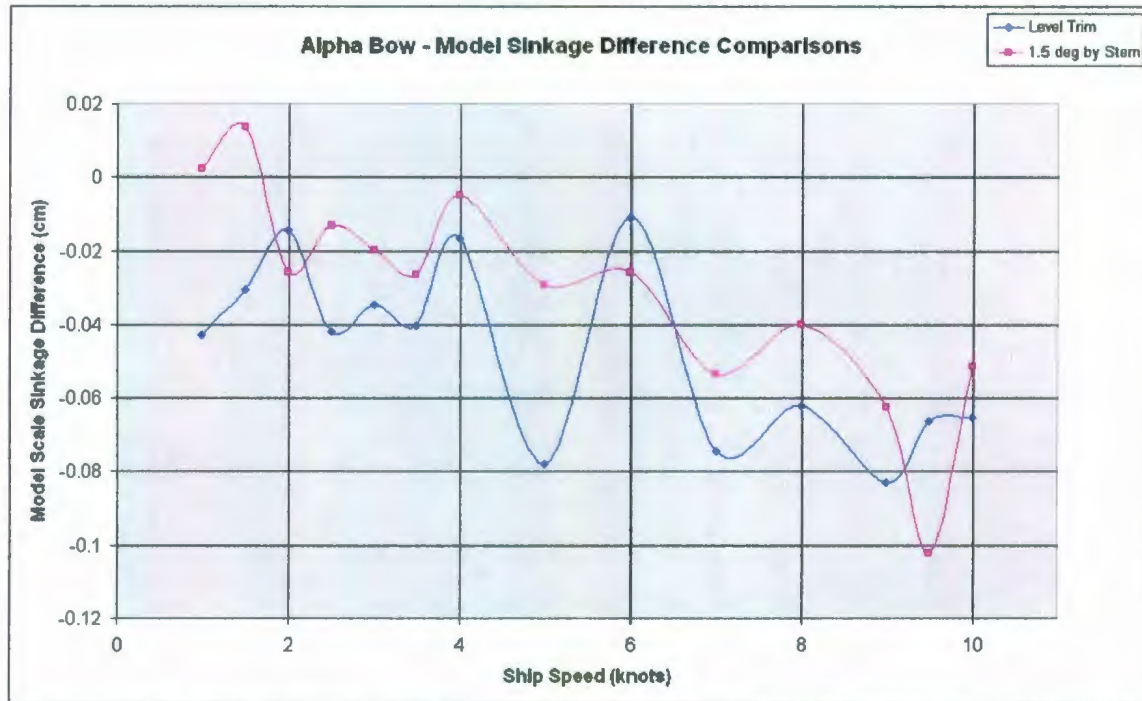


Figure 41: Difference Comparison of Sinkage Data for Alpha and Alpha2 Tests at Level Trim and 1.5° by Stern

5.8.2 Bulbous Bows

There are two purposes of a bulbous bow; one is to minimize the pitching motions of a vessel in seas and the second is to reduce the overall resistance of the vessel. Pitching minimization is analyzed by way of seakeeping tests in waves, using a soft-moored model for benchmarking a seakeeping simulation model, or the model remotely controlled in an offshore basin. For the purpose of this report only the resistance reduction are considered in detail. The results shown are in terms of full scale effective power for the bulbous bows as well.

The bulbous bow works by creating an additional wave just ahead of the bow wave created by the vessel. If this wave operates out of phase or partially out of phase from the bow wave then the two waves interfere such that the wave generated over the hull of the vessel is reduced. A bulbous bow increases the frictional resistance of a vessel; this generally leads to an overall increase of resistance at the lower speeds where wave making resistance is not as significant as frictional resistance. However, at higher speeds (i.e. $F_n = 0.24$ and higher), when the wave making resistance begins to have a significant impact on overall resistance the effects of the bulbous bow should begin to take effect.

Beta Bow

Table 11: Effective Power for Vessel with Beta Bow

Effective Power for Beta Bow (W)			
Speed (knots)	Level Trim	1.5° by Stern Trim	3.0° by Stern Trim
1	16	33	42
2	131	178	171
3	486	663	843
4	1322	1783	2035
5	2581	3632	4320
6	5098	6762	8695
7	9905	11553	15425
8	21694	21211	24548
9	41812	34735	39835
10	77034	61412	67510



Figure 42: Effective Power with Beta Bow

It is shown that the model at level trim performs better than trimmed by the stern up to about 8 knots when compared to 1.5° by stern, and up to about 9 knots when compared to 3.0° by stern. After this however, trimming the model by 1.5° reduces the required effective power significantly. For example, at 10 knots the required effective power is reduced by more than 12% by statically trimming the model 1.5° by the stern.

From the dynamic trim data it is known that the model is trimmed approximately 1.0° by the head at 10 knots for the static level trim condition. For the 1.5° by stern condition it is known that the model dynamically trims by the stern approximately 0.7°, for a total trim angle of about 2.2° by the stern. For the 3.0° by stern condition it is known that the model dynamically trims by the stern approximately 1.85°, for a total trim angle of about 4.85° by the stern. Based on this data it is known that the model will be at dynamic level trim at 10 knots full scale when the model is statically trimmed approximately 0.43° by the stern. It may therefore be interesting to go back and complete testing at this static trim condition for comparisons.

Gamma Bow

The model outfitted with Gamma bow was tested at 0°, 0.75° by stern, and 1.5° by stern trim levels. The trim condition of 3.0° by stern was taken out as results from testing on the other bows showed that the required effective power at this trim level is significantly larger than at level trim or at 1.5° by stern.

Table 12: Effective Power for Vessel with Gamma Bow

Effective Power for Gamma Bow (W)			
Speed (knots)	Level Trim	0.75° by Stern Trim	1.5° by Stern Trim
1	41	25	68
2	205	201	174
3	665	733	723
4	1605	2029	2073
5	3105	3997	4748
6	5234	6586	8441
7	9288	10765	12809
8	18236	18964	20152
9	35191	34229	34344
10	64981	62961	64012

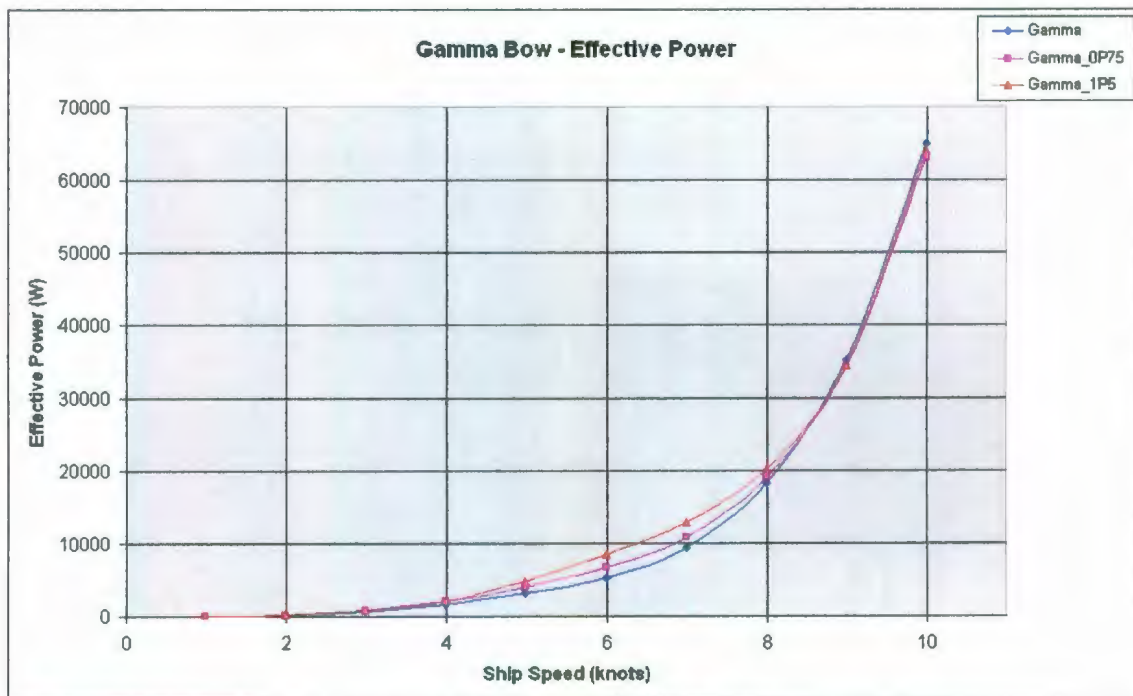


Figure 43: Effective Power with Gamma Bow

It can be seen that the effect of trimming the model is much less significant than was the case for Beta and Epsilon bows. Above 9 knots there is no significant difference in required effective power with changing static trim angle. Below this point the required effective power is significantly higher for the model trimmed 1.5° by the stern.

Video footage was taken for the Gamma bulbous bow also. The following series of pictures show the model with Gamma bow attached at 0° , 0.75° , and 1.5° by stern trim angles while traveling at the full scale speed of 10 knots.

From this footage it can be seen that as the trim angle increases there is less water spray off to the sides at the bow. However, there still is some water spray at 0.75° trim, and at 1.5° there looks as if there is a secondary wave spray created in the area where the bulb intersects with the bow. This may provide one explanation as to why the increasing trim angle by the stern is not reducing the effective power to the extent that was seen with Beta and Epsilon bows.

From the dynamic trim data it is known that the model is trimmed approximately 0.48° by the stern at 10 knots for the static level trim condition. For the 0.75° by stern condition it is known that the model dynamically trims by the stern approximately 0.92° , for a total trim angle of about 1.67° by the stern. For the 3.0° by stern condition it is known that the model dynamically trims by the stern approximately 1.33° , for a total trim angle of about 2.83° by the stern. Based on this data it is known that the model will be at dynamic level trim at 10 knots full scale when the model is statically trimmed approximately 0.3° by the head. It may therefore be interesting to go back and complete testing at this static trim condition for comparisons.



Figure 44: Gamma Bow Test at Level Trim – Speed of 10 knots



Figure 45: Gamma Bow Test at 0.75° by Stern – Speed of 10 knots



Figure 46: Gamma Bow Test at 1.5° by Stern – Speed of 10 knots

Epsilon Bow

For this bow a fourth trim condition (0.75° by stern) was added. This was done because results from testing on the first two bows showed that the required effective power at 3.0° by stern is significantly larger than at level trim or at 1.5° by stern. Also, it was found that the model was not trimming by the head as much as originally estimated.

Table 13 Effective Power for Vessel with Epsilon Bow

Effective Power for Epsilon Bow (W)				
Speed (knots)	Level Trim	0.75° by Stern Trim	1.5° by Stern Trim	3.0° by Stern Trim
1	49	25	20	23
2	209	152	122	194
3	586	606	506	713
4	1480	1682	1666	1998
5	2915	3687	3907	4328
6	4357	5945	6861	8485
7	8560	9635	10879	14645
8	19181	19056	19425	24378
9	37225	34426	33018	38255
10	68828	64235	63293	69675

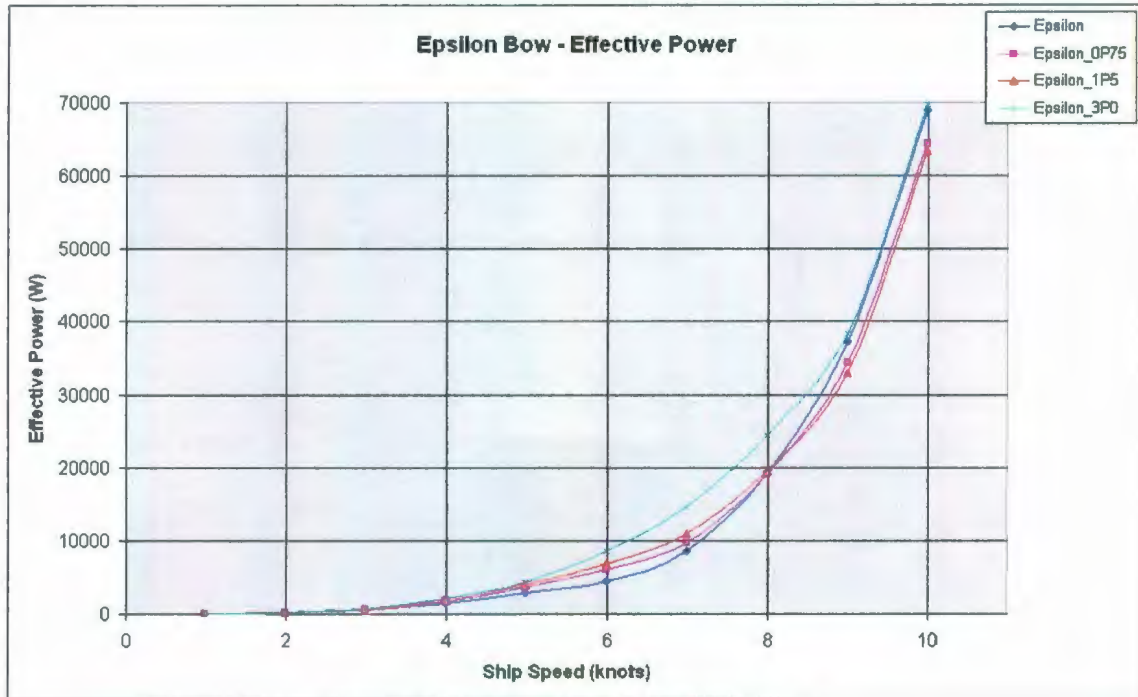


Figure 47: Effective Power with Epsilon Bow

The first observation to be clearly made is that the model trimmed 3.0° gives a higher required effective power than level trim right up to 10 knots. Also, at almost exactly 8 knots both 0.75° and 1.5° start to become more efficient than level trim. The other obvious observation to make is that there is very little difference in required effective power between 0.75° and 1.5° trim levels.

The following series of pictures show the model with Epsilon bow attached at 0° , 0.75° , 1.5° , and 3.0° by stern trim angles while traveling at the full scale speed of 10 knots. From the following figures it can be seen that there is a significant reduction in water spray off the bow with increasing trim by the stern. It can also be seen that the flow of water across the hull is much smoother with increasing trim angle.

At the trim condition of 3.0° it is shown that the front of the bulb is sticking out of the water. This is one possible explanation for the fact that the effective power at the condition is higher than at the level trim condition.

From the dynamic trim data it is known that the model is trimmed approximately 0.2° by the head at 10 knots for the static level trim condition. For the 0.75° by stern condition it is known that the model dynamically trims by the stern approximately 0.53° , for a total trim angle of about 1.28° by the stern. For the 1.5° by stern condition it is known that the model dynamically trims by the stern approximately 1.14° , for a total trim angle of about 2.64° by the stern. For the 3.0° by stern condition it is known that the model dynamically trims by the stern approximately 2.02° , for a total trim angle of about 5.02° by the stern. Based on this data it is known that the model will be at dynamic level trim at 10 knots full scale when the model is statically trimmed approximately 0.1° by the stern. Again, it may be interesting to go back and complete testing at this static trim condition for comparisons.



Figure 48: Epsilon Bow Test at Level Trim – Speed of 10 knots



Figure 49: Epsilon Bow Test at 0.75° by Stern – Speed of 10 knots



Figure 50: Epsilon Bow Test at 1.5° by Stern – Speed of 10 knots

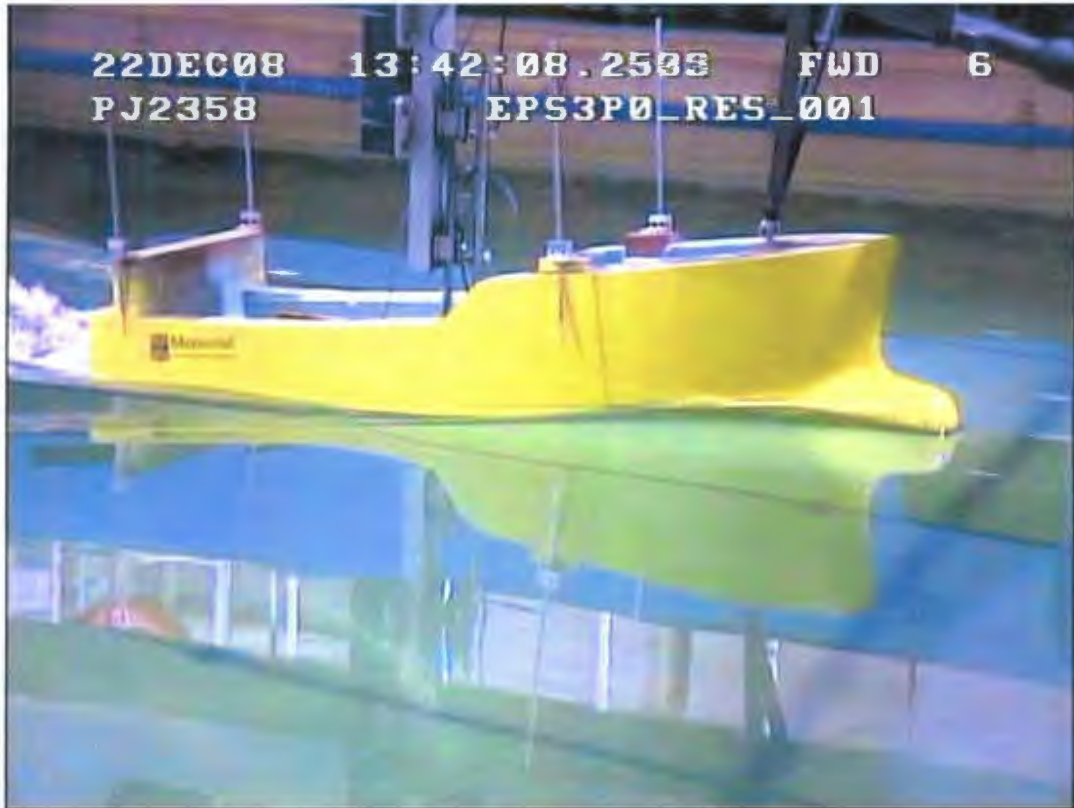


Figure 51: Epsilon Bow Test at 3.0° by Stern – Speed of 10 knots

5.8.3 Bow Comparisons

The following sections show plots of the effective power for all of the bows tested at each of the four trim angles. A few things to note here; firstly not all bows were tested at both 0.75° and 3.0° by stern trim conditions. The results for ‘Alpha’ are not reliable as they are the results from the tests when the model was misaligned. Hence, they are not included in these comparisons. Lastly, all comparisons are made with the conventional bow at the static level trim condition since this is the best operating condition for it over the full speed range.

Trim Condition – Level Trim



Figure 52: Effective Power Comparison at Level Trim

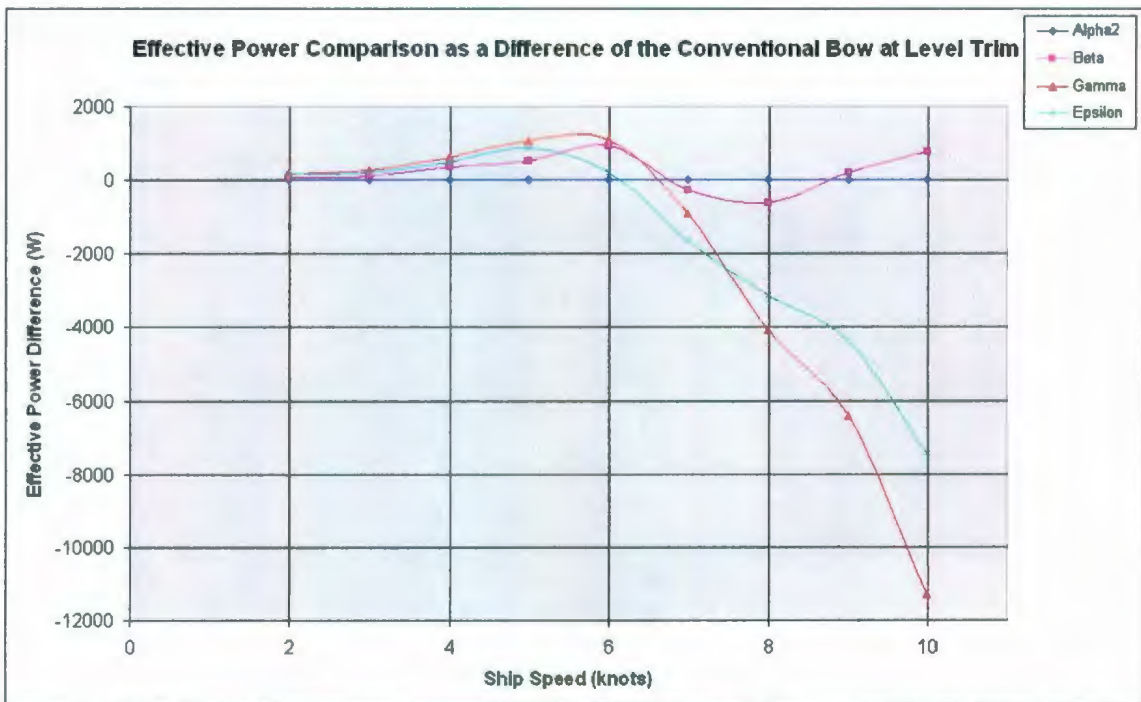


Figure 53: Effective Power Comparison as the Difference from the Conventional Bow at Level Trim

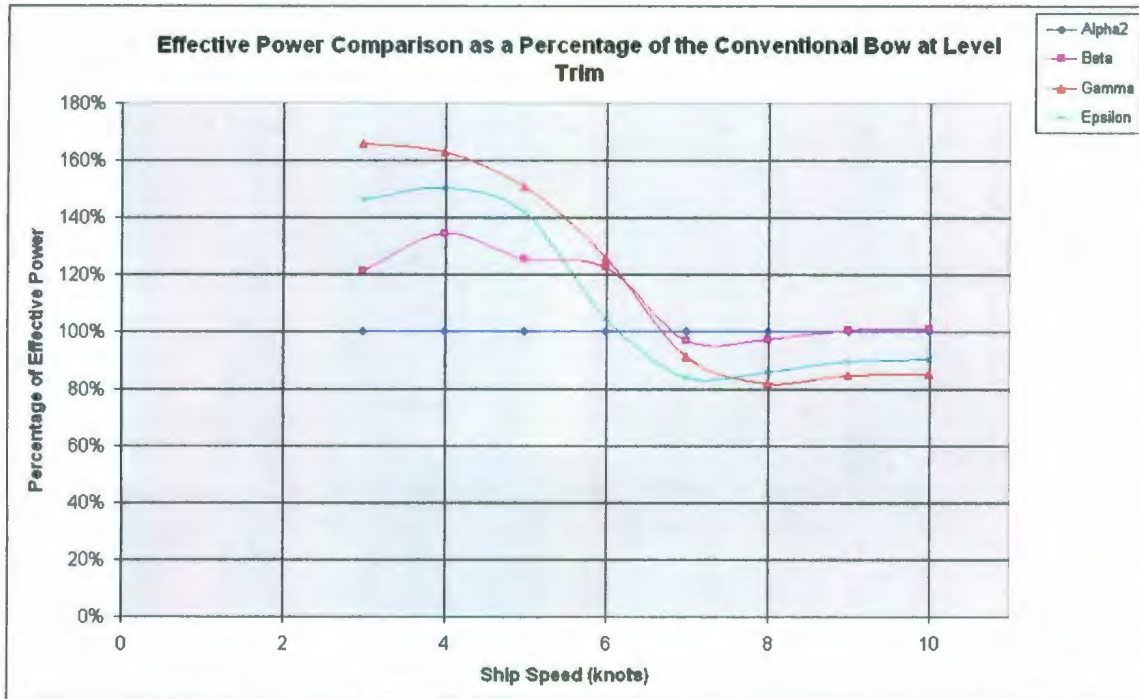


Figure 54: Effective Power Comparison as a Percentage of the Conventional Bow at Level Trim

Table 14: Effective Power Comparison as a Percentage of the Conventional Bow at Level Trim

Percentage of Conventional Bow at Level Trim (%)				
Speed (knots)	Alpha2	Beta	Gamma	Epsilon
3	100.00	121.37	165.93	146.34
4	100.00	134.29	163.04	150.29
5	100.00	125.39	150.85	141.65
6	100.00	122.42	125.69	104.63
7	100.00	97.10	91.05	83.91
8	100.00	97.22	81.72	85.96
9	100.00	100.43	84.53	89.42
10	100.00	100.99	85.19	90.23

The above three plots show that the bulbous bows begin to outperform the conventional bow between approximately 6 – 7 knots ($F_n = 0.27 - 0.32$). This is consistent with what was found in basically all of the experimental papers discussed in the literature review. It is also consistent with what is provided in *Principles of Naval Architecture* (1988).

It can be seen that Epsilon bow begins to outperform the conventional bow at slightly above 6 knots. Gamma bow begins to outperform Alpha bow just shy of 7 knots, and begins to outperform Epsilon bow at approximately 7.5 knots. Beta bow performs slightly better than the conventional bow in the region between about 7 – 9 knots.

So in the design operating range of 8 – 10 knots ($F_n = 0.36 - 0.45$), it is shown that Epsilon bow provides a decrease in required effective power of roughly 10%. Gamma bow performs a little better than this, reducing the required effective power 15 – 20% in the same speed range. Beta bow does not perform as well; reducing the required effective power by approximately 3.8% at 8 knots but increasing it by 0.5% and 1% at 9 and 10 knots respectively.

The papers outlined in the experimental section of the literature review list decreases in required effective power anywhere between 5 – 35%. The numbers listed for the studies included in the literature review are for different hull forms and different bulbous bow designs. However, it is reasonable to conclude that the numbers found for reductions in required effective power for this hull form with bulbous bows are in the same range as those found for most of the hulls of studies included in the literature review.

Trim Condition – 0.75° by Stern



Figure 55: Effective Power Comparison at 0.75° by Stern Trim

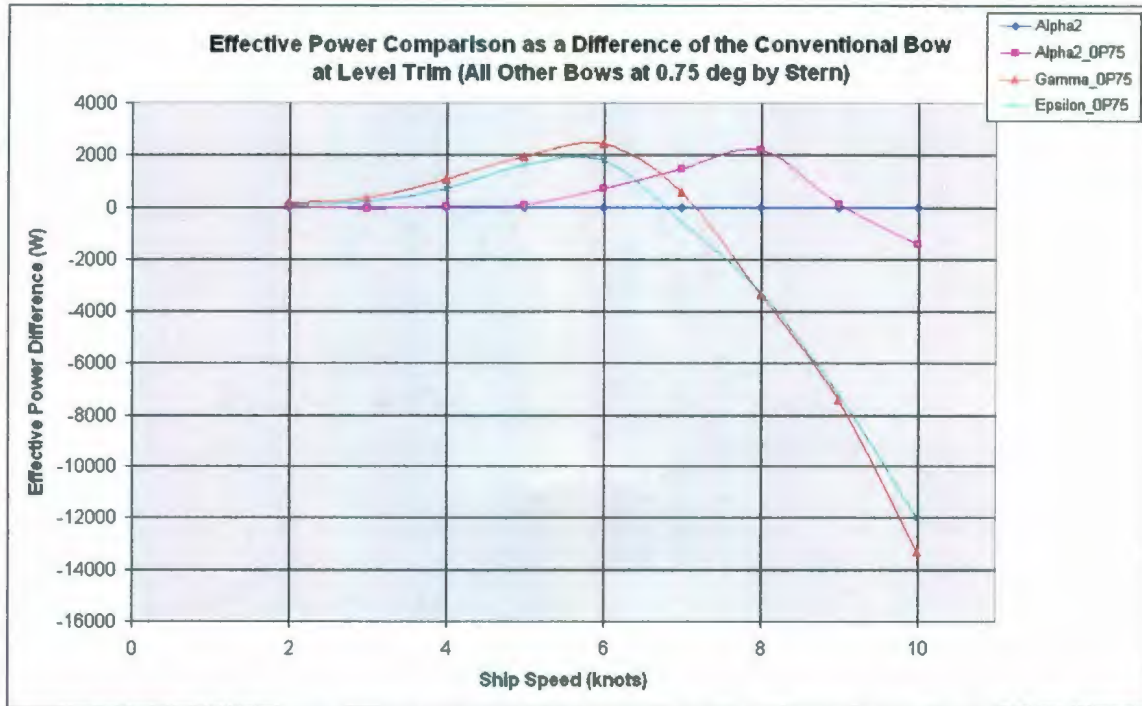


Figure 56: Effective Power Comparison as the Difference from the Conventional Bow at Level Trim (All Other Bows at 0.75° by Stern)

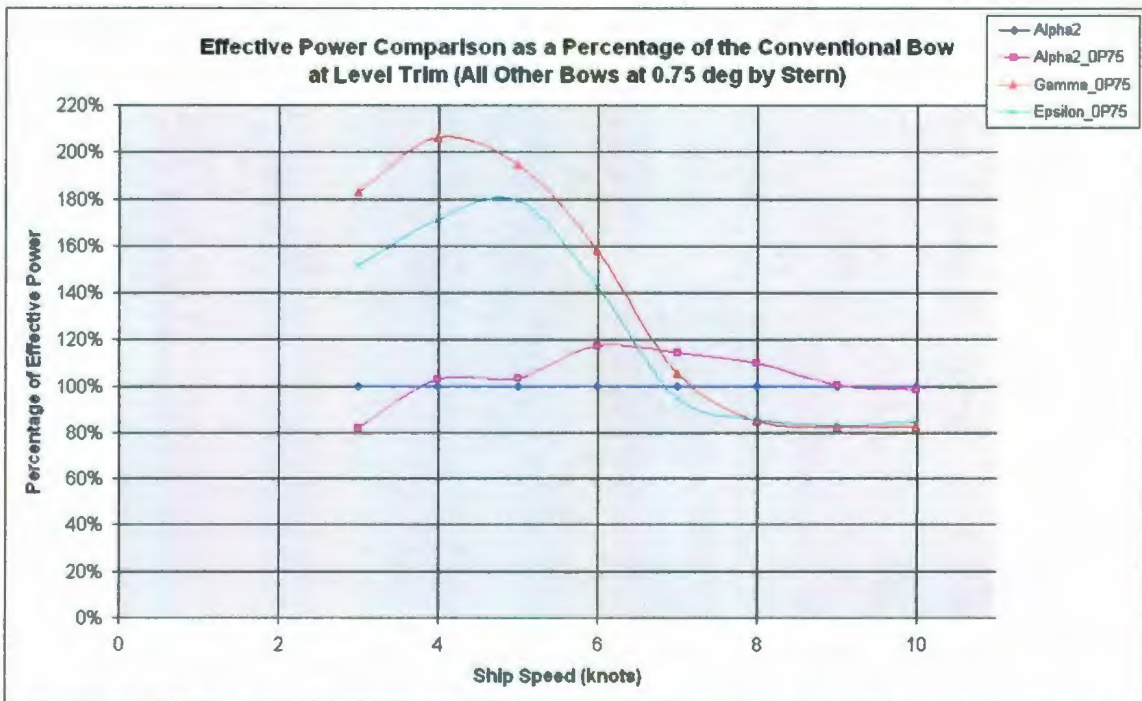


Figure 57: Effective Power Comparison as a Percentage of the Conventional Bow at Level Trim (All Other Bows at 0.75° by Stern)

Table 15: Effective Power Comparison as a Percentage of the Conventional Bow at Level Trim (All Other Bows at 0.75° by Stern)

Percentage of Conventional Bow at Level Trim (%)				
Speed (knots)	Alpha2	Alpha2_0P75	Gamma_0P75	Epsilon_0P75
3	100.00	82.07	182.94	151.39
4	100.00	102.64	206.12	170.88
5	100.00	103.35	194.19	179.17
6	100.00	117.31	158.14	142.75
7	100.00	114.24	105.53	94.45
8	100.00	109.74	84.99	85.40
9	100.00	100.24	82.22	82.69
10	100.00	98.12	82.54	84.21

For this trim condition it can be seen that both Gamma and Epsilon bows begin to outperform the conventional bow at roughly 7 knots. It can be seen that for both bulbous bows a reduction in required effective power of almost 20% throughout the design speed range. At 10 knots there is a decrease of effective power of 12 kW for Epsilon bow and roughly 13.5 kW for Gamma bow.

Trim Condition – 1.5° by Stern

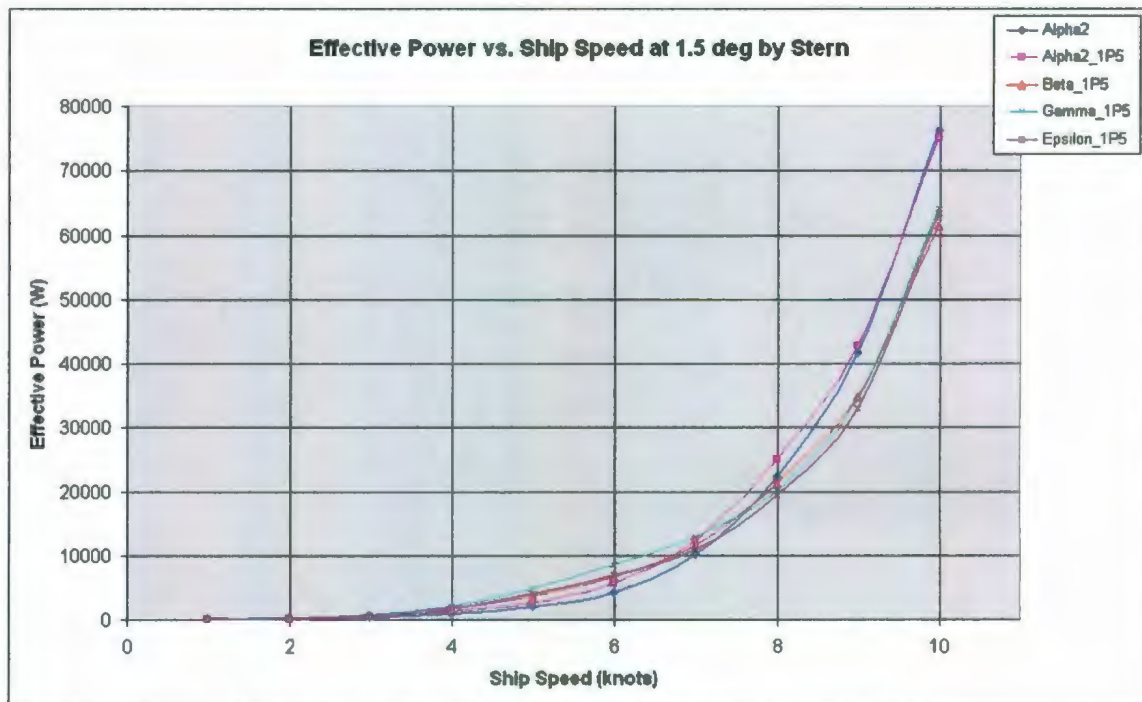


Figure 58: Effective Power Comparison at 1.5° by Stern Trim



Figure 59: Effective Power Comparison as the Difference from the Conventional Bow at Level Trim (All Other Bows at 1.5° by Stern)



Figure 60: Effective Power Comparison as a Percentage of the Conventional Bow at Level Trim (All Other Bows at 1.5° by Stern)

Table 16: Effective Power Comparison as a Percentage of the Conventional Bow at Level Trim (All Other Bows at 1.5° by Stern)

Percentage of Conventional Bow at Level Trim (%)					
Speed (knots)	Alpha2	Alpha2_1P5	Beta_1P5	Gamma_1P5	Epsilon_1P5
3	100.00	96.14	165.49	180.53	126.39
4	100.00	119.58	181.10	210.55	169.23
5	100.00	126.29	176.45	230.67	189.82
6	100.00	134.01	162.38	202.70	164.76
7	100.00	120.01	113.26	125.57	106.65
8	100.00	111.59	95.05	90.31	87.05
9	100.00	102.42	83.44	82.50	79.31
10	100.00	98.56	80.51	83.92	82.97

It can be seen that Epsilon bow performs the best at this trim condition. It begins to outperform the conventional bow just after 7 knots. Beta and Gamma bow perform roughly the same in this condition, both giving similar reductions of required effective power in the 8 – 10 knot range. At 10 knots Beta provides a reduction of effective power of roughly 15 kW, Epsilon almost 13 kW, and Gamma more than 12 kW.

Trim Condition – 3.0° by Stern

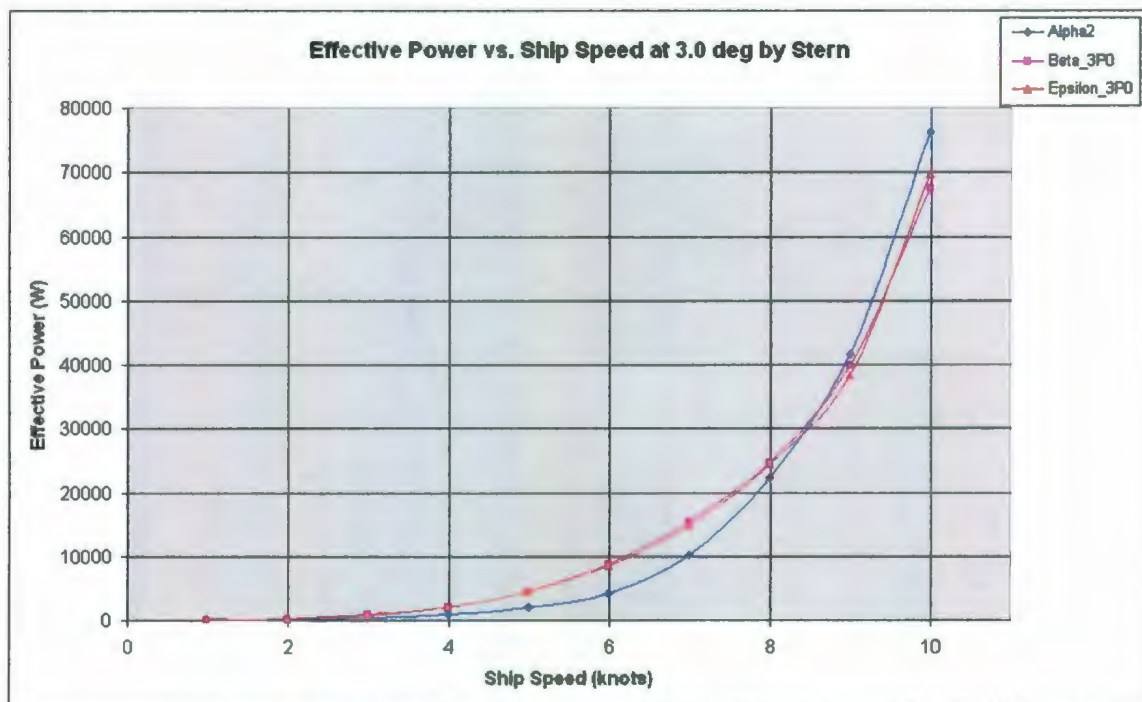


Figure 61: Effective Power Comparison at 3.0° by Stern Trim

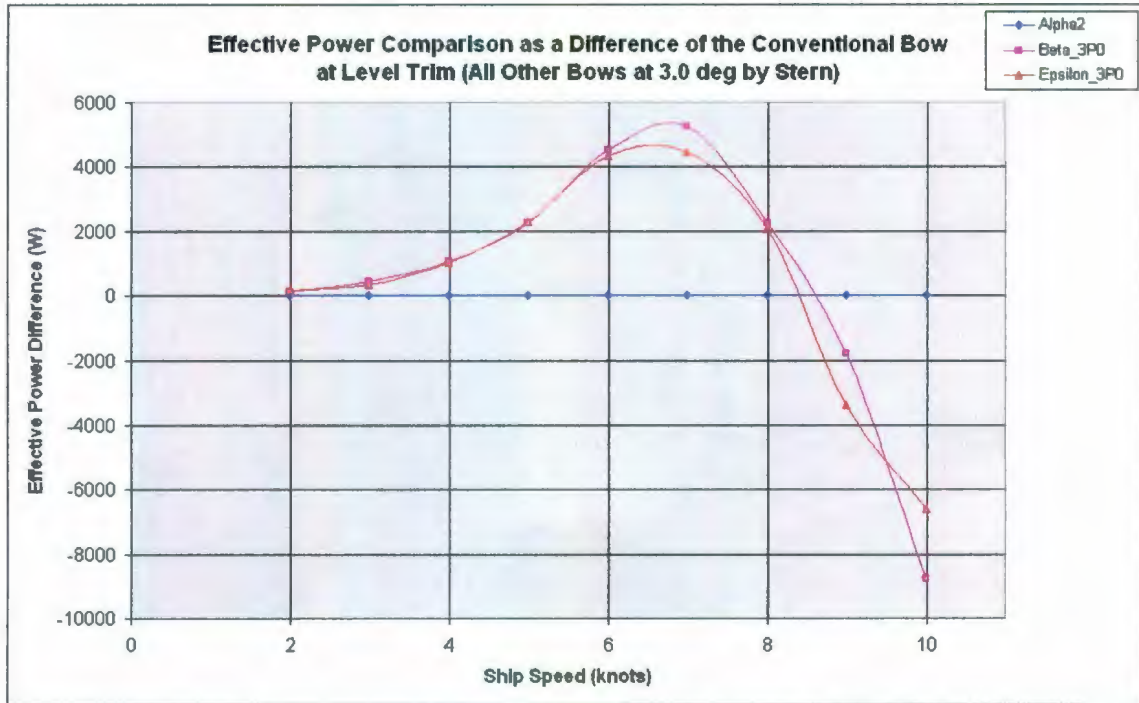


Figure 62: Effective Power Comparison as a Difference of the Conventional Bow at Level Trim (All Other Bows at 3.0° by Stern)

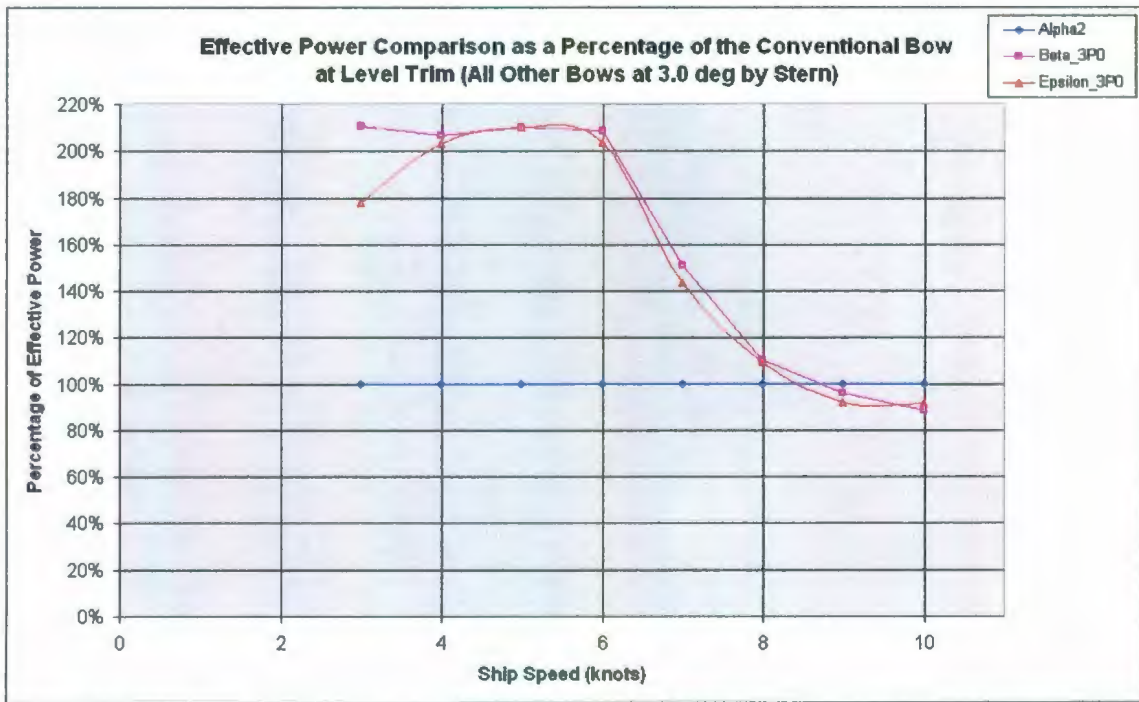


Figure 63: Effective Power Comparison as a Percentage of the Conventional Bow at Level Trim (All Other Bows at 3.0° by Stern)

Table 17: Effective Power Comparison as a Percentage of the Conventional Bow at Level Trim (All Other Bows at 3.0° by Stern)

Percentage of Conventional Bow at Level Trim (%)			
Speed (knots)	Alpha2	Beta_3P0	Epsilon_3P0
3	100.00	210.40	177.90
4	100.00	206.74	202.97
5	100.00	209.88	210.27
6	100.00	208.80	203.75
7	100.00	151.21	143.57
8	100.00	110.01	109.25
9	100.00	95.68	91.89
10	100.00	88.50	91.34

It can be seen that at this trim condition the bulbous bows do not perform as well as at the lower trim conditions tested. It can be seen that both Beta and Epsilon bows do not begin to outperform the conventional bow until roughly 8.5 knots. Between 9 – 10 knots Beta provides a reduction of required effective power of roughly 5 – 10%. Epsilon provides a reduction of about 10% through this range.

At 10 knots Beta provides a reduction of nearly 9 kW effective power and Epsilon provides only about 6.5 kW.

Optimal Trim Conditions

It is also useful to determine the optimal initial trim condition for each bow at each speed tested. The following table outlines the best trim condition for each of the bows tested. Again note here that for Alpha bow the retest data are provided.

Table 18: Optimal Trim Conditions for Each Bow

Optimal Trim Condition				
Speed (knots)	Alpha2	Beta	Gamma	Epsilon
2	level trim	level trim	0.75° by stern	1.5° by stern
3	0.75° by stern	level trim	level trim	1.5° by stern
4	level trim	level trim	level trim	level trim
5	level trim	level trim	level trim	level trim
6	level trim	level trim	level trim	level trim
7	level trim	level trim	level trim	level trim
8	level trim	1.5° by stern	level trim	0.75° by stern
9	level trim	1.5° by stern	0.75° by stern	1.5° by stern
10	0.75° by stern	1.5° by stern	0.75° by stern	1.5° by stern

So, in general it is shown that at lower speeds it is better to operate the vessel at static level trim. However, when we get into the design speed range of 8 – 10 knots it is generally better to have the vessel trimmed by the stern from a resistance point of view.

The following figure and table provide a percentage comparison of the optimal effective power for each bow to the conventional bow at level trim.



Figure 64: Effective Power Comparison at Optimal Trim Conditions as a Percentage of the Conventional Bow at Level Trim

Table 19: Effective Power Comparison at Optimal Trim Conditions as a Percentage of the Conventional Bow at Level Trim

Speed (knots)	Percentage of Conventional Bow at Level Trim (%)				
	Alpha2 Level Trim	Alpha2 Optimal Trim	Beta Optimal Trim	Gamma Optimal Trim	Epsilon Optimal Trim
3	100.00	82.07	121.37	165.93	126.39
4	100.00	100.00	134.29	163.04	150.29
5	100.00	100.00	125.39	150.85	141.65
6	100.00	100.00	122.42	125.69	104.63
7	100.00	100.00	97.10	91.05	83.91
8	100.00	100.00	95.05	81.72	85.40
9	100.00	100.00	83.44	82.22	79.31
10	100.00	98.12	80.51	82.54	82.97

It can be seen from this that all three bulbous bows begin to outperform the conventional bow around the 7 knot mark. Also, in the design speed range of 8 – 10 knots Gamma and Epsilon bows tend to perform the best; providing a 15 – 20% reduction in required effective power.

5.8.4 Dynamic Trim Results

The following four figures show comparisons of the model dynamic trim for each bow at each static trim condition tested. Two things should be noted here; firstly note that the static trim condition is not actually shown in each plot, that is each plot starts at zero degrees. Secondly, note that negative values signify the model trimming by the head and positive trimming by the stern.

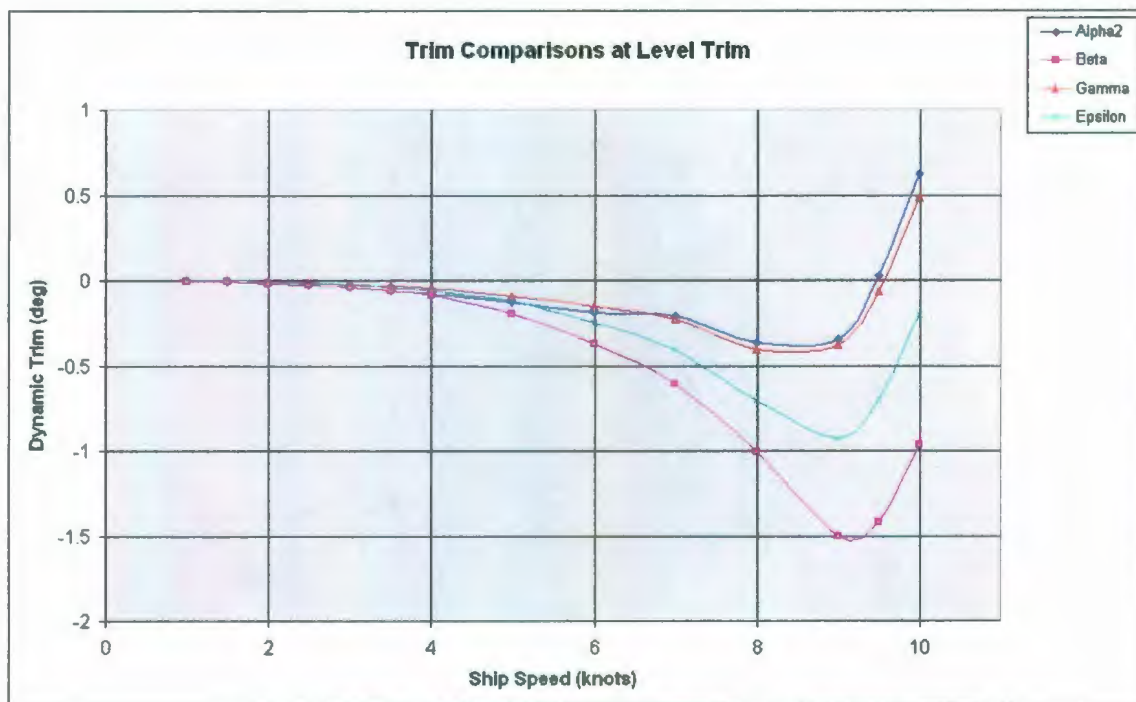


Figure 65: Dynamic Trim Comparison at Static Level Trim

From the above figure it can be seen that all bows have a tendency to trim by the head up to about 8.5 – 9 knots ($F_n = 0.38 - 0.41$) and then drastically begin to trim more and more by the stern with increasing speed. This is consistent with the studies conducted by Johnson (1958) and Friis et al. (2008). In the study by Johnson it was found that the

model would trim by the head up to $F_n = 0.35 - 0.37$ while Friis et al. found that the model would trim by the head up to $F_n = 0.36 - 0.43$.

Beta and Epsilon have a maximum around 9 knots. Alpha2 and Gamma have a maximum at a slightly lower point, between 8 – 9 knots. It can also be noted that Beta and Epsilon have a much larger magnitude of dynamic trim than Gamma bow.

Note here that Beta has the largest top bulb area as well as largest amount of bulb submergence, Epsilon the next largest, and Gamma the smallest. ‘Top bulb area’ is the extra waterplane area added due to the presence of each bulb respectively. ‘Bulb submergence’ is taken as the added underwater volume due to the presence of each bulb respectively. This is calculated by determining the underwater volume with each bulb attached and subtracting the underwater volume with the conventional bow attached. This will then yield only the underwater volume of each bulb respectively.

These results along with previous testing by Johnson (1958) and Friis et al. (2008) indicate that dynamic trim by the head is likely a function of bulb submergence, top bulb area, and pressure distribution around the stern section. The possible explanations are given below:

- The presence of a bulb at the stem causes an increase in water velocity around the fore body of the model (i.e. the water has to speed up to get around the added volume of the bulb). The increase in water velocity results in a reduction of pressure in the area around the bow of the model. This reduction of pressure then translates into a reduction in ‘lift’ at the bow section, which means that the bow section tends to trim further into the water.
- The presence of a bulb at the stem causes a beaching effect with increasing speed, where water flows up onto the top of the bulb. The flowing water over the top of the bulb then provides a downward force on the bulb, thereby forcing the bulb further down into the water.

- The flow past the hull causes an area of high velocity at the stern due to the streamlines closing in; which in turn reduces the pressure at the stern. As hull speed is increased the magnitude of this low pressure is increased, thereby causing even lower pressure at the stern section. This results in 'suction' at the stern section which tends to pull the stern section of the hull further into the water.

Therefore, the dynamic trim is determined by the balance of the pressure drops at the bow and the stern. When the pressure drop at the bow plus the build up of water on the bulb exceeds the suction force at the stern the hull tends to trim dynamically by the head. When the speed gets high enough the suction at the stern will tend to dominate and the hull will trim dynamically by the stern.

In order to determine the extent of each of the above phenomena on the dynamic trim characteristics of this model it would be possible to perform further resistance tests with pressure sensors placed around the bow and stern sections. This would then provide details of how the pressure distributions over the bow and stern are changing with increasing speed as well as different initial trim conditions; and how these pressures affect the dynamic trim of the model.

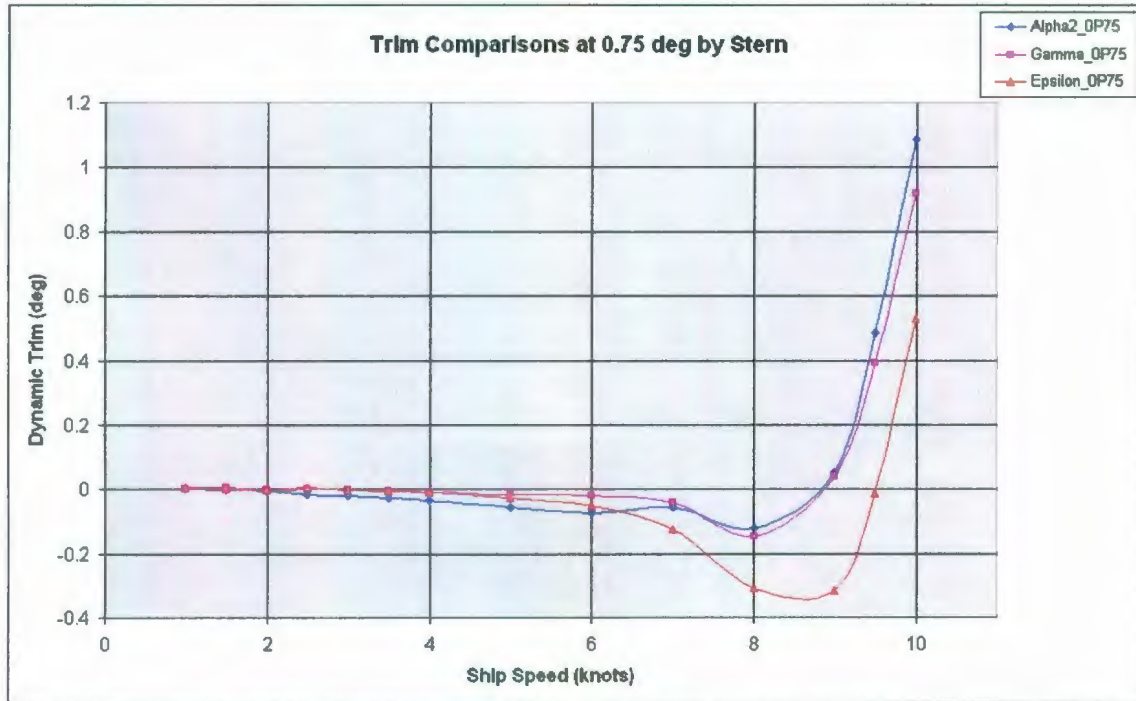


Figure 66: Dynamic Trim Comparison at 0.75° by Stern Trim

Here a similar trend for 0.75° by the stern as was seen in the level trim condition can be seen. Epsilon bow provides a much larger trim by the head than does Gamma bow, although it is a much smaller magnitude than was seen in the static level trim condition.

The lower magnitude of dynamic trimming by the head is likely attributed to less bulb submergence. In fact, the following two figures agree with this trend of less and less trim by the head around the 8 – 9 knot speed range. At 3.0° by stern static trim condition it can be seen that there is no dynamic trim by the head for any of the bows tested. For the 1.5° by stern case only Beta provides any trim by the head.

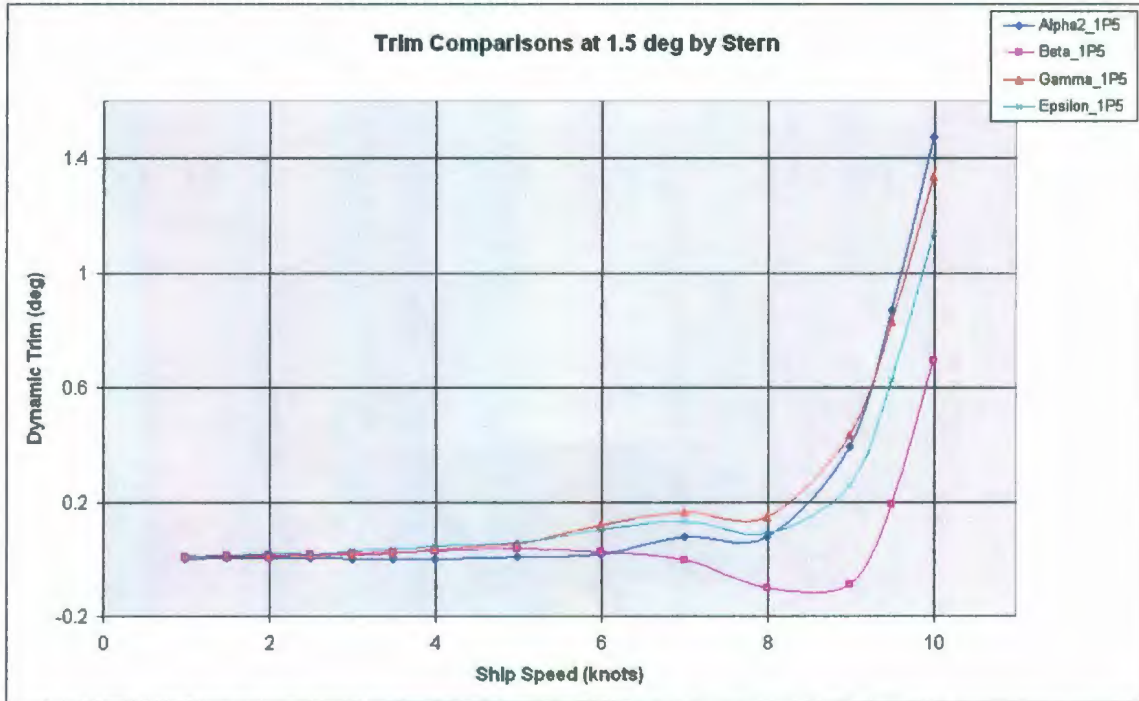


Figure 67: Dynamic Trim Comparison at 1.5° by Stern Trim



Figure 68: Dynamic Trim Comparison at 3.0° by Stern Trim

5.8.5 Sinkage Results

The 'squat' effect is a hydrodynamic phenomenon which occurs when a hull is moving through a fluid. An area of low pressure is created under the hull which then causes the hull to sink, or 'squat', down into the water. This is known to be due to a reduction in buoyancy caused by a downward hydrodynamic force created by flow-induced pressures.

The following four figures show comparisons of the model sinkage for each bow at each static trim condition tested. Note that negative values signify the model squatting down at speed. Also note there that model sinkage is measured at the tow point.

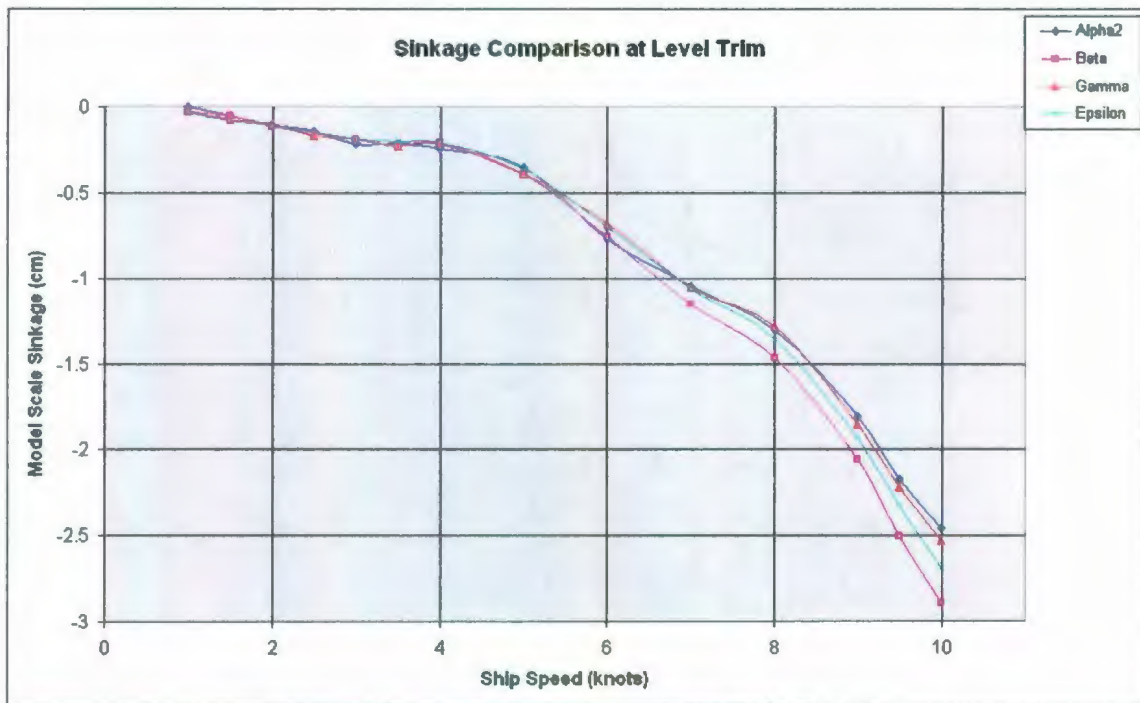


Figure 69: Sinkage Comparison at Static Level Trim

From the above figure it can be seen that all bows tend to sink, or 'squat', down at an increasing rate with increasing speed. It can also be shown that the top bulb area seems to have an influence on the magnitude of sinkage. Beta bow tends to sink more than either other bow from 7 knots and above. Epsilon generally has the second largest model sinkage while Gamma has the smallest model sinkage out of the bulbs tested. Again, note here that Beta has the largest amount of bulb submergence as well as top bulb area, Epsilon the next largest, and Gamma the smallest.

Similarly to the conclusions from the dynamic trim results, these results along with previous testing by Johnson (1958) and Friis et al. (2008) indicate that model sinkage is likely a function of bulb submergence, top bulb area, and the pressure distribution around the stern section.

In order to determine the extent of each of the above phenomena on the sinkage characteristics of this model it would be necessary to perform further resistance tests with pressure sensors placed around the bow and stern sections. This would provide details of how the pressure distributions over the bow and stern change with increasing speed as well as different initial trim conditions; and how these pressures affect the model sinkage.



Figure 70: Sinkage Comparison at 0.75° by Stern Trim

Here it is shown again that both bulbous bows result in a larger model sinkage than the conventional bow. Also, in the design speed range it is found that Epsilon bow sinks slightly more than Gamma bow, which has a smaller bulb submergence and top bulb area.

For the two trim conditions shown below, 1.5° by stern and 3.0° by stern, it can be seen that the same general trend continues as for the previous two cases.

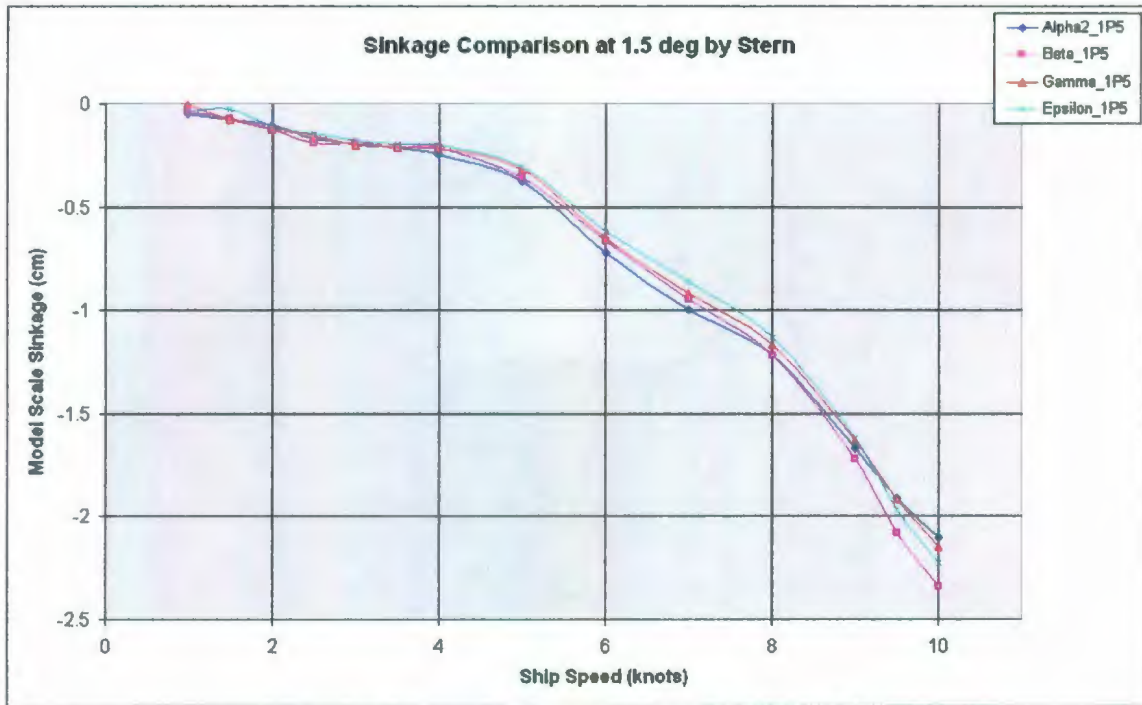


Figure 71: Sinkage Comparison at 1.5° by Stern Trim

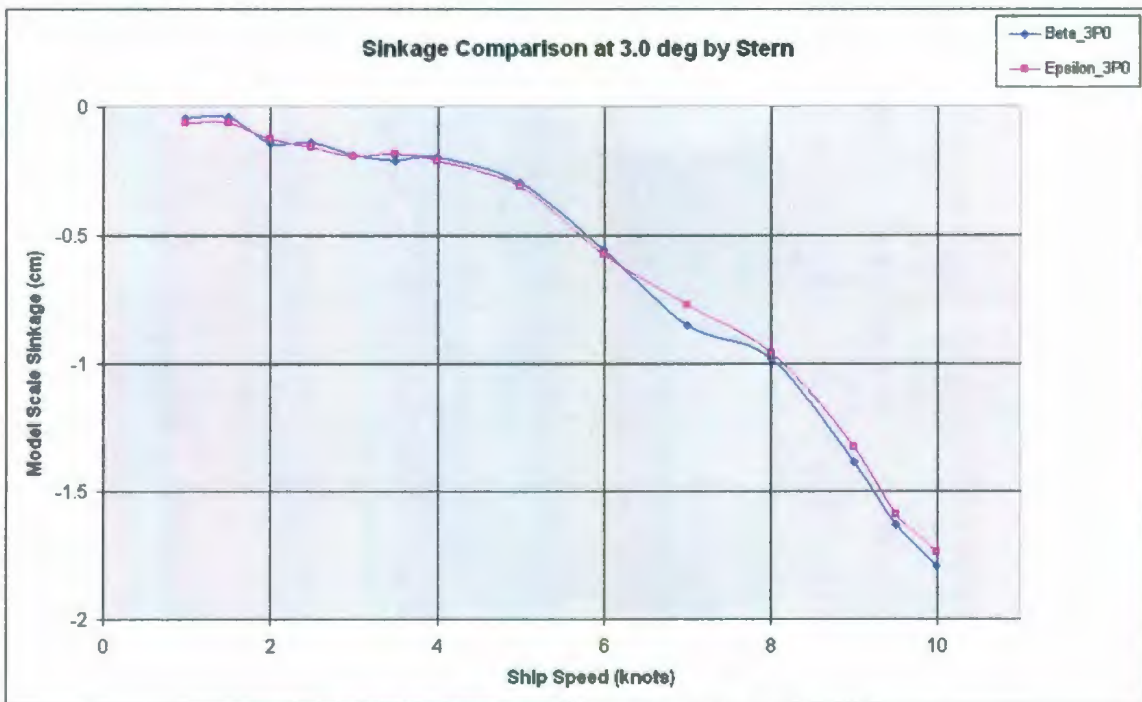


Figure 72: Sinkage Comparison at 3.0° by Stern Trim

Chapter 6 - MUN Bare Hull Resistance Tests

The resistance tests carried out in the MUN towing tank was conducted to determine the full scale effective power of the vessel with each of the nine bows attached. They were also conducted in order to validate the results obtained from the resistance tests carried out in the IOT ice tank. These tests were carried out in two different periods: from February 24, 2009 – February 27, 2009 and from September 14, 2009 – September 18, 2009. The objective was completed by testing the model over speeds corresponding to 0 – 12 knots full scale. This analysis was done using the International Towing Tank Conference - 1957 (ITTC-57) procedures.

6.1 MUN Test Facility

The towing tank facility at MUN (<http://www.engr.mun.ca/oerc/towtank.php>) has a length of 54.7 m, is 4.5 m wide, and has a water depth of 2.2 m. The tank is equipped with a 3.9 tonne towing carriage which has a maximum towing speed of 5.0 m/s. The tank is equipped with a hydraulically operated wave maker which is capable of generating regular or irregular waves up to 0.3 m significant wave height. The tank is fitted with passive wave absorbers on three sides of the tank, which consist of: pool dividers along the length of the tank, and a passive wire mesh beach at the north end of the tank. Located in the facility is a precision dynamometer, a 16 channel data acquisition system, along with other instrumentation; all of which allows for various types of testing to be completed at the facility.

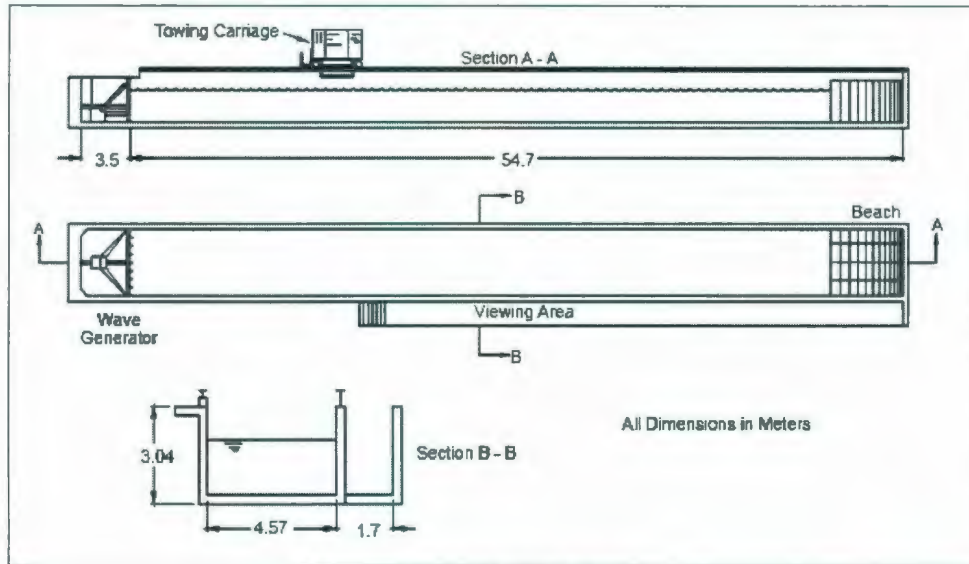


Figure 73: MUN Tank Schematic

6.2 Test Instrumentation

Towing Dynamometer

The towing dynamometer used was a *Kempf & Remmers* R 47 resistance dynamometer. The balance contains a load cell which has a rating of ± 50 lbs (approximately ± 220 N). It also contains a LVDT which has the ability to measure heave motion up to 400 mm. This dynamometer was used to measure both model resistance and heave motion of the model. This dynamometer allows the model to pitch and heave; it restricts it from yawing, surging, swaying, as well as rolling.



Figure 74: Towing Dynamometer

Inclinometer

To measure pitch angles a Servo Inclinometer from *Jewell Instruments LLC* was used. The inclinometer is fully self-contained and designed to operate in hostile environments. It is designed to operate from a standard DC power source. The output is an analog DC signal which is directly proportional to the sine of the angle of tilt; in level (horizontal) position, the DC output is zero. In one direction the output is 0 to +5 V and in the other it is 0 to -5 V.

Data Acquisition System

The data for each of the test conditions was collected through four channels (one each for resistance, heave, pitch, as well as carriage speed). The voltage data outputs for the tests were collected using an *IOTech* Daqbook data acquisition system (Daqbook 2000) connected to a computer running DaqView software. For these tests, the data were collected with a sampling rate of 50 Hz. The raw data was collected in ASCII format and post processed using Microsoft EXCEL.

6.2.1 Instrumentation Calibrations

The same calibration procedures were used as is outlined for the IOT bare hull resistance tests, given in Section 5.2.1.

6.3 Model Set-up

The same model set-up was used as is outlined for the IOT bare hull resistance tests, given in Section 5.3.

6.4 Test Plan

The test plan included testing each of the five remaining bulbous bows at the design draft of 0.188 m model scale and three different trim angles (level trim, 0.75° by stern, and 1.5° by stern). The vessel speed was originally set to range from 2 – 12 knots full scale. The following table shows the original test plan for the following bows: Delta, Eta, Iota, Theta, and Zeta.

**Table 20: Test Plan for Resistance Tests at MUN
For Each Trim Condition**

Run #	V _S (knots)	V _M (m/s)
Roughup	6	1.115
Roughup	6	1.115
1	2	0.372
2	4	0.743
3	6	1.115
4	8	1.487
5	10	1.859
6	12	2.230
7	11	2.044
8	9	1.673
9	7	1.301
10	5	0.929

Along with these tests the four bows tested previously in the IOT ice tank were retested in the MUN towing tank at level trim condition only. The vessel speed was set to range from 2 – 12 knots full scale. The thought here is that if good comparisons are found between the MUN and IOT tests at level trim, then the trimmed tests carried out at IOT

could be taken as correct. The following table shows the original test plan for the following bows: Alpha, Beta, Gamma, and Epsilon.

Table 21: Test Plan for MUN Resistance Retests

Run #	V _S (knots)	V _M (m/s)
Roughup	6	1.115
Roughup	6	1.115
1	2	0.372
2	6	1.115
3	9	1.673
4	12	2.230
5	10	1.859
6	8	1.487
7	4	0.743

6.5 Description of Experiment (ITTC-57 Method)

The same method was used as in the IOT bare hull resistance tests, as outlined in Section 5.5.

6.6 Blockage Corrections

The same blockage correction was used as in the IOT bare hull resistance tests, as outlined in Section 5.6.

6.7 Description of Data Analysis

6.7.1 Online Data Analysis

The data were acquired in ASCII (*.txt files) format and transferred to Microsoft EXCEL on the tow tank carriage workstation during testing to verify the integrity of the acquired data.

The resistance online data analysis is described as follows:

- The basic resistance channels (carriage speed, tow force, sinkage, and trim) are plotted on the screen in the time domain. The following plot shows a typical plot of a run down the tank, shown here is the speed data:

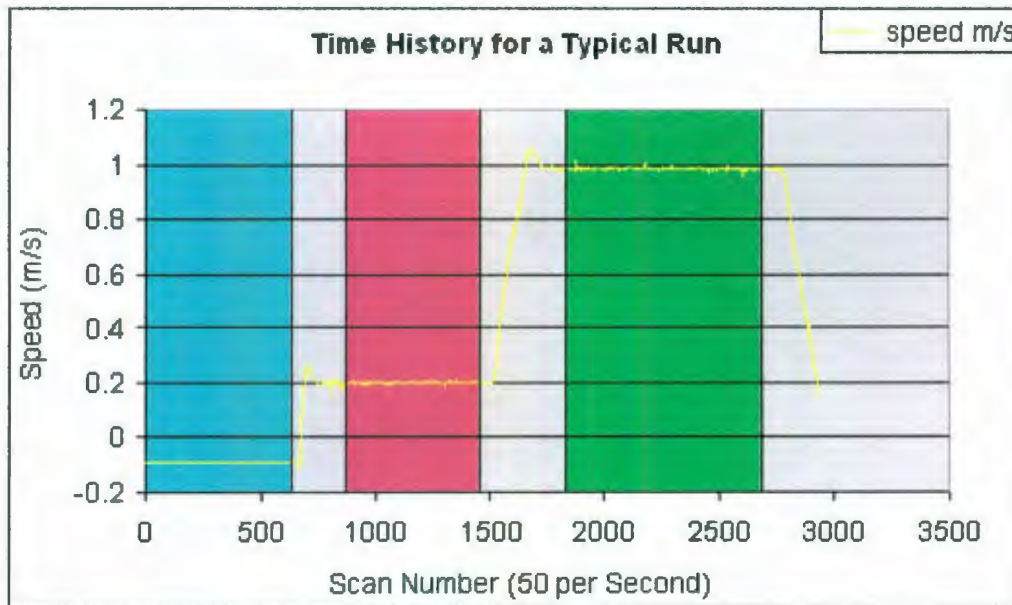


Figure 75: Typical Plot of Carriage Speed for One Run during Resistance Tests

- The above plot shows three distinct stages:
 - 1) The carriage is stopped; the resistance, pitch, and heave recorded at this stage will be used as tare values
 - 2) The carriage is up to steady state forward speed; resistance, pitch, and heave are all recorded
 - 3) The carriage is at the next forward speed; this can be done if the speeds are low enough that 10 seconds of data can be gathered for each speed.
- Start and end times are chosen for the initial tare segment as well as for each steady state segment. The averages are then computed and the tare values are subtracted from the steady state forward speed data.
- The following four plots are displayed on the same screen:
 - 1) Resistance (N) vs. Froude Number

- 2) Trim (degrees) vs. Froude Number
 - 3) Sinkage (cm) vs. Froude Number
 - 4) $10^3 C_{TM}$ vs. Froude Number
- Mean values of carriage speed (m/s), resistance (N), sinkage (cm), and trim (degrees) computed over each steady state time segment were output in tabular form for all runs completed up to the given run.

6.7.2 Offline Data Analysis

The following data analysis was carried out to assess the hull resistance using the IOT Standard Resistance Procedure (2006). Within this standard the effective power is estimated using the ITTC-57 Method (1957).

- Carriage speed (m/s), resistance (N), sinkage (cm) and trim (degrees) values were output in tabular form for all runs carried out for the model.
- The model resistance coefficients were then plotted against Froude Number and $\log_{10} R_{eM}$. Coefficients plotted include C_{TM} , blockage corrected C_{TM} (corrected using Scott's Method (1976)), and C_{FM} .
- A plot of effective power vs. ship speed (knots) using the ITTC-57 methodology was generated.
- A table of ship resistance and effective power using the ITTC-57 prediction method was provided for the ship in salt water and including the tank blockage correction using Scott's Method. The table includes: V_S (knots), P_E (kW), R_{TS} (kN), F_n , R_{nS} , C_{TS} , C_{FS} , and C_R .
- A table of sinkage and trim information was also generated and included: V_S (knots), Z_V , and θ_V .

6.8 Results and Discussions

This section is intended to give an overview of the results obtained from the analysis of the testing. The effective power results shown in this report are scaled to a full scale vessel of 45.93 ft in length. The detailed results are contained in Appendix C.

6.8.1 Conventional Bow

The following table and figure gives the required effective power for the vessel with Alpha bow. Effective power is defined as the power required to overcome the hull resistance at a given speed.

Table 22: Effective Power for Vessel with Alpha Bow

Effective Power for Alpha Bow (W)	
Ship Speed (knots)	Level Trim
1.6	226
3.7	1075
4.7	2341
5.8	6096
6.8	12274
7.9	24899
8.9	42788
10.0	74284
11.0	125493
12.1	194584

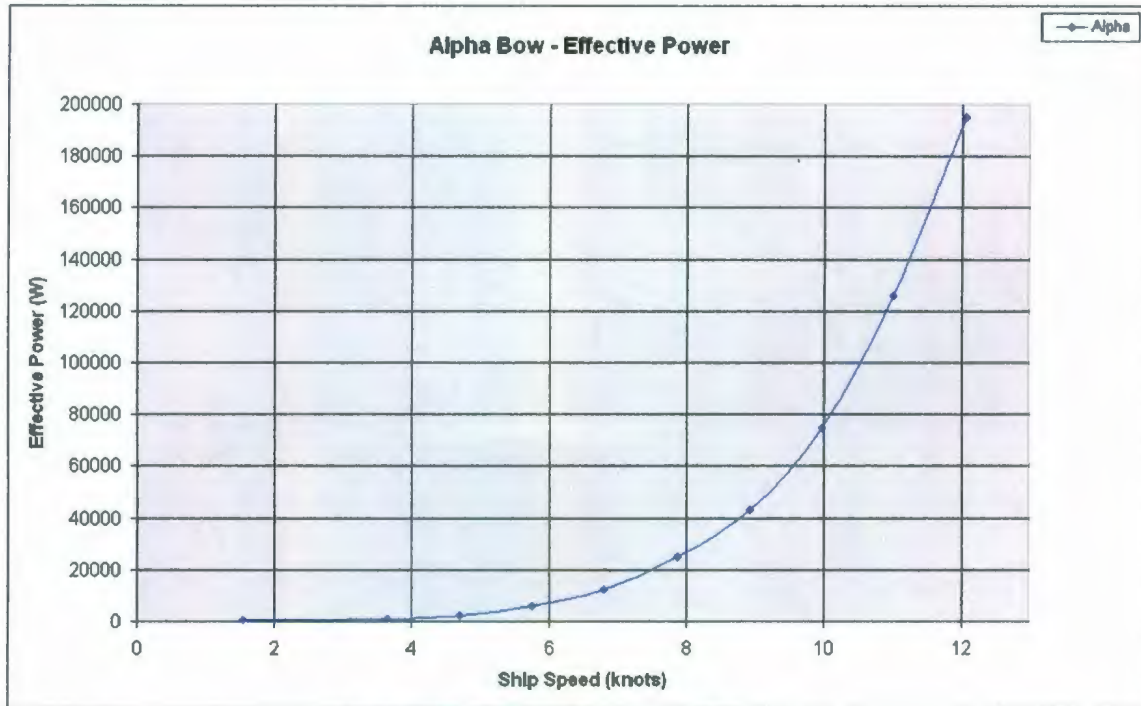


Figure 76: Effective Power with Alpha Bow

It can be seen that the effective power starts to significantly increase at speeds above approximately 8 knots full scale. Therefore, significant amounts of extra power would be required to enable the vessel to go every extra knot in calm water conditions.

The following figure is a picture taken during testing. The picture shows the model with Alpha bow for the level trim condition at a speed of 10 knots full scale. From the photo it can be seen that there is a large bow wave created. There is quite a bit of spray at the stem, which increases the overall resistance of the hull.



Figure 77: Alpha Bow Test at Level Trim – Speed of 10 knots

6.8.2 Bulbous Bows

This section provides the determined powering requirements of the vessel with each of the bulbous bows as tested in the MUN towing tank.

Beta Bow

The following table and figure gives the required effective power for the vessel with Beta bow.

Table 23: Effective Power for Vessel with Beta Bow

Effective Power for Beta Bow (W)	
Ship Speed (knots)	Level Trim
1.6	112
3.7	1469
4.7	2822
5.8	4893
6.8	9491
7.9	18709
8.9	35185
10.0	64742
11.0	113848
12.1	168010

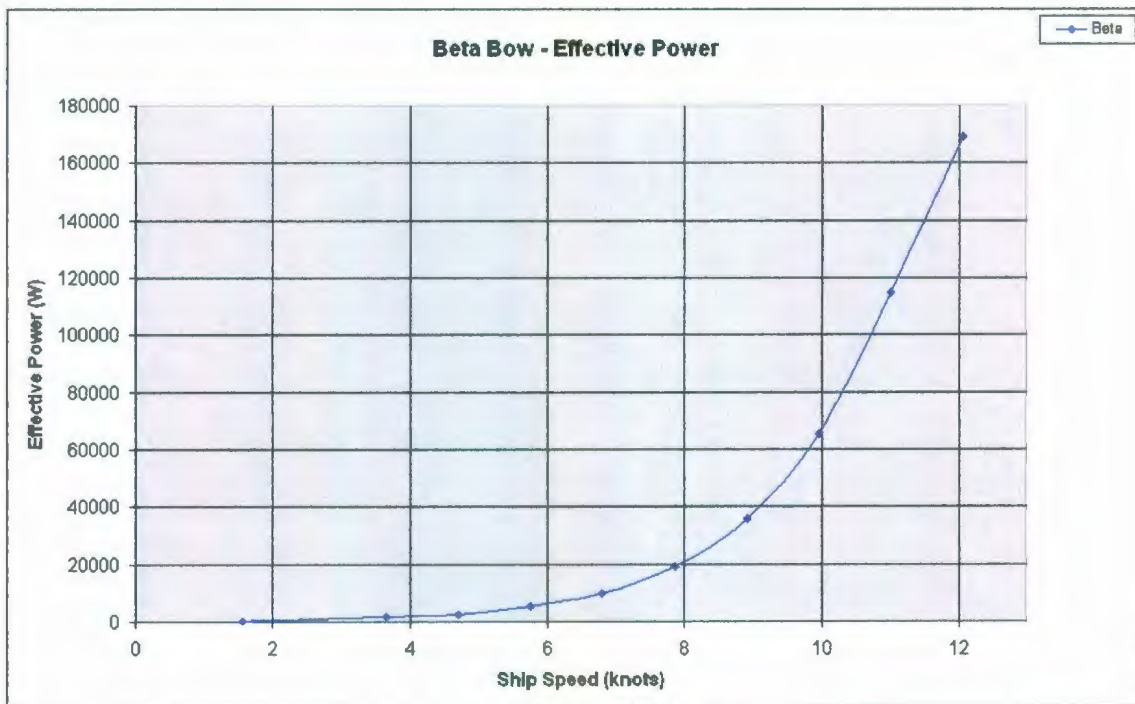


Figure 78: Effective Power with Beta Bow

There is a similar trend for this bow as for the conventional bow; that is there begins to be a significant increase in required power above speeds of around 8 knots full scale.

The following figure is a picture taken during testing. The picture shows the model with Beta bow for the level trim condition at a speed of 10 knots full scale. From the photo it can be seen that there is a fairly large bow wave created and there is quite a bit of spray at the stem.

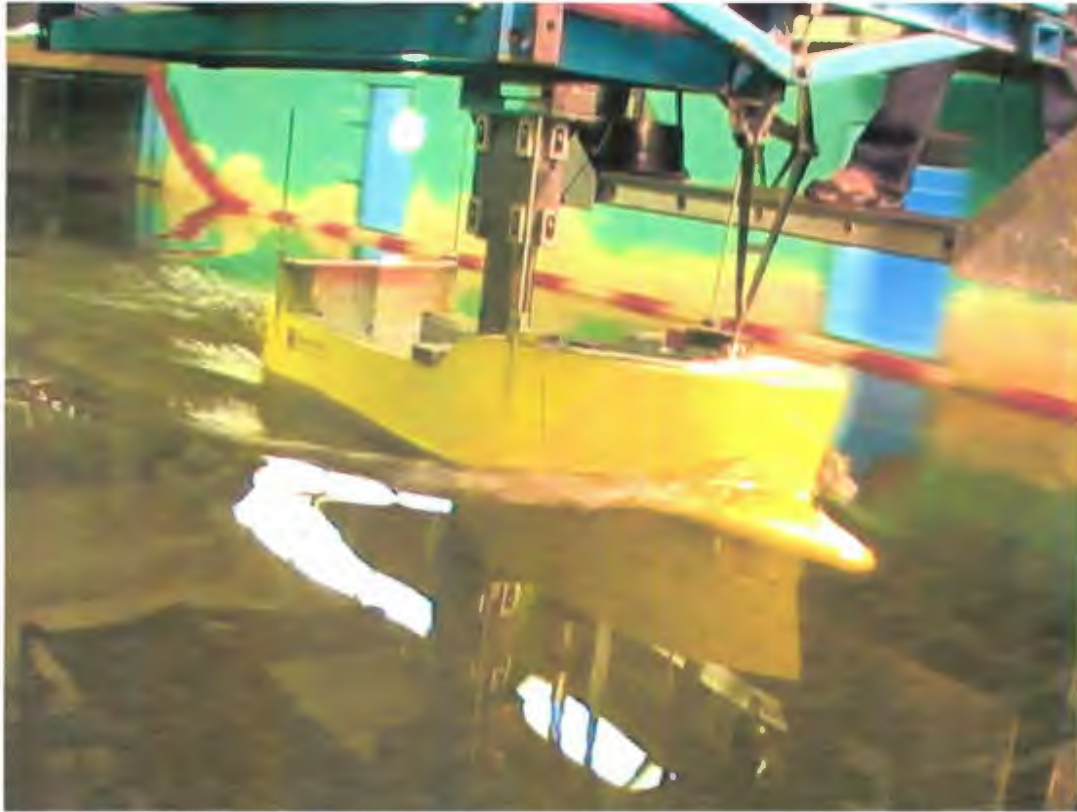


Figure 79: Beta Bow Test at Level Trim – Speed of 10 knots

Delta Bow

The following table and figure gives the required effective power for the vessel with Delta bow.

Table 24: Effective Power for Vessel with Delta Bow

Effective Power for Delta Bow (W)			
Ship Speed (knots)	Level Trim	0.75° by Stern Trim	1.5° by Stern Trim
1.6	65	66	101
3.7	1174	1442	1386
4.7	2611	3053	3433
5.8	4765	5520	7110
6.8	7420	8947	10481
7.9	17164	18091	19312
8.9	30728	33181	31565
10	61227	57907	56995
11	106452	101578	102346
12.1	175036	175654	177188

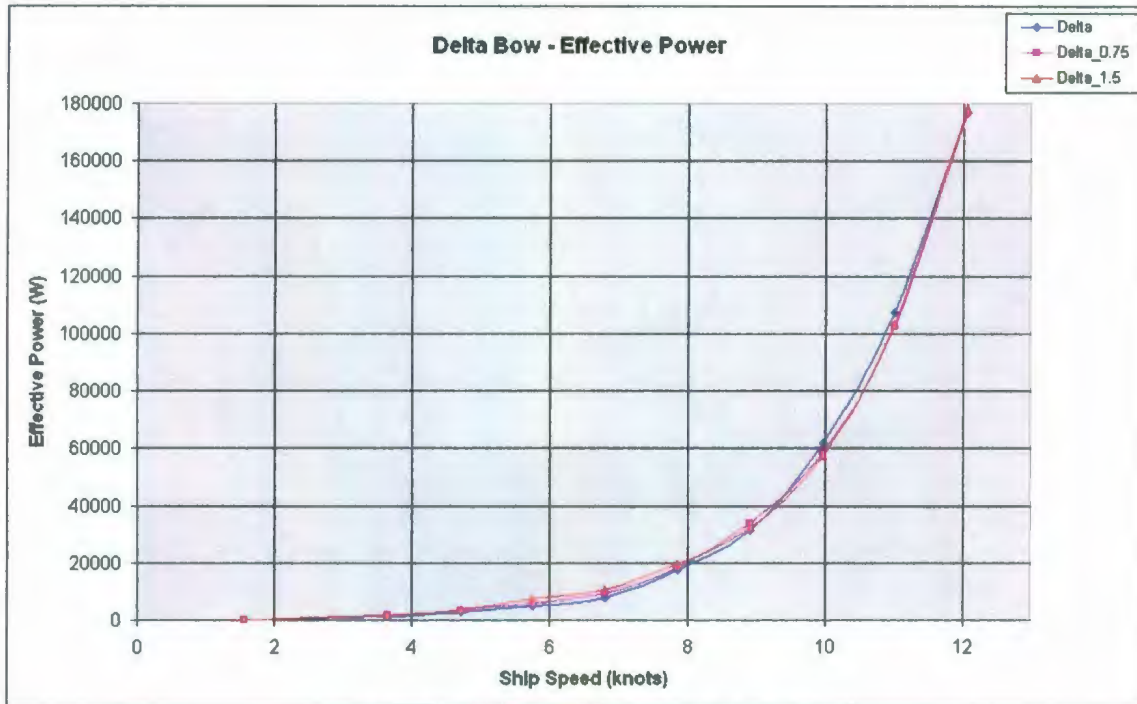


Figure 80: Effective Power with Delta Bow

It can be shown that there is not a large effect due to the static trim of the model with regards to the powering performance of the model with Delta bow. Below 9 knots the model at level trim outperforms the trimmed by the stern conditions slightly. From 9 – 11 knots both of the trimmed conditions slightly outperform the level trim condition. There is no real significant difference in required effective power at 12 knots. At 10 knots the required effective power is reduced by approximately 7.3% by statically trimming the model 1.5° by the stern. Similarly, it's reduced by about 5.6% by trimming it 0.75° by the stern.

The following series of pictures show the model with Delta bow attached at 0°, 0.75°, and 1.5° by stern trim angles while traveling at the full scale speed of 10 knots. From the following figures it can be seen that there is a significant reduction in water spray off the bow with increasing static trim by the stern.



Figure 81: Delta Bow Test at Level Trim – Speed of 10 knots



Figure 82: Delta Bow Test at 0.75° by Stern Trim – Speed of 10 knots

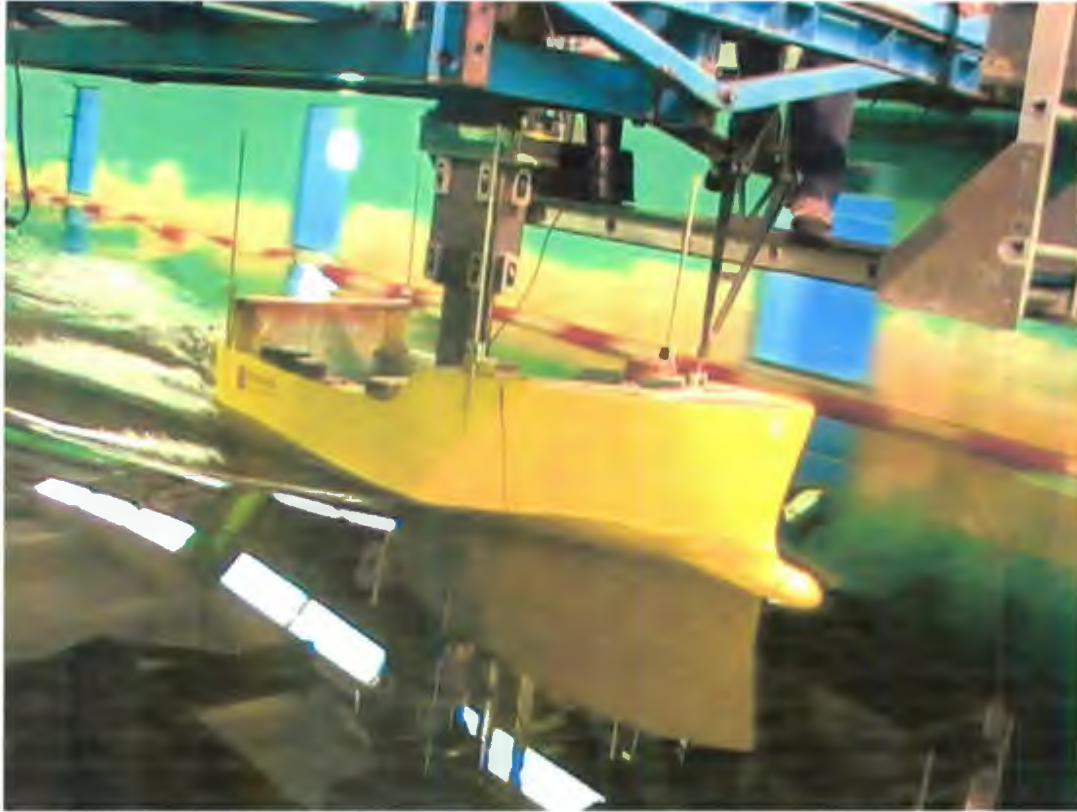


Figure 83: Delta Bow Test at 1.5° by Stern Trim – Speed of 10 knots

It is difficult to see exactly from the figures, but it is known from the dynamic trim data that the model is at approximately level trim at 10 knots for the static level trim condition. For the 0.75° by stern condition it is known that the model dynamically trims by the stern an additional 0.5°, for a total trim angle of about 1.25° by the stern. Likewise, for the 1.5° by stern condition it is known that the model dynamically trims by the stern an additional 1.0°, for a total trim angle of about 2.5° by the stern.

This may explain why there is not a large reduction in effective power from the static level trim condition to the trim by the stern conditions. One possible explanation is that if the model is further trimmed by the stern then the submerged transom area is increased, thereby increasing the wake and hence required effective power. This increase in submerged transom then partially cancels out the positive effect of reduction in water spray off the bow with increasing static trim by the stern.

Gamma Bow

The following table and figure gives the required effective power for the vessel with Gamma bow.

Table 25: Effective Power for Vessel with Gamma Bow

Effective Power for Gamma Bow (W)	
Ship Speed (knots)	Level Trim
1.6	170
3.7	979
4.7	2269
5.8	5224
6.8	8697
7.9	16873
8.9	32952
10	58127
11	102051
12.1	174502

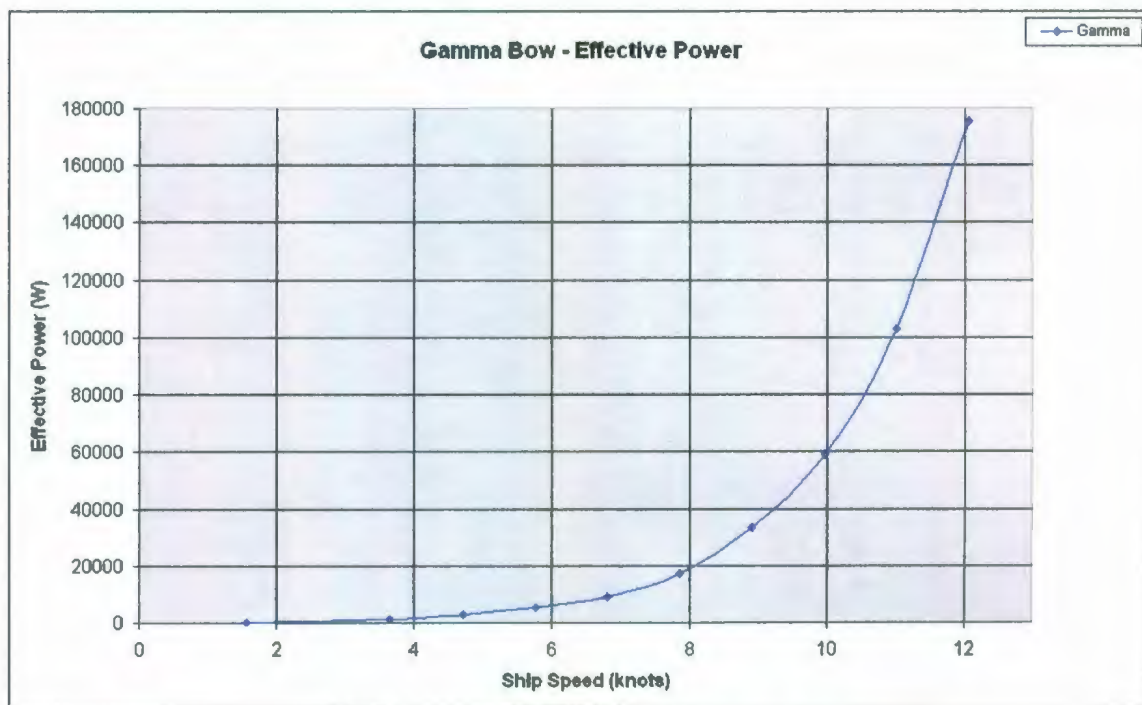


Figure 84: Effective Power with Gamma Bow

So again it can be seen there a significant increase in required power above speeds of around 7 – 8 knots full scale.

The following figure is a picture taken during testing. The picture shows the model with Gamma bow for the level trim condition at a speed of 10 knots full scale. From the photo it can be seen that there is a much smaller bow wave created than was seen for Alpha, Beta, or Delta bow at this trim condition.



Figure 85: Gamma Bow Test at Level Trim – Speed of 10 knots

Epsilon Bow

The following table and figure gives the required effective power for the vessel with Epsilon bow.

Table 26: Effective Power for Vessel with Epsilon Bow

Effective Power for Epsilon Bow (W)	
Ship Speed (knots)	Level Trim
1.6	-31
3.7	833
4.7	1739
5.8	3667
6.8	7647
7.9	16233
8.9	29552
10	58561
11	99339
12.1	165525

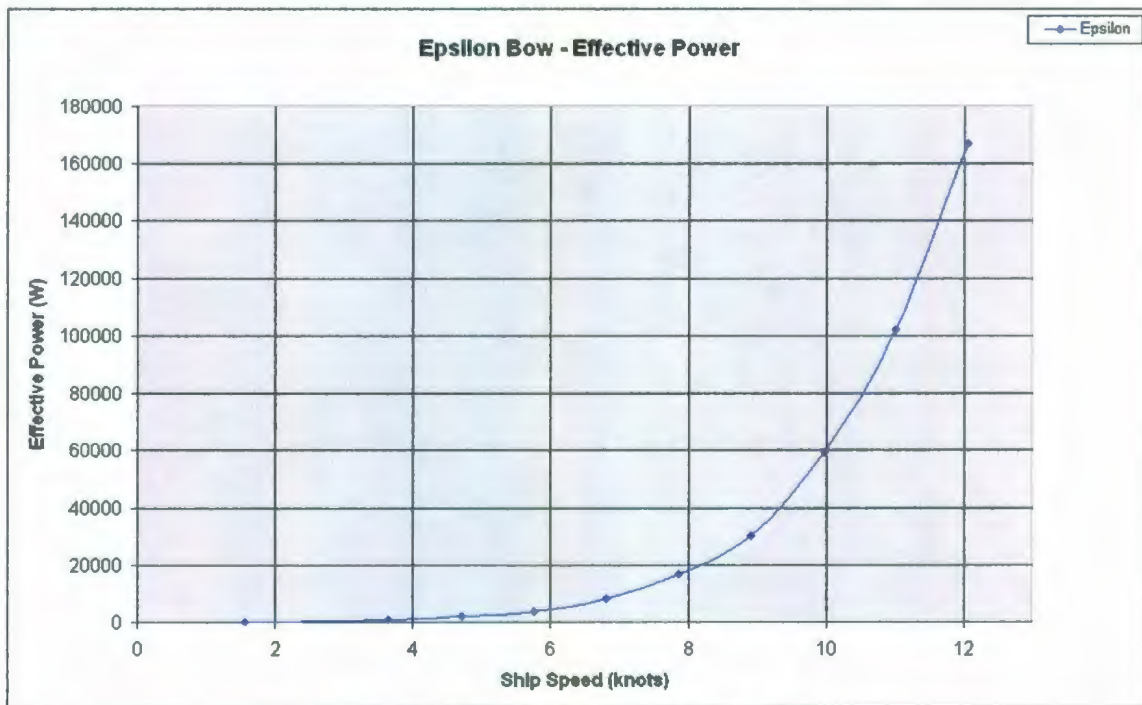


Figure 86: Effective Power with Epsilon Bow

Once more, it can be seen that there a significant increase in required power above speeds of around 7 – 8 knots full scale.

The following figure is a picture taken during testing. The picture shows the model with Epsilon bow for the level trim condition at a speed of 10 knots full scale. From the photo it can be seen that there is a fairly large bow wave created and there is quite a bit of spray at the stem.

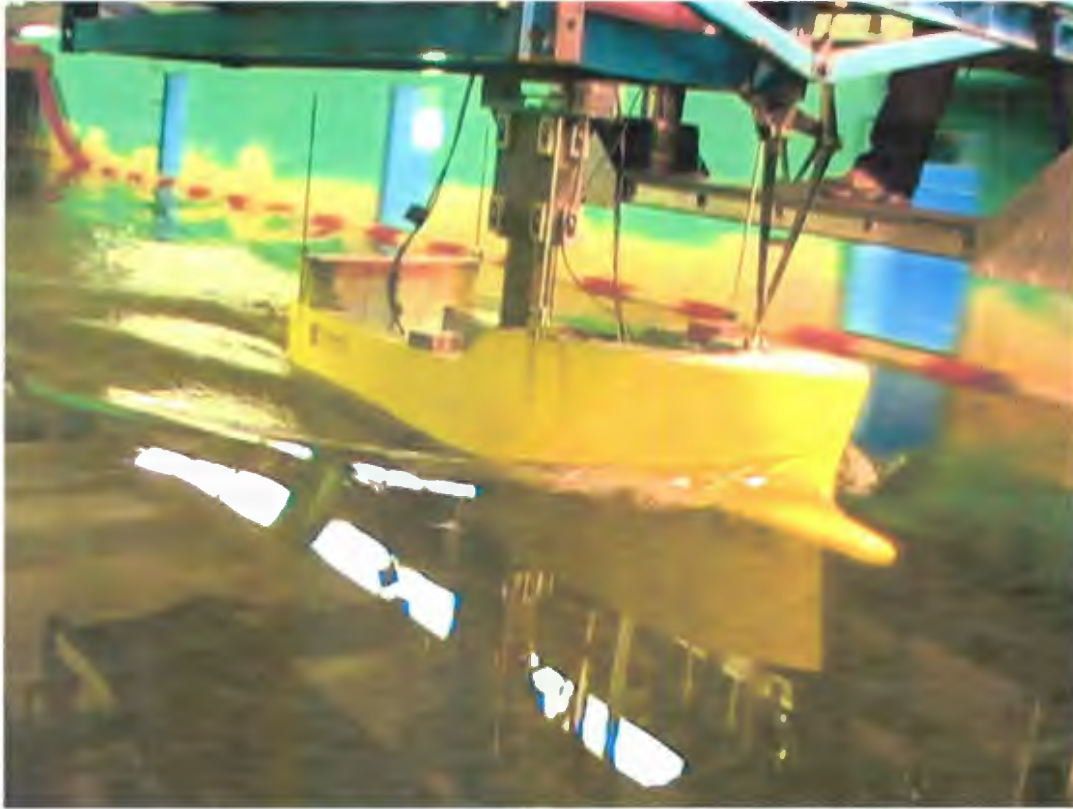


Figure 87: Epsilon Bow Test at Level Trim – Speed of 10 knots

Eta Bow

The following table and figure gives the required effective power for the vessel with Eta bow.

Table 27: Effective Power for Vessel with Eta Bow

Effective Power for Eta Bow (W)			
Ship Speed (knots)	Level Trim	0.75° by Stern Trim	1.5° by Stern Trim
1.6	59	100	106
3.7	990	1338	1282
4.7	2238	2661	3288
5.8	5329	5937	6766
6.8	10004	10822	12383
7.9	19617	19751	20882
8.9	35082	34706	33282
10	67483	59473	54173
11	111792	98468	91699
12.1	171454	159493	154709



Figure 88: Effective Power with Eta Bow

It can be seen that below 8 or 9 knots there is no significant effect due to the static trim of the model with regards to the powering performance. Above 9 knots both the trim conditions of 0.75° and 1.5° by stern significantly outperform the static level trim condition. At 10 knots the required effective power is reduced by approximately 19.5% by statically trimming the model 1.5° by the stern. Similarly, it's reduced by almost 11.8% by trimming it 0.75° by the stern.

The following series of pictures show the model with Delta bow attached at 0° , 0.75° , and 1.5° by stern trim angles while traveling at the full scale speed of 10 knots. From the following figures it can be seen that there is a significant reduction in water spray off the bow with increasing static trim by the stern. It can also be seen that the flow of water across the hull is much smoother with increasing static trim angle.



Figure 89: Eta Bow Test at Level Trim – Speed of 10 knots



Figure 90: Eta Bow Test at 0.75° by Stern Trim – Speed of 10 knots

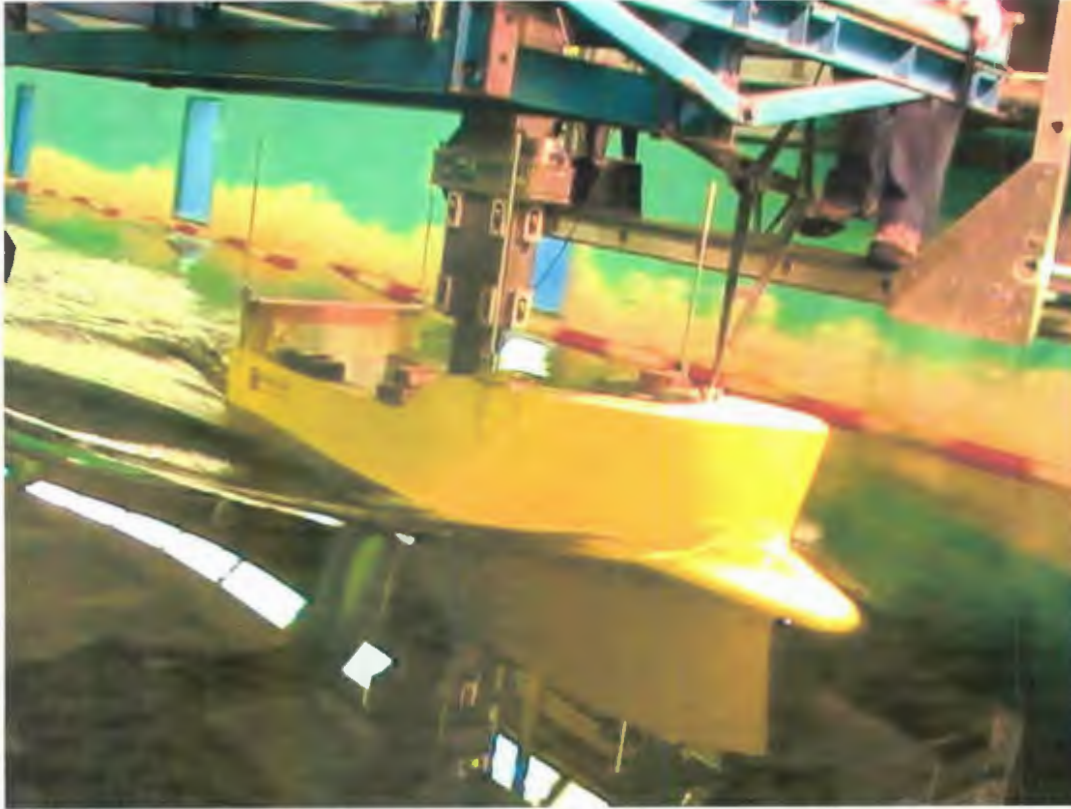


Figure 91: Eta Bow Test at 1.5° by Stern Trim – Speed of 10 knots

From the dynamic trim data it is known that the model is trimmed approximately 1.7° by the head at 10 knots for the static level trim condition. For the 0.75° by stern condition it is known that the model dynamically trims by the head approximately 0.8°, which brings the model to level trim at speed. For the 1.5° by stern condition it is known that the model dynamically trims by the stern an approximately 0.1°, for a total dynamic trim angle of about 1.6° by the stern.

This may help explain why there is a 12% reduction from the level trim to 0.75° by stern conditions. For the static level trim condition the model is trimmed significantly by the head at 10 knots which creates a large bow wave. Whereas, for the 0.75° by stern condition the model is leveled out at 10 knots, thereby reducing the bow wave and hence the total resistance on the model. At the 1.5° by stern condition the model is actually trimmed by the stern by about 1.6°, however the bow wave is significantly reduced and the flow around the hull is much smoother. This then explains why the effective power is reduced even further even though the submerged transom area is increased.

Iota Bow

The following table and figure gives the required effective power for the vessel with Iota bow.

Table 28: Effective Power for Vessel with Iota Bow

Effective Power for Iota Bow (W)			
Ship Speed (knots)	Level Trim	0.75° by Stern Trim	1.5° by Stern Trim
1.6	142	50	55
3.7	1191	1658	1547
4.7	2997	3628	4280
5.8	6040	7010	8662
6.8	8402	10538	13192
7.9	16338	17313	19736
8.9	29522	29838	29388
10	58142	55556	52854
11	104041	98010	96618
12.1	168857	168854	170425

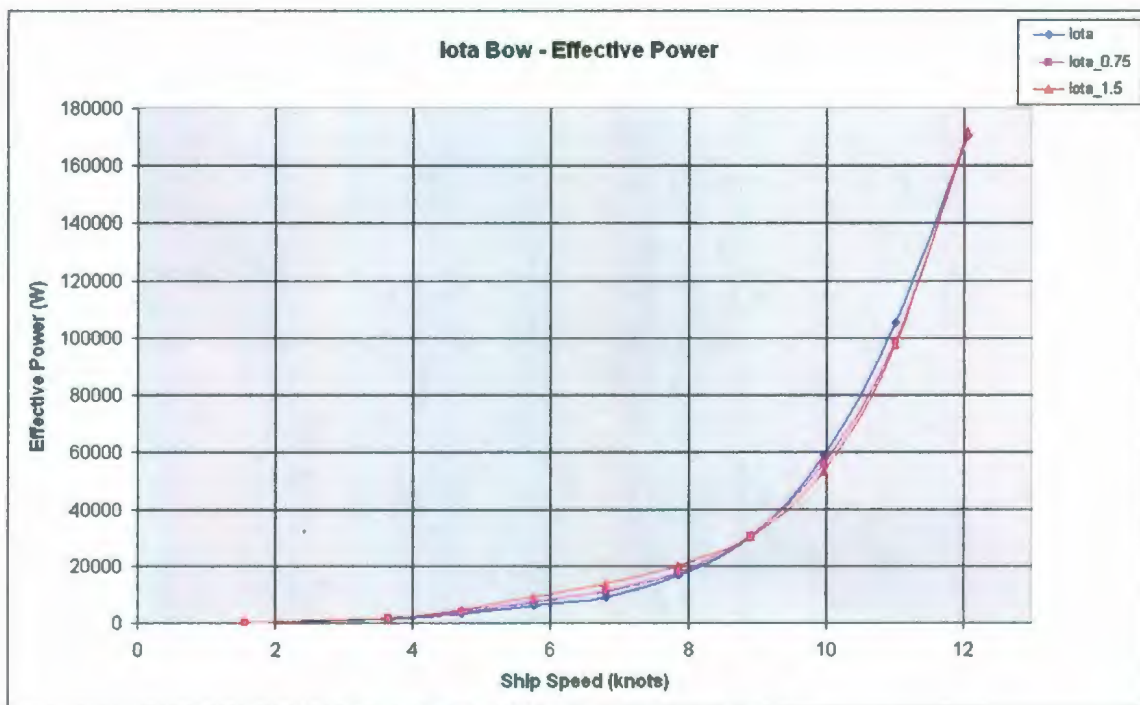


Figure 92: Effective Power with Iota Bow

Here it can be seen that below 9 knots full scale the best performance occurs when the model is at static level trim. From 9 – 11 knots both of the trimmed conditions slightly outperform the level trim condition. There is no real significant difference in required effective power at 12 knots. At 10 knots the required effective power is reduced by

approximately 9.1% by statically trimming the model 1.5° by the stern. Similarly, it's reduced approximately 4.4% by trimming it 0.75° by the stern.

The following series of pictures show the model with Iota bow attached at 0°, 0.75°, and 1.5° by stern trim angles while traveling at the full scale speed of 10 knots. From the following figures it can be seen that there is a significant reduction in water spray off the bow with increasing static trim by the stern. It can also be seen that the flow of water across the hull is much smoother with increasing static trim angle.



Figure 93: Iota Bow Test at Level Trim – Speed of 10 knots

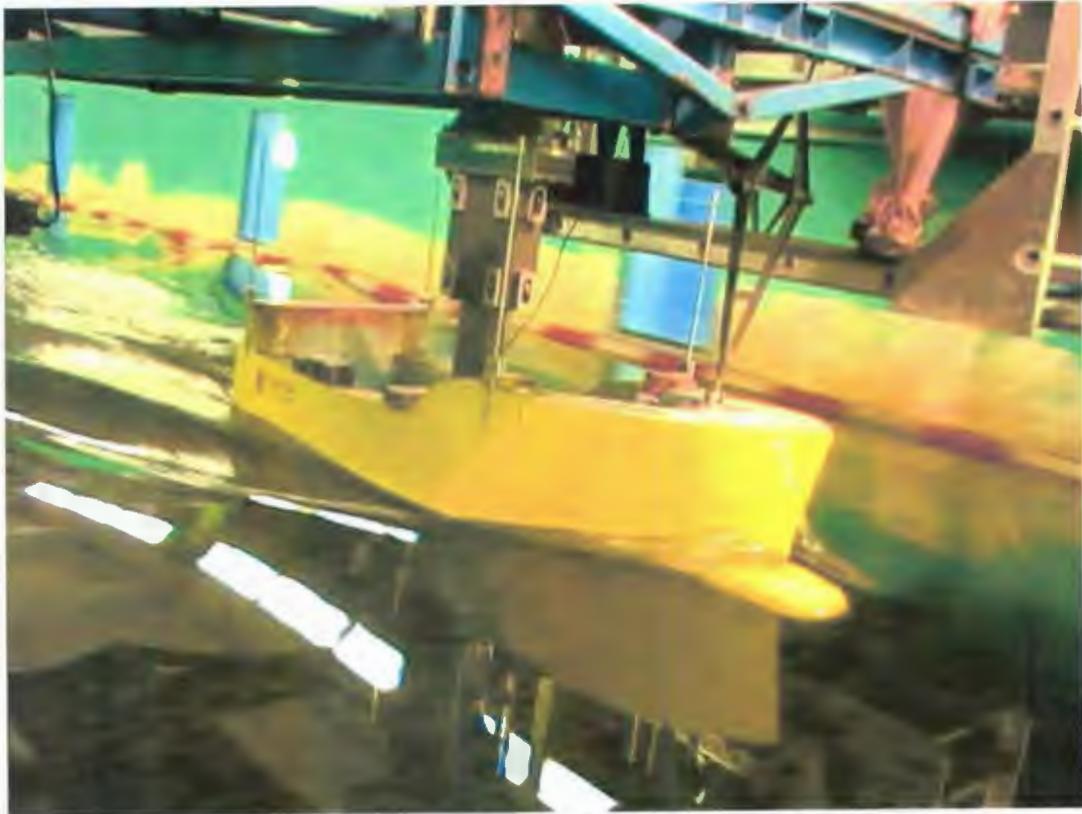


Figure 94: Iota Bow Test at 0.75° by Stern Trim – Speed of 10 knots

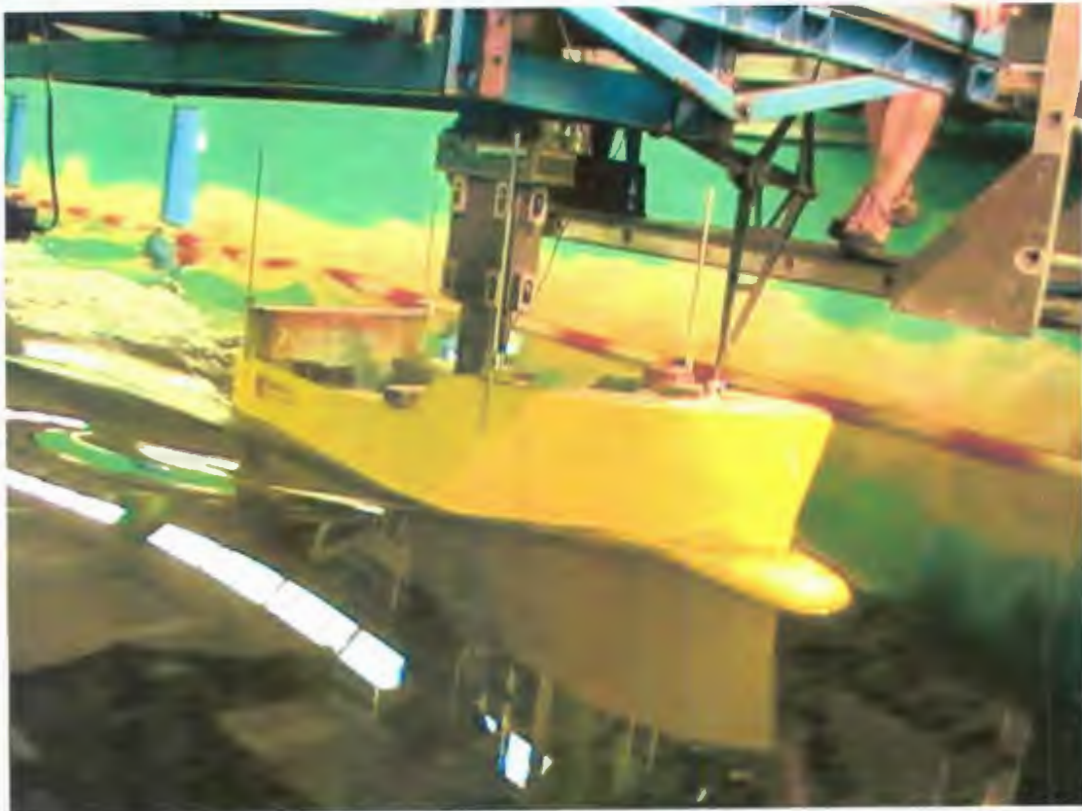


Figure 95: Iota Bow Test at 1.5° by Stern Trim – Speed of 10 knots

It is known from the dynamic trim data that the model is trimmed approximately 0.5° by the head at 10 knots for the static level trim condition. For the 0.75° by stern condition it is known that the model dynamically trims by the stern an additional 0.1° , for a total trim angle of about 0.85° by the stern. Likewise, for the 1.5° by stern condition it is known that the model dynamically trims by the stern an additional 0.7° , for a total trim angle of about 2.2° by the stern. Based on this data it is known that the model will be at dynamic level trim at 10 knots full scale when the model is statically trimmed approximately 0.28° by the stern. It may therefore be interesting to go back and complete testing at this static trim condition for comparisons.

This is a similar scenario as in the Delta bow case, where the model is further trimmed by the stern in both the 0.75° and 1.5° static trim conditions. This then leads to a greater submerged transom area for these two cases; and therefore not as much of a reduction in required effective power even though the flow around the hull is much smoother with increasing static trim angle.

Theta Bow

The following table and figure gives the required effective power for the vessel with Theta bow.

Table 29: Effective Power for Vessel with Theta Bow

Effective Power for Theta Bow (W)			
Ship Speed (knots)	Level Trim	0.75° by Stern Trim	1.5° by Stern Trim
1.6	80	99	61
3.7	1481	1328	1278
4.7	2527	3055	3119
5.8	5710	6052	6467
6.8	10377	11119	12206
7.9	20965	20912	21942
8.9	37675	37814	37097
10	71560	64015	59690
11	119041	106658	99819
12.1	178372	170145	166673



Figure 96: Effective Power with Theta Bow

It can be seen that below 9 knots the effect due to the static trim of the model with regards to the powering performance is insignificant. Above 9 knots both the trim conditions of 0.75° and 1.5° by stern significantly outperform the static level trim condition. At 10 knots the required effective power is reduced by approximately 16.7% by statically trimming the model 1.5° by the stern. Similarly, it's reduced by about 10.5% by trimming it 0.75° by the stern.

The following series of pictures show the model with Theta bow attached at 0° , 0.75° , and 1.5° by stern trim angles while traveling at the full scale speed of 10 knots. From the following figures it can be seen that there is a significant reduction in water spray off the bow with increasing static trim by the stern. It can also be seen that the flow of water across the hull is much smoother with increasing static trim angle.

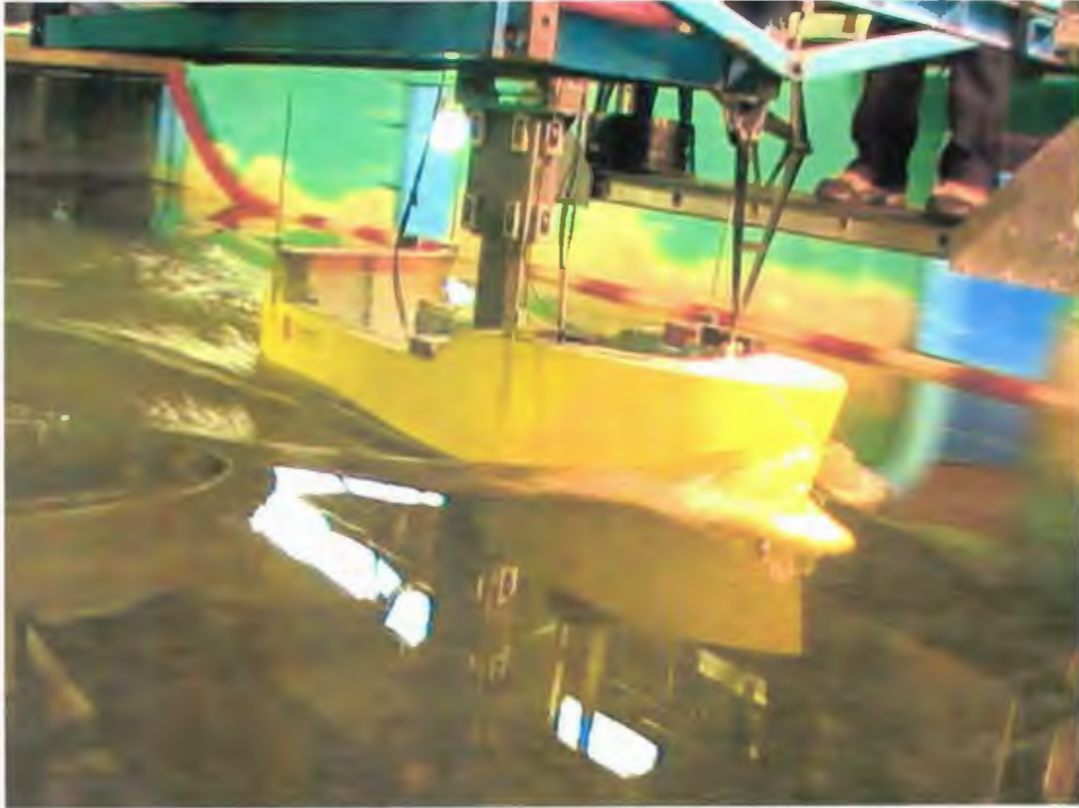


Figure 97: Theta Bow Test at Level Trim – Speed of 10 knots



Figure 98: Theta Bow Test at 0.75° by Stern Trim – Speed of 10 knots

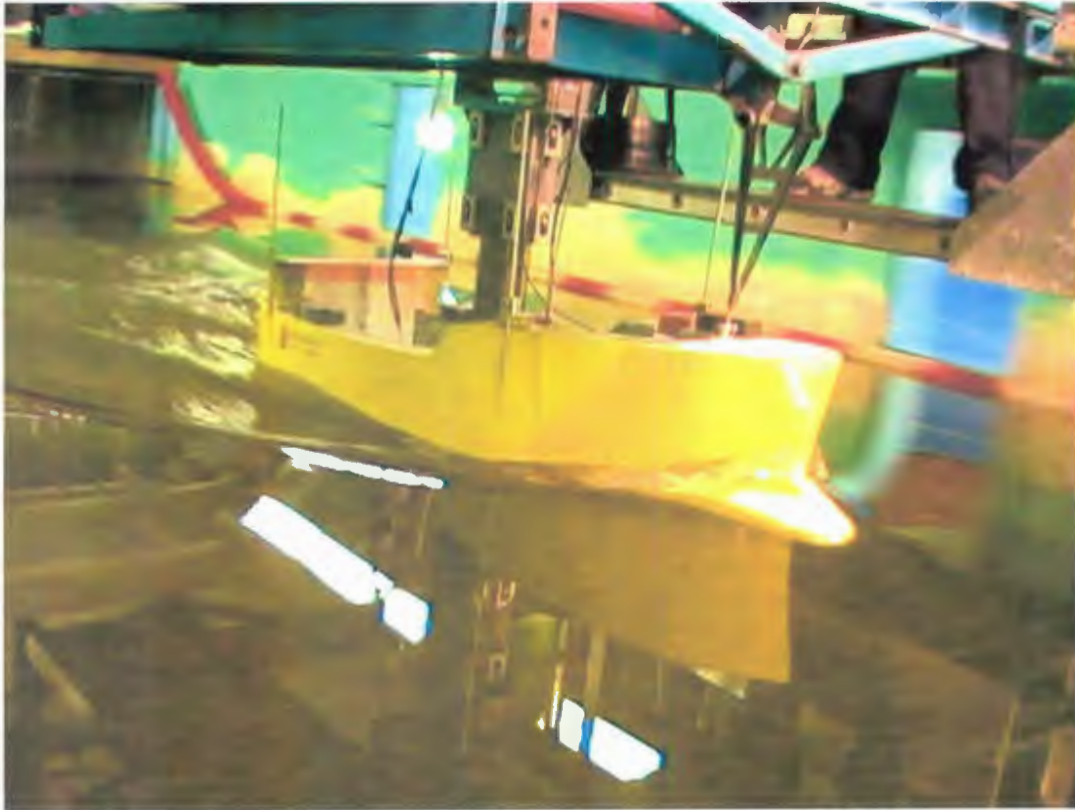


Figure 99: Theta Bow Test at 1.5° by Stern Trim – Speed of 10 knots

From the dynamic trim data it is known that the model is trimmed approximately 1.7° by the head at 10 knots for the static level trim condition. For the 0.75° by stern condition it is known that the model dynamically trims by the head approximately 0.9°, for a total trim angle of about 0.15° by the head. For the 1.5° by stern condition it is known that the model does not dynamically trim at 10 knots, so the total trim angle is 1.5° by the stern. Based on this data it is known that the model will be at dynamic level trim at 10 knots full scale when the model is statically trimmed approximately 0.82° by the stern. It may therefore be interesting to go back and complete testing at this static trim condition for comparisons.

This is a similar scenario as in the Eta bow case; where the model is trimmed by the head for the static level trim condition thereby creating a large bow wave for this condition. The model is nearly at level trim for the 0.75° condition thereby reducing the bow wave and hence the total resistance on the model. At the 1.5° by stern condition the model is still trimmed by the stern at 10 knots but the bow wave is significantly reduced and the

flow around the hull is much smoother. This may explain why the effective power is reduced even further even though the submerged transom is actually increased.

Zeta Bow

The following table and figure gives the required effective power for the vessel with Zeta bow.

Table 30: Effective Power for Vessel with Zeta Bow

Effective Power for Zeta Bow (W)			
Ship Speed (knots)	Level Trim	0.75° by Stern Trim	1.5° by Stern Trim
1.6	110	89	90
3.7	868	1113	1240
4.7	2414	2615	3216
5.8	4719	5344	6107
6.8	8674	8520	9810
7.9	18700	18423	18695
8.9	35803	33781	33656
10	67386	59633	58028
11	111728	101802	98616
12.1	177687	170288	167961

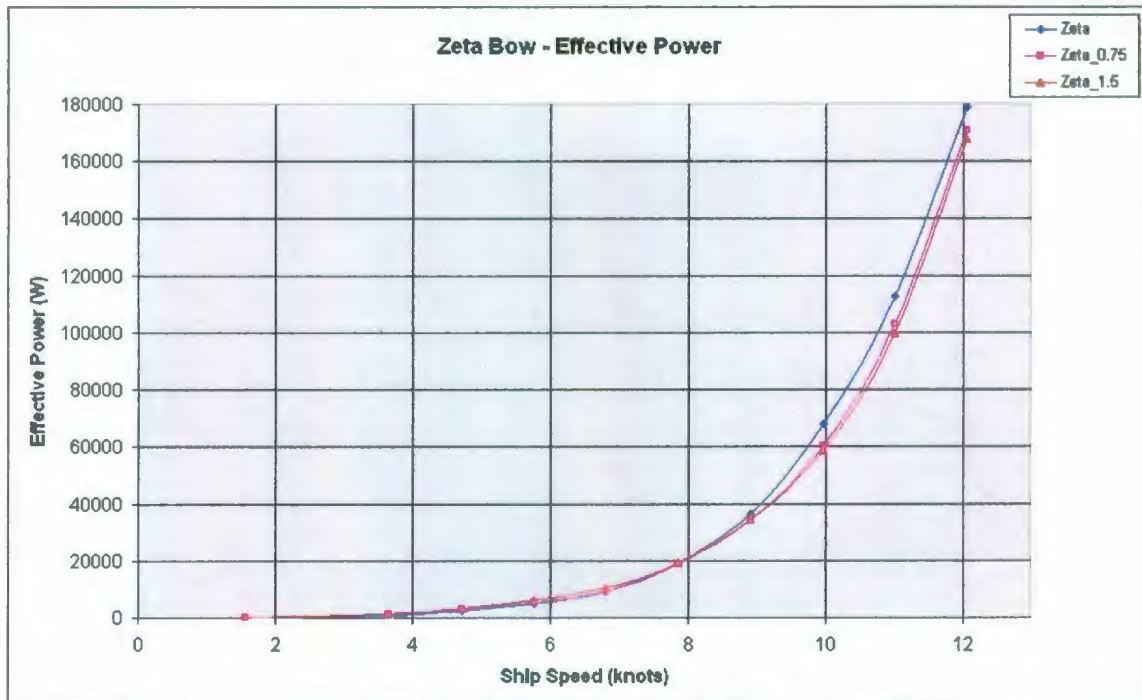


Figure 100: Effective Power with Zeta Bow

Again, it can be seen that below 8 – 9 knots the effect due to the static trim of the model with regards to the powering performance is basically insignificant. Above 9 knots both the trim conditions of 0.75° and 1.5° by stern significantly outperform the static level trim condition. At 10 knots the required effective power is reduced by approximately 13.8% by statically trimming the model 1.5° by the stern. Similarly, it's reduced by about 11.4% by trimming it 0.75° by the stern.

The following series of pictures show the model with Zeta bow attached at 0° , 0.75° , and 1.5° by stern trim angles while traveling at the full scale speed of 10 knots. From the following figures it can be seen that there is a significant reduction in water spray off the bow with increasing static trim by the stern. It can also be seen that the flow of water across the hull is much smoother with increasing static trim angle.



Figure 101: Zeta Bow Test at Level Trim – Speed of 10 knots

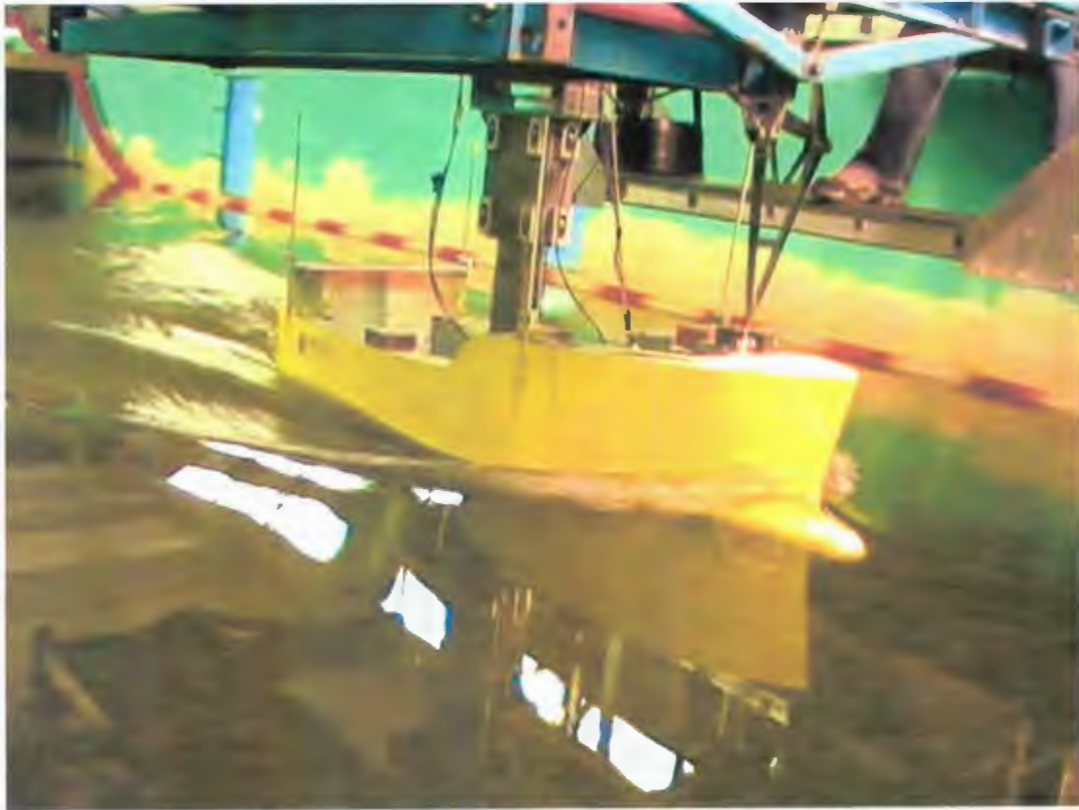


Figure 102: Zeta Bow Test at 0.75° by Stern Trim – Speed of 10 knots



Figure 103: Zeta Bow Test at 1.5° by Stern Trim – Speed of 10 knots

From the dynamic trim data it is known that the model is trimmed approximately 0.9° by the head at 10 knots for the static level trim condition. For the 0.75° by stern condition it is known that the model dynamically trims by the head approximately 0.3° , for a total trim angle of about 0.45° by the stern. For the 1.5° by stern condition it is known that the model dynamically trims by the stern an approximately 0.4° , for a total trim angle of about 1.9° by the stern. Based on this data it is known that the model will be at dynamic level trim at 10 knots full scale when the model is statically trimmed approximately 0.5° by the stern. It may therefore be interesting to go back and complete testing at this static trim condition for comparisons.

This case is basically in between the Delta and Eta cases shown above. At static level trim the model is trimmed 0.9° by the head, which is approximately in the middle of what was found for Delta and Eta. Looking at the three figures of each of these bows at the level trim condition it is clear that Eta has the largest bow wave, then Zeta, and finally Delta.

For the 0.75° trim condition the model is trimmed 0.45° by the stern at 10 knots, which again is approximately in the middle of what was found for Delta and Eta. Similar wave patterns are found for this trim condition as was found for the static level trim condition, which is that Eta has the largest bow wave, followed by Zeta, and finally Delta. It is also found here that there is around an 11.5% reduction in required power from the static level trim condition for both Zeta and Eta bows, but only a 5.6% reduction for Delta bow.

For the 1.5° trim condition the model is trimmed 1.9° by the stern at 10 knots, which again is approximately in the middle of what was found for Delta and Eta. Once more, similar wave patterns are found for this trim condition as was found for the static level trim condition as well as the 0.75° by stern trim condition, which is that Eta has the largest bow wave, followed by Zeta, and finally Delta. It was also found here that there is a 19.5% reduction in required power from the static level trim condition for Eta bow, 13.8% reduction for Zeta bow, and a 7.3% reduction for Delta bow.

6.8.3 Bow Comparisons

The following sections show plots of the effective power for all of the bows tested at each of the three trim angles (i.e. level trim, 0.75° by stern, and 1.5° by stern). In each section three figures are given to show comparisons of the required effective power for the vessel with each of the bows tested. Each individual plot shows a different way of comparing the data.

Trim Condition – Level Trim



Figure 104: Effective Power Comparison at Level Trim

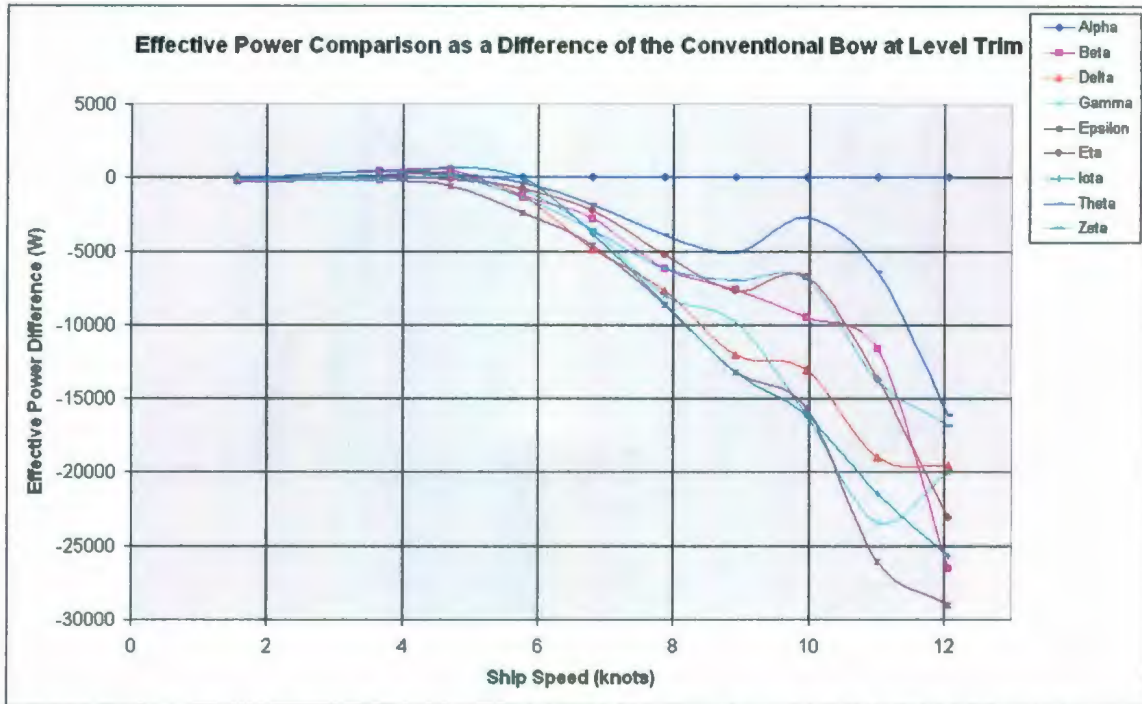


Figure 105: Effective Power Comparison as a Difference of the Conventional Bow at Level Trim

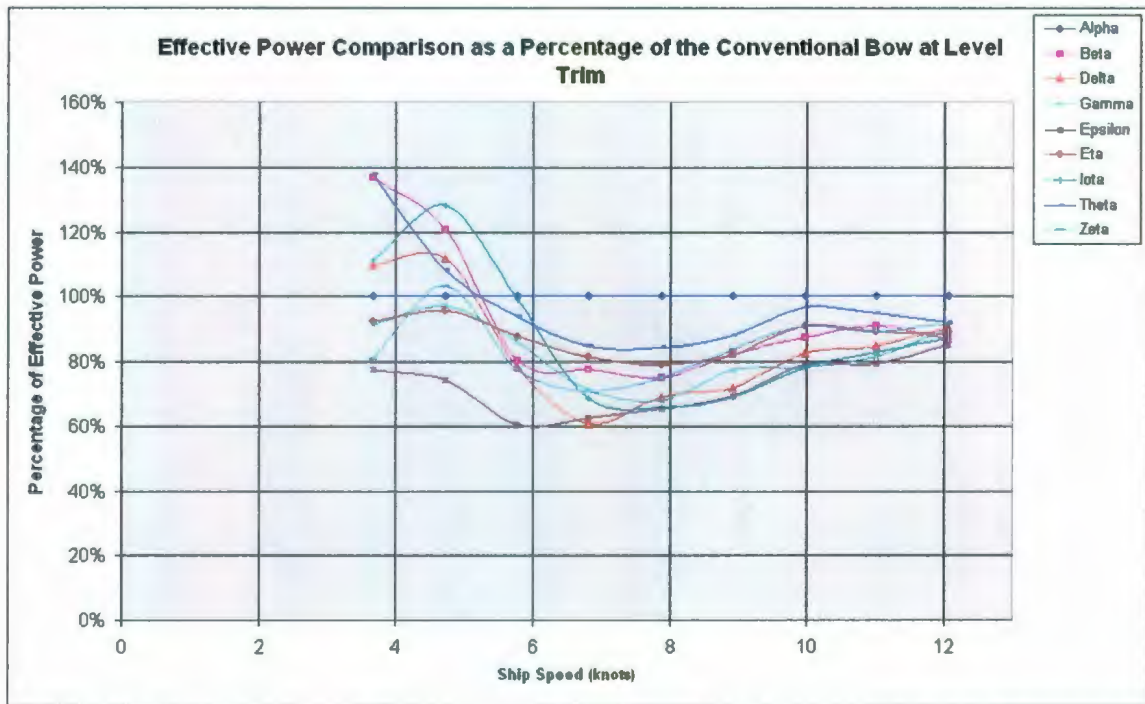


Figure 106: Effective Power Comparison as a Percentage of the Conventional Bow at Level Trim

Table 31: Effective Power Comparison as a Percentage of the Conventional Bow

Percentage of Conventional Bow at Level Trim (%)									
Speed (knots)	Alpha	Beta	Delta	Gamma	Epsilon	Eta	Iota	Theta	Zeta
3.7	100.00	136.62	109.26	91.11	77.51	92.11	110.82	137.78	80.76
4.7	100.00	120.53	111.52	96.91	74.29	95.59	128.03	107.95	103.11
5.8	100.00	80.27	78.15	85.69	60.14	87.41	99.07	93.67	77.41
6.8	100.00	77.33	60.45	70.86	62.30	81.51	68.45	84.55	70.67
7.9	100.00	75.14	68.93	67.76	65.19	78.79	65.62	84.20	75.10
8.9	100.00	82.23	71.81	77.01	69.07	81.99	69.00	88.05	83.67
10.0	100.00	87.15	82.42	78.25	78.83	90.84	78.27	96.33	90.71
11.0	100.00	90.72	84.83	81.32	79.16	89.08	82.91	94.86	89.03
12.1	100.00	86.34	89.95	89.68	85.07	88.11	86.78	91.67	91.32

From above it can be seen that each bulb begins to outperform the conventional bow between 5 – 6 knots (i.e. $F_n = 0.23 - 0.27$), with the exception of Gamma, Epsilon, and Eta (which are actually always below the conventional bow). Above approximately 6 knots all of the bulbous bows outperform the conventional bow from a calm water resistance point of view. This is consistent with what was found in basically all of the experimental papers discussed in the literature review. It is also consistent with what is provided in *Principles of Naval Architecture* (1988).

In the design speed range of 8 – 10 knots ($F_n = 0.36 - 0.45$) reductions in required effective power on the order of 3.7 – 34.2% are found. These are similar numbers to those found in the papers outlined in the experimental section of the literature review. The numbers listed in the various papers in the literature review are for different hull forms and different bulbous bow designs. However, it is reasonable to conclude that the numbers found for reductions in required effective power for this hull form with bulbous bows are in the same range as those found for most of the hulls of studies included in the literature review.

Both Iota and Epsilon bows perform the best from a resistance point of view; with each providing nearly a 35% reduction in required effective power at 8 knots and 21 – 31% reduction at 9 and 10 knots respectively.

The following table provides a ranking of the best bulbous bow based on the average reduction of required effective power in the design speed range for all bows tested at static level trim condition. Also shown are the main parameters of each of the bulbous bows tested.

Table 32: Ranking of Bulbous Bows at Level Trim

Rank	Fairing Type	Added Length (ft)	% A_m (%)	R_F (ft)	A_{TP} (deg)
Iota	None	0.425	29.47	0.236	16.7
Epsilon	S-Shaped	0.59	17.64	0.309	13
Gamma	None	0.59	17.64	0.309	13
Delta	None	0.425	17.64	0.236	16.7
Beta	Straight Line	0.59	17.64	0.309	13
Zeta	S-Shaped	0.425	17.64	0.236	16.7
Eta	Straight Line	0.59	23.48	0.309	13
Theta	Straight Line	0.425	23.48	0.236	16.7

Based on the above table it looks as if one could say that the fairing type does play a major role in the reduction of required effective power. The three bulbs with no fairing are in the top four rankings, and the three bulbs with straight line fairing are in the bottom four.

Interesting comparisons can also be made between bulbs which have only different lengths. Delta and Gamma both have no fairing and a front cross-sectional area of 17.64% of the amidships sectional area; the only difference between the two is the length of each. Between these two bows Gamma bow, which has a longer length, performs an average of about 0.05% better than Delta bow in the design speed range. Looking at the figures above it can be seen that the trends for Delta bow take a slight dip at 9 knots. This could explain why Delta bow performs nearly as well as Gamma bow on average in the design speed range. It may be worthwhile to retest Delta bow around this speed range to ensure the model scale resistance data is satisfactory.

Two more similar comparisons can be made; firstly between Epsilon and Zeta, which both have s-shaped fairings. Between these two bows Epsilon, which has a longer length, performs on average about 12.1% better than Zeta in the design speed range. Finally, a comparison can be made between Eta and Theta; both of these bows have straight line

fairing and a front cross-sectional area of 23.48% of the amidships sectional area. Between these two bows Eta, which has a longer length, performs on average about 5.7% better than Theta in the design speed range.

When all of three of these comparisons are considered it is reasonable to conclude that a bulb with the longer length will outperform a bulb with the shorter length if all other parameters are the same. It should also be noted here that the fairing radius and top profile angle of the bulb both change linearly with bulb length. That is a bulb with a length of 0.425 ft has a fairing radius of 0.236 ft and a top profile slope of 16.7°. Whereas a bulb which has a length of 0.590 ft has a fairing radius of 0.309 ft and a top profile slope of 13°. In order to determine which parameter has the greatest effect on reducing resistance a statistical analysis would likely have to be performed.

Also, from the above table it can clearly be seen that there is some sort of correlation between resistance reduction and the front cross-sectional area of the bulb. With the exception of Iota bow, it can be seen that the bulbs with a front cross-sectional area corresponding to 17.64% of the amidships sectional area are clearly better performers than the bulbs with a front cross-sectional area corresponding to 23.48% of the amidships sectional area. The only direct comparison that can be made is between Beta and Eta bows; these bows have all the same bulb parameters other than the front cross-sectional area. Beta bow, which has a smaller front cross-sectional area, reduces the required effective power by about 2.4% more than Eta bow, which has a larger front cross-sectional area.

Further investigation should be completed into why Iota bulb, with a shorter length and larger front cross-sectional area, performs very well in the design speed range. This may be done by constructing additional bulbous bows with varying front cross-sectional areas, fairing radii as well as top profile angles and testing them in the MUN towing tank. It could also be possibly completed by use of some Computational Fluid Dynamics (CFD) computer simulations.

Trim Condition – 0.75° by Stern



Figure 107: Effective Power Comparison at 0.75° by Stern Trim



Figure 108: Effective Power Comparison as a Difference of the Conventional Bow at Level Trim (All Other Bows at 0.75° by Stern)



Figure 109: Effective Power Comparison as a Percentage of the Conventional Bow at Level Trim (All Other Bows at 0.75° by Stern)

Table 33: Effective Power Comparison as a Percentage of the Conventional Bow at Level Trim (All Other Bows at 0.75° by Stern)

Percentage of Conventional Bow at Level Trim (%)						
Speed (knots)	Alpha	Delta_0.75	Eta_0.75	Iota_0.75	Theta_0.75	Zeta_0.75
3.7	100.00	134.15	124.46	154.24	123.52	103.51
4.7	100.00	130.40	113.67	154.96	130.48	111.72
5.8	100.00	90.54	97.39	114.98	99.26	87.66
6.8	100.00	72.89	88.17	85.85	90.59	69.42
7.9	100.00	72.66	79.32	69.53	83.99	73.99
8.9	100.00	77.55	81.11	69.73	88.37	78.95
10.0	100.00	77.95	80.06	74.79	86.18	80.28
11.0	100.00	80.94	78.47	78.10	84.99	81.12
12.1	100.00	90.27	81.97	86.78	87.44	87.51

From above it can be seen that each bulb begins to outperform the conventional bow somewhere between approximately 5 – 6.5 knots. Above this point and all of the bulbous bows outperform the conventional bow from a resistance point of view.

In the design speed range of 8 – 10 knots Iota bow outperforms all other bows, providing reductions between approximately 25.2 – 30.5% in required effective power.

The following table provides a ranking of the best bulbous bow based on the average reduction of required effective power in the design speed range for all bows tested at 0.75° by the stern trim condition. Also shown are the main parameters of each of the bulbous bows tested.

Table 34: Ranking of Bulbous Bows at 0.75° by Stern

Rank	Fairing Type	Added Length (ft)	% A_m (%)	R_F (ft)	A_{TP} (deg)
Iota_0.75	None	0.425	29.47	0.236	16.7
Delta_0.75	None	0.425	17.64	0.236	16.7
Zeta_0.75	S-Shaped	0.425	17.64	0.236	16.7
Eta_0.75	Straight Line	0.590	23.48	0.309	13
Theta_0.75	Straight Line	0.425	23.48	0.236	16.7

This table again shows that fairing type most likely plays a major role in the ability to reduce the hulls resistance. The two bulbs with no fairing are in the top two rankings, and the two bulbs with straight line fairing are in the bottom two.

Only comparison can be made to determine the effect of bulb length/fairing radius/top profile angle, and that is between Eta and Theta. From this comparison it can be seen that Eta bow, with a longer length, performs on average about 6% better than Theta. So this supports the conclusions from the level trim condition.

There is also a similar relation in the front cross-sectional area and resistance reduction as in the level trim case. Again, further investigation into this phenomenon is warranted.

Trim Condition – 1.5° by Stern



Figure 110: Effective Power Comparison at 1.5° by Stern Trim



Figure 111: Effective Power Comparison as a Difference of the Conventional Bow at Level Trim (All Other Bows at 1.5° by Stern)

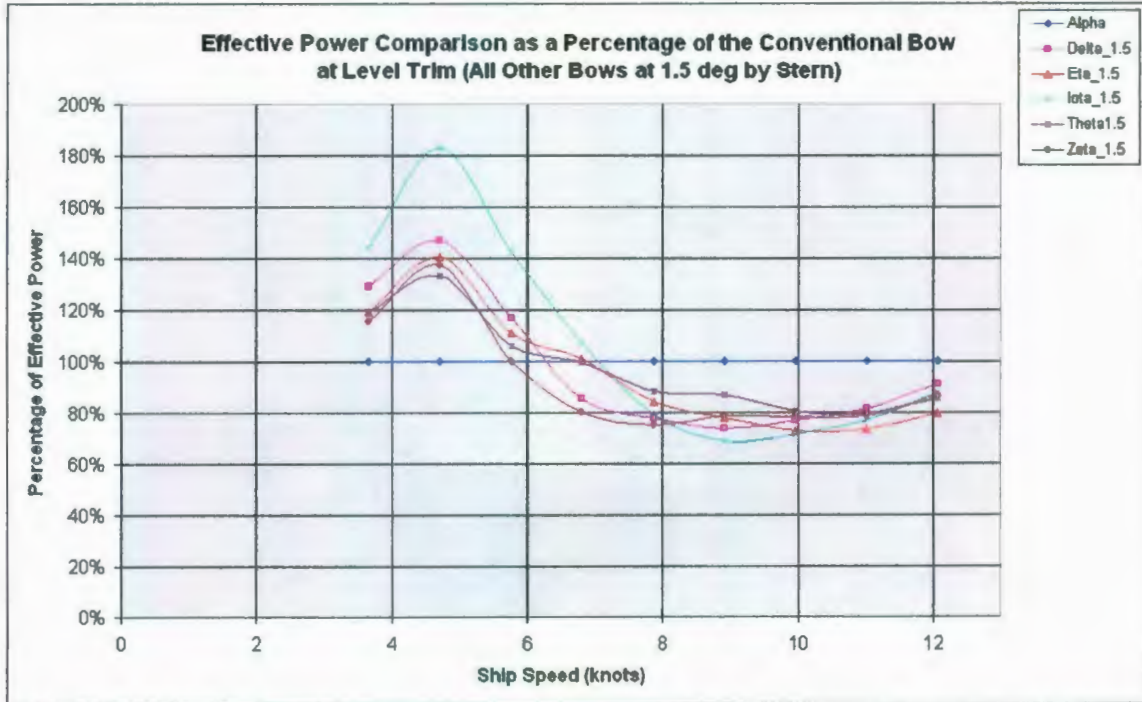


Figure 112: Effective Power Comparison as a Percentage of the Conventional Bow at Level Trim (All Other Bows at 1.5° by Stern)

Table 35: Effective Power Comparison as a Percentage of the Conventional Bow at Level Trim (All Other Bows at 1.5° by Stern)

Percentage of Conventional Bow at Level Trim (%)						
Speed (knots)	Alpha	Delta_1.5	Eta_1.5	Iota_1.5	Theta_1.5	Zeta_1.5
3.7	100.00	128.96	119.27	143.87	118.89	115.32
4.7	100.00	146.66	140.47	182.81	133.22	137.38
5.8	100.00	116.62	110.98	142.08	106.08	100.18
6.8	100.00	85.39	100.88	107.48	99.44	79.93
7.9	100.00	77.56	83.86	79.27	88.12	75.08
8.9	100.00	73.77	77.78	68.68	86.70	78.66
10.0	100.00	76.73	72.93	71.15	80.35	78.12
11.0	100.00	81.56	73.07	76.99	79.54	78.58
12.1	100.00	91.06	79.51	87.58	85.66	86.32

From above it can be seen that each bulb begins to outperform the conventional bow somewhere between approximately 5.5 – 7 knots. Above this point and all of the bulbous bows outperform the conventional bow from a resistance point of view.

In the design speed range of 8 – 10 knots Iota bow outperforms all other bows, providing reductions between approximately 20.7 – 31.3% in required effective power.

The following table provides a ranking of the best bulbous bow based on the average reduction of required effective power in the design speed range for all bows tested at 1.5° by the stern trim condition. Also shown are the main parameters of each of the bulbous bows tested.

Table 36: Ranking of Bulbous Bows at 1.5° by Stern

Rank	Fairing Type	Added Length (ft)	% A_m (%)	R_F (ft)	A_{TP} (deg)
Iota_1.5	None	0.425	29.47	0.236	16.7
Delta_1.5	None	0.425	17.64	0.236	16.7
Zeta_1.5	S-Shaped	0.425	17.64	0.236	16.7
Eta_1.5	Straight Line	0.590	23.48	0.309	13
Theta_1.5	Straight Line	0.425	23.48	0.236	16.7

These are the exact same bulb rankings as for the 0.75° by stern trim condition. Therefore, all of the same conclusions can be applied to this trim condition.

Optimal Trim Conditions

It is also useful to determine the optimal trim condition for each bow at each speed tested. The following table outlines the best trim condition for each of the bows tested. Note here that Beta, Gamma, and Epsilon bows are not shown in this section; as they were only tested at level trim during the MUN resistance tests.

Table 37: Optimal Trim Conditions for Each Bow

Optimal Trim Condition					
Speed (knots)	Delta	Eta	Iota	Theta	Zeta
1.6	level trim	level trim	0.75° by stern	1.5° by stern	0.75° by stern
3.7	level trim	level trim	level trim	1.5° by stern	level trim
4.7	level trim	level trim	level trim	level trim	level trim
5.8	level trim	level trim	level trim	level trim	level trim
6.8	level trim	level trim	level trim	level trim	0.75° by stern
7.9	level trim	level trim	level trim	0.75° by stern	0.75° by stern
8.9	level trim	1.5° by stern	level trim	1.5° by stern	1.5° by stern
10.0	1.5° by stern	1.5° by stern	1.5° by stern	1.5° by stern	1.5° by stern
11.0	0.75° by stern	1.5° by stern	1.5° by stern	1.5° by stern	1.5° by stern
12.1	level trim	1.5° by stern	level trim	1.5° by stern	1.5° by stern

In general it can be seen that at lower speeds it is better to operate the vessel at static level trim. However, around the design speed range of 8 – 10 knots it is generally better to have the vessel trimmed by the stern from a resistance point of view.

The following figure and table provide a percentage comparison of the optimal effective power for each bow to the conventional bow at level trim.

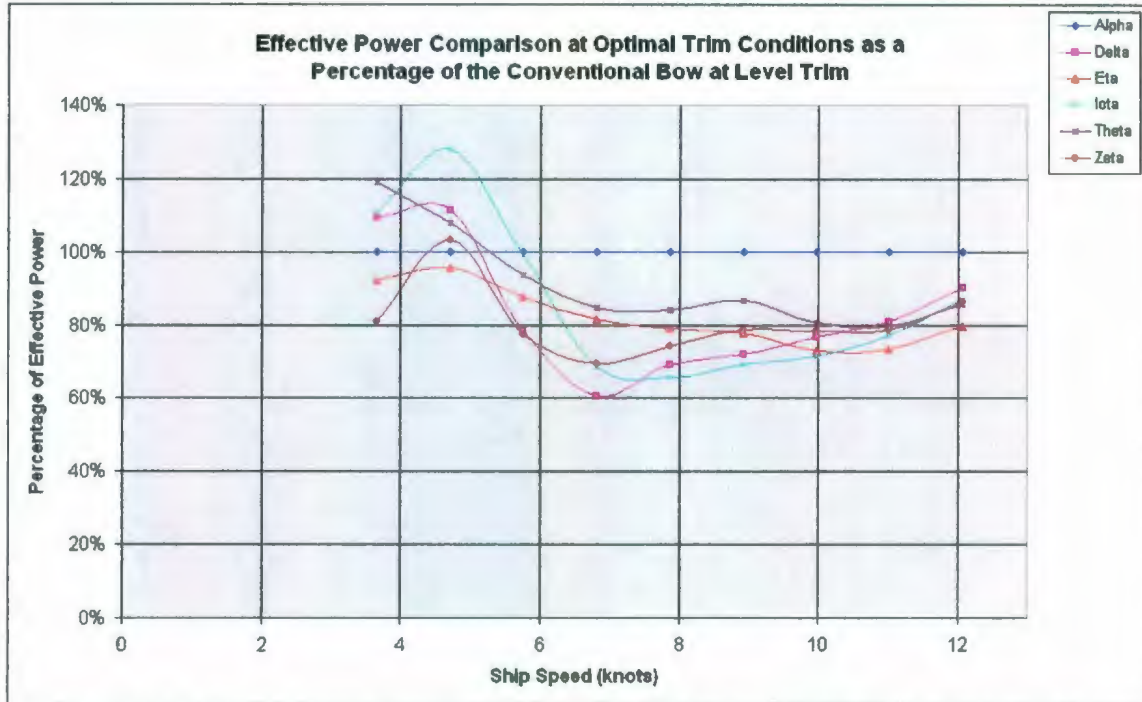


Figure 113: Effective Power Comparison at Optimal Trim Conditions as a Percentage of the Conventional Bow at Level Trim

Table 38: Effective Power Comparison at Optimal Trim Conditions as a Percentage of the Conventional Bow at Level Trim

Speed (knots)	Percentage of Conventional Bow at Level Trim (%)					
	Alpha Level Trim	Delta Optimal Trim	Eta Optimal Trim	Iota Optimal Trim	Theta Optimal Trim	Zeta Optimal Trim
3.7	100.00	109.26	92.11	110.82	118.89	80.76
4.7	100.00	111.52	95.59	128.03	107.95	103.11
5.8	100.00	78.15	87.41	99.07	93.67	77.41
6.8	100.00	60.45	81.51	68.45	84.55	69.42
7.9	100.00	68.93	78.79	65.62	83.99	73.99
8.9	100.00	71.81	77.78	69.00	86.70	78.66
10	100.00	76.73	72.93	71.15	80.35	78.12
11	100.00	80.94	73.07	76.99	79.54	78.58
12.1	100.00	89.95	79.51	86.78	85.66	86.32

It can be seen from this that each bulbous bow begins to outperform the conventional bow between 5 – 6 knots, except for Eta bow (which is always below the conventional bow). Also, in the design speed range of 8 – 10 knots Iota bow tends to perform the best; providing approximately a 28.9 – 34.4% reduction in required effective power. Delta provides anywhere between a 23.3 – 31.1% reduction in the same speed range.

Again, note here that Beta, Gamma, and Epsilon data are not provided within this section as they were only tested at level trim. Both Gamma and Epsilon would most likely outperform Delta bow, and Epsilon would likely be as effective as Iota bow in reducing the required effective power.

6.8.4 Dynamic Trim Results

The following section shows comparisons of the model dynamic trim for each bow at each static trim condition tested. Note that the static trim condition is not actually shown in each plot, that is each plot starts at zero degrees. Also note that negative values signify the model trimming by the head and positive trimming by the stern.

Trim Condition – Level Trim

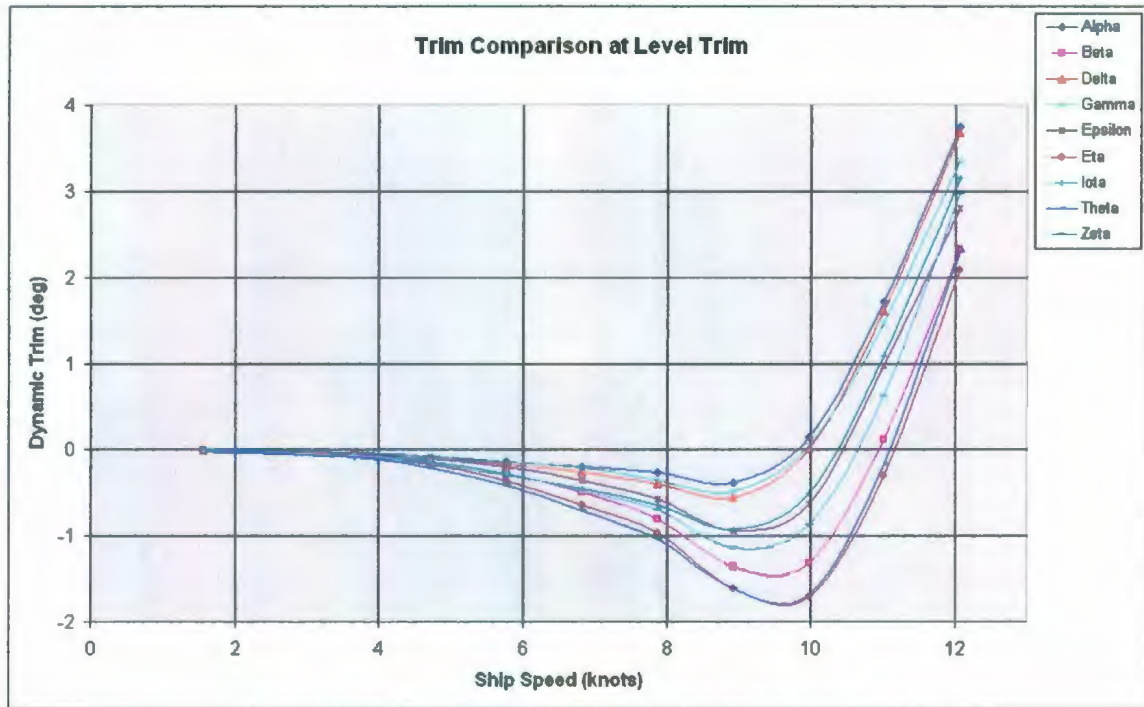


Figure 114: Dynamic Trim Comparison at Static Level Trim

From the above figure it can be seen that all bows have a tendency to trim by the head up to between 8.75 – 9.65 knots ($F_n = 0.39 - 0.44$) and then drastically begin to trim more and more by the stern with increasing speed. Again, this is fairly consistent with the study conducted by Johnson (1958) where it was found that the model would trim by the head up to $F_n = 0.35 - 0.37$. Similarly, the study conducted by Friis et al. found that the model would trim by the head up to $F_n = 0.36 - 0.43$.

Eta, Theta, and Beta bows all have a maximum trim by the head at approximately 9.5 knots. Epsilon, Iota, and Zeta bows all have a maximum at approximately 9 knots. Alpha, Delta, and Gamma bows have a maximum around 8.5 knots.

The following table shows the ranking of each bulb tested with respect to the speed at which the maximum trim by the head occurs. So, for example, Eta bow is ranked number one because it has a maximum trim by the head at the highest speed. Likewise, Gamma

bow is ranked last as it has a maximum trim by the head at the lowest speed of all the bulbous bows.

Note that in the following series of tables ‘top bulb area’ is the extra waterplane area added due to the presence of each bulb respectively. ‘Bulb submergence’ is taken as the added underwater volume due to the presence of each bulb respectively. This is calculated by determining the underwater volume with each bulb attached and subtracting the underwater volume with the conventional bow attached. This will then yield only the underwater volume of each bulb respectively.

Table 39: Ranking of Bulbous Bows in Order of Speed at which Maximum Trim by the Head Occurs at Static Level Trim

Speed of Max Trim by Head - Static Level Trim					
Rank	Speed (knots)	Added Length (ft)	% A_m (%)	Top Bulb Area (ft ²)	Bulb Submergence (ft ³)
Eta	9.65	0.590	23.48	0.5215	0.2788
Theta	9.65	0.425	23.48	0.4315	0.2304
Beta	9.5	0.590	17.64	0.4348	0.2390
Zeta	9.15	0.425	17.64	0.2360	0.1599
Epsilon	9.05	0.590	17.64	0.2745	0.1832
Iota	8.9	0.425	29.47	0.2194	0.1554
Delta	8.75	0.425	17.64	0.1135	0.0843
Gamma	8.75	0.590	17.64	0.1458	0.1035

From the above table there seems to be a strong correlation between both the top bulb area and bulb submergence with the speed at which maximum trim by the head occurs.

A plot showing the speed at which maximum trim by the head is reached vs. both the top bulb area and bulb submergence is shown below. Regression lines are fit through both sets of data to determine the goodness of fit. The regression lines fitted for both the top bulb area and bulb submergence shows that there is a strong correlation between both the top bulb area and bulb submergence with the speed at which maximum trim by the head occurs.

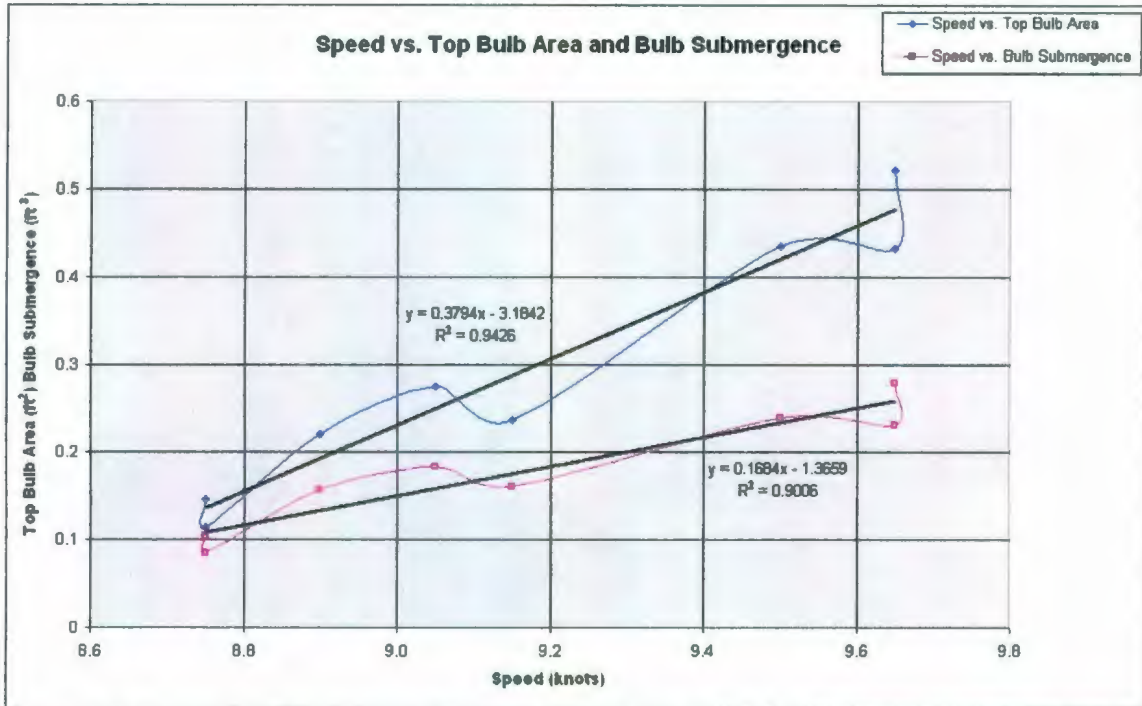


Figure 115: Regression Lines through Comparisons of Speed of Maximum Trim by the Head vs. Top Bulb Area and Bulb Submergence

A ranking can also be completed for the maximum magnitude of the trim by the head, as is shown in the following table.

Table 40: Ranking of Bulbous Bows in Order of the Magnitude of Maximum Trim by the Head at Static Level Trim

Magnitude of Max Trim by Head - Static Level Trim					
Rank	Max Trim (deg)	Added Length (ft)	% A_m (%)	Top Bulb Area (ft ²)	Bulb Submergence (ft ³)
Eta	1.82	0.590	23.48	0.5215	0.2788
Theta	1.8	0.425	23.48	0.4315	0.2304
Beta	1.46	0.590	17.64	0.4348	0.2390
Zeta	1.15	0.425	17.64	0.2360	0.1599
Epsilon	0.95	0.590	17.64	0.2745	0.1832
Iota	0.93	0.425	29.47	0.2194	0.1554
Delta	0.59	0.425	17.64	0.1135	0.0843
Gamma	0.51	0.590	17.64	0.1458	0.1035

From this table it can be seen that there is the exact same ranking as that for the speed of maximum trim by the head. So there also seems to be a correlation between both the top bulb area and bulb submergence with the magnitude of maximum trim by the head.

The following plot shows the maximum trim by the head vs. both the top bulb area and bulb submergence. The regression lines fitted for both the top bulb area and bulb submergence shows that there is a strong correlation between both the top bulb area and bulb submergence with the maximum trim by the head.

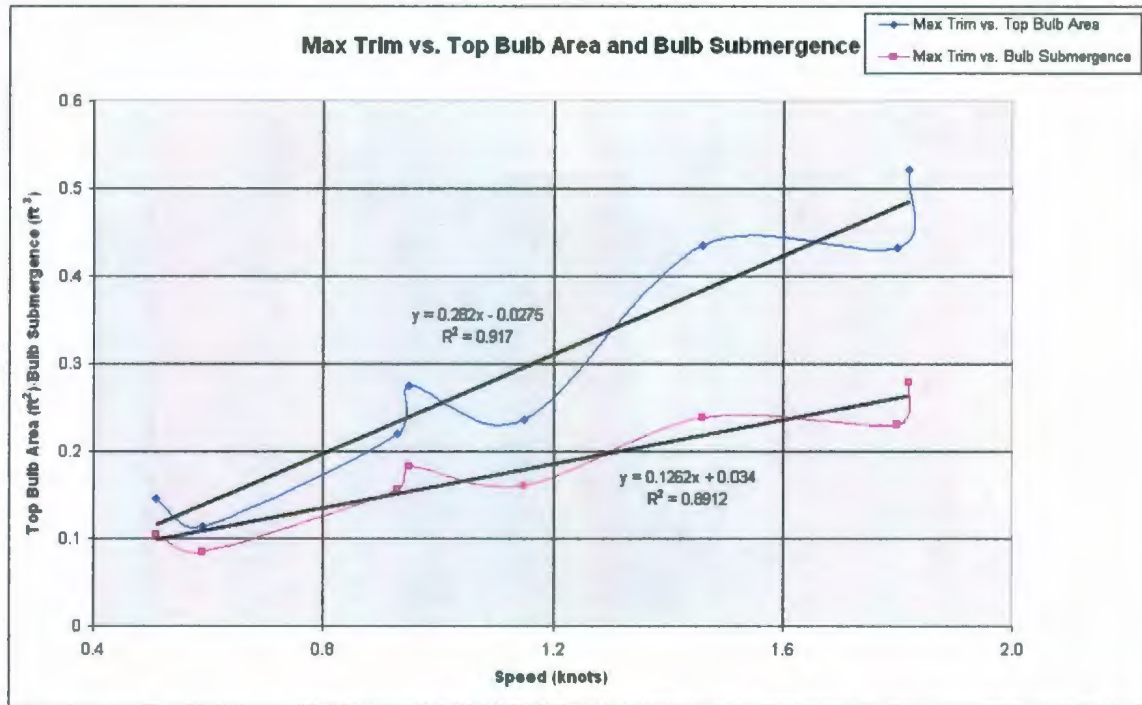


Figure 116: Regression Lines through Comparisons of Maximum Trim by the Head vs. Top Bulb Area and Bulb Submergence

These results along with those from the IOT bare hull resistance tests as well as previous testing by Johnson (1958) and Friis et al. (2008) indicate that dynamic trim by the head is likely a function of bulb submergence, top bulb area and pressure distribution around the stern section. Again, the possible explanations are given below:

- The presence of a bulb at the stem causes an increase in water velocity around the fore body of the model (i.e. the water has to speed up to get around the added volume of the bulb). The increase in water velocity results in a reduction of pressure in the area around the bow of the model. This reduction of pressure then translates into a reduction in ‘lift’ at the bow section, which means that the bow section tends to trim further into the water.

- The presence of a bulb at the stern causes a beaching effect with increasing speed, where water flows up onto the top of the bulb. The flowing water over the top of the bulb then provides a downward force on the bulb, thereby forcing the bulb further down into the water.
- The flow past the hull causes an area of high velocity at the stern due to the streamlines closing in; which in turn reduces the pressure at the stern. As hull speed is increased the magnitude of this low pressure is increased, thereby causing even lower pressure at the stern section. This results in 'suction' at the stern section which tends to pull the stern section of the hull further into the water.

Trim Condition – 0.75° by Stern

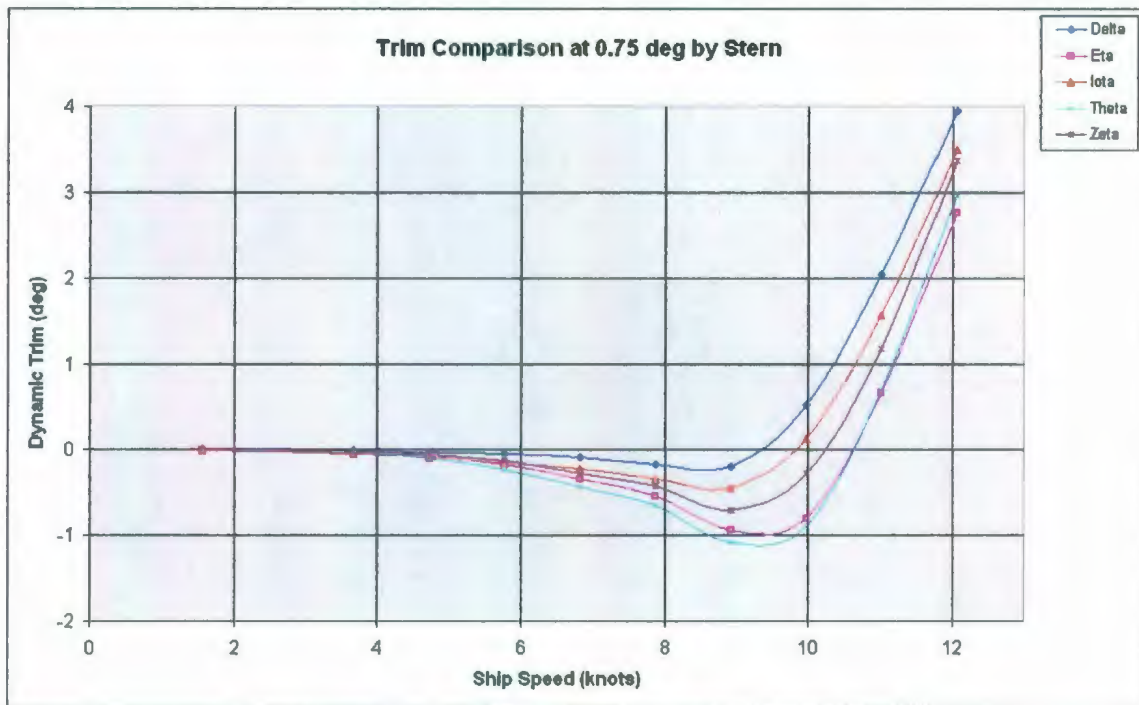


Figure 117: Dynamic Trim Comparison at 0.75° by Stern Trim

Here a similar trend is found for the 0.75° by the stern condition as was seen in the level trim condition. Theta and Eta bows provide a larger trim by the head than does Iota and Delta bows; although all are much smaller magnitudes than was seen in the static level

trim condition. The generally lower magnitude of dynamic trimming by the head is likely attributed to less bulb submergence.

The following two tables show rankings of the speed at which the maximum trim by the head occurs as well as the maximum magnitude of the trim by the head.

Table 41: Ranking of Bulbous Bows in Order of Speed at which Maximum Trim by the Head Occurs at 0.75° by Stern Trim Condition

Speed of Max Trim by Head - 0.75° by Stern					
Rank	Speed (knots)	Added Length (ft)	% A _m (%)	Top Bulb Area (ft ²)	Bulb Submergence (ft ³)
Eta	9.4	0.590	23.48	0.5215	0.2788
Theta	9.35	0.425	23.48	0.4315	0.2304
Zeta	8.9	0.425	17.64	0.2360	0.1599
Iota	8.65	0.425	29.47	0.2194	0.1554
Delta	8.5	0.425	17.64	0.1135	0.0843

Table 42: Ranking of Bulbous Bows in Order of the Magnitude of Maximum Trim by the Head at 0.75° by Stern Trim Condition

Magnitude of Max Trim by Head - 0.75° by Stern					
Rank	Max Trim (deg)	Added Length (ft)	% A _m (%)	Top Bulb Area (ft ²)	Bulb Submergence (ft ³)
Theta	1.11	0.425	23.48	0.4315	0.2304
Eta	0.98	0.590	23.48	0.5215	0.2788
Zeta	0.71	0.425	17.64	0.2360	0.1599
Iota	0.48	0.425	29.47	0.2194	0.1554
Delta	0.25	0.425	17.64	0.1135	0.0843

From the above tables it can be seen that similar results are found for this trim condition as was found for the static level trim condition. Again, there seems to be a correlation between both the top bulb area and bulb submergence with the speed at which maximum trim by the head occurs as well as the magnitude of maximum trim by the head. In general, as both the top bulb area and bulb submergence decreases both the speed at which maximum trim by the head occurs as well as the magnitude of maximum trim by the head tends to decrease.

Trim Condition – 1.5° by Stern

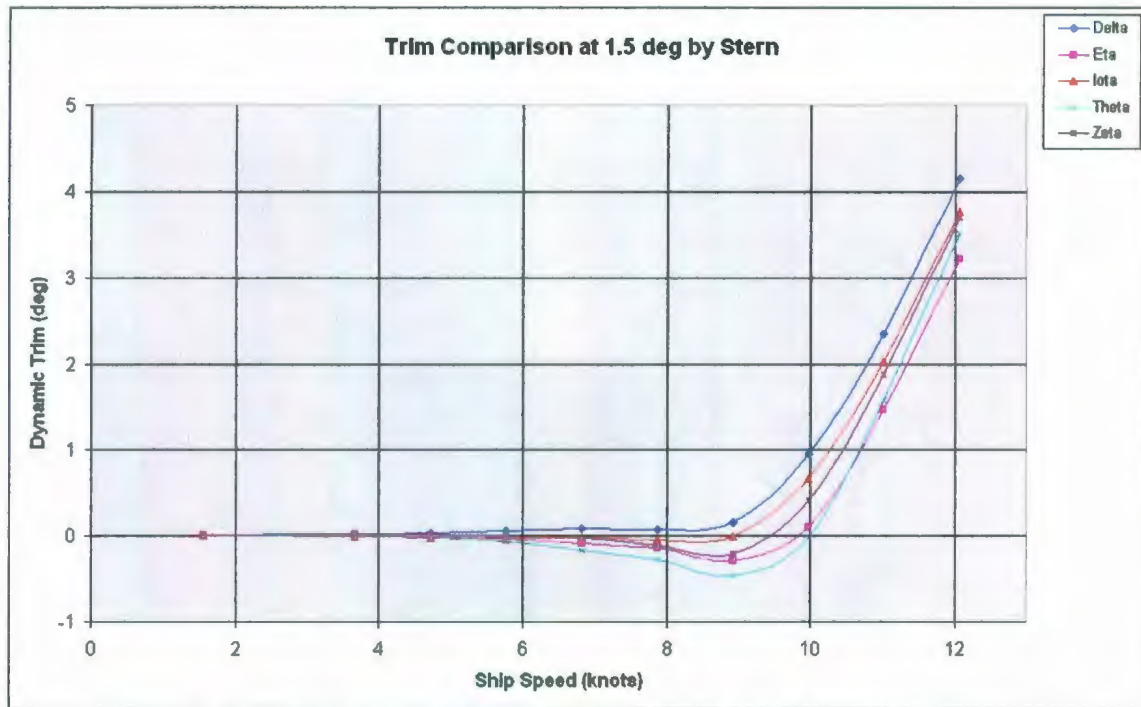


Figure 118: Dynamic Trim Comparison at 1.5° by Stern Trim

Once again a similar trend is found for the 1.5° by the stern condition as was seen in the first two trim conditions. There are much smaller magnitudes of trim by the head in this condition than was seen in either of the first two. The lower magnitude of dynamic trimming by the head is likely attributed to less bulb submergence.

The following two tables show rankings of the speed at which the maximum trim by the head occurs as well as the maximum magnitude of the trim by the head.

Table 43: Ranking of Bulbous Bows in Order of Speed at which Maximum Trim by the Head Occurs at 1.5° by Stern Trim Condition

Speed of Max Trim by Head - 1.5° by Stern					
Rank	Speed (knots)	Added Length (ft)	% A_m (%)	Top Bulb Area (ft ²)	Bulb Submergence (ft ³)
Theta	8.85	0.425	23.48	0.4315	0.2304
Eta	8.8	0.590	23.48	0.5215	0.2788
Zeta	8.65	0.425	17.64	0.2360	0.1599
Iota	8.4	0.425	29.47	0.2194	0.1554
Delta	-	0.425	17.64	0.1135	0.0843

Table 44: Ranking of Bulbous Bows in Order of the Magnitude of Maximum Trim by the Head at 1.5° by Stern Trim Condition

Magnitude of Max Trim by Head - 1.5° by Stern					
Rank	Max Trim (deg)	Added Length (ft)	% A_m (%)	Top Bulb Area (ft ²)	Bulb Submergence (ft ³)
Theta	0.48	0.425	23.48	0.4315	0.2304
Eta	0.3	0.590	23.48	0.5215	0.2788
Zeta	0.24	0.425	17.64	0.2360	0.1599
Iota	0.08	0.425	29.47	0.2194	0.1554
Delta	-	0.425	17.64	0.1135	0.0843

These are similar bulb rankings as for the 0.75° by stern trim condition. Therefore, all of the same conclusions can be applied to this trim condition.

Individual Bulbs

It is also possible to look at the dynamic trim for each of the bulbs tested individually. The following five plots show each bow tested in static level trim, 0.75° by stern, as well as 1.5° by stern condition at MUN.

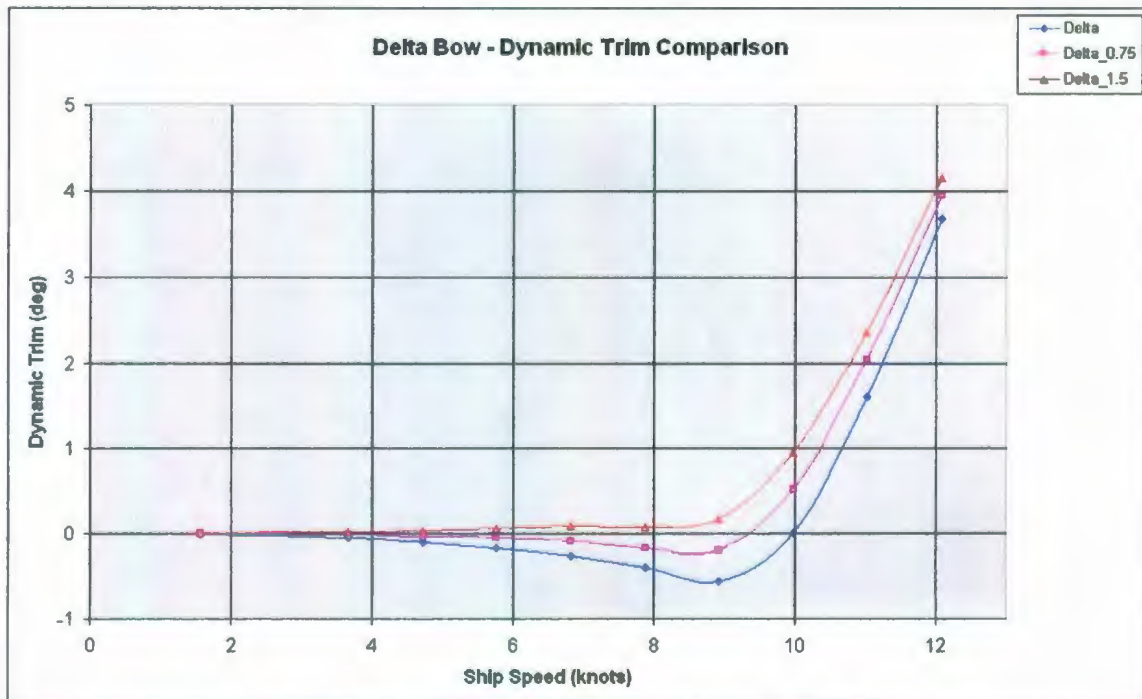


Figure 119: Dynamic Trim Comparison for Delta Bow

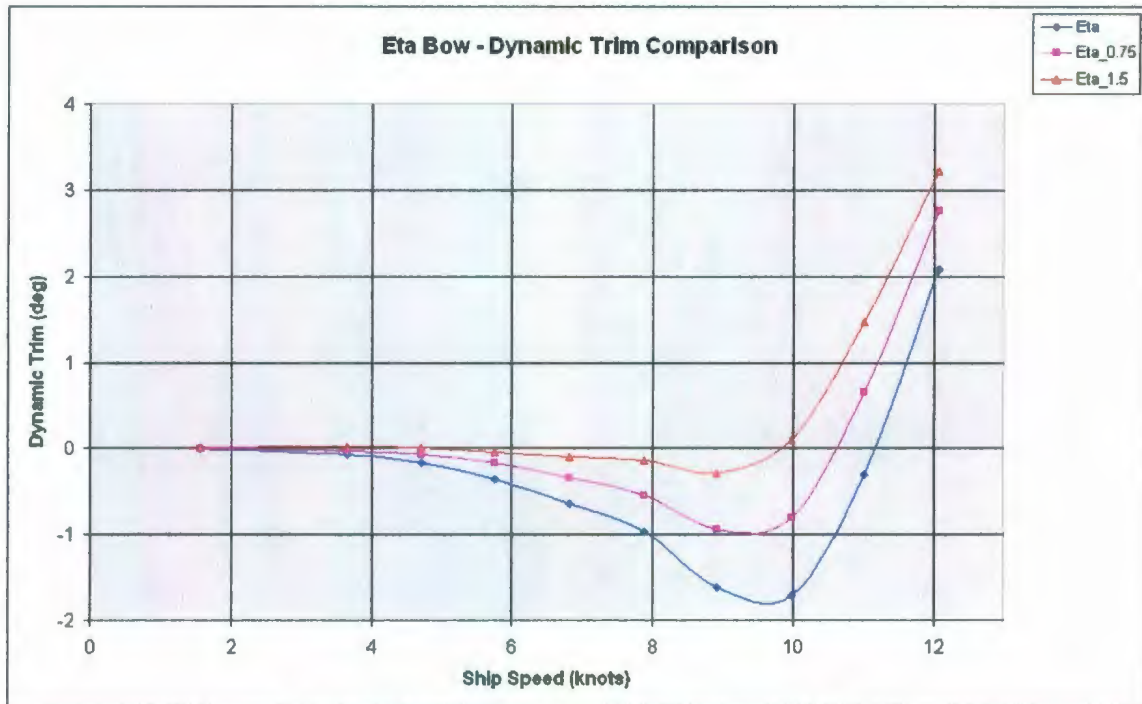


Figure 120: Dynamic Trim Comparison for Eta Bow

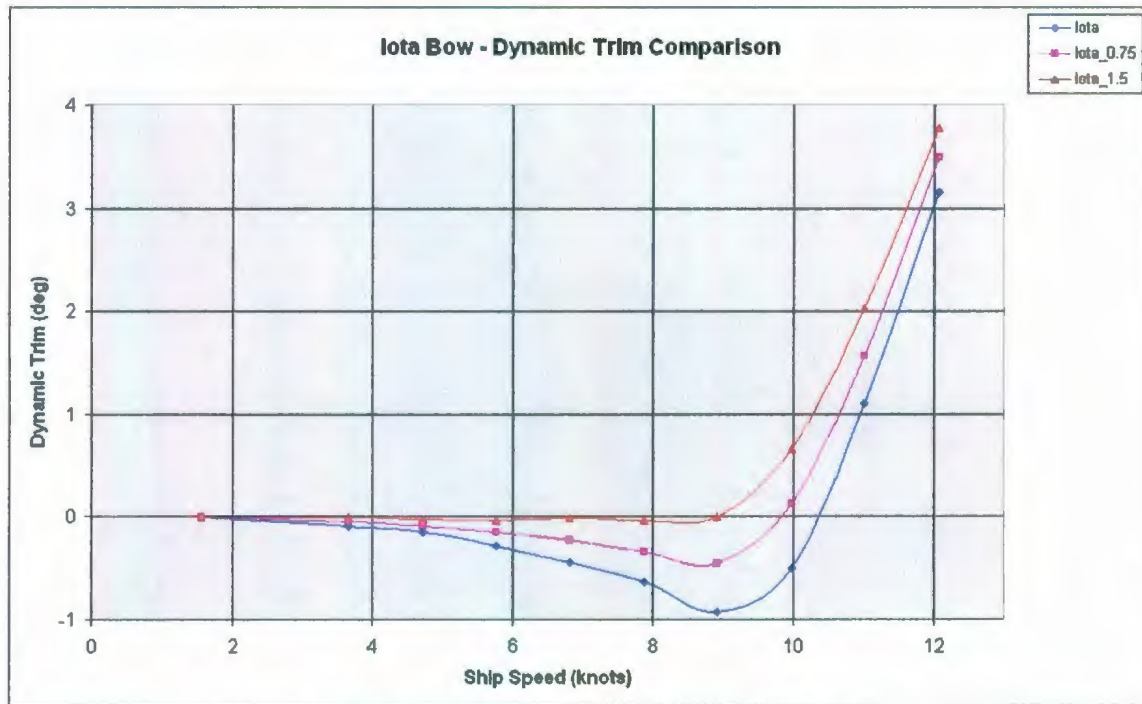


Figure 121: Dynamic Trim Comparison for Iota Bow

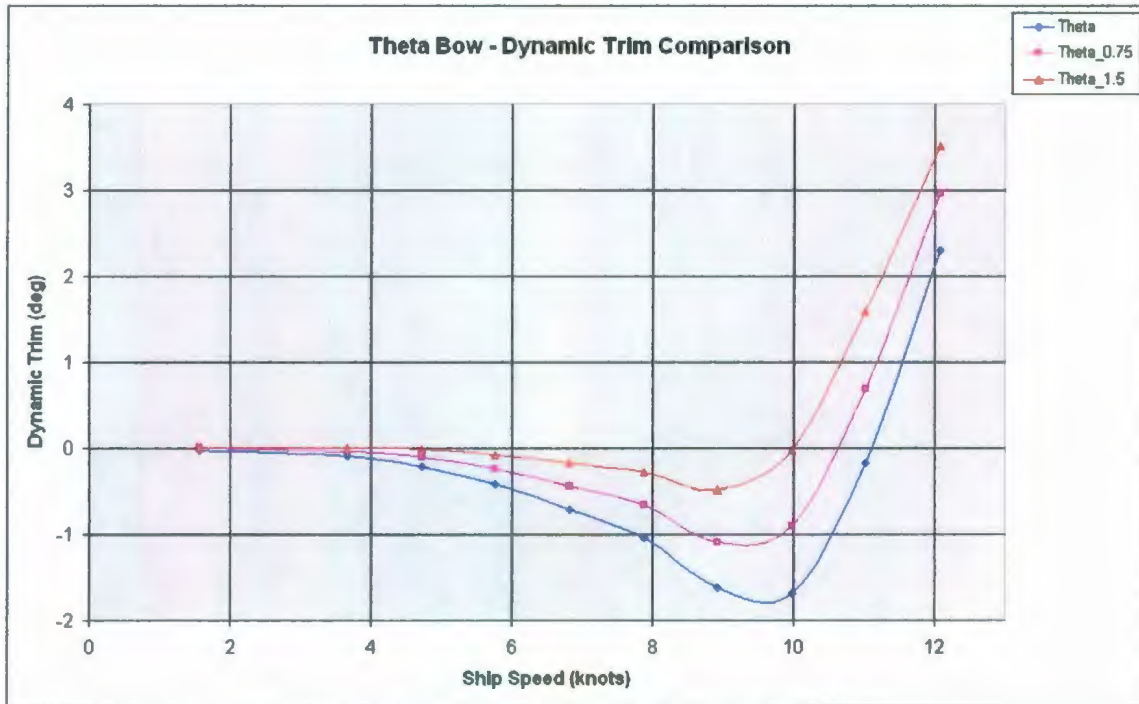


Figure 122: Dynamic Trim Comparison for Theta Bow

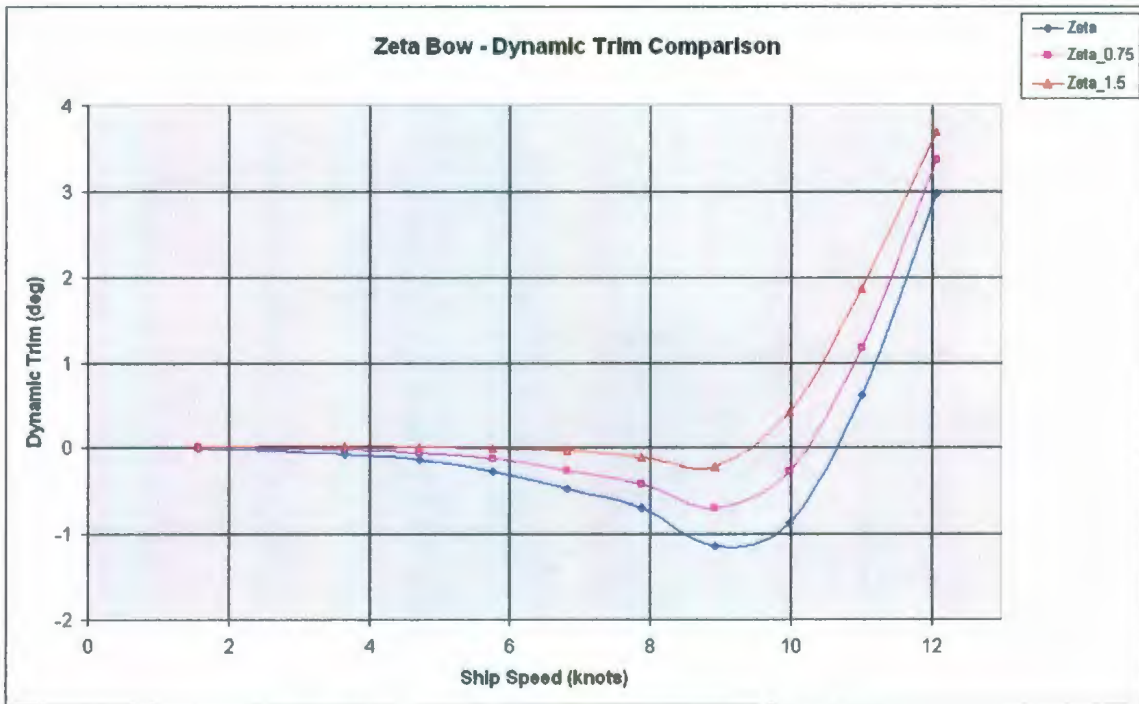


Figure 123: Dynamic Trim Comparison for Zeta Bow

From the above five figures it can be seen that with any bulb as the static trim angle increases the magnitude of dynamic trim by the head as well as the speed at which the maximum trim by the head occurs tend to decrease significantly. Take Zeta bow for

example, the following table provides a breakdown of the magnitude of maximum dynamic trim by the head as well as the speed at which this maximum occurs for each static trim condition tested.

Table 45: Breakdown of Dynamic Trim for Zeta Bow

Dynamic Trim for Zeta Bow		
Static Trim Angle (deg)	Max Trim (deg)	Speed of Max Trim (knots)
0.0	1.15	9.15
0.75	0.71	8.9
1.5	0.25	8.65

The above table shows that there is definitely a strong correlation between the initial trim angle and the maximum magnitude of dynamic trim by the head. It also suggests that there is a correlation between the initial trim angle and speed of the maximum trim by the head. Similar results are found for each of the bulbs tested.

It is known that as the initial trim angle by the stern is increased the bulb submergence is reduced while the top bulb area increases. It was suggested that if the top bulb area is increased then the magnitude of maximum dynamic trim by the head should also increase; which is not what is found here.

However, the correlation between top bulb area and dynamic trim by the head may not be the best comparison in this case. The relationship between water flow over the top of the bulb with dynamic trim is likely a more suitable comparison. It is known from pictures taken during testing that as the static trim by the stern is increased that the water flow over the top of the bulb is generally reduced. This will result in less downward force acting on the top of the bulb, and act as if the 'top bulb area' is reduced.

The results from the individual bulbs then agree with the results from bulb comparisons for each static trim condition. That is the dynamic trim is likely a function bulb submergence, top bulb area, and pressure distribution around the stern section.

6.8.5 Sinkage Results

The following section shows comparisons of the model sinkage for each bow at each static trim condition tested. Note here that negative values signify the model squatting down at speed.

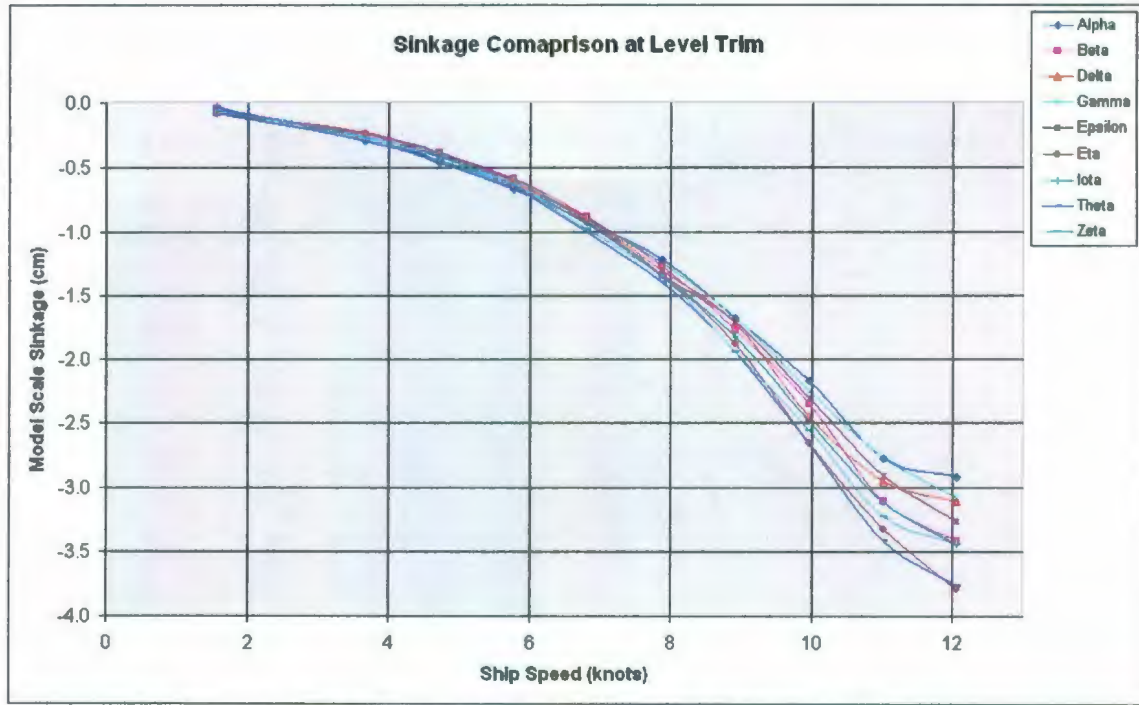


Figure 124: Sinkage Comparison at Static Level Trim

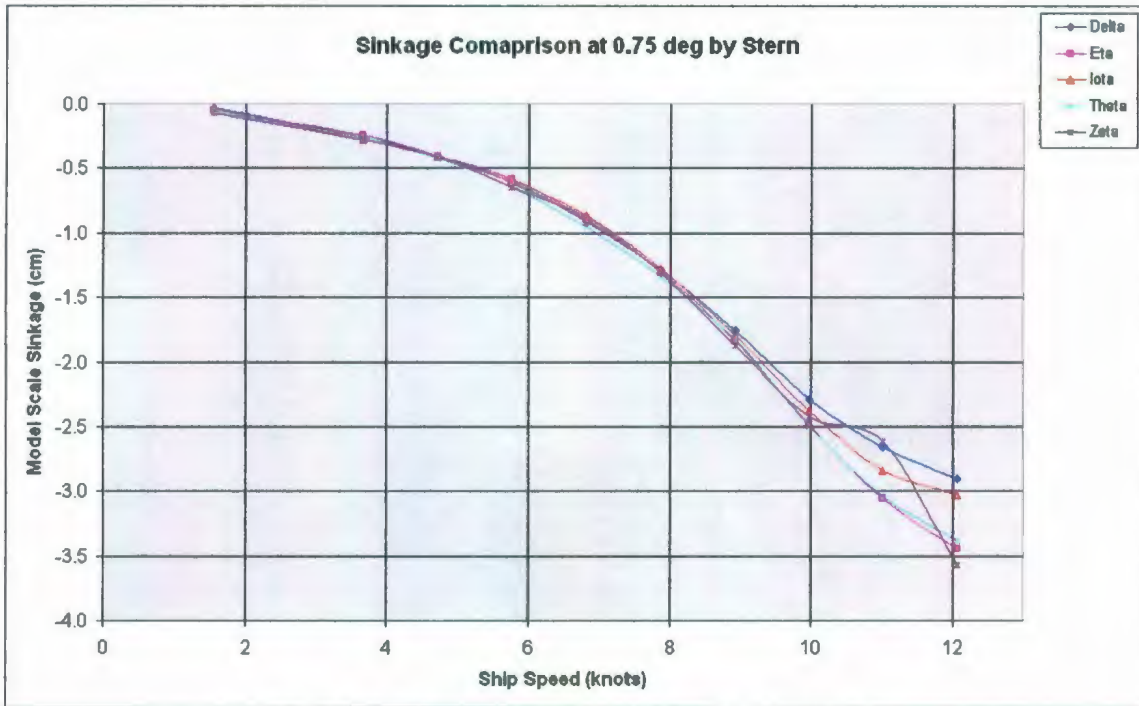


Figure 125: Sinkage Comparison at 0.75° by Stern Trim

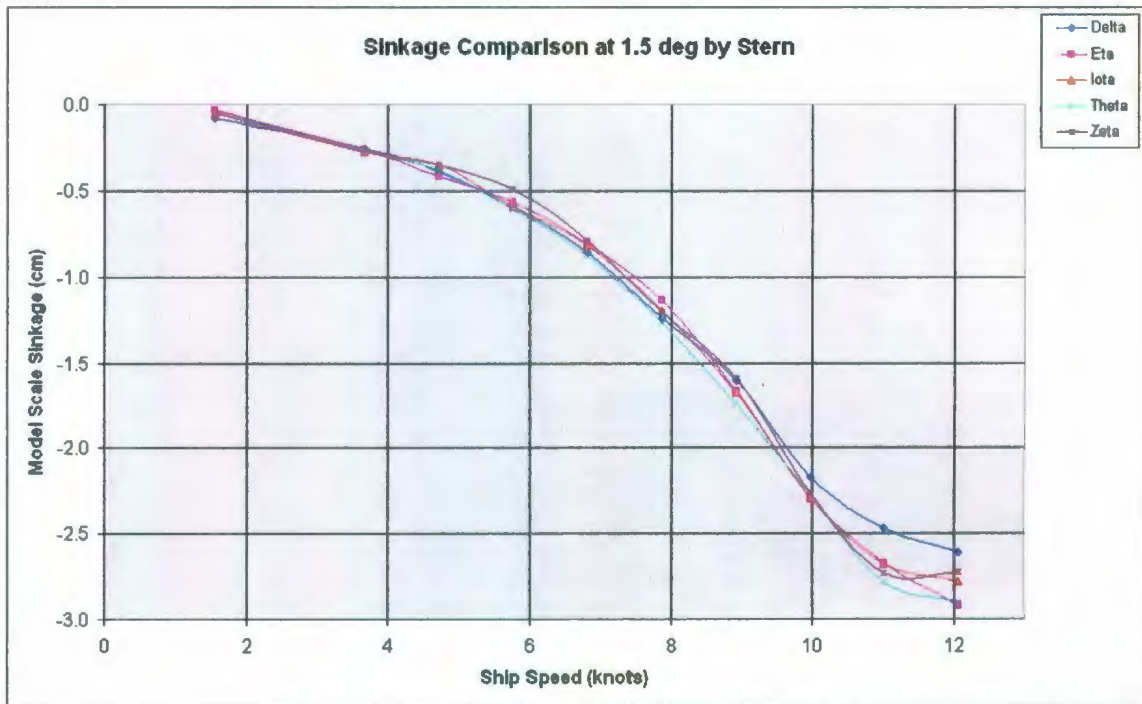


Figure 126: Sinkage Comparison at 1.5° by Stern Trim

From the above figures it can be seen that all bows tend to sink, or 'squat', down at an increasing rate with increasing speed. Upon examining the results it was found that there is some correlation between the top bulb area and bulb submergence of each bulbous bow

with the magnitude of sinkage. For each trim condition at lower speeds, say 7 knots and below, it was found that no real correlation exists. This may be due to the fact that there are small magnitudes of sinkage below these speeds. However, above these speeds there seems to be a definite correlation between the magnitude of sinkage with both the top bulb area and bulb submergence. It was found that there is a general trend of higher magnitudes of sinkage with increasing top bulb area and bulb submergence. This was found for each trim condition tested.

Again, these results along with those found in the IOT bare hull resistance tests as well as previous testing by Johnson (1958) and Friis et al. (2008) indicate that model sinkage is likely a function of bulb submergence, top bulb area and pressure distribution around the stern section.

Individual Bulbs

It is also possible to look at the sinkage for each of the bulbs tested individually. The following five plots show each bow tested in static level trim, 0.75° by stern, as well as 1.5° by stern condition at MUN.

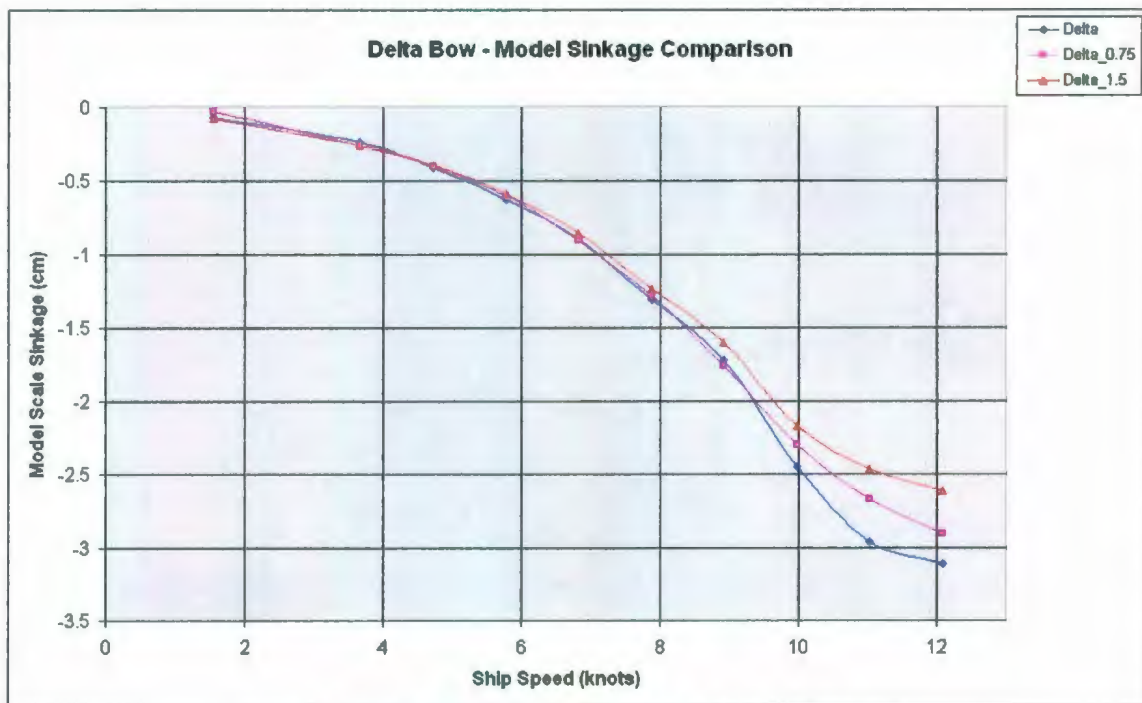


Figure 127: Sinkage Comparison for Delta Bow

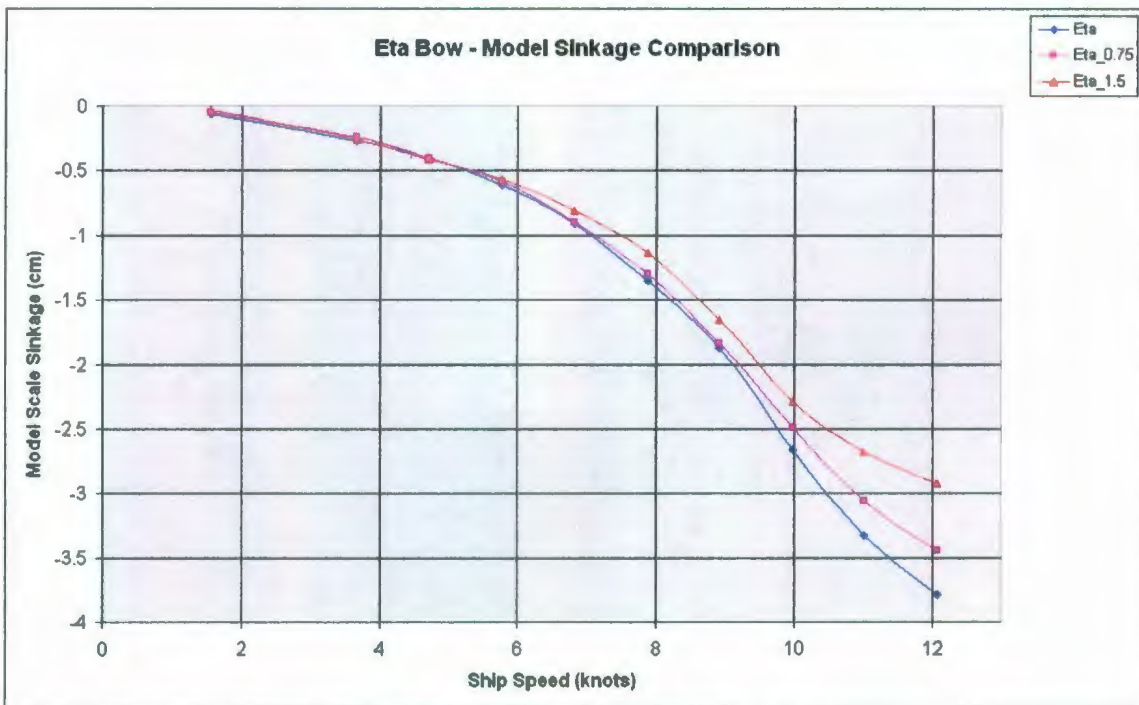


Figure 128: Sinkage Comparison for Eta Bow

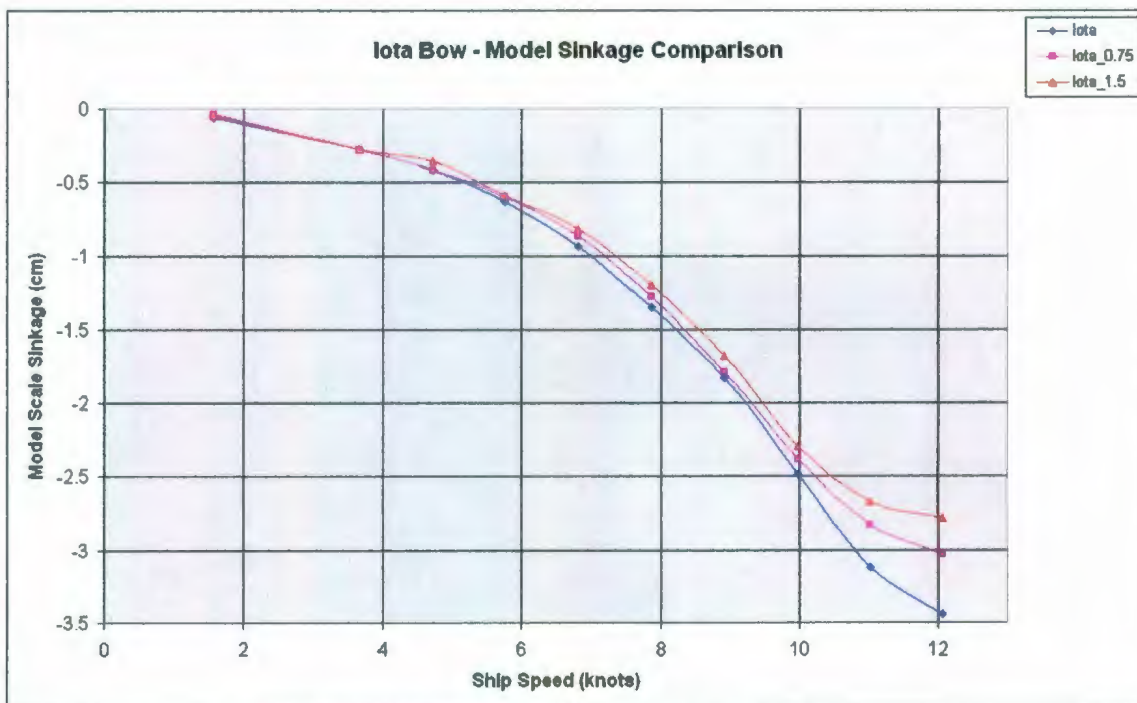


Figure 129: Sinkage Comparison for Iota Bow

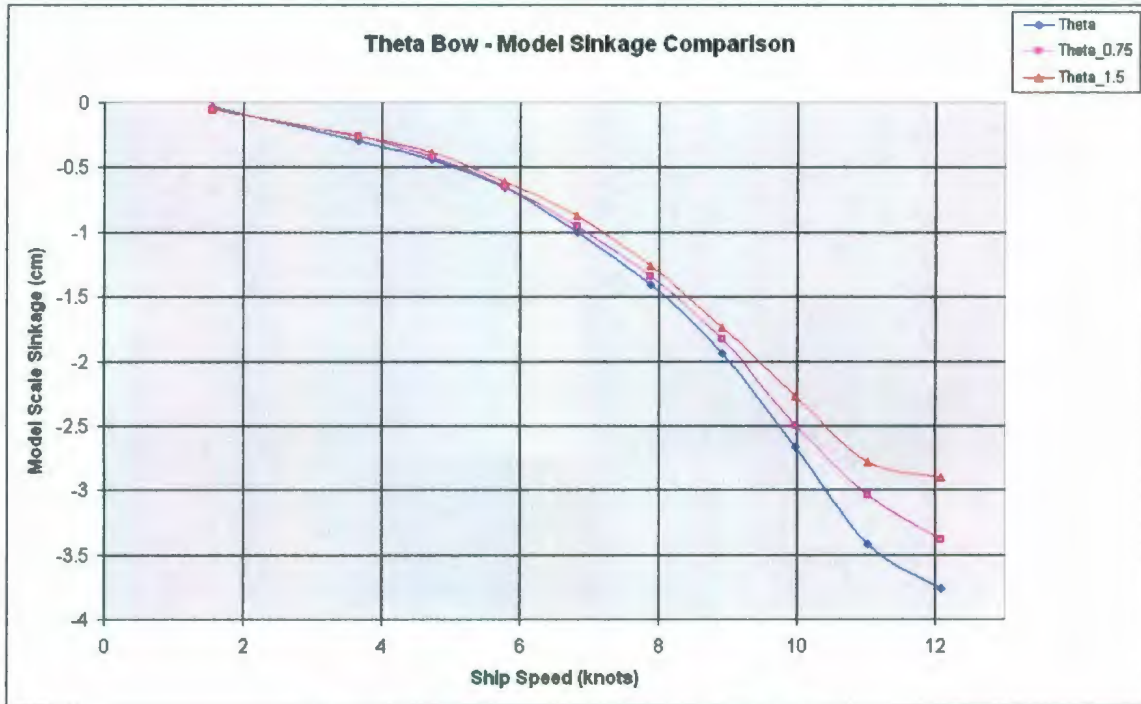


Figure 130: Sinkage Comparison for Theta Bow



Figure 131: Sinkage Comparison for Zeta Bow

From the above five figures it can be seen that with any bulb as the static trim angle increases the magnitude of model sinkage tends to decrease. Similar conclusions can be drawn here as for the dynamic trim results for individual bulbs. That is there is a

correlation between the water flow over the top of the bulb with the magnitude of model sinkage. As the water flow is decreased the magnitude of model sinkage also decreases.

This means that the model sinkage and dynamic trim by the head are both functions of pressure distributions around the hull; and maybe more importantly the pressure distributions around the bow and stern sections.

To reiterate the conclusion from the IOT bare hull resistance tests results, it may be possible to complete resistance tests on each of the bows with pressure sensors placed on the underwater portion of the hull, with emphasis on the bow and stern sections. This type of testing would provide a good idea of the pressure changes occurring due to increasing speed as well as the initial static trim condition. It may then also be possible to estimate how these pressures are affecting the magnitudes of dynamic trim and model sinkage.

Chapter 7 - MUN/IOT Comparisons

This section is intended to draw comparisons between the testing completed in the IOT ice tank with those from the testing completed in the MUN towing tank. The calculated effective powers, dynamic trim as well as model sinkage will be compared. Also note here that the data presented for the conventional bow from the IOT tests is that collected for the 'Alpha2' tests (i.e. the retests which were completed after realignment).

For the effective power comparisons one chart and one table will be provided for each bow comparison. The plot will show the actual calculated values from the testing. The table will show the 'standardized' effective power; which means a polynomial curve is fit through the plotted data and it is these two curves that are being compared. The reason for doing this is that the model was not tested at exactly the same speeds for both sets of tests. Therefore one cannot actually directly compare the two sets of data without standardizing it first.

7.1 Conventional Bow

7.1.1 Effective Power Comparison

The following figure shows a comparison of the effective power calculated in the IOT and MUN test programs at static level trim.

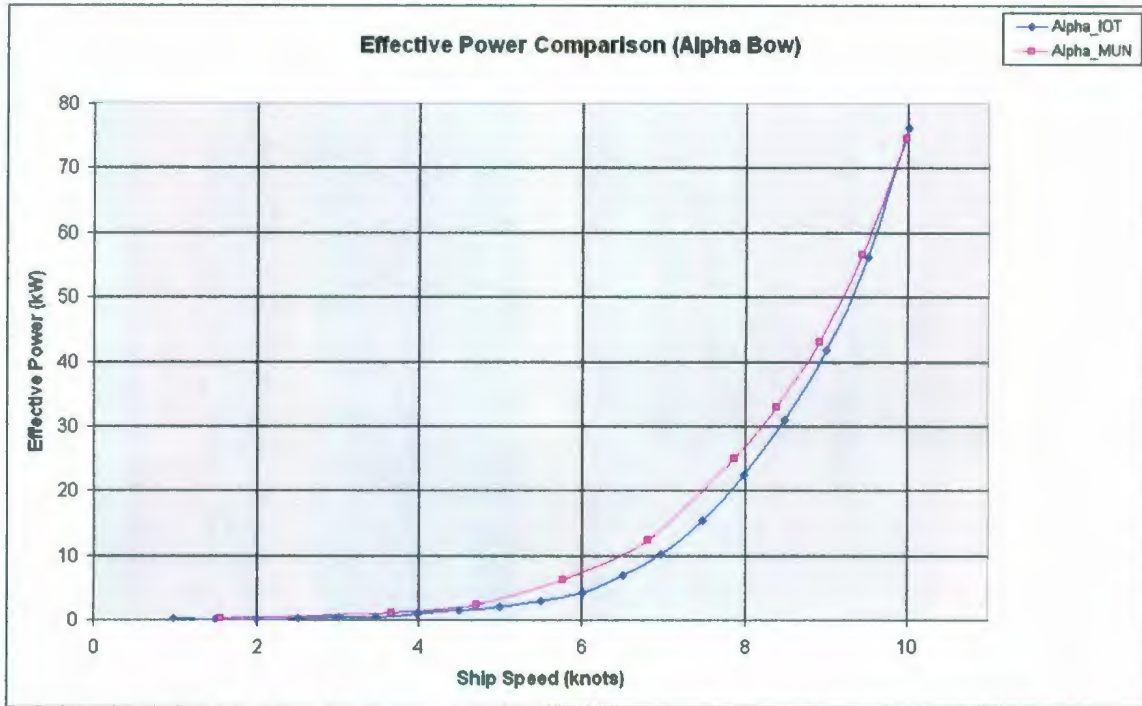


Figure 132: Effective Power Comparison of Alpha Bow Tested at IOT and MUN

Table 46: Standardized Effective Power Comparison of Alpha Bow Tested at IOT and MUN

Ship Speed (knots)	EP (IOT) (kW)	EP (MUN) (kW)	Difference (kW)	Percent Difference (%)
2	0.07	0.15	0.08	107.25%
2.5	0.13	0.21	0.08	66.78%
3	0.28	0.42	0.14	50.80%
3.5	0.55	0.88	0.34	61.25%
4	0.94	1.27	0.33	34.55%
4.5	1.46	2.17	0.71	48.64%
5	2.07	3.39	1.31	63.46%
5.5	2.54	5.04	2.50	98.57%
6	4.10	7.26	3.16	76.96%
6.5	6.55	10.24	3.69	56.34%
7	10.15	14.19	4.04	39.76%
7.5	15.22	19.36	4.14	27.18%
8	22.11	26.04	3.94	17.81%
8.5	31.18	34.55	3.38	10.82%
9	42.86	45.26	2.40	5.59%
9.5	57.59	58.54	0.95	1.64%
10	75.87	74.84	-1.03	-1.36%

From above it can be seen that the MUN tests give lower effective powers than the IOT tests above about 9.5 knots. Below those speeds and the MUN testing provide higher

effective powers than the IOT tests. In the design speed range there is a difference in required effective power between about -1.4 – 17.8%.

It is known that there were misalignment issues for the testing completed in the IOT ice tank. This could then explain why the powering data from the IOT tests tend to increase relative to the MUN powering data with increasing speed. If the model was misaligned for these tests then one would expect to see higher relative resistances with increasing model speed.

7.1.2 Trim Comparison

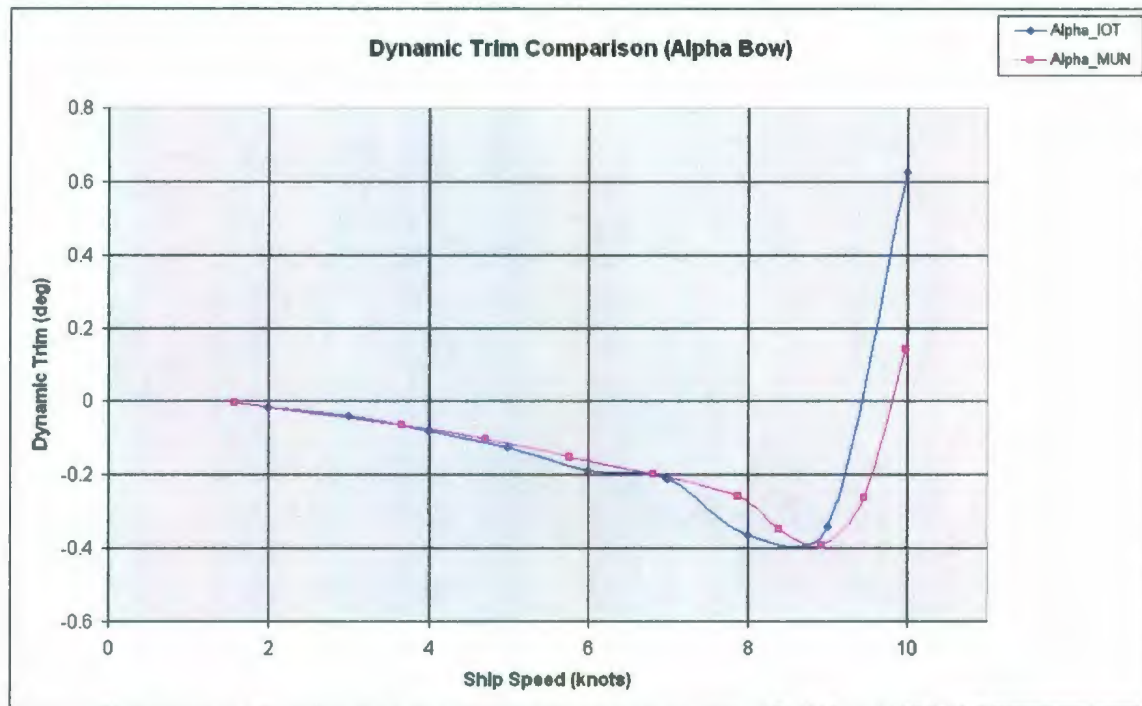


Figure 133: Dynamic Trim Comparison of Alpha Bow Tested at IOT and MUN

The above plot shows that the dynamic trim for the model in the MUN program is lower than that in the IOT program after about 9 knots. This may be due to a slightly different tow points in the two instrumentation set-ups at IOT and MUN respectively. It is known that the tow point in the MUN test program was about 1 inch higher and 1 – 1.5 inches further aft than in the IOT test program.

A different tow point means a slightly different axis about which the model will pitch. Ideally one would like to have the tow point as close as possible to the centroid of the resistance on the underwater portion of the hull in the vertical direction. Any difference in the tow point will result in a trimming moment on the hull.

From the 3D drawing it is known that the centroid of the underwater portion of the hull with any of the bows attached is approximately 0.152 m from the baseline. In the IOT tests the tow point was also located approximately 0.152 m from the baseline. While in the MUN tests, due to model constraints, the tow point was located approximately 0.178 m from the baseline. Therefore, during the MUN test program there was a 0.026 m moment arm due to this difference. This moment arm will induce a trimming moment on the model which will tend to trim it by the head.

Trimming moment, M_{Trim} , is calculated using the following equation:

$$M_{Trim} = (R_{TM})(T_{Diff}) \quad (23)$$

Where: T_{Diff} = Difference between tow point and centroid of the underwater portion of the hull (0.026 m)

The following figure shows how the trimming moment changes with increasing speed. This shows that the trimming moment increases at the same rate as resistance with increasing speed. Therefore, as the model speed is increased to the higher speeds there is a larger magnitude of trimming moment. This would explain why the model in the MUN test program tends to trim by the head further at the higher speeds than in the IOT test program.

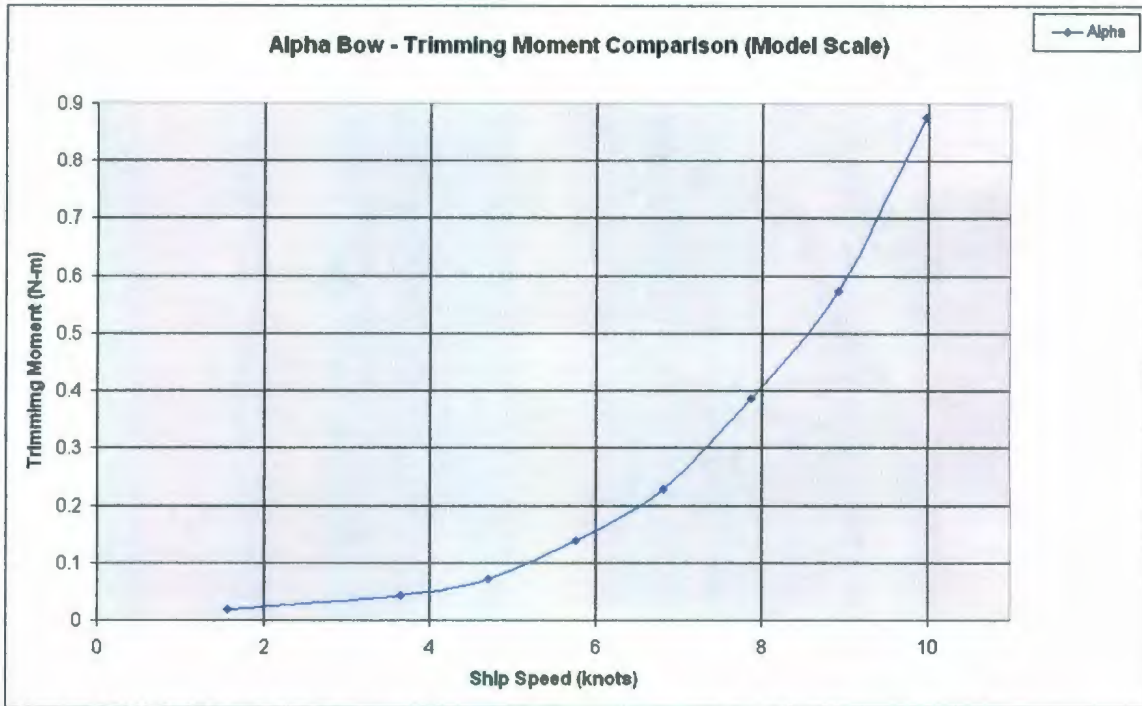


Figure 134: Trimming Moment Comparison of Alpha Bow Tested at MUN

7.1.3 Sinkage Comparison

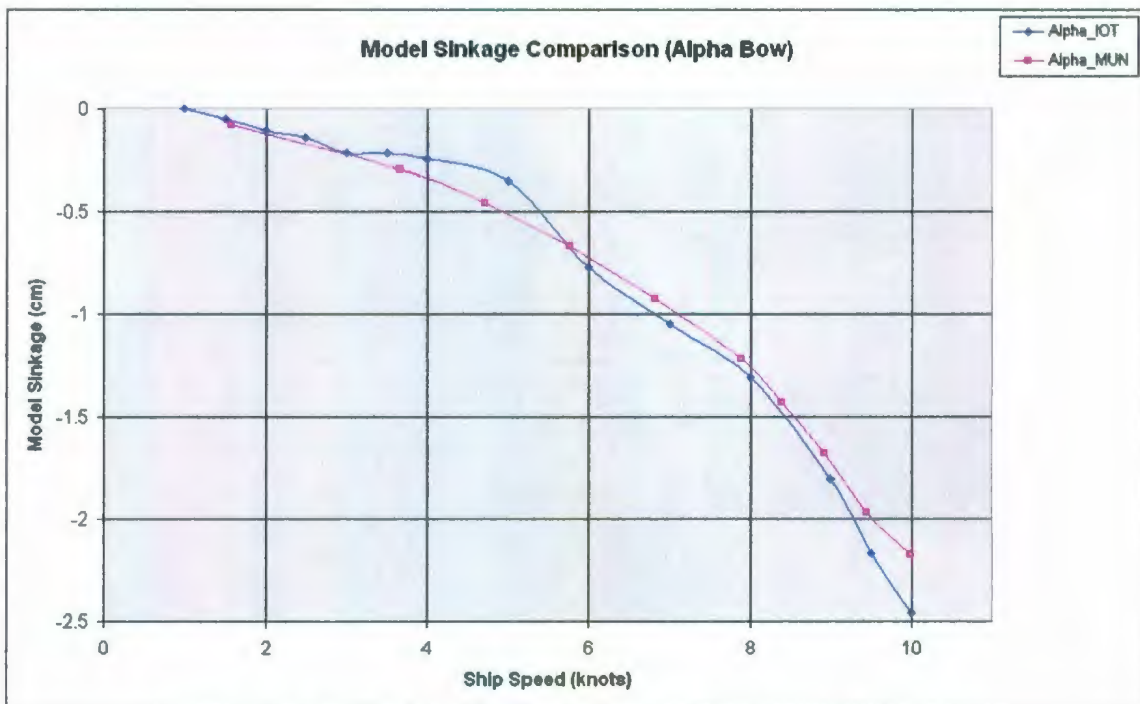


Figure 135: Sinkage Comparison of Alpha Bow Tested at IOT and MUN

The above plot shows that the model sinkage for the model in the MUN program is lower than that in the IOT program above approximately 6 knots. This is actually the opposite of what one would expect to occur; as a vessel in a confined channel (i.e. the MUN towing tank) tends to sink more than if it is in open water (i.e. IOT ice tank). A slightly differing tow point may at least partially explain this difference.

7.2 Bulbous Bows

7.2.1 Effective Power Comparisons

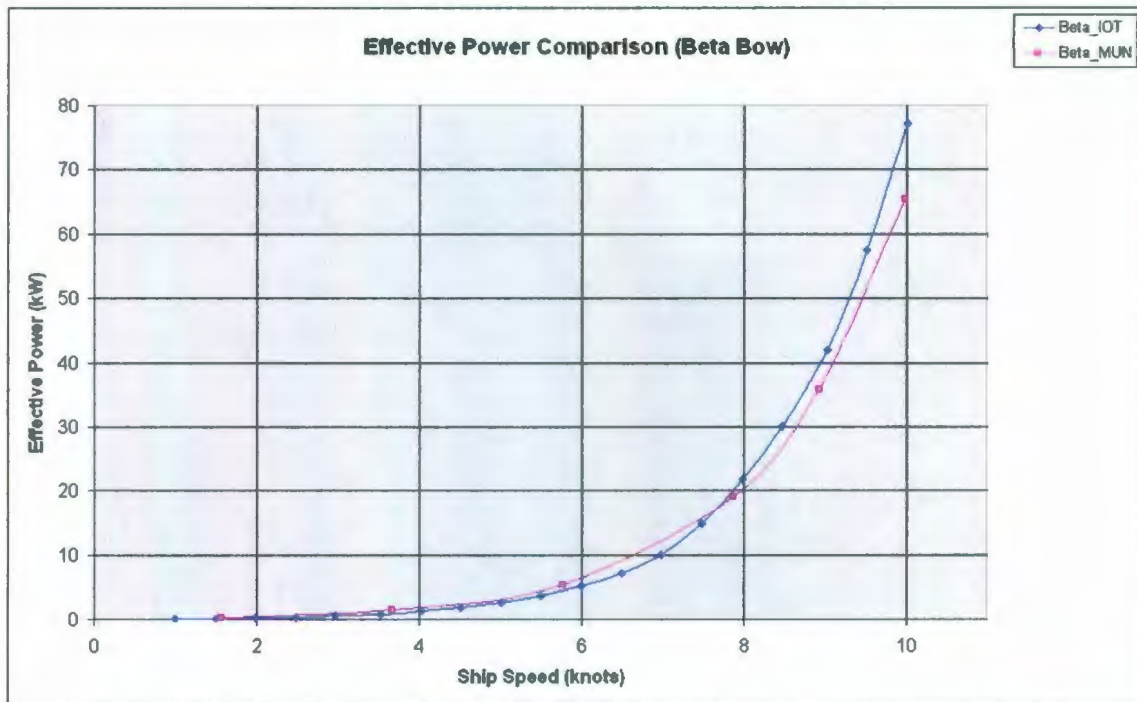


Figure 136: Effective Power Comparison of Beta Bow Tested at IOT and MUN

Table 47: Standardized Effective Power Comparison of Beta Bow Tested at IOT and MUN

Ship Speed (knots)	EP (IOT) (kW)	EP (MUN) (kW)	Difference (kW)	Percent Difference (%)
2	0.10	0.21	0.12	122.57%
2.5	0.39	0.45	0.06	15.55%
3	0.71	0.67	-0.04	-6.00%
3.5	1.04	1.26	0.22	21.66%
4	1.37	1.93	0.56	40.83%
4.5	1.77	2.67	0.90	50.54%
5	2.35	3.53	1.17	49.83%
5.5	3.27	4.61	1.33	40.79%
6	4.73	6.06	1.33	28.05%
6.5	6.98	8.08	1.10	15.75%
7	10.32	10.92	0.60	5.86%
7.5	15.10	14.90	-0.20	-1.31%
8	21.71	20.36	-1.35	-6.21%
8.5	30.59	27.71	-2.88	-9.42%
9	42.24	37.41	-4.83	-11.43%
9.5	57.20	49.98	-7.22	-12.62%
10	76.04	65.96	-10.08	-13.25%

This shows that the results obtained from the MUN testing give lower effective powers than those from the IOT testing above about 7 knots. In the design speed range the MUN tests give about 6.2 – 13.3% lower required effective power than for the IOT tests.

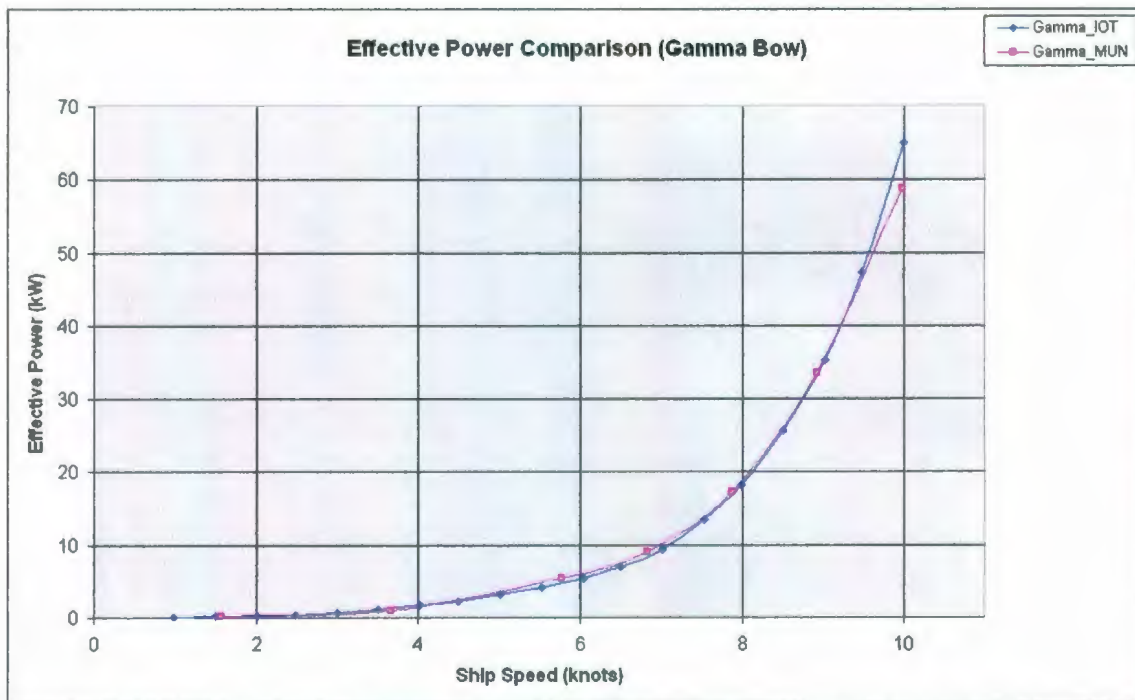


Figure 137: Effective Power Comparison of Gamma Bow Tested at IOT and MUN

Table 48: Standardized Effective Power Comparison of Gamma Bow Tested at IOT and MUN

Ship Speed (knots)	EP (IOT) (kW)	EP (MUN) (kW)	Difference (kW)	Percent Difference (%)
2	0.16	0.16	0.01	5.76%
2.5	0.38	0.29	-0.09	-23.67%
3	0.71	0.50	-0.21	-29.20%
3.5	1.13	0.99	-0.14	-12.57%
4	1.65	1.58	-0.07	-4.29%
4.5	2.26	2.26	0.00	0.14%
5	3.01	3.10	0.09	2.95%
5.5	3.96	4.16	0.20	5.08%
6	5.24	5.59	0.35	6.70%
6.5	7.02	7.56	0.53	7.59%
7	9.55	10.27	0.72	7.52%
7.5	13.14	13.99	0.84	6.40%
8	18.21	19.00	0.79	4.36%
8.5	25.25	25.66	0.41	1.62%
9	34.88	34.33	-0.54	-1.56%
9.5	47.82	45.45	-2.37	-4.96%
10	64.94	59.48	-5.46	-8.41%

From above it can be seen that there is adequate agreement between the data from both sets of tests. However, a trend of increasing difference with increasing speed continuing above 10 knots is evident in the above plot. In the design speed range there is a difference in required effective power of about -8.4 – 4.4%.

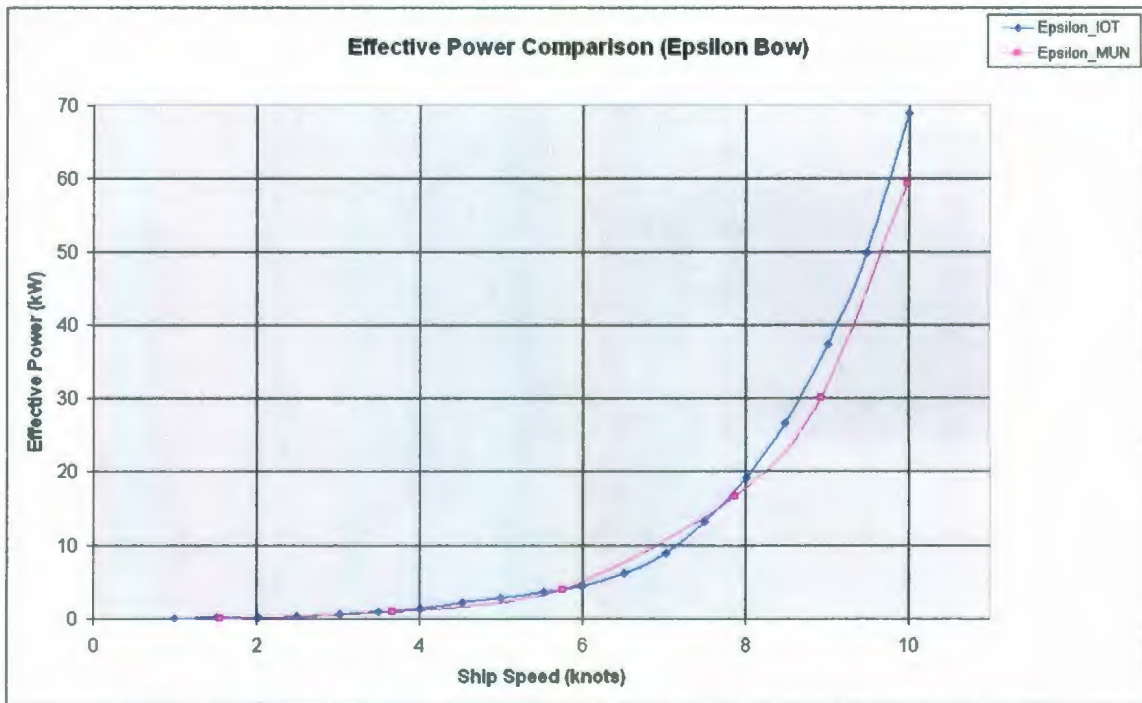


Figure 138: Effective Power Comparison of Epsilon Bow Tested at IOT and MUN

Table 49: Standardized Effective Power Comparison of Epsilon Bow Tested at IOT and MUN

Ship Speed (knots)	EP (IOT) (kW)	EP (MUN) (kW)	Difference (kW)	Percent Difference (%)
2	0.24	0.26	0.02	9.70%
2.5	0.38	0.42	0.04	10.70%
3	0.75	0.63	-0.12	-15.76%
3.5	1.14	0.82	-0.32	-28.37%
4	1.56	1.20	-0.36	-22.85%
4.5	2.00	2.01	0.01	0.29%
5	2.56	2.86	0.30	11.73%
5.5	3.35	3.82	0.47	14.11%
6	4.54	5.02	0.48	10.55%
6.5	6.35	6.63	0.28	4.49%
7	9.06	8.93	-0.14	-1.51%
7.5	13.04	12.22	-0.81	-6.24%
8	18.68	16.91	-1.77	-9.47%
8.5	26.47	23.43	-3.04	-11.48%
9	36.96	32.30	-4.66	-12.61%
9.5	50.80	44.11	-6.69	-13.17%
10	68.68	59.49	-9.19	-13.38%

This shows that the results obtained from the MUN testing give lower effective powers than those from the IOT testing again above about 7 knots. In the design speed range the MUN tests give about 9.5 – 13.4% lower required effective power than for the IOT tests.

7.2.2 Trim Comparisons

The three figures below all show that the dynamic trim by the head measured in the MUN tests is generally lower than the trim by the head measured in the IOT tests up to approximately 8 – 9 knots. Above this point however, and the dynamic trim measured in the MUN tests begin to become higher than measured in the IOT tests. This is consistent with what was found for the conventional bow.

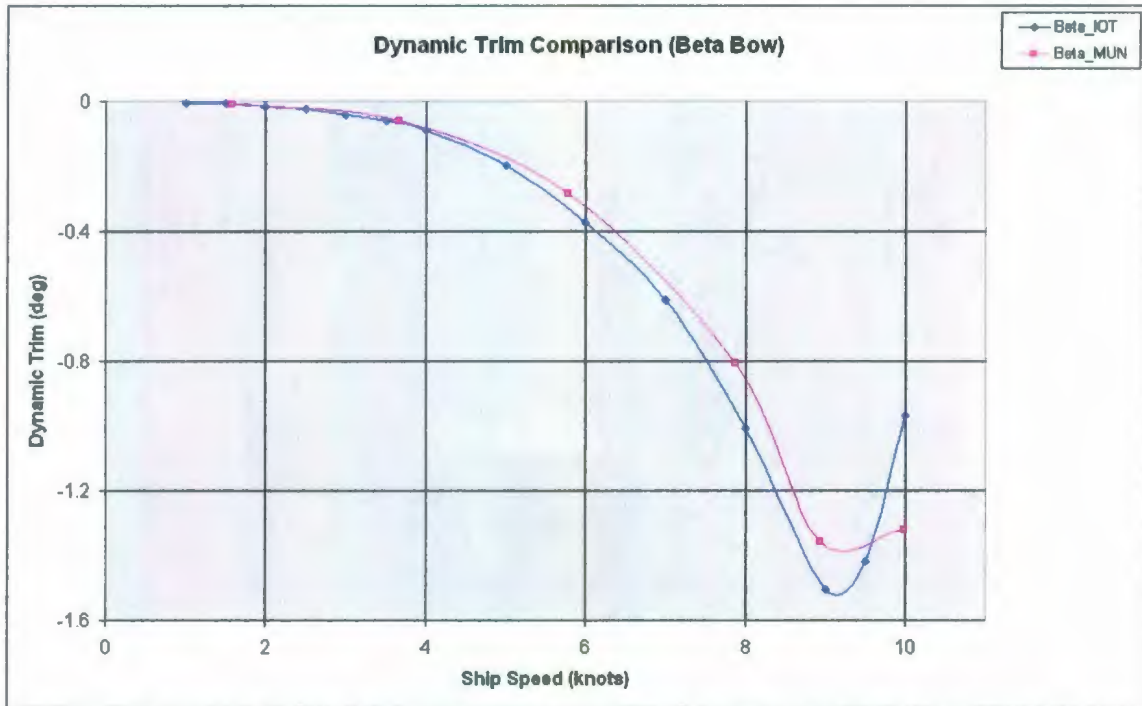


Figure 139: Dynamic Trim Comparison of Beta Bow Tested at IOT and MUN

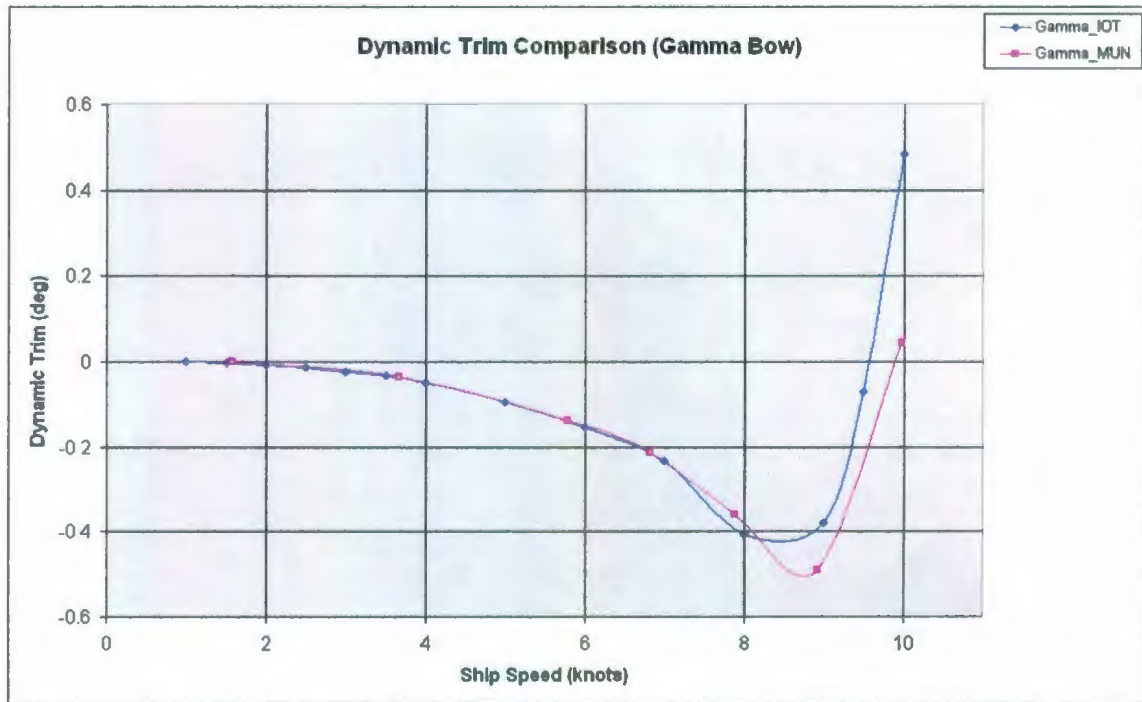


Figure 140: Dynamic Trim Comparison of Gamma Bow Tested at IOT and MUN

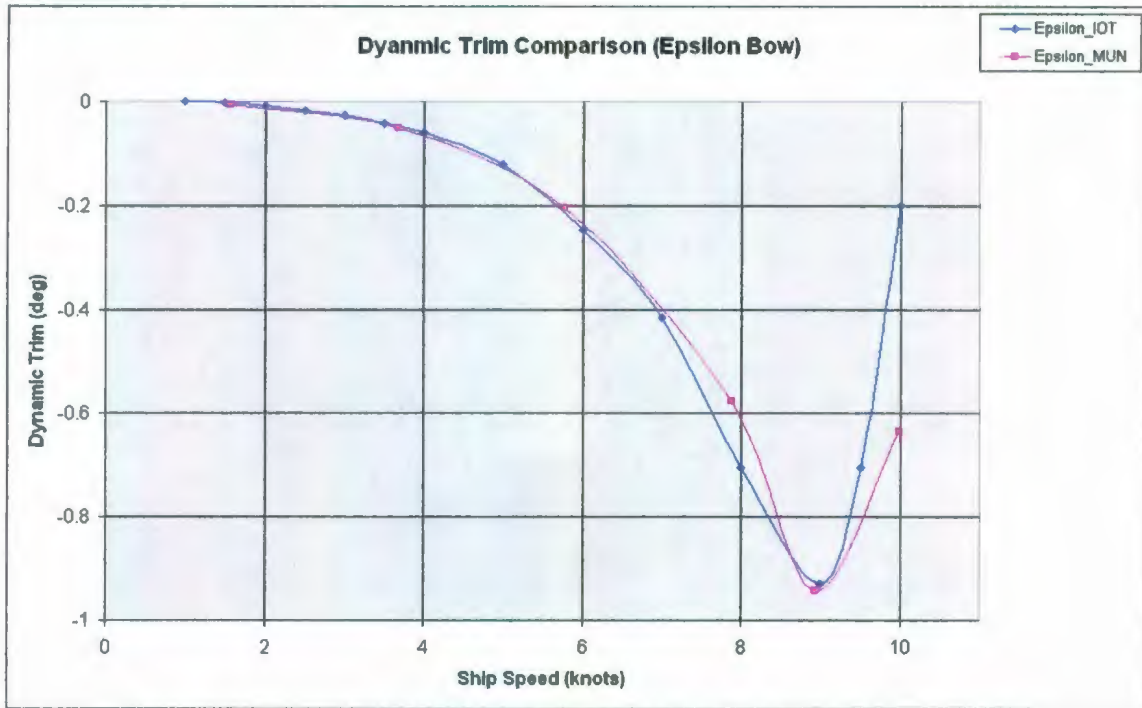


Figure 141: Dynamic Trim Comparison of Epsilon Bow Tested at IOT and MUN

The following figure shows the trimming moments for each of the bulbous bows.

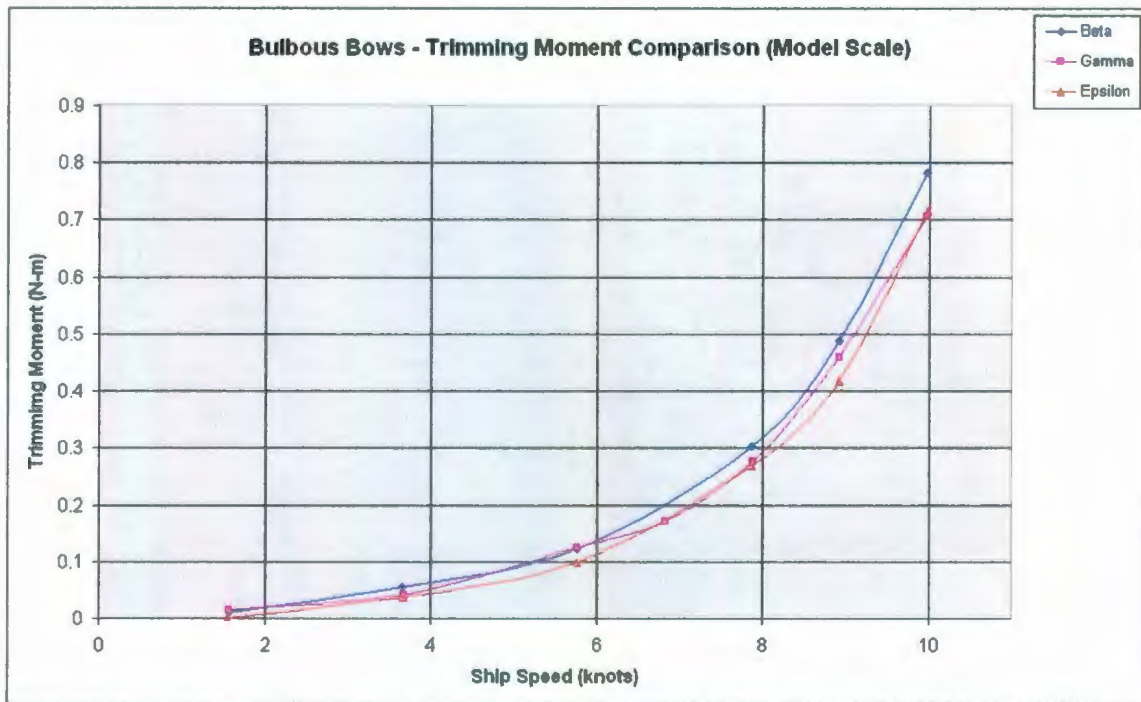


Figure 142: Trimming Moment Comparison of Bulbous Bows Tested at MUN

Again, the higher dynamic trim by the head in the lower speeds in the IOT test program is likely due to the misalignment issues. However, as can be seen from the above plot, the trimming moment in the MUN test program begins to become more relevant as speed is increased. It is likely that the trimming moment begins to become more significant than the misalignment at higher speeds, and therefore this cross over is found for every bow in the 8 – 9 knot range.

7.2.3 Sinkage Comparisons

The three figures below all show that the sinkage for each set of tests is fairly consistent up to approximately 5 – 6 knots. Above this point however, and the sinkage measured in the IOT tests begin to become significantly higher than measured in the MUN tests. This is consistent with what was found for the conventional bow. Again, a slightly differing tow point may at least partially explain this difference.

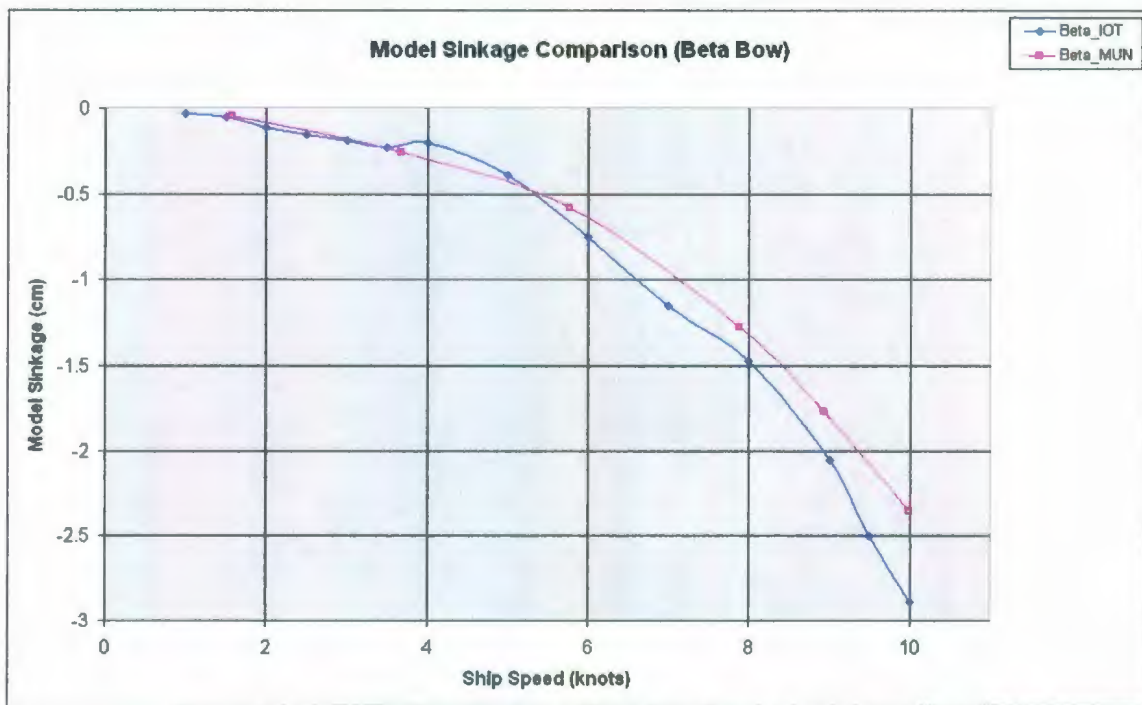


Figure 143: Sinkage Comparison of Beta Bow Tested at IOT and MUN

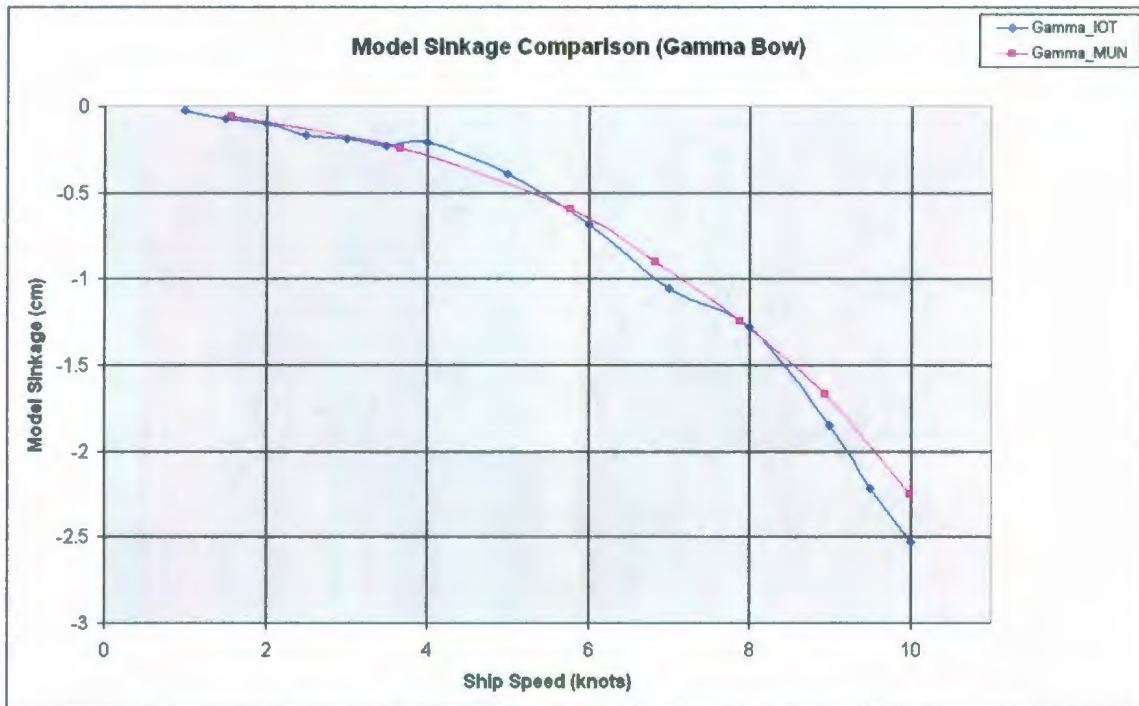


Figure 144: Sinkage Comparison of Gamma Bow Tested at IOT and MUN

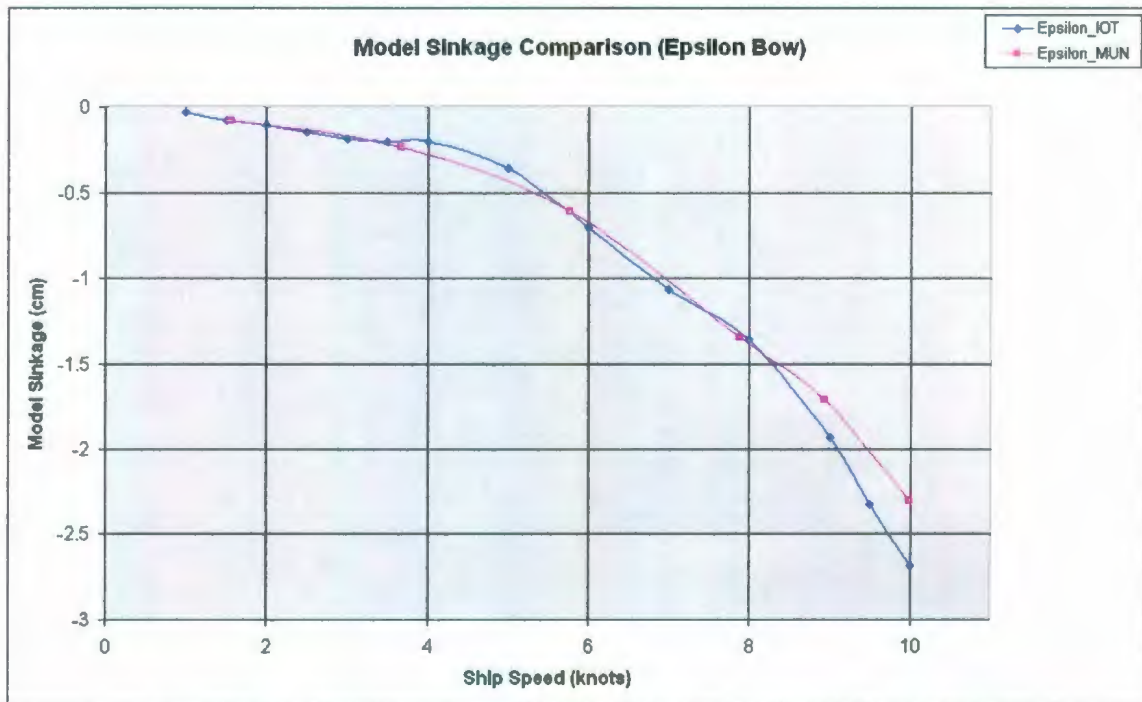


Figure 145: Sinkage Comparison of Epsilon Bow Tested at IOT and MUN

7.3 Overall Comparisons

Effective Power

The following two plots show the difference between the calculated effective power from the IOT tests and the MUN tests. The first plot shows the magnitude of the differences between the two test programs. The differences are taken as the required effective powers calculated in the IOT tests subtracted from the required effective powers calculated in the MUN tests; hence a negative value means that the MUN tests provide a lower effective power. The plot shows the differences for all four bows tested.

The second plot shows the percentage of difference between the two test programs. This is taken as the required effective powers calculated in the MUN tests divided by the required effective powers calculated in the IOT tests; hence a value less than 100% means that the MUN tests provide a lower effective power.

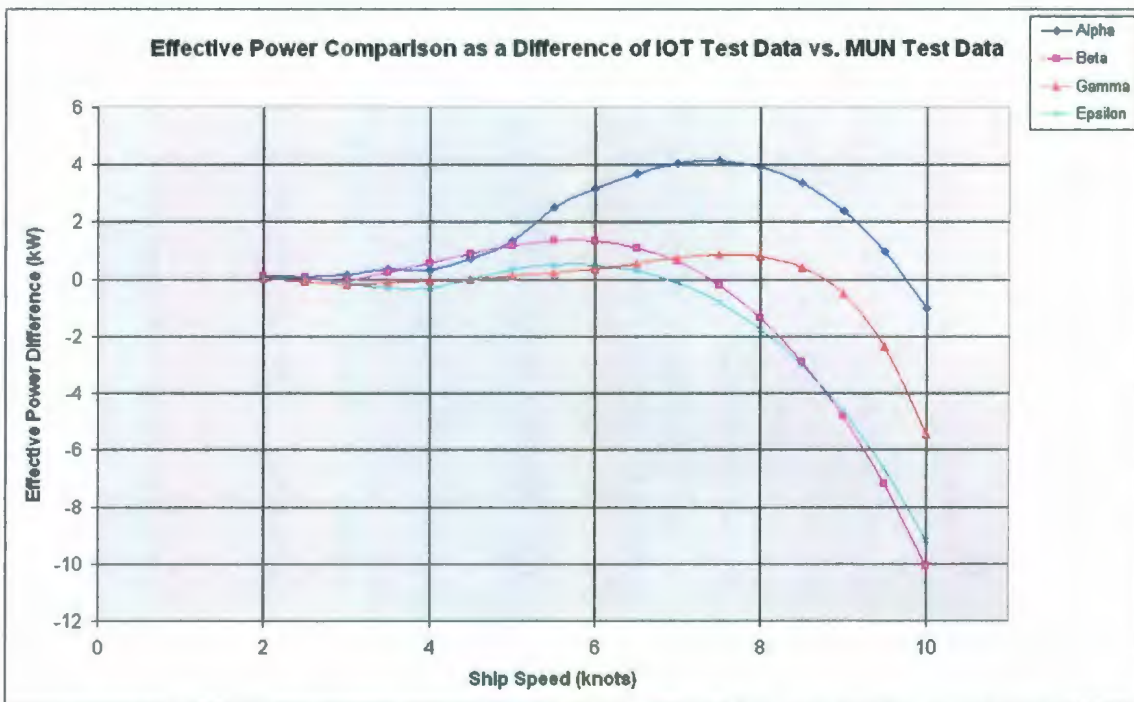


Figure 146: Effective Power Comparison as a Difference IOT Test Data vs. MUN Test Data

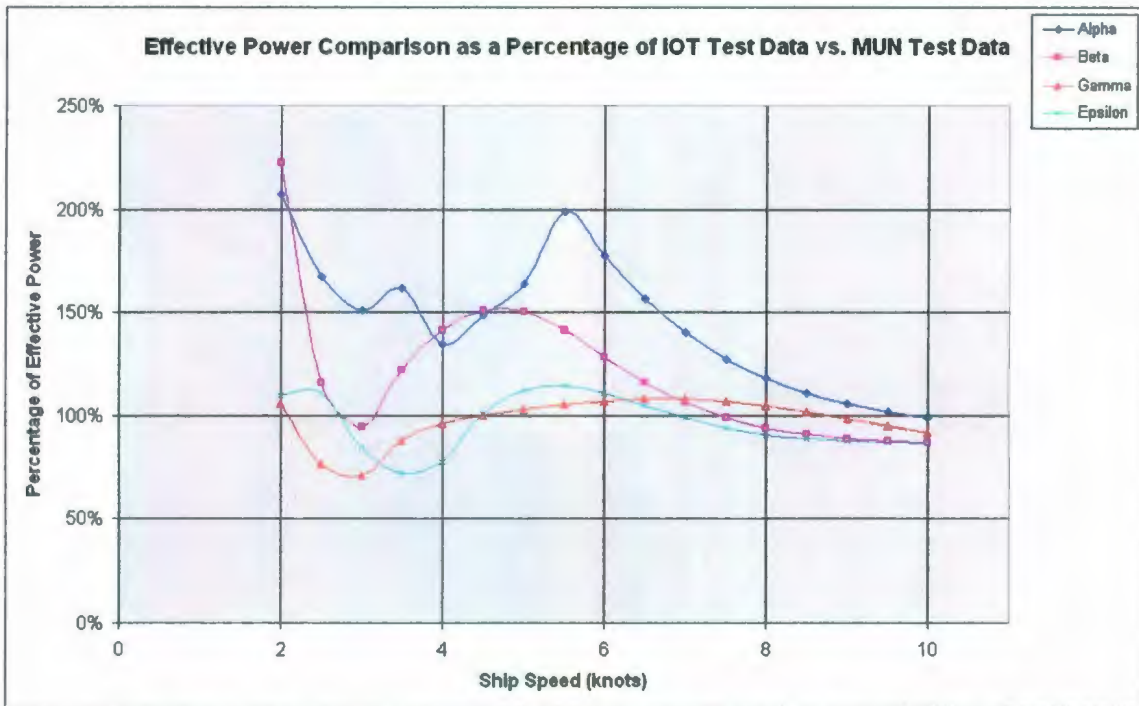


Figure 147: Effective Power Comparison as a Percentage IOT Test Data vs. MUN Test Data

From the first plot it is evident that, depending on the individual bow, above 5 – 7 knots the differences are tending to go towards negative values. The second plot shows that above between 5 – 7 knots and the percentages begin to generally decrease. These both point to the conclusion that the MUN tests are generally providing decreasing effective power values with increasing speed relative to the data from the IOT tests.

Dynamic Trim

The next two plots show similar comparisons as above using the dynamic trim data.

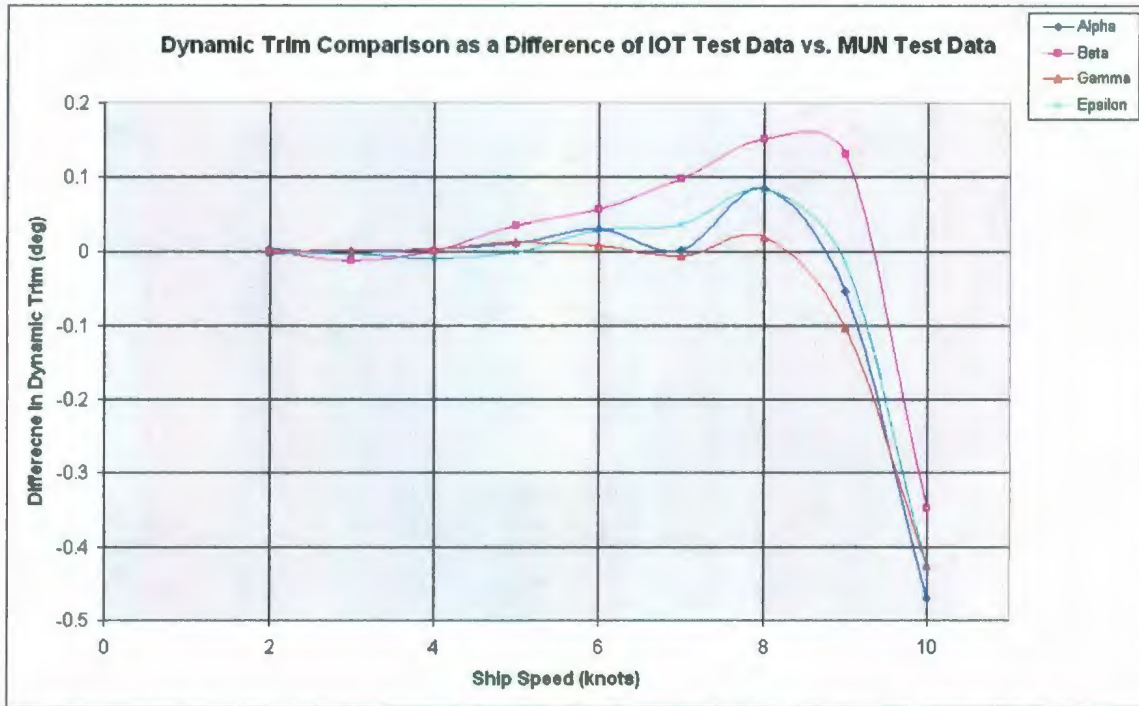


Figure 148: Dynamic Trim Comparison as a Difference IOT Test Data vs. MUN Test Data

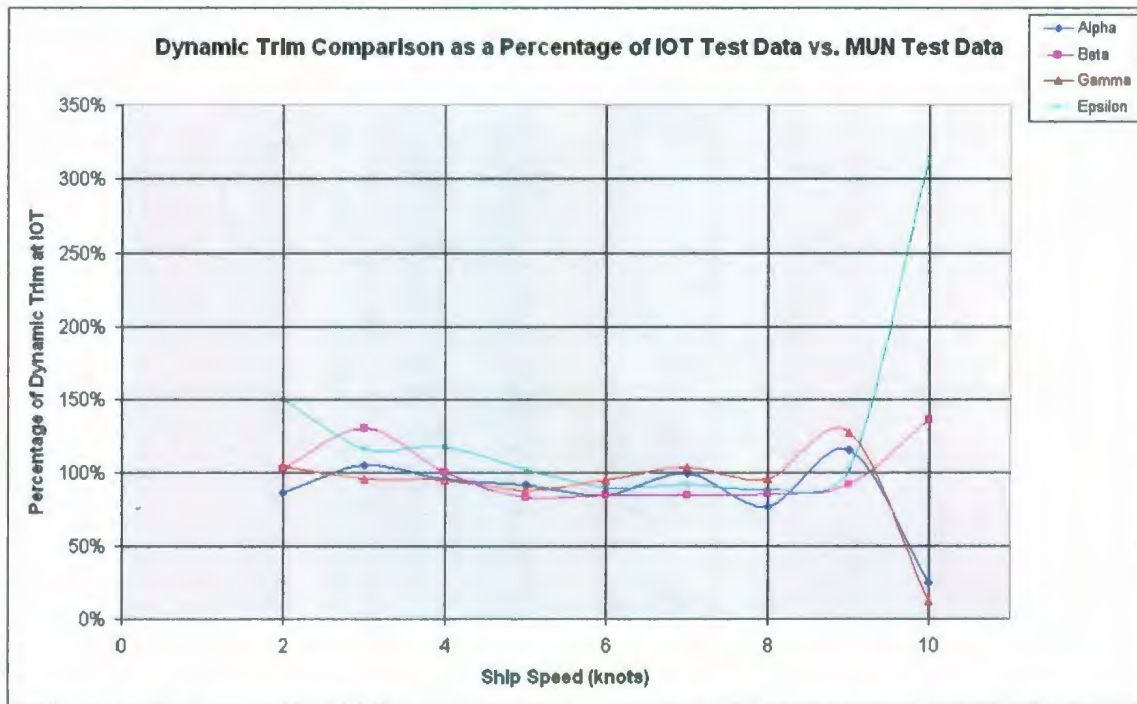


Figure 149: Dynamic Trim Comparison as a Percentage IOT Test Data vs. MUN Test Data

The first plot shows that for each bow there is a sharp decline in the difference between the dynamic trim data for the two test programs above approximately 8 knots. This

means that the model with each of the four bows attached in the MUN test program is trimming more by the head at higher speeds than in the IOT test program.

The second plot shows that the MUN test program generally has about 10% less dynamic trim by the head than in the IOT test program up to about 8 – 9 knots. It can be seen that above this point the percent differences tend to either decrease or increase significantly. The percent difference for both Epsilon and Beta bows tend towards positive values as the dynamic trim data for both the IOT and MUN tests are still negative values (i.e. the model is still trimmed by the head in both test programs). For Alpha and Gamma bows however the model is trimmed by the stern at 10 knots in both programs; this is the reason that the percent differences tend towards more negative values.

Both of the above two plot point to the conclusion that the MUN tests generally provide lower dynamic trim by the head in the lower speed range but then increasing dynamic trim by the head at higher speeds relative to the data from the IOT tests.

Model Sinkage

Finally, the next two plots show similar comparisons as above using the model sinkage data.

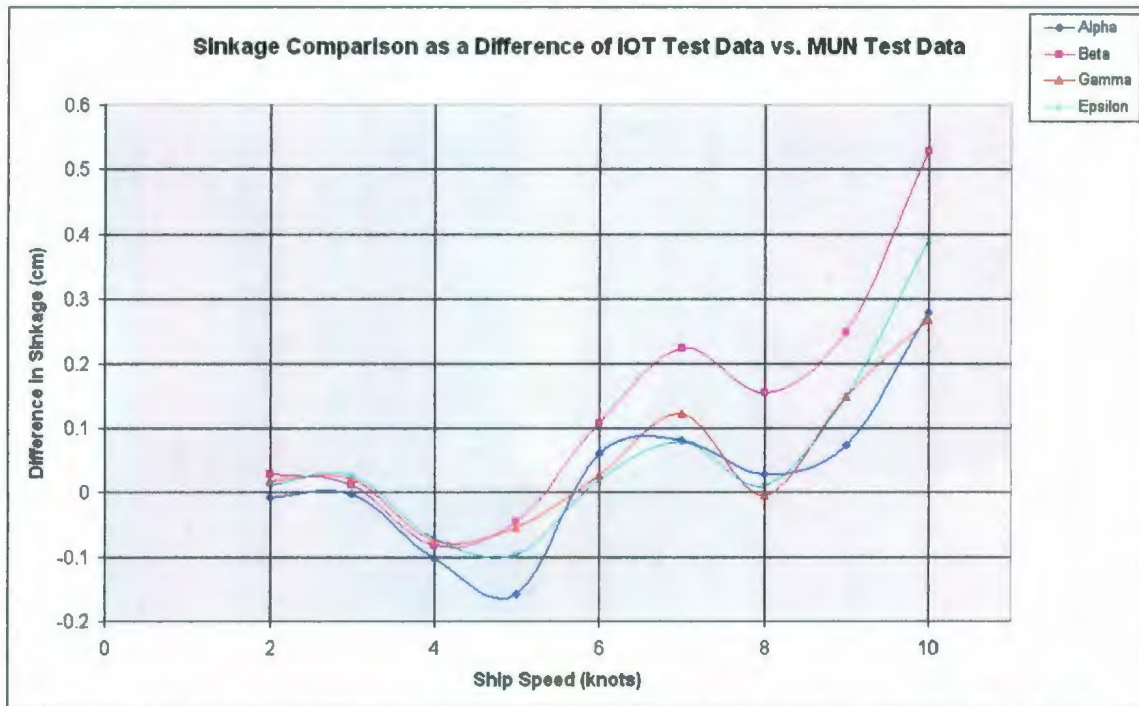


Figure 150: Model Sinkage Comparison as a Difference IOT Test Data vs. MUN Test Data

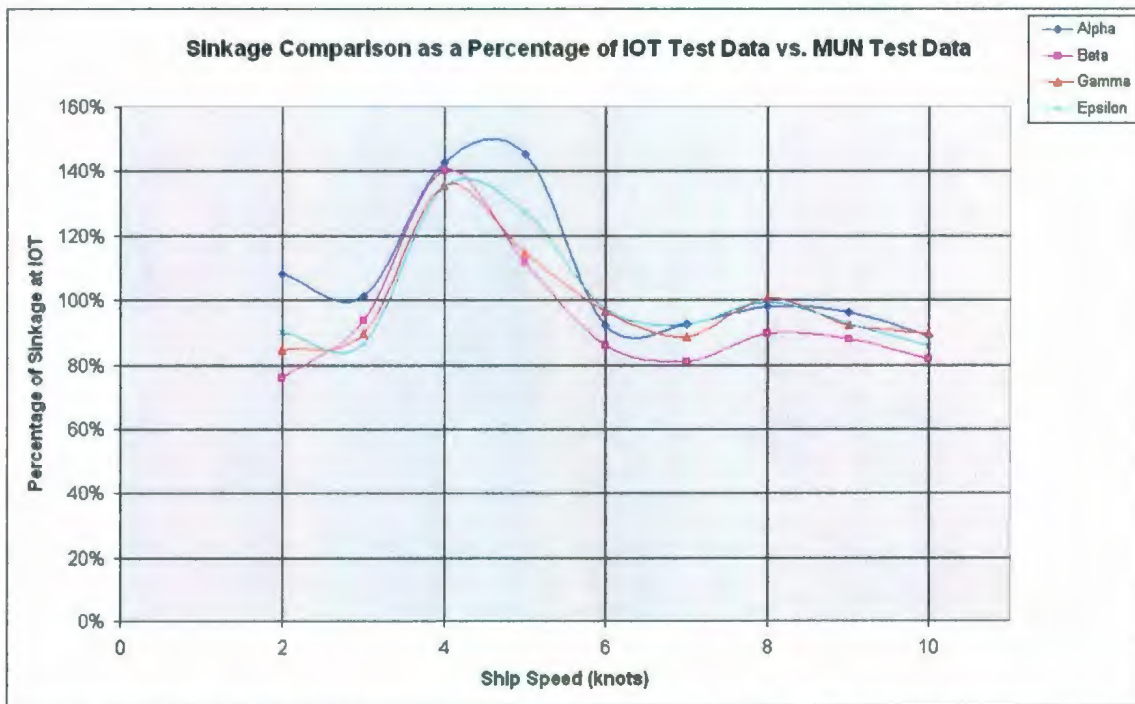


Figure 151: Model Sinkage Comparison as a Percentage IOT Test Data vs. MUN Test Data

The first thing to stand out in both of the above plots is that there are two prominent humps in the comparison curves for each of the bows; the first occurs around 4 – 5 knots and the second at around 8 – 9 knots. It can be seen in the sinkage data, see previous two

sections, for the IOT tests that with each bow tested there is a slight decrease in the downward sinkage trend around these two points. It is unclear what exactly would cause this, but it is likely due to the instrumentation set-up used during the IOT test program as the same kind of trends are not found in the MUN test data for any of the four bows tested.

With the exception of points around 4 – 5 and 8 – 9 knots the first plot shows a general trend of increasing difference in model sinkage with increasing speed. This means that the model sinkage in the IOT tests is generally increasing relative to the MUN tests with speed. The second plot shows that the percent difference is relatively consistent and 90% through the whole speed range, again with the exception of data around 4 – 5 and 8 – 9 knots.

If the data at 4, 5, 8, and 9 knots are removed then a clear trend of a slightly decreasing percent difference is found. This means that as the model speed is increased then the model in the IOT tests is generally sinking further into the water than in the MUN tests.

Final Remarks

There are several possible explanations for the trends in differences. Firstly, with regards to the powering data, there were two different load cells used for each of the two test programs. Each of the load cells used are rated for ± 220 N. The load cell used in the IOT test program was calibrated up to ± 189 N, while the load cell used in the MUN test program was calibrated up to ± 167 N. Since similarly rated load cells were used and the calibration equations were perfectly linear for each suggests that this is not the cause of the discrepancies in powering data.

It is known that there were misalignment issues for the testing completed in the IOT ice tank. Because there were misalignment issues during the IOT test program there would be a point when the model starts to roll very slightly due to the difference in resistance on the two sides of the model. This in turn increases this difference and causes more roll and consequently even larger yawing moment. The model will start yawing

infinitesimally more since the yaw restraint is not totally rigid. This will result in an increase in resistance as speed increases as well as resulting in differences in both trim and sinkage.

Two different instrumentation set-ups were used for each test program. The tests carried out in the IOT ice tank used a gimbal which was free to pitch and roll. This gimbal was mounted in the model via a gimbal plate attached directly to the top part of the inner keel. The tests carried out in the MUN towing tank used a base plate that attached to the bottom of the tow post. The base plate was attached to the sides of the inner keel using two ball joint linkages which allowed it to pitch. This particular set-up was used in the MUN tests as it would allow for fitment of a dynamometer during self-propulsion testing.

Because there were two separate instrumentation set-ups used there was a slightly differing tow point for each test program. It is known that the tow point in the MUN test program was about 1 inch higher and 1 – 1.5 inches further aft than in the IOT test program. Having a higher tow point would lead to higher trim by the head values with increasing speed, as quantified earlier, because there is a moment applied around the tow point by way of the force acting on the underwater portion of the hull.

Chapter 8 - Self-Propulsion Tests

The purpose of self-propulsion tests is to evaluate the performance of the propeller behind the hull as well as determine the interaction effects between the propeller and hull. This is generally done by determining the wake and thrust deduction fractions as well as the relative rotative efficiencies from the test results. These tests were carried out in two different periods: from May 21, 2009 – May 22, 2009 and from October 14, 2009 – October 23, 2009. The objective was completed by testing the model at three hull speeds while running the propeller at five different shaft speeds for each model speed.

Wake is the difference between the ships speed and the speed of advance (i.e. speed through propeller race area). The wake fraction is a percentage value which expresses the reduction in fluid flow through the propeller race relative to the vessels speed. For example, wake fraction values of 0.1 means that the speed of water flowing into the propeller race is 10% lower than the speed of the model. It is calculated using the following equation:

$$w = 1 - \frac{V_A}{V_M} = 1 - \frac{J_O}{J_P} \quad (24)$$

Where: w = wake fraction

V_A = Speed of advance in propeller open water test (m/s)

V_M = Model Speed (m/s)

J_O = Advance coefficient in propeller open water test

J_P = Advance coefficient for model in self-propulsion test

The wake fraction is made up of three components:

1) Frictional wake: the frictional drag of the hull, which tends to slow down the flow of water over the hull surface due to frictional forces.

2) Potential wake: the pressure distribution over the stern section of the hull is always increased due to the streamlines closing in. This results in a lower water velocity past this section of the hull than the model speed.

3) Wave wake: the models wave pattern also affects the speed of water flow into the propeller wake. The water particles in a wave crest will have a forward velocity while in a trough they will have a velocity towards the stern. So depending on whether the propeller race is in a crest or trough there may be either a small increase or decrease in water flow speed due to wave action.

This is therefore a complex mixture of several phenomena. It is known that the presence of a bulbous bow will alter the wave pattern over the hull surface, thereby affecting the wake and thrust deduction fractions somewhat. Likewise, a bulb will increase the frictional drag on the surface of the hull, increasing the wake somewhat along with it. However, it is more difficult to say how the presence of a bulb will affect the pressure distribution over the hull form. Therefore, it is important to conduct self-propulsion tests to determine the overall magnitudes of these interactions for each bow.

The thrust deduction fraction comes about due to the fact that the resistance of a self-propelled hull form is greater than that of the same hull form towed (i.e. by a carriage) at the same speed. This is due to the fact that there is an area of high pressure at the stern decreasing the overall resistance on the hull when it is being towed. This same area of high pressure is reduced by the action of the propeller when it is being self-propelled. One can also think of this increase in resistance as a deduction of the thrust available at the propeller. So although the propeller provides a thrust of T , there is only a R_T amount available to overcome the hulls resistance. This "loss of thrust" ($T - R_T$) expressed as a fraction of the thrust T is the thrust deduction fraction, and is generally given as:

$$t = \frac{T - R_T}{T} \quad (25)$$

Where: t = Thrust deduction fraction

T = Propeller thrust

R_T = Resistance of towed hull form

The thrust deduction fraction is mainly affected by the pressure distribution over the stern section of the hull. In bare hull resistance tests there is a region of high pressure over the stern section which results in a lower water velocity past this section of the hull than the model speed. In self-propulsion tests the propeller tends to lower this pressure at the stern and hence increases the relative water velocity over the stern section as well as the resistance on the hull.

The relative rotative efficiency, η_R , is the difference between the torque measured in the behind hull and open water conditions. It is due to the following two reasons:

- 1) Wake condition: during the self-propulsion tests the propeller is operating in a non-homogeneous flow, which leads to a decreased efficiency of the propeller blades.
- 2) Relative amount of laminar and turbulent flow: there is generally more turbulence in the water during the self-propulsion tests than when the propeller is tested in the open water condition. This also leads to a decrease in efficiency during the self-propulsion testing.

Resistance tests and open water propeller tests are required prior to the self-propulsion tests. The resistance tests were completed as stated above; the results from the MUN tests were used during this self-propulsion test program and analysis. The propeller tests have been completed on a previous project that was run in the MUN towing tank.

8.1 MUN Test Facility

The same test facility as was used for the self-propulsion testing as for the MUN bare hull resistance tests, as outlined in Section 6.1.

8.2 Test Instrumentation

The following figures show the instrumentation used for the self-propulsion tests carried out in the MUN Towing Tank installed in the model.

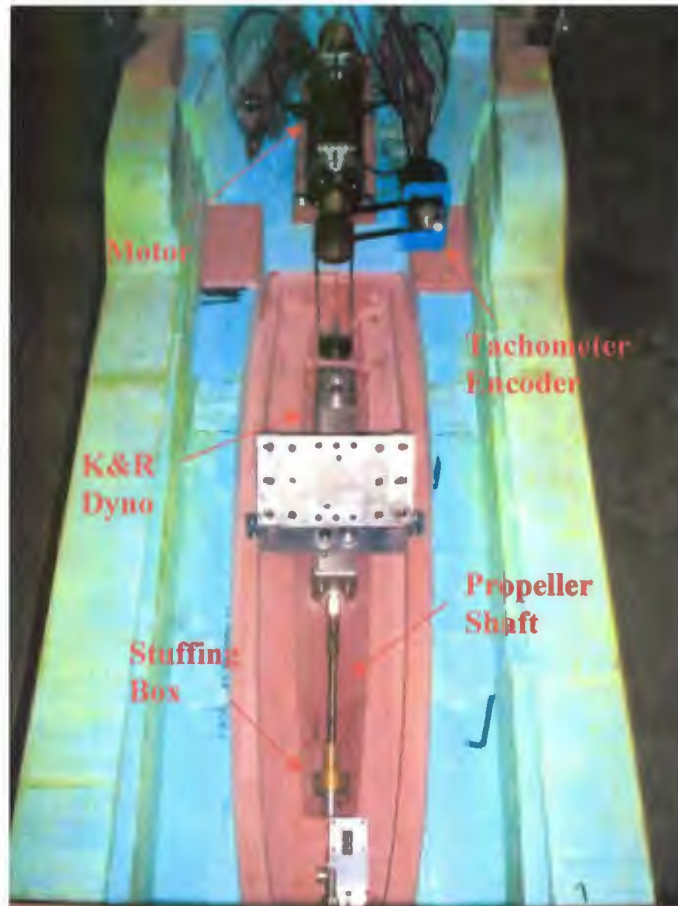


Figure 152: Outline of Self-Propulsion Instrumentation

Towing Dynamometer

The same towing dynamometer was used during self-propulsion tests as was used in the MUN bare hull resistance tests.

Inclinometer

The same inclinometer was used during self-propulsion tests as was used in the MUN bare hull resistance tests.

Motor and Motor Controller

The motor and motor controller used is from *Electro-Craft Corporation*. The motor is a permanent magnet servo motor; model number E 644 A-MGB. Further details can be found online by searching the name and product number.



Figure 153: Motor used in Self-Propulsion Tests



Figure 154: Motor Controller used in Self-Propulsion Tests

Tachometer Encoder

An encoder was used to determine the propeller shaft speed. It was directly coupled to the drive shaft of the motor at the opposite end from the dynamometer. The encoder measures the frequency of the motor shaft and is read into Daqbook via a special channel.



Figure 155: Tachometer Encoder Installed in Model

Thrust and Torque Dynamometer

A K&R dynamometer was used to measure propeller thrust and torque. The type used is rated for ± 25 kg (or ± 245 N) of thrust and ± 100 kg-cm (or ± 9.81 N-m) of torque. Their light weight and small dimensions make them ideal for such applications as they can be easily handled and fit in tight spaces such as in the bottom of the opens boat where they will be well protected.



Figure 156: Thrust and Torque Dynamometer Installed in Model

Data Acquisition System

The data for each of the test conditions was collected through seven channels (one each for resistance, propeller thrust, propeller torque, shaft speed, heave, pitch, as well as carriage speed). The voltage data outputs for the tests were collected using an *IOTech* Daqbook data acquisition system (Daqbook 2000) connected to a computer running DaqView software. For these tests, the data were collected with a sampling rate of 50 Hz. The raw data was collected in *.txt format and post processed using Microsoft Excel.

8.2.1 Instrumentation Calibrations

The same calibration procedures were used for the load cell, inclinometer, and LVDT as for the IOT bare hull resistance tests, as outlined in Section 5.2.1.

The motor controller was calibrated by hooking it up to the electric motor and adjusting the motor controller dial until the motor shaft was rotating and known increments (i.e. increments of 3 rps). The motor shaft speed was measured using an optical tachometer. Markings were then made on the motor controller dial which corresponds to known motor shaft speeds. This was then used as a rough guide when setting the propeller shaft speed for each run.

The tachometer encoder was calibrated by hooking it up to the motor and running the motor at various shaft speeds. The rotational speed of the tachometer was then measured using an optical tachometer. The measured rotational speeds were then plotted against the measured voltages for each measured rotational speed. The equation of this linear relationship was then used during testing.

Thrust is calibrated by adding weights incrementally to induce a known force on the end of the K&R dynamometer. The weight added should be sufficient to cover at least the expected range of force expected during testing. After all the weights are added a plot can be made of the known force vs. voltage reading. The plot should be exactly linear; if it is then the equation of this line can be used during the testing to convert the voltage

reading from the dyno into a force reading that will be used during the analysis of the data.

The torque is calibrated in much the same way as thrust, except a lever arm (which has a known length) is attached to the end of the dynamometer from which the weight will be added. The torque is then calibrated using the same procedure as thrust.



Figure 157: K&R Dyno Torque Calibration

8.3 Model Set-up

The same model set-up was used as was outlined for the IOT bare hull resistance tests, as described in Section 5.3.

8.4 Test Plan

The test plan included testing each of the nine bows at the design draft of 0.188 m model scale and one trim angle (level trim). The tests are carried out by running the model at a

given speed down the tank while running the propeller at five different shaft speeds around the expected self-propulsion point. It is typical to test at least two shaft speeds above and below the expected self-propulsion point so a curve can be fit through the data to pin point the exact point where the tow force is equal to zero.

This set of tests included testing each bow at 8, 9, and 10 knots full scale. The following table shows the original test plan for all bows.

Table 50: Test Plan for Self-Propulsion Tests at MUN

Run #	V _S (knots)	V _M (m/s)	F _n	Shaft Speed (rps)
1	9	1.673	0.406	15.0
2	9	1.673	0.406	15.0
3	8	1.487	0.361	6.0
4	8	1.487	0.361	9.0
5	8	1.487	0.361	12.0
6	8	1.487	0.361	15.0
7	8	1.487	0.361	18.0
8	9	1.673	0.406	10.0
9	9	1.673	0.406	13.0
10	9	1.673	0.406	16.0
11	9	1.673	0.406	19.0
12	9	1.673	0.406	22.0
13	10	1.859	0.451	14.0
14	10	1.859	0.451	17.0
15	10	1.859	0.451	20.0
16	10	1.859	0.451	23.0
17	10	1.859	0.451	26.0

It was found during testing that the pulley belts would begin slipping at propeller shaft speeds above approximately 23 – 24 rps. Therefore, the shaft speed of 23 rps was reduced to approximately 22 rps and the shaft speed of 26 rps was reduced to as high as was possible (usually about 23.5 rps). This ensured that there was still at least two points above the self-propulsion point.

8.5 Description of Experiment

To calculate the components of the hull forms propulsive efficiency the IOT Standard Test Method for the Prediction of Ship Powering (2006) was used as a guideline. Note here that this standard was not used exclusively to analyze the self-propulsion data

contained within. The following series of steps were taken to determine the components of the propulsive efficiency:

1) Determine the full scale self-propulsion point for each model speed. Since there is a scale factor between the model and full scale hull (i.e. 7.654) the full scale self-propulsion point is not the same as the model scale self-propulsion point. The model scale self-propulsion point is simply the point where the propeller thrust equals the resistance on the hull (i.e. there is zero tow force). In order to determine the full scale self-propulsion point corrections must first be made. This is determined by completing a series of sub steps.

- i) Calculate the total resistance coefficient for ship including correlation allowance:

$$C_{TS} = C_{TM} + (C_{FS} - C_{FM}) + C_A - \Delta C_T \quad (26)$$

Where: C_{TM} = total resistance coefficient for model (from resistance tests)

C_{FS} = ship frictional resistance coefficient (from resistance tests)

C_{FM} = model frictional resistance coefficient (from resistance tests)

C_A = correlation allowance (taken as 0.0004)

ΔC_T = blockage correction (from resistance tests)

- ii) Calculate the total model resistance coefficient at the propulsion test temperature:

$$C_{TMP} = C_{TM15} + (C_{FMP} - C_{FM15}) \quad (27)$$

Where: C_{TM15} = total resistance coefficient for model at 15°C (from resistance tests)

C_{FMP} = frictional resistance coefficient for model at propulsion test temperature

C_{FM15} = frictional resistance coefficient for model at 15°C (from resistance tests)

iii) Calculate the skin friction correction coefficient in propulsion test:

$$C_{FD} = C_{TS} - C_{TMP} \quad (28)$$

iv) Calculate the skin friction correction (N) in self-propulsion test:

$$F_{DMP} = 0.5\rho_M V_M^2 S_M C_{FD} \quad (29)$$

Where: ρ_M = Water density (kg/m^3)

V_M = Model speed (m/s)

S_M = Wetted surface area of model scale vessel (m^2)

v) The full scale self-propulsion point can now be found by plotting propeller shaft speed versus tow force. A polynomial line is run through the data and the equation of the line is used to determine the exact propeller shaft speed corresponding to the skin friction correction. This is then called the 'self-propulsion point'. This will result in a higher required shaft speed (hence higher propeller thrust) than is required for the model scale self-propulsion point.

2) Determine the values of propeller thrust and torque at the self-propulsion point by plotting propeller shaft speed versus both propeller thrust and torque respectively. A polynomial line is run through both sets of data and the equations of the lines are used to determine the thrust and torque at the propeller shaft speed corresponding to the self-propulsion point.

3) Calculate the value of J_P at the self-propulsion point for each model speed using:

$$J_P = \frac{V_M}{n_P D_M} \quad (30)$$

Where: n_p = Propeller shaft speed at self-propulsion point (rps)

D_M = Model propeller diameter (0.1205 m)

4) Calculate the values of K_{TP} , K_{QP} , and η_{OP} at the self-propulsion point for each model speed using the following three equations:

$$K_{TP} = \frac{T_P}{\rho_M D_M^4 n_P^2} \quad (31)$$

$$K_{QP} = \frac{Q_P}{\rho_M D_M^5 n_P^2} \quad (32)$$

$$\eta_{OP} = \frac{J_P K_{TP}}{2\pi K_{QP}} \quad (33)$$

Where: K_{TP} = Propeller thrust coefficient in self-propulsion tests

K_{QP} = Propeller torque coefficient in self-propulsion tests

η_{OP} = Propeller efficiency in self-propulsion tests

T_P = Propeller thrust at self-propulsion point (N)

Q_P = Propeller torque at self-propulsion point (N-m)

5) Set the above propeller thrust coefficient (K_{TP}) equal to the propeller thrust coefficient from the propeller open water tests (K_{TO}) in order to determine the advance coefficient from propeller open water tests (J_O), propeller torque coefficient from propeller open water tests (K_{QO}), as well as the propeller open water efficiency (η_O) at the self-propulsion point.

This is completed by plotting J_O , K_{QO} , and η_O versus K_{TO} separately. A polynomial line is run through the data in each plot and the equation of the line is used to determine the values of J_O , K_{QO} , and η_O corresponding to the value of $K_{TO} = K_{TP}$ at the self-propulsion point.

6) Calculate the wake fraction at the self-propulsion point for each model speed using:

$$w = 1 - \frac{J_O}{J_P} \quad (34)$$

7) Determine the total resistance coefficient for the ship, denoted as C_{TS} , corresponding to each speed tested in the self-propulsion test (i.e. 8, 9, and 10 knots in this case). Note that this coefficient was calculated in the bare hull resistance tests.

8) Calculate the thrust deduction fraction at the self-propulsion point for each model speed using:

$$t = 1 - \frac{S_S}{2D_S^2} \frac{C_{TS} J_P^2}{K_{TP}} \quad (35)$$

Where: S_S = Wetted surface area of full scale vessel (m^2)

D_S = Full scale propeller diameter (m)

C_{TS} = Total resistance coefficient for the ship (from resistance tests)

8) Calculate the hull efficiency, denoted as η_H , using:

$$\eta_H = \frac{1-t}{1-w} \quad (36)$$

9) Calculate the relative rotative efficiency, denoted as η_R , using:

$$\eta_R = \frac{K_{QO}}{K_{QP}} \quad (37)$$

Again note that both coefficients are at the self-propulsion point.

10) Calculate the open water efficiency, denoted as η_o , for each model speed corresponding to the value of K_{TP} at the self-propulsion point. Note that this was explained in step 5.

11) Calculate the quasi-propulsive coefficient, denoted QPE, for each model speed by using:

$$QPE = \eta_H \eta_R \eta_o \quad (38)$$

12) Calculate the installed power required (W) at each model speed using:

$$P_{ins} = \frac{(1 + WA)P_E}{(QPE)(ET)(NC)} \quad (39)$$

Where: WA = Weather allowance

P_E = Effective power (W) (From bare hull resistance tests)

QPE = Quasi-propulsive coefficient

ET = Transmission efficiency

NC = Normal continuous rating

The transmission efficiency for the gearing and shafting system is assumed to be 98%. The normal continuous power output for the engine is assumed to be 90% of the rated power. Also, a weather allowance for the service condition is assumed to be 25%.

8.6 Description of Experimental Procedure

The data analysis procedure for the self-propulsion tests is very similar to that used for the bare hull resistance tests carried out in the MUN towing tank. However, there are a few differences that should be addressed within this section. Firstly, the torque in the system due to shaft friction has to be measured at the beginning and end of each test day. This is completed by running the propeller shaft with a dummy hub in place of the propeller at various speeds which cover the range that will be used during the actual tests.

Lines of best fit are then fit through the data for the beginning and end of each day and an average taken. This data is then used in the analysis spreadsheet.

During the actual self-propulsion tests there are different stages than in a typical run for bare hull resistance tests. Each run begins with the model stopped and the propeller turning over slowly (i.e. at approximately 1 rps), which is then used to tare the propeller thrust and torque. The next stage begins when the propeller shaft speed is turned up to whichever shaft speed is being tested during that particular run. This then provides the bollard pull of the propeller at that shaft speed. The third stage is when the model is up to running speed and the propeller is still turning over at the set rps. At each stage there is a minimum of 10 seconds of data gathered for each parameter included.

In a similar fashion to that used in the bare hull resistance tests, after the averages are taken for each run the interpreted data can be transferred to a new Microsoft Excel sheet where it is sorted accordingly. The wake and thrust deduction fractions can then be calculated for the vessel using the above description of experiment.

8.7 Results and Discussion

This section is intended to give an overview of the results obtained from the analysis of the self-propulsion tests. The detailed results are contained in Appendix D.

8.7.1 Conventional Bow

The following table and figure shows the thrust deduction and wake fractions for the model outfitted with the conventional bow.

From below it can be seen that both the thrust deduction and wake fractions are significantly lower at 10 knots than at the first two speeds. Since this general trend is found for both fractions it suggests that there is some phenomenon present which significantly changes the flow of water at the stern of the vessel. The frictional drag would be expected to increase with increased hull speed thereby increasing the wake

fraction. It was observed in the screen captures of testing that the stern section was in a trough at 7.9 knots and a partial crest at 10 knots. This would also suggest an increasing wake fraction with speed. Therefore, the decreasing fractions are most likely attributed to the differing pressure distributions over the stern section of the hull with changing speed.

It may be a good idea to complete further self-propulsion tests for this bow running the model at several speeds which cover a wider range of ship speeds than what was tested so far. This would then provide a better idea of what exactly is happening with Alpha bow attached.

Table 51: Thrust Deduction and Wake Fractions for Alpha Bow

Alpha Bow		
Speed (knots)	w	t
7.9	0.0927	0.1823
8.9	0.0732	0.1844
10.0	0.0069	0.0979

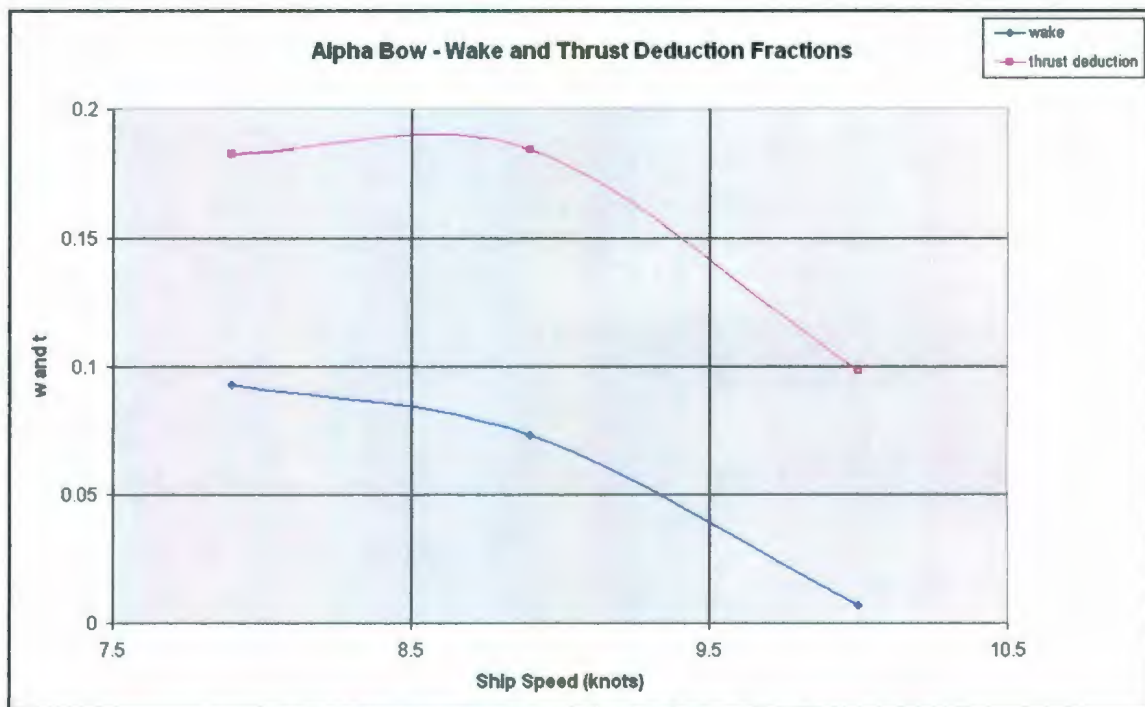


Figure 158: Thrust Deduction and Wake Fractions for Alpha Bow

The following table and figure shows the hull efficiencies calculated for Alpha bow. The hull efficiency is the ratio between the work done on the hull to the work done by the propeller. So a value less than 1.0 (as is the case for all shown in the table below) means that the propeller has to work harder to propel the vessel at a given speed.

Table 52: Hull Efficiencies for Alpha Bow

Alpha Bow	
Speed (knots)	η_H
7.9	0.901
8.9	0.880
10	0.908

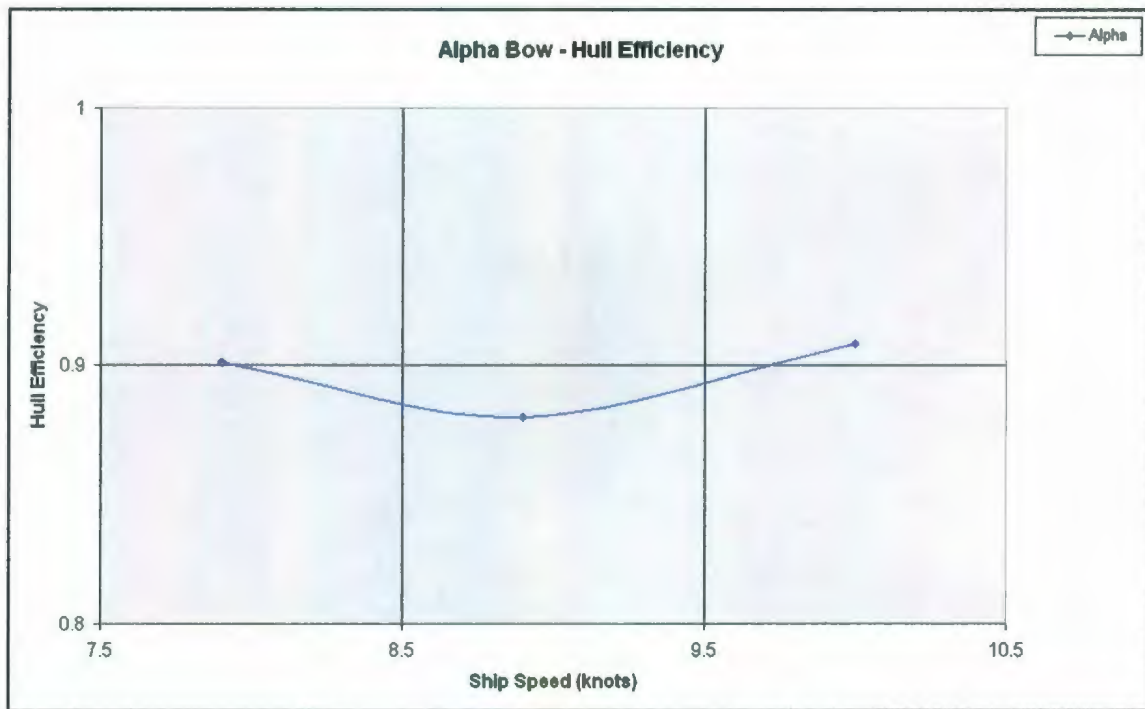


Figure 159: Hull Efficiencies for Alpha Bow

The following table and figure shows the relative rotative efficiencies calculated for Alpha bow. The relative rotative efficiency is the ratio of propeller torque in open water at a given speed to that in the behind hull condition at the same speed. There are two main reasons why the torque would vary between the two conditions. Firstly, in open water the propeller is operating in a uniform flow, which means the efficiency is likely to be higher. Secondly, there is likely to be more turbulence in the water for the behind hull condition, which would likely decrease efficiency in this condition.

As can be seen from the below table, the relative rotative efficiency is anywhere between approximately 1.103 – 1.180. The values found for this model agree well with what is written in *Principles of Naval Architecture* (1988), which concludes that for single-screw vessels the relative rotative efficiencies are expected to be in the range of 1.0 – 1.1.

Table 53: Relative Rotative Efficiencies for Alpha Bow

Alpha Bow	
Speed (knots)	η_R
7.9	1.180
8.9	1.103
10	1.130

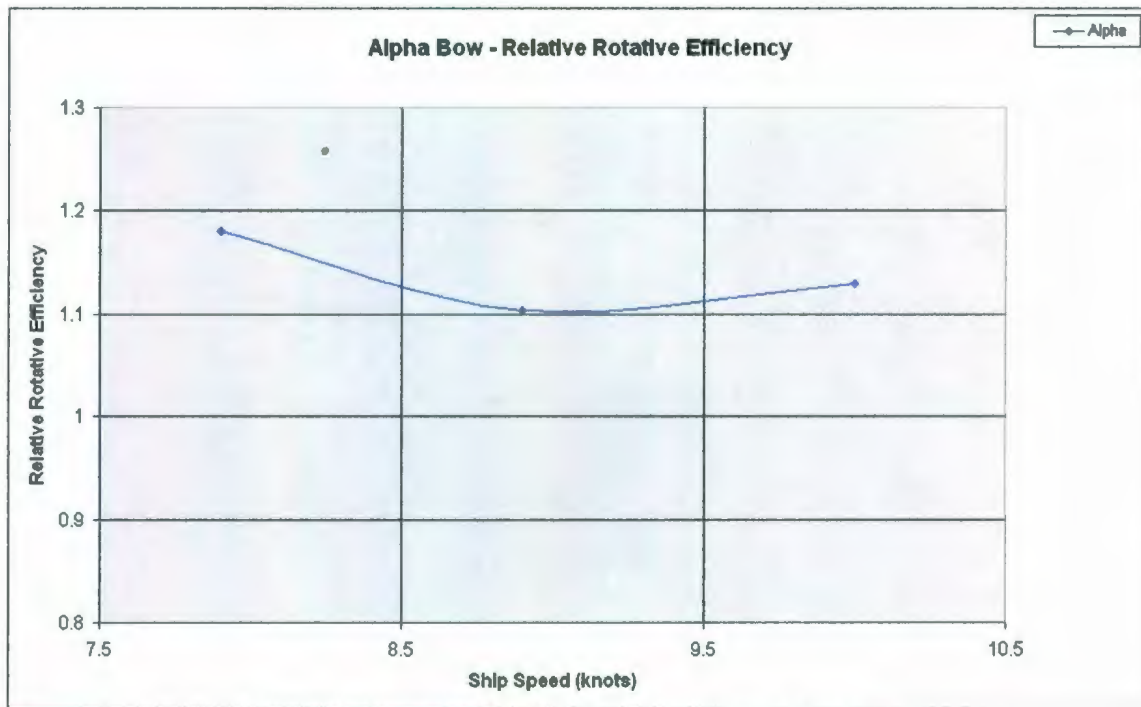


Figure 160: Relative Rotative Efficiencies for Alpha Bow

8.7.2 Bulbous Bows

The following table and figure shows the wake fractions calculated for each of the bulbous bows tested.

From below it can be seen that, with the exception of Delta and Eta bows, there is generally a slight increase of wake fraction with increasing speed. Upon comparing the screen captures taken during testing it was found that for every bow the change in wave

pattern from 7.9 to 8.9 to 10 knots is very similar. For each bow that waves crest tends to move from approximately amidships at 7.9 knots to just before the transom stern at 10 knots. Therefore, the differences in the trends of the wake fractions are most likely due to differing pressure distributions over the stern section. The frictional drag would also be slightly different for each bulb; this may play a small part in explaining the differences in the trends of the wake fractions.

Table 54: Wake Fractions for all Bulbous Bows

Speed (knots)	wake fraction							
	Beta	Delta	Gamma	Epsilon	Eta	Iota	Theta	Zeta
7.9	0.0511	0.1258	0.0387	0.0963	0.1949	0.1013	0.0334	0.0212
8.9	0.0807	0.1250	0.0469	0.1154	0.1519	0.1244	0.1070	0.0363
10.0	0.0534	0.1079	0.1040	0.1151	0.1449	0.1204	0.1296	0.0261

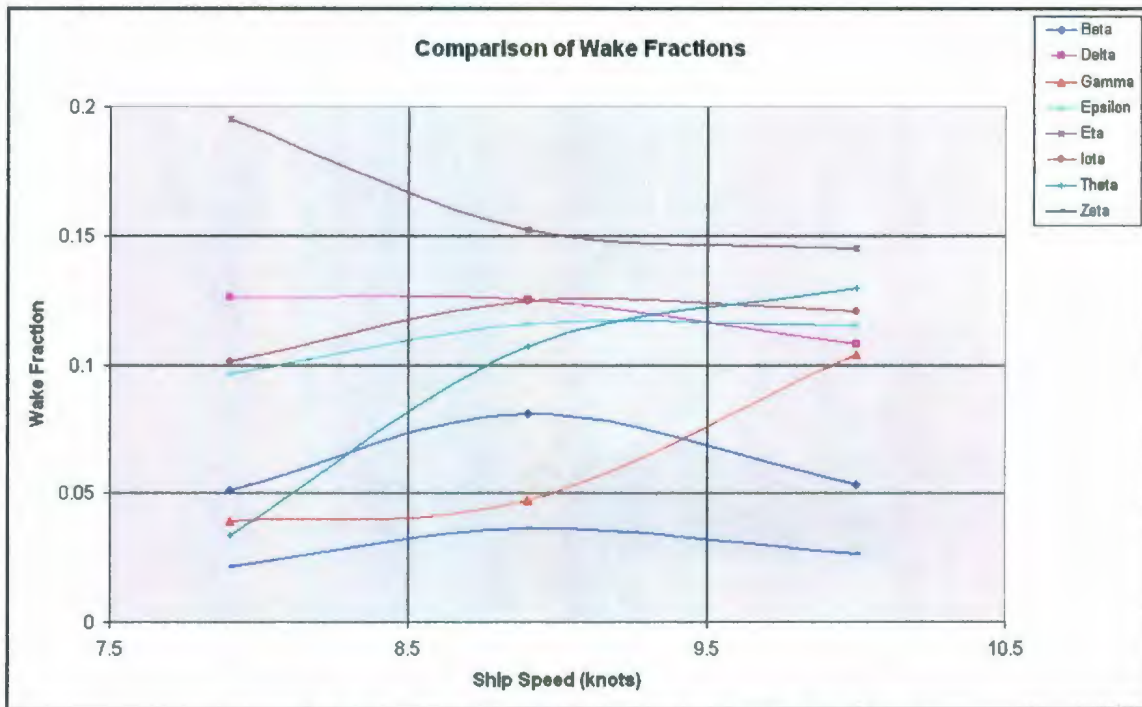


Figure 161: Comparison of Wake Fractions for Bulbous Bows

The following table and figure shows the thrust deduction fractions calculated for each of the bulbous bows tested.

From below it can be seen that, with the exception of Theta, there is generally a slight decrease of thrust deduction fraction with increasing speed. This too is most likely explained by a difference in the pressure distribution over the stern section of the hull with Theta bow present. It may be the case that with the other bows the pressure is increasing with increasing speed, which would therefore decrease the thrust deduction fraction with increasing speed. However, with Theta bow the pressure may be decreasing with increasing speed. This may be something that should be considered in more detail in further phases of the project.

Also of note there is that the thrust deduction fraction for Gamma bow takes a big dip at 8.9 knots. The wake fraction for Gamma also takes somewhat of a dip at 8.9 knots, which suggests that there may be some unusual phenomena happening to cause these unusual dips. Again, it may be a good idea to complete further self-propulsion tests for this bow running the model at several speeds which cover a wider range of ships speeds than what was tested so far. This would then provide a better idea of what is happening with Gamma bow attached.

Table 55: Thrust Deduction Fractions for all Bulbous Bows

thrust deduction fraction								
Speed (knots)	Beta	Delta	Gamma	Epsilon	Eta	Iota	Theta	Zeta
7.9	0.2567	0.3678	0.2609	0.3423	0.3423	0.2718	0.1871	0.2730
8.9	0.2620	0.3109	0.1673	0.2856	0.2297	0.2548	0.2043	0.1770
10.0	0.2023	0.2211	0.2111	0.2787	0.2321	0.2253	0.2169	0.1667

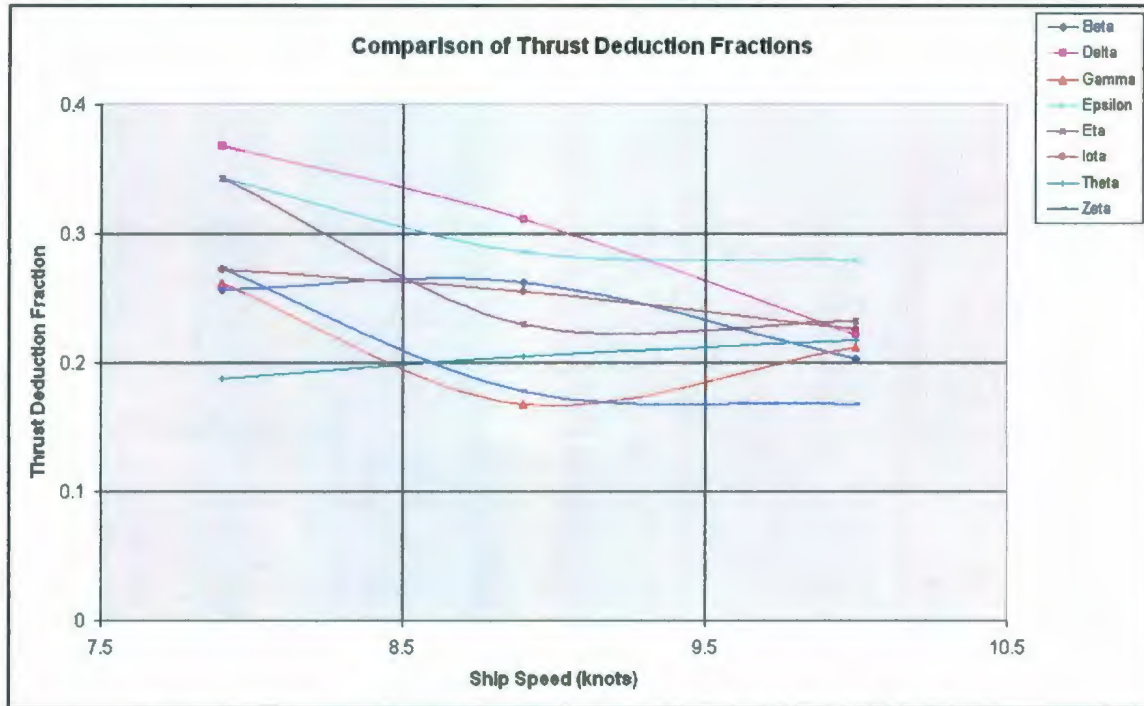


Figure 162: Comparison of Thrust Deduction Fractions for Bulbous Bows

The following table and figure shows the hull efficiencies calculated for each of the bulbous bows tested. It can be seen from below that all hull efficiencies are below 1.0. This means that the propeller has to work harder to propel the vessel at a given speed. It can be seen from below that the hull efficiency generally increases with speed. This is due to the fact that the thrust deduction fraction is generally decreasing with speed and the wake fraction is generally slightly increasing with speed. Either of these will provide an increase in hull efficiency.

Table 56: Hull Efficiencies for all Bulbous Bows

Speed (knots)	η_H							
	Beta	Delta	Gamma	Epsilon	Eta	Iota	Theta	Zeta
7.9	0.783	0.723	0.769	0.728	0.817	0.810	0.841	0.743
8.9	0.803	0.787	0.874	0.808	0.908	0.851	0.891	0.854
10.0	0.843	0.873	0.880	0.815	0.898	0.881	0.900	0.856



Figure 163: Comparison of Hull Efficiencies for Bulbous Bows

The following table and figure shows the relative rotative efficiencies calculated for each of the bulbous bows tested. The relative rotative efficiency is generally between 1.0 – 1.2 for the bulbs. The one exception is the relative rotative efficiency for Theta bow, which has lower efficiencies over the whole speed range. After looking at the test data it looks as if the torque readings for this bow may be slightly high. This data was used during the following analysis; however it may be a good idea to complete further self-propulsion tests on Theta bow to ensure that the propeller torque readings are accurate.

Table 57: Relative Rotative Efficiencies for all Bulbous Bows

Speed (knots)	η_R							
	Beta	Delta	Gamma	Epsilon	Eta	Iota	Theta	Zeta
7.9	1.099	1.160	1.064	1.116	1.103	1.148	0.986	1.015
8.9	1.089	1.076	1.071	1.078	1.101	1.121	0.965	1.088
10	1.119	0.998	1.123	1.098	1.110	1.061	0.803	1.043

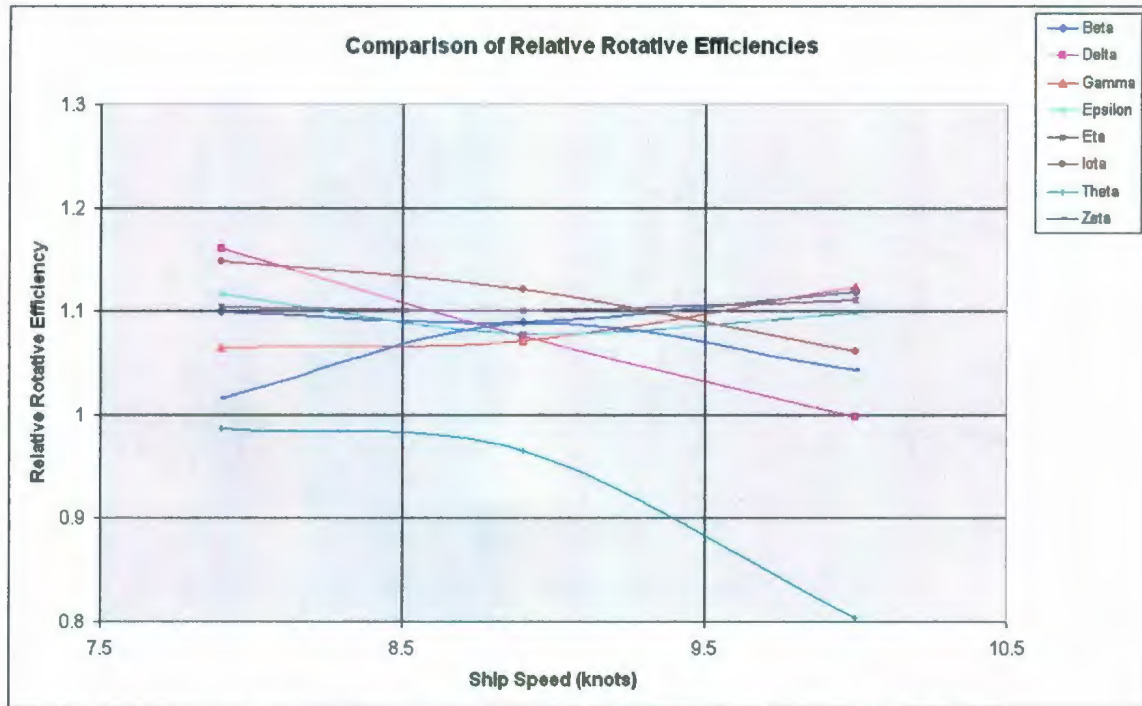


Figure 164: Comparison of Relative Rotative Efficiencies for Bulbous Bows

8.7.3 Bow Comparisons

It is also useful to compare the self-propulsion data for the conventional bow with that found for the bulbous bows. The following section provides a breakdown of all of the self-propulsion data gathered in this phase of the project.

The figure below shows the wake fractions calculated for all bows tested.

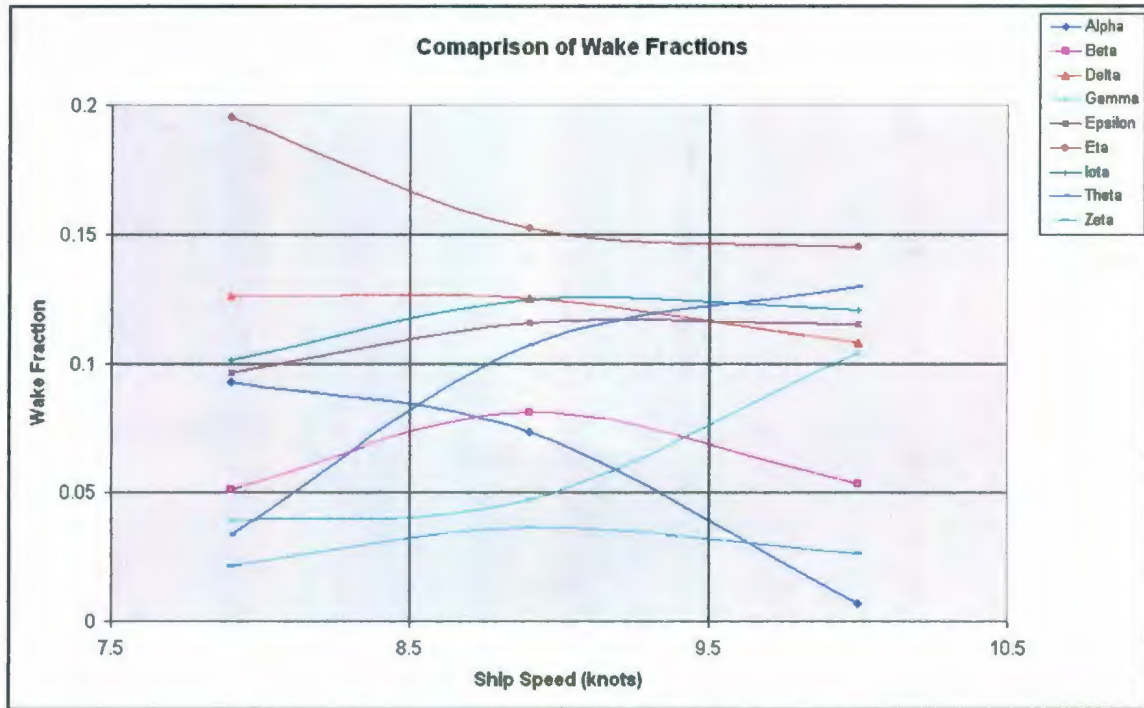


Figure 165: Comparison of Wake Fractions for All Bows

The figure below shows the thrust deduction fractions calculated for all bows tested.

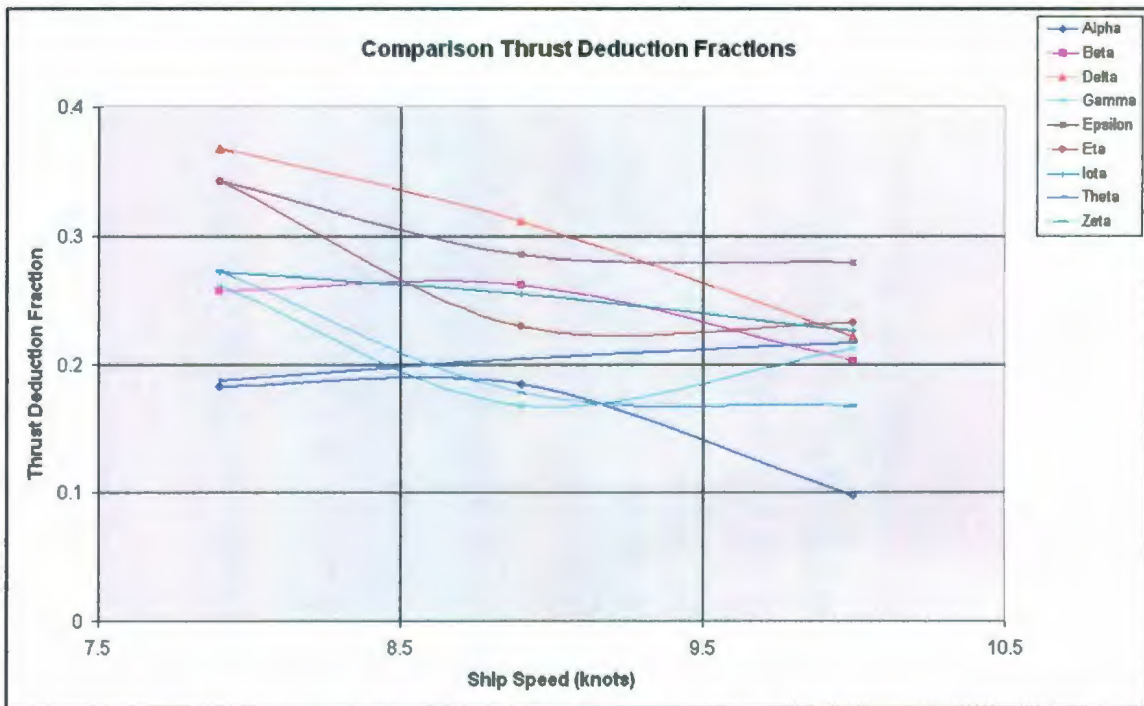


Figure 166: Comparison of Thrust Deduction Fractions for All Bows

From the above two figures it can be seen that the wake values for Alpha bow are in the same range as for the bulbous bows (with the exception of 10 knots). A study by NORDCO (1990) on a 65 ft Newfoundland type fishing found that the wake fractions were slightly higher for a bulb than for a conventional bow. However, a study by Friis et al. (2008) on a 90 ft fishing vessel found that the wake fractions were generally lower for a bulb than for a conventional bow. Since this hull form type falls somewhere in between the two aforementioned hulls it is reasonable to conclude that the wake fractions calculated for this hull form are satisfactory.

It can be seen that the thrust deduction values are generally lower for Alpha bow than the bulbs (with the exception of Gamma and Zeta bows at 8.9 knots). This is consistent with what was found by Johnson (1958), NORDCO (1990), and Friis et al. (2008).

Since the thrust deduction fractions are generally lower for Alpha bow it can be stated with reasonable confidence that there is less of a reduction in pressure at the stern with the conventional bow (i.e. some phenomena are occurring when a bulbous bow is attached which results in a greater reduction of pressure at the stern when the propeller is operating).

It is then possible to attempt to deduce what is occurring so that the wake values for Alpha at the lower speeds are in the same range as for the bulbs. If the pressure at the stern is relatively higher for Alpha bow then the wake fraction should also be higher. Since this is not the case, then there must be some phenomena which results in wake fraction values on the same order as is found for the bulbs. From pictures taken during testing it is known that the wave trains are similar for the conventional bow as for the bulbous bows. Obviously the wave heights are slightly larger for the conventional bow, but the difference in magnitudes doesn't seem large enough to fully explain the similarity in wave fraction values.

It is also known that a higher frictional drag on the hull will increase the wake fraction. The conventional bow will no doubt have a lower frictional drag than any of the bulbous

bows; therefore this may offer the best explanation of why at the lower speeds the wake values for Alpha are similar to those found for the bulbous bows. It could also explain why the wake fraction for Alpha bow is lower at 10 knots than any of the bulbous bows. As speed increases the frictional drag on the model outfitted with a bulb is likely to increase at a faster rate than the model outfitted with the conventional bow. This would result in a relatively lower wake value for the conventional bow.

The figure below shows the hull efficiencies calculated for all bows tested. It shows that the hull efficiency for Alpha bow is generally higher than that of any of the bulbous bows (with the exception of Eta and Theta bows at 8.9 knots). This is due to the fact that the thrust deduction fractions for the conventional bow are generally lower than for the bulbous bows. This is consistent with what was concluded from tests completed by Johnson (1958), NORDCO (1990), and Friis et al. (2008).

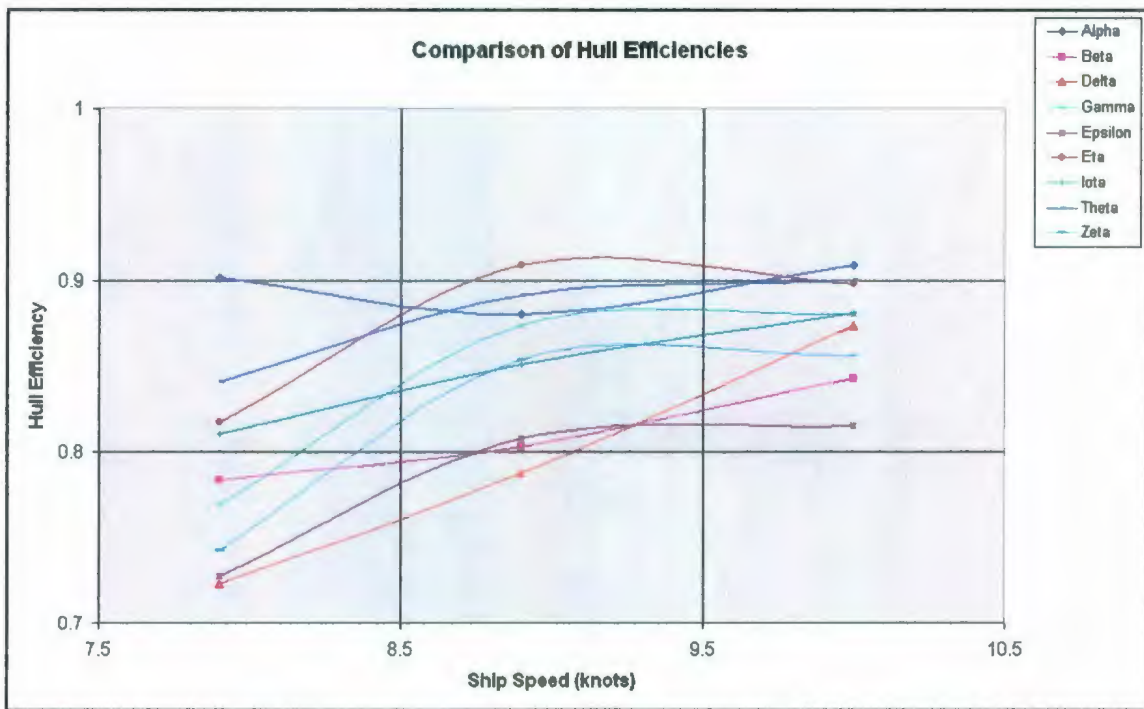


Figure 167: Comparison of Hull Efficiencies for All Bows

The figure below shows the relative rotative efficiencies calculated for all bows tested. It shows that the relative rotative efficiency for Alpha bow is generally slightly higher than that of any of the bulbous bows (with the exception of Iota bow at 8.9 knots). This is

strange, as one would expect that the propeller is operating in a more uniform flow behind the hull outfitted with a bulbous bow. However, this suggests that the propeller is operating in a more uniform flow behind the hull outfitted with a conventional bow, and hence is more efficient behind this hull.

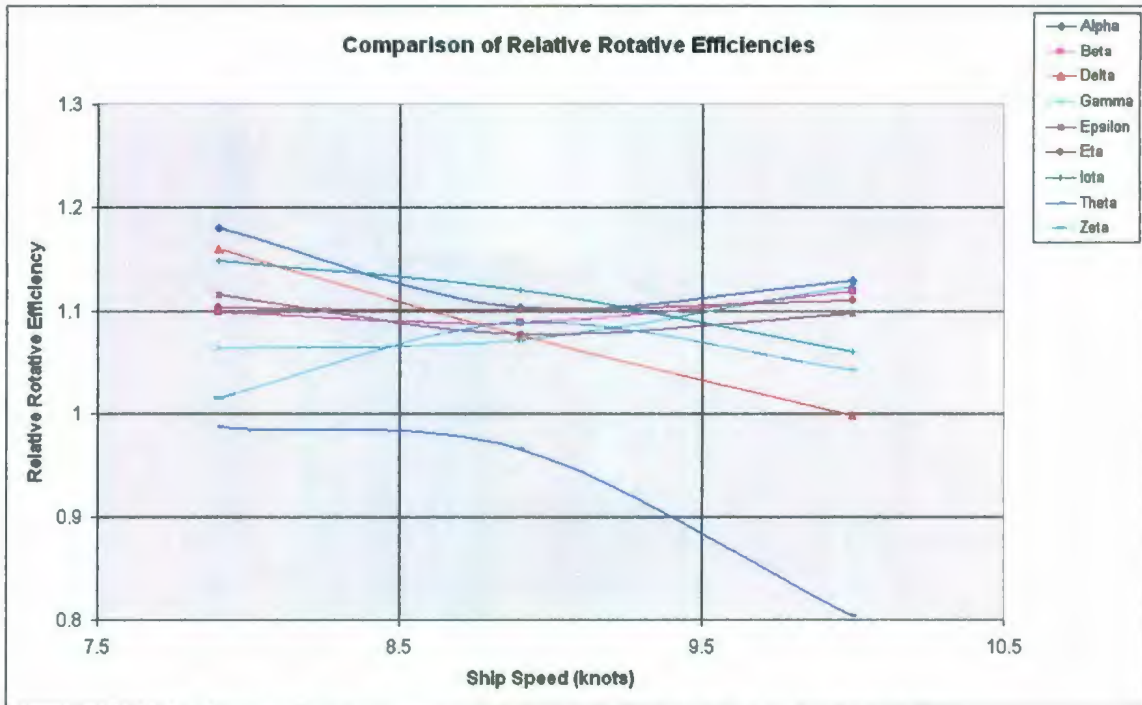


Figure 168: Comparison of Relative Rotative Efficiencies for All Bows

Since both the hull efficiency and relative rotative efficiency for the conventional is generally higher than for the bulbous bows the QPE for the conventional bow is generally higher than for the bulbous bows. This general trend can be seen in the table and figure below.

Table 58: Quasi Propulsive Efficiencies for All Bows

Speed (knots)	QPE								
	Alpha	Beta	Delta	Gamma	Epsilon	Eta	Iota	Theta	Zeta
7.9	0.496	0.417	0.398	0.401	0.389	0.399	0.450	0.400	0.366
8.9	0.443	0.404	0.386	0.451	0.402	0.443	0.441	0.386	0.440
10.0	0.470	0.425	0.388	0.443	0.393	0.422	0.414	0.305	0.407

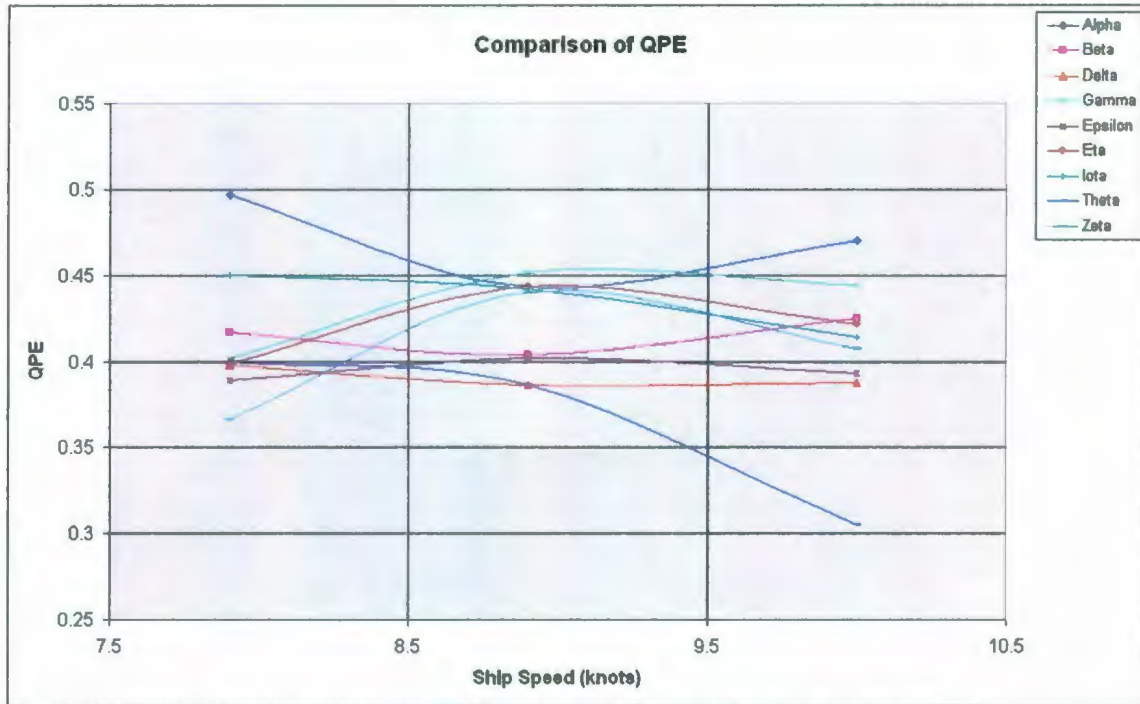


Figure 169: Comparison of Quasi Propulsive Efficiencies for All Bows

A study by Doust (1960) found that there was an increase in QPE when a bulbous bow is used. The hull form used in that study had a length to beam ratio of approximately 5.6, whereas the hull form in this study has a length to beam ratio of 3.15. The flow into the propeller race for the hull form with a length to beam ratio of 5.6 is likely much smoother than for the hull with a length to beam ratio of 3.15. Therefore, it would be difficult to directly compare the results from the two sets of tests.

8.7.4 Installed Power Values

Using the above self-propulsion data it is possible to calculate the required installed power to propel the vessel at a given speed. The installed power is the actual power required by the engine and typically used when deciding on a suitable engine that is capable of powering the vessel.

Equation 39 is used to calculate the installed power for the vessel. The transmission efficiency for the gearing and shafting system is assumed to be 98%. The normal continuous power output for the engine is assumed to be 90% of the rated power. Also, a

weather allowance for the service condition is assumed to be 25%; which is meant to take into account the vessel operating in rough weather.

Using the above equation the following three figures and table were created. These show three different ways of making comparisons of the required installed power for the vessel outfitted with the conventional bow to the vessel outfitted with each of the bulbous bows.



Figure 170: Installed Power Comparison

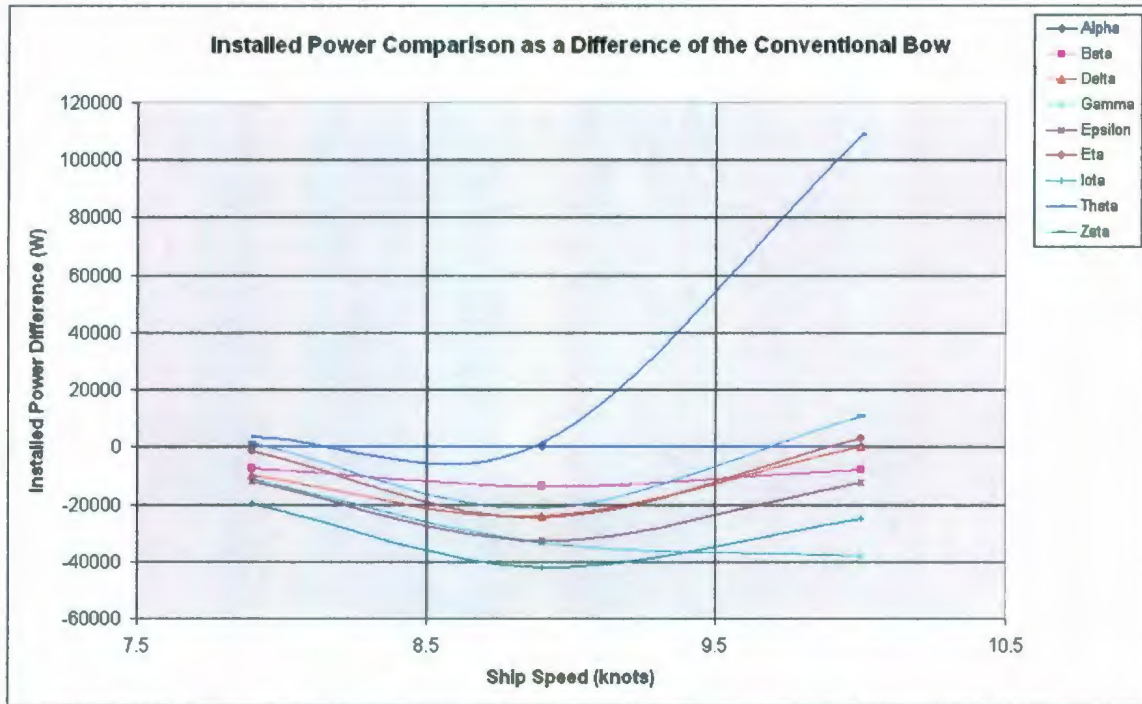


Figure 171: Installed Power Comparison as the Difference from Conventional Bow

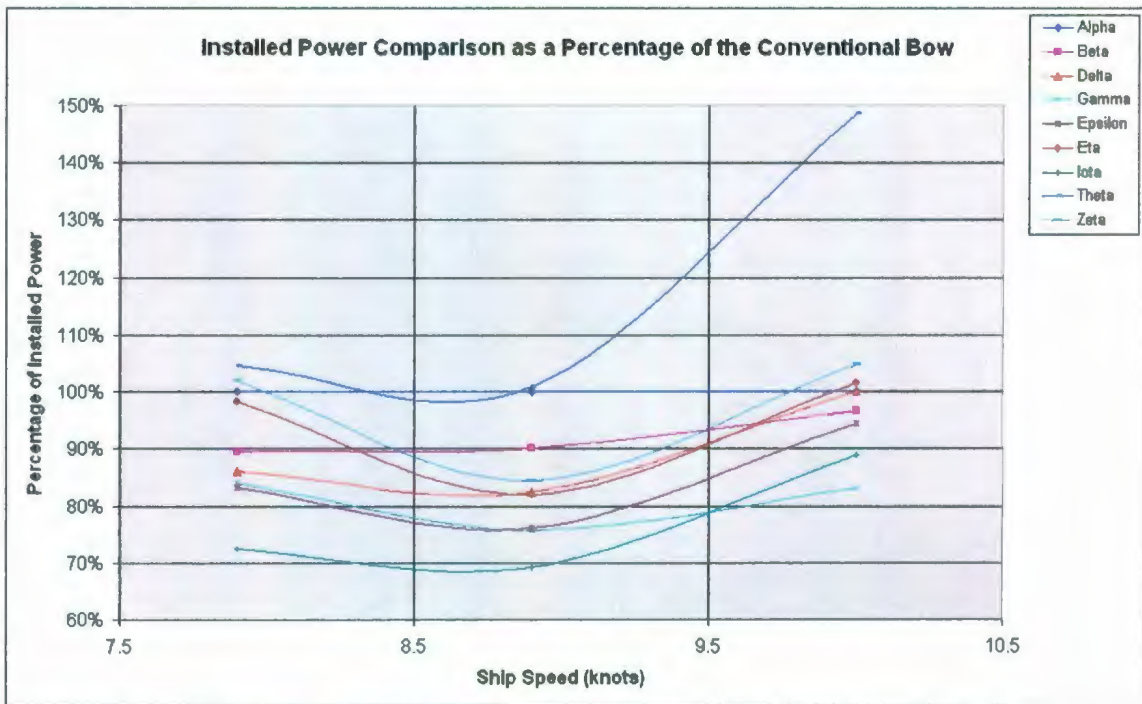


Figure 172: Installed Power Comparison as a Percentage of the Conventional Bow

Table 59: Installed Power Comparison

P_{ins} (W)									
Speed (knots)	Alpha	Beta	Delta	Gamma	Epsilon	Eta	Iota	Theta	Zeta
7.9	71082	63639	61183	59677	59152	69758	51486	74345	72442
8.9	136975	123425	112727	103486	104252	112248	94805	138244	115447
10	223833	215957	223921	185760	211243	226891	198935	332601	234405

Table 60: Installed Power Comparison the Difference from the Conventional Bow

Difference in Required Installed Power (W)									
Speed (knots)	Alpha	Beta	Delta	Gamma	Epsilon	Eta	Iota	Theta	Zeta
7.9	0.0	-7443	-9899	-11405	-11930	-1324	-19595	3263	1360
8.9	0.0	-13551	-24249	-33489	-32723	-24727	-42171	1269	-21528
10	0.0	-7876	88	-38073	-12590	3058	-24898	108768	10572

Table 61: Installed Power Comparison as a Percentage of the Conventional Bow

% Savings in Required Installed Power (%)									
Speed (knots)	Alpha	Beta	Delta	Gamma	Epsilon	Eta	Iota	Theta	Zeta
7.9	100.00	89.53	86.07	83.96	83.22	98.14	72.43	104.59	101.91
8.9	100.00	90.11	82.30	75.55	76.11	81.95	69.21	100.93	84.28
10	100.00	96.48	100.04	82.99	94.38	101.37	88.88	148.59	104.72

From above it can be seen that not all bows outperform the conventional bow from a powering point of view over the design speed range of 8 – 10 knots. Theta bow never performs better than the conventional bow in this speed range. However this may have to do with the fact that the torque values seemed high for this bow during the self-propulsion tests which in turn influenced the relative rotative efficiencies. In this speed range Iota and Gamma bows are generally the two best performers.

At 7.9 knots Iota bow requires about 19.6 kW less power than the conventional bow. At this speed Epsilon bow is the next best performer, requiring approximately 11.9 kW less power. At 8.9 knots Iota requires approximately 42.2 kW less power and Gamma almost 33.5 kW less. Finally, at 10 knots Gamma requires almost 38.1 kW less power, while Iota requires about 24.9 kW less.

The following table provides a ranking of the best bulbous bow based on the average reduction of required installed power over the design speed range. Also shown are the main parameters of each of the bulbous bows tested.

Table 62: Ranking of Bulbous Bows based on Installed Power Requirements

Rank	Fairing Type	Length (ft)	% A_m (%)
Iota	None	0.425	29.47
Gamma	None	0.59	17.64
Epsilon	S-Shaped	0.59	17.64
Delta	None	0.425	17.64
Beta	Straight Line	0.59	17.64
Eta	Straight Line	0.59	23.48
Zeta	S-Shaped	0.425	17.64
Theta	Straight Line	0.425	23.48

The above rankings are similar to the rankings of bulbous bow performance based on required effective power. This indicates that the quasi-propulsive efficiencies of all bulbous bows are similar in magnitude, as can be seen in the previous section.

Chapter 9 - Uncertainty Analysis

In order to determine any errors involved in experimental testing an uncertainty analysis must be completed. This procedure has been completed for the bare hull resistance tests that have been carried out in the IOT ice tank as well as the MUN towing tank. Based on the findings from this analysis it is possible to determine how each facility may influence the findings from each set of resistance tests. This can then be used to determine if the comparisons made in Chapter 7 between the IOT and MUN test data are still reliable, or if the errors associated with testing are responsible for the discrepancies in data between the two test programs.

9.1 Bare Hull Resistance Tests

The uncertainty analysis performed was based on guidelines provided by the International Towing Tank Conference (ITTC); more specifically the ITTC Recommended Procedures and Guidelines: Uncertainty Analysis – 7.5-02-01-01 (1999). The ITTC Recommended Procedures and Guidelines: Uncertainty Analysis, Example for Resistance Test – 7.5-02-02-02 (2002) was also used as a reference for creating a spreadsheet to complete the analysis. The methodology used in the above standards is based on material from Coleman and Steele (1999). The details from the analysis of both sets of resistance tests can be found in Appendix E, which includes a detailed outline of the methodology used throughout the analysis.

Based upon the methodology outlined in the above guideline experimental errors can be considered to be composed of two components: a bias component and a precision component. The bias component is composed of errors which are inherent in the system; these are considered to be systematic errors. Bias errors may be reduced through calibration. The precision component is composed of errors which are variable in nature; these are considered to be random errors. Precision errors may be reduced through the use of multiple readings (i.e. multiple test runs).

9.1.1 Test Design

Since the analysis is performed on the non-dimensional performance coefficients it is important to first identify all of the variables contained in each of the data reduction equations. This will later help identify which of the variables are the major contributors of uncertainty in the system, which in turn could be useful in identifying how to reduce the overall uncertainty in the system. The data reduction equations of interest, which have been discussed earlier in Chapter 5, are listed as:

$$C_{TM} = \frac{R_{TM}}{\frac{1}{2} \rho_M V_M^2 S_M} \quad (2)$$

Where: R_{TM} = total model resistance measured

ρ_M = fresh water density (which is a function of water temperature)

V_M = model speed (i.e. carriage speed)

S_M = model wetted surface area

$$C_{FM} = \frac{0.075}{(\log_{10} R_{nM} - 2)^2} \quad (3)$$

Where R_{nM} is given as:

$$R_{nM} = \frac{V_M L_M}{\nu_M} \quad (4)$$

Where: L_M = model length on waterline

ν_M = kinematic viscosity for fresh water

$$C_R = C_{TM} - C_{FM} \quad (5)$$

9.1.2 Measurement System and Procedure

The bias limits that contribute to the total uncertainty are estimated for the following individual variables: hull geometry, speed, resistance, temperature, density, and viscosity. The elementary bias limits for each variable are estimated for the following categories: calibration, data acquisition, data reduction, and conceptual bias. Note that not all categories are applicable for every variable. Using the above equations for C_{TM} , C_R , and C_{FN} the bias limits are then reduced to B_{CT} , B_{CR} , and B_{CF} respectively.

The precision limits for the total resistance coefficient at a temperature of 15°C, P_{CT} , residuary resistance coefficient, P_{CR} , and frictional resistance coefficient, P_{CF} , are estimated by an end-to-end method where all of the precision errors for speed, resistance, temperature, density, and viscosity are included.

9.1.3 Calculating the Total Uncertainties

The total uncertainty for both the total resistance and residual resistance coefficients are determined using the root sum square (RSS) of the uncertainties of the total bias and precision limits. This is demonstrated in the two equations below:

$$(U_{CT})^2 = (B_{CT})^2 + (P_{CT})^2 \quad (40)$$

$$(U_{CR})^2 = (B_{CR})^2 + (P_{CR})^2 \quad (41)$$

$$(U_{CF})^2 = (B_{CF})^2 + (P_{CF})^2 \quad (42)$$

The error estimates used in the determination of both the bias and precision limits in this analysis are assumed to be made at a 95% confidence level. This means that the true value of the quantity is expected to be within the $\pm U$ interval about the experimentally determined value 95 times out of 100.

The bias limit for the total resistance coefficient can be calculated as:

$$(B_{CT})^2 = \left(\frac{\partial C_T}{\partial S} B_S \right)^2 + \left(\frac{\partial C_T}{\partial V} B_V \right)^2 + \left(\frac{\partial C_T}{\partial R_x} B_{R_x} \right)^2 + \left(\frac{\partial C_T}{\partial \rho} B_\rho \right)^2 \quad (43)$$

Where: B_S = wetted surface area error

B_V = speed error

B_{R_x} = resistance error

B_ρ = density error

The bias limit for the residual resistance coefficient can then be calculated as:

$$(B_{CR})^2 = \left(\frac{\partial C_R}{\partial C_T} B_{CT} \right)^2 + \left(\frac{\partial C_R}{\partial C_F} B_{CF} \right)^2 \quad (44)$$

Where B_{CF} , which is the bias limit for the frictional resistance coefficient, is given as:

$$(B_{CF})^2 = \left(\frac{\partial C_F}{\partial V} B_V \right)^2 + \left(\frac{\partial C_F}{\partial L} B_L \right)^2 + \left(\frac{\partial C_F}{\partial R_v} B_v \right)^2 \quad (45)$$

Where: B_L = model length error

B_v = water viscosity error

The precision limits for multiple runs can be calculated according to the following two equations:

$$P_{CT} = \frac{K \cdot S_{DEVCT}}{\sqrt{M}} \quad (46)$$

$$P_{CR} = \frac{K \cdot S_{DEVCR}}{\sqrt{M}} \quad (47)$$

$$P_{CF} = \frac{K \cdot S_{DEVCF}}{\sqrt{M}} \quad (48)$$

Where: K = coverage factor (taken as equal to 2 according to the methodology)

S_{DevCT} = standard deviation for C_T (established by multiple runs)

S_{DevCR} = standard deviation for C_R (established by multiple runs)

S_{DevCF} = standard deviation for C_F (established by multiple runs)

M = number of runs for which the precision limit is to be established

9.1.4 Uncertainty Analysis Results for IOT Testing

The results from the uncertainty analysis for the resistance tests carried out in the IOT ice tank are contained within this section. The analysis was carried out only on the test data for each bow at the static level trim condition.

The bias errors were determined for each variable by estimating the elementary error associated with each of the following categories: calibration, data acquisition, data reduction, and conceptual bias. Note that the categories not applicable for each respective variable have been left out.

The following table shows the estimates for the individual bias errors as well as the total bias limit for each of the variables included in the data reduction equations shown above. Note that only the data for Alpha bow (data from 'Alpha2' tests) at 10 knots full scale is given within this section; and is intended to be used as an example of how the uncertainty is calculated for any given test condition. It would be too space consuming to list all of the bias errors for each bow at all of the speeds tested. Again, the complete details of the procedure, including explanations for the individual bias error estimates for each variable, and analysis are outlined for each bow tested at every speed in Appendix E.

Table 63: Bias Errors for Alpha Bow Test Carried out in the IOT Ice Tank at 10 knots Full Scale

Alpha Test @ IOT- 10 knots Full Scale		
Variable	Bias Errors	Bias Limit
Model Length	Data Acquisition: ± 0.002 m	
Wetted Surface Area	Data Acquisition: ± 0.003946 m ² Calibration: ± 0.000860 m ²	Total: ± 0.004038 m ²
Speed	Pulse Count: ± 0.0058255 m/s Wheel Diameter: ± 0.0004276 m/s Time Base: ± 0.0001906 m/s	Total: ± 0.005844 m/s
Resistance	Calibration: ± 0.001739 N Data Acquisition: ± 0.194895 N	Total: ± 0.194975 N
Temperature	Calibration: ± 0.5 °C Data Acquisition: ± 0.1 °C	Total: ± 0.5099 °C
Density	Calibration: ± 0.075873 kg/m ³ Data Reduction: ± 0.07 kg/m ³	Total: ± 0.103232 kg/m ³
Viscosity	Calibration: $\pm 1.534805E-08$ m ² /s Data Reduction: $4.15E-10$ m ² /s	Total: $\pm 1.535366E-08$ m ² /s

The bias errors in the above table are then combined using equations 43 – 45 to determine the total bias limits for the resistance coefficients C_T , C_R , and C_F . The values for Alpha bow at 10 knots are as follows:

$$B_{CT} = \pm 0.000162$$

$$B_{CR} = \pm 0.000162$$

$$B_{CF} = \pm 1.0261E-05$$

The precision errors, as calculated using the method outlined above, had to be estimated using the data gathered during the MUN resistance test program. This is due to the fact that there were very few repeat runs conducted during the IOT test program. Since there were few repeat runs it would be difficult to determine the standard deviation for the resistance coefficients with any accuracy. However, during the MUN test program there was a total of ten runs that were repeated. Because both test programs use very similar test instrumentation and both programs were conducted according to the IOT Standard Resistance Procedure (2006) it is likely that the precision errors are very similar in both test programs. Therefore the MUN data was used to come up with the values for the precision limits for C_T , C_R , and C_F .

The precision limits are calculated according to equations 46 – 48. Therefore the standard deviations for both C_T and C_R had to be estimated. These were both calculated based on the ten runs in the MUN towing tank which were repeated. The standard deviation was calculated for each of the ten repeats and an average taken for both the standard deviations for C_T , C_R , and C_F . The following precision limits were calculated for C_T , C_R , and C_F .

$$P_{CT} = \pm 0.0002263$$

$$P_{CR} = \pm 0.0002333$$

$$P_{CF} = \pm 7.336E-07$$

The total bias limits and precision limits are finally combined using equations 40 – 41 to obtain the total uncertainty for C_T , C_R , and C_F . The values for Alpha bow at 10 knots are as follows:

$$U_{CT} = \pm 0.000278$$

$$U_{CR} = \pm 0.000284$$

$$U_{CF} = \pm 1.0287E-05$$

These uncertainties then have to be applied to the test data in order to determine the precise effects on the full scale resistance data. It is known from the ITTC-57 method that the total resistance coefficient for a full scale ship, as calculated using equation 8, is:

$$C_{TS} = C_{FS} + C_R + C_A \quad (8)$$

The above equation can be rewritten to include the uncertainties in both the frictional resistance coefficient and the residual resistance coefficient as follows:

$$C_{TS} = (C_{FS} \pm U_{CF}) + (C_R \pm U_{CR}) + C_A \quad (49)$$

The maximum and minimum values of C_{TS} can then be inserted into equations 9 and 10 to determine the maximum and minimum values of the required effective power for each bow. The following four tables show the calculated effective powers for each bow at each full scale speed tested in the IOT test program. In each table is the maximum and minimum possible effective power as calculated using the above uncertainty analysis; the difference between the actual calculated effective power and the maximum and minimum effective powers; as well as the percentage of the calculated effective power for both the maximum and minimum effective powers.

Table 64: Max/Min Full Scale Effective Powers for Alpha Bow during IOT Tests

Alpha @ IOT – Level Trim Condition					
Ship Speed	P_E	Maximum P_E	Minimum P_E	Average Difference from calculated P_E	Percentage of calculated P_E
(knots)	(kW)	(kW)	(kW)	(kW)	(%)
1	0.130	0.177	0.083	0.047	36.09%
2	0.057	0.152	-0.038	0.095	166.04%
3	0.401	0.547	0.253	0.147	36.73%
4	0.985	1.185	0.782	0.202	20.47%
5	2.058	2.335	1.777	0.279	13.55%
6	4.164	4.543	3.776	0.384	9.21%
7	10.598	11.119	10.052	0.533	5.03%
8	22.314	23.018	21.559	0.730	3.27%
9	41.631	42.587	40.578	1.005	2.41%
10	76.280	77.569	74.813	1.378	1.81%

Table 65: Max/Min Full Scale Effective Powers for Beta Bow during IOT Tests

Beta @ IOT – Level Trim Condition					
Ship Speed	P_E	Maximum P_E	Minimum P_E	Average Difference from calculated P_E	Percentage of calculated P_E
(knots)	(kW)	(kW)	(kW)	(kW)	(%)
1	0.016	0.066	-0.034	0.050	308.20%
2	0.140	0.236	0.030	0.103	73.19%
3	0.515	0.667	0.349	0.159	30.92%
4	1.322	1.503	1.069	0.217	16.44%
5	2.581	2.859	2.258	0.300	11.63%
6	5.098	5.531	4.707	0.412	8.08%
7	9.905	10.602	9.473	0.565	5.70%
8	22.542	22.906	21.386	0.760	3.37%
9	41.812	42.500	40.439	1.031	2.47%
10	77.034	78.370	75.602	1.384	1.80%

Table 66: Max/Min Full Scale Effective Powers for Gamma Bow during IOT Tests

Gamma @ IOT – Level Trim Condition					
Ship Speed	P_E	Maximum P_E	Minimum P_E	Average Difference from calculated P_E	Percentage of calculated P_E
(knots)	(kW)	(kW)	(kW)	(kW)	(%)
1	0.041	0.090	-0.009	0.049	121.17%
2	0.205	0.301	0.098	0.101	49.54%
3	0.665	0.833	0.520	0.157	23.60%
4	1.670	1.829	1.400	0.214	12.83%
5	3.105	3.381	2.789	0.296	9.53%
6	5.234	5.703	4.892	0.406	7.76%
7	9.288	9.873	8.760	0.556	5.99%
8	18.236	18.953	17.459	0.747	4.10%
9	35.191	35.953	33.929	1.012	2.88%
10	64.981	66.592	63.884	1.354	2.08%

Table 67: Max/Min Full Scale Effective Powers for Epsilon Bow during IOT Tests

Epsilon @ IOT – Level Trim Condition					
Ship Speed	P_E	Maximum P_E	Minimum P_E	Average Difference from calculated P_E	Percentage of calculated P_E
(knots)	(kW)	(kW)	(kW)	(kW)	(%)
1	0.049	0.098	-0.001	0.050	102.45%
2	0.209	0.318	0.114	0.102	48.71%
3	0.586	0.742	0.426	0.158	26.94%
4	1.480	1.665	1.234	0.216	14.57%
5	2.915	3.205	2.609	0.298	10.22%
6	4.357	4.803	3.986	0.408	9.37%
7	8.560	9.266	8.146	0.560	6.54%
8	19.181	19.708	18.203	0.752	3.92%
9	37.225	38.128	36.089	1.020	2.74%
10	68.828	70.458	67.726	1.366	1.98%

The following plot shows a comparison of the required effective power calculated for each of the four bows tested during the IOT test program. The plot also includes error bars which correspond to the errors calculated in the uncertainty analysis. Again, the error bars represent the 95% confidence interval estimate of the uncertainty in the data.



Figure 173: Effective Power Comparison with Error Bars at Level Trim for IOT Tests

From the above tables and figure it can be stated that the results obtained from the resistance tests conducted in the IOT ice tank provide a good representation of the actual performance of the hull form under the specific test conditions.

The figure and table below both show a comparison of the maximum possible effective powers for each bow to the minimum possible effective power for Alpha bow; which is essentially a comparison of the worst case scenario for each bow with the best case scenario for the conventional bow. This shows that both Epsilon and Gamma bows will still outperform the conventional bow above approximately 7 knots. In the speed range of 8 – 10 knots Gamma requires approximately 11 – 12.1% less effective power than Alpha bow. In this range Epsilon requires between approximately 5.8 – 8.6% less effective power. Beta would require between 4.8 – 6.3% more effective power in this range.

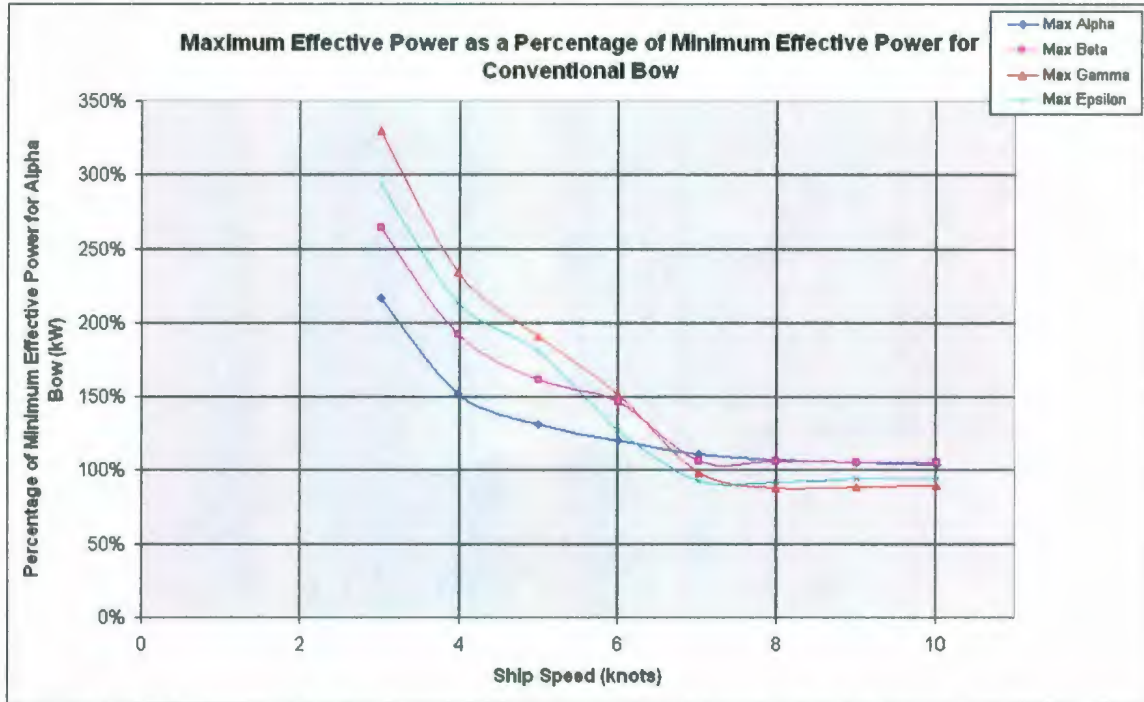


Figure 174: Maximum Effective Power as Percentage of Minimum Effective Power for Conventional Bow from IOT Tests

Table 68: Maximum Effective Power as Percentage of Minimum Effective Power for Conventional Bow from IOT Tests

% of Minimum Effective Power for Conventional Bow (%)				
Speed (knots)	Alpha	Beta	Gamma	Epsilon
3	216.34	263.72	329.54	293.40
4	151.55	192.29	233.93	213.01
5	131.40	160.90	190.29	180.35
6	120.32	146.48	151.05	127.20
7	110.61	105.48	98.22	92.18
8	106.77	106.25	87.91	91.41
9	104.95	104.74	88.60	93.96
10	103.68	104.75	89.01	94.18

9.1.5 Uncertainty Analysis Results from MUN Tests

The results from the uncertainty analysis for the resistance tests carried out in the MUN towing tank are contained within this section. The same procedure was applied to the data from the MUN resistance test program as in the IOT test program. The maximum and minimum values of the required effective power for each bow were determined using the method described above. The complete details of the procedure and analysis are outlined in Appendix E.

The following nine tables show the calculated effective powers for each bow at each full scale speed tested in the MUN test program. In each table is the maximum and minimum possible effective power as calculated using the above uncertainty analysis; the difference between the actual calculated effective power and both the maximum and minimum effective powers; as well as the percentage of the calculated effective power for both the maximum and minimum effective powers.

Table 69: Max/Min Full Scale Effective Powers for Alpha Bow during MUN Tests

Alpha @ MUN – Level Trim Condition					
Ship Speed	P_E	Maximum P_E	Minimum P_E	Average Difference from calculated P_E	Percentage of calculated P_E
(knots)	(kW)	(kW)	(kW)	(kW)	(%)
1.6	0.226	0.343	0.110	0.116	51.39%
3.7	1.075	1.354	0.796	0.279	25.99%
4.7	2.341	2.715	1.967	0.374	15.99%
5.8	6.096	6.589	5.604	0.492	8.07%
6.8	12.274	12.916	11.632	0.642	5.23%
7.9	24.899	25.749	24.050	0.850	3.41%
8.9	42.788	43.905	41.671	1.117	2.61%
10	74.284	75.765	72.803	1.481	1.99%
11	125.493	127.454	123.531	1.962	1.56%
12.1	194.584	197.148	192.021	2.564	1.32%

Table 70: Max/Min Full Scale Effective Powers for Beta Bow during MUN Tests

Beta @ MUN – Level Trim Condition					
Ship Speed	P_E	Maximum P_E	Minimum P_E	Average Difference from calculated P_E	Percentage of calculated P_E
(knots)	(kW)	(kW)	(kW)	(kW)	(%)
1.6	0.112	0.238	-0.014	0.126	112.33%
3.7	1.469	1.771	1.166	0.302	20.60%
4.7	2.822	3.226	2.417	0.404	14.33%
5.8	4.893	5.421	4.366	0.527	10.78%
6.8	9.491	10.173	8.810	0.681	7.18%
7.9	18.709	19.596	17.823	0.886	4.74%
8.9	35.185	36.336	34.033	1.151	3.27%
10	64.742	66.241	63.243	1.499	2.32%
11	113.848	115.789	111.907	1.941	1.70%
12.1	168.010	170.493	165.527	2.483	1.48%

Table 71: Max/Min Full Scale Effective Powers for Delta Bow during MUN Tests

Delta @ MUN – Level Trim Condition					
Ship Speed	P _E	Maximum P _E	Minimum P _E	Average Difference from calculated P _E	Percentage of calculated P _E
(knots)	(kW)	(kW)	(kW)	(kW)	(%)
1.6	0.065	0.187	-0.057	0.122	187.13%
3.7	1.174	1.466	0.883	0.292	24.86%
4.7	2.611	3.001	2.220	0.390	14.95%
5.8	4.765	5.274	4.255	0.509	10.68%
6.8	7.420	8.077	6.763	0.657	8.86%
7.9	17.164	18.019	16.309	0.855	4.98%
8.9	30.728	31.837	29.619	1.109	3.61%
10	61.227	62.671	59.782	1.444	2.36%
11	106.452	108.317	104.586	1.866	1.75%
12.1	175.036	177.441	172.630	2.405	1.37%

Table 72: Max/Min Full Scale Effective Powers for Gamma Bow during MUN Tests

Gamma @ MUN – Level Trim Condition					
Ship Speed	P _E	Maximum P _E	Minimum P _E	Average Difference from calculated P _E	Percentage of calculated P _E
(knots)	(kW)	(kW)	(kW)	(kW)	(%)
1.6	0.170	0.294	0.045	0.124	73.20%
3.7	0.979	1.277	0.681	0.298	30.43%
4.7	2.269	2.667	1.870	0.399	17.57%
5.8	5.224	5.744	4.704	0.520	9.95%
6.8	8.697	9.368	8.026	0.671	7.72%
7.9	16.873	17.746	16.000	0.873	5.17%
8.9	32.952	34.086	31.819	1.133	3.44%
10	58.127	59.599	56.654	1.473	2.53%
11	102.051	103.952	100.150	1.901	1.86%
12.1	174.502	176.958	172.046	2.456	1.41%

Table 73: Max/Min Full Scale Effective Powers for Epsilon Bow during MUN Tests

Epsilon @ MUN – Level Trim Condition					
Ship Speed	P _E	Maximum P _E	Minimum P _E	Average Difference from calculated P _E	Percentage of calculated P _E
(knots)	(kW)	(kW)	(kW)	(kW)	(%)
1.6	-0.031	0.094	-0.156	0.125	-404.26%
3.7	0.833	1.133	0.533	0.300	36.01%
4.7	1.739	2.140	1.338	0.401	23.06%
5.8	3.667	4.190	3.144	0.523	14.26%
6.8	7.647	8.323	6.972	0.675	8.83%
7.9	16.233	17.111	15.355	0.878	5.41%
8.9	29.552	30.691	28.413	1.139	3.86%
10	58.561	60.044	57.078	1.483	2.53%
11	99.339	101.251	97.426	1.912	1.93%
12.1	165.525	167.987	163.064	2.462	1.49%

Table 74: Max/Min Full Scale Effective Powers for Eta Bow during MUN Tests

Eta @ MUN – Level Trim Condition					
Ship Speed	P_E	Maximum P_E	Minimum P_E	Average Difference from calculated P_E	Percentage of calculated P_E
(knots)	(kW)	(kW)	(kW)	(kW)	(%)
1.6	0.059	0.186	-0.067	0.126	213.58%
3.7	0.990	1.294	0.686	0.304	30.67%
4.7	2.238	2.644	1.832	0.406	18.15%
5.8	5.329	5.859	4.799	0.530	9.94%
6.8	10.004	10.688	9.320	0.684	6.84%
7.9	19.617	20.508	18.727	0.890	4.54%
8.9	35.082	36.238	33.926	1.156	3.29%
10	67.484	68.991	65.976	1.507	2.23%
11	111.793	113.739	109.847	1.946	1.74%
12.1	171.455	173.952	168.957	2.497	1.46%

Table 75: Max/Min Full Scale Effective Powers for Iota Bow during MUN Tests

Iota @ MUN – Level Trim Condition					
Ship Speed	P_E	Maximum P_E	Minimum P_E	Average Difference from calculated P_E	Percentage of calculated P_E
(knots)	(kW)	(kW)	(kW)	(kW)	(%)
1.6	0.142	0.265	0.018	0.124	87.17%
3.7	1.191	1.488	0.894	0.297	24.92%
4.7	2.997	3.394	2.600	0.397	13.25%
5.8	6.040	6.558	5.522	0.518	8.57%
6.8	8.402	9.070	7.734	0.668	7.95%
7.9	16.338	17.207	15.469	0.869	5.32%
8.9	29.523	30.650	28.396	1.127	3.82%
10	58.143	59.609	56.676	1.466	2.52%
11	104.042	105.937	102.147	1.895	1.82%
12.1	168.859	171.297	166.421	2.438	1.44%

Table 76: Max/Min Full Scale Effective Powers for Theta Bow during MUN Tests

Theta @ MUN – Level Trim Condition					
Ship Speed	P_E	Maximum P_E	Minimum P_E	Average Difference from calculated P_E	Percentage of calculated P_E
(knots)	(kW)	(kW)	(kW)	(kW)	(%)
1.6	0.080	0.205	-0.044	0.124	154.66%
3.7	1.481	1.779	1.183	0.298	20.14%
4.7	2.527	2.926	2.128	0.399	15.79%
5.8	5.710	6.231	5.190	0.520	9.11%
6.8	10.377	11.049	9.705	0.672	6.48%
7.9	20.965	21.840	20.090	0.875	4.17%
8.9	37.675	38.812	36.538	1.137	3.02%
10	71.560	73.043	70.076	1.484	2.07%
11	119.040	120.958	117.121	1.919	1.61%
12.1	178.370	180.830	175.910	2.460	1.38%

Table 77: Max/Min Full Scale Effective Powers for Zeta Bow during MUN Tests

Zeta @ MUN – Level Trim Condition					
Ship Speed	P_E	Maximum P_E	Minimum P_E	Average Difference from calculated P_E	Percentage of calculated P_E
(knots)	(kW)	(kW)	(kW)	(kW)	(%)
1.6	0.110	0.232	-0.013	0.122	111.72%
3.7	0.868	1.162	0.574	0.294	33.85%
4.7	2.414	2.807	2.021	0.393	16.28%
5.8	4.720	5.232	4.207	0.512	10.86%
6.8	8.675	9.336	8.013	0.662	7.63%
7.9	18.701	19.562	17.839	0.861	4.61%
8.9	35.805	36.924	34.686	1.119	3.13%
10	67.390	68.848	65.931	1.459	2.16%
11	111.734	113.617	109.851	1.883	1.69%
12.1	177.697	180.121	175.273	2.424	1.36%

The following plot shows a comparison of the required effective power calculated for each of the four bows tested during the MUN test program. The plot also includes error bars which correspond to the errors calculated in the uncertainty analysis. Again, the error bars represent the 95% confidence interval estimate of the uncertainty in the data.

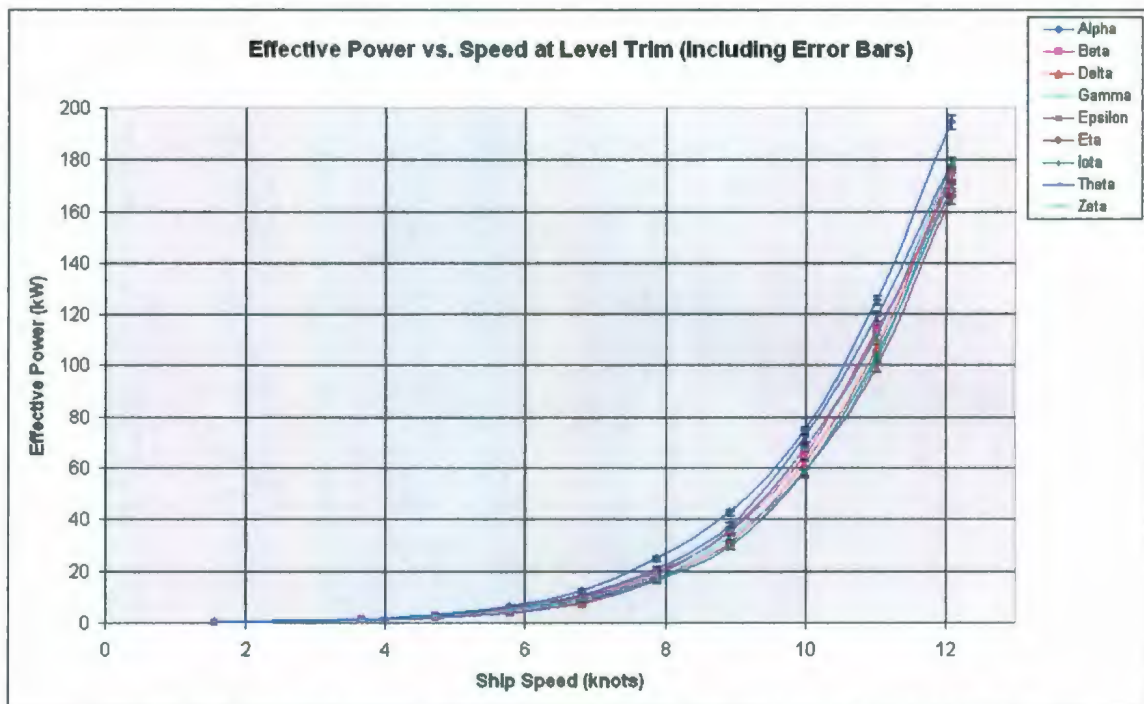


Figure 175: Effective Power Comparison with Error Bars at Level Trim for MUN Tests

From the above tables and figure it can be stated that the results obtained from the resistance tests conducted in the MUN towing tank provide a good representation of the actual performance of the hull form under the specific test conditions.

The figure and table below both show a comparison of the maximum possible effective powers for each bow to the minimum possible effective power for Alpha bow. Again, this is a comparison of the worst case scenario for each bow with the best case scenario for the conventional bow. These show that above 6.8 knots all of the bulbous bows, with the exception of Theta bow at 10 knots, will outperform the conventional bow even in the worst case scenario.

In the speed range of 8 – 10 knots there are minimum reductions in required effective power on the order of -0.3 – 28.9% for the bulbous bows. At 8 knots Epsilon provides a 28.9% reduction from the minimum effective power for Alpha bow. At 10 knots Theta requires 0.3% more effective power than the minimum effective power for Alpha bow.

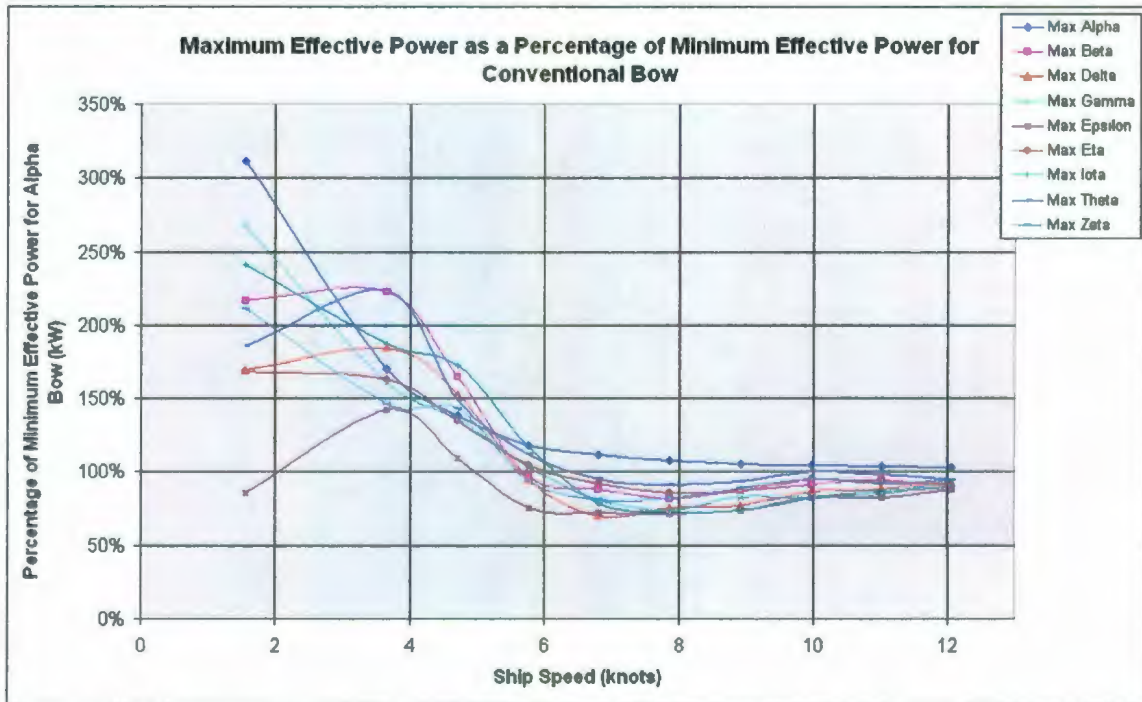


Figure 176: Maximum Effective Power as Percentage of Minimum Effective Power for Conventional Bow from MUN Tests

Table 78: Maximum Effective Power as Percentage of Minimum Effective Power for Conventional Bow from MUN Tests

% of Minimum Effective Power for Conventional Bow (%)									
Speed (knots)	Alpha	Beta	Delta	Gamma	Epsilon	Eta	Iota	Theta	Zeta
1.6	311.44	216.25	169.45	266.79	85.41	168.66	241.10	185.80	210.70
3.7	170.24	222.62	184.33	160.57	142.45	162.64	187.06	223.67	146.07
4.7	138.08	164.04	152.61	135.63	108.83	134.44	172.60	148.78	142.74
5.8	117.56	96.72	94.10	102.49	74.75	104.54	117.01	111.18	93.36
6.8	111.04	87.45	69.43	80.53	71.55	91.88	77.97	94.99	80.26
7.9	107.06	81.48	74.92	73.79	71.15	85.27	71.55	90.81	81.34
8.9	105.36	87.20	76.40	81.80	73.65	86.96	73.55	93.14	88.61
10	104.07	90.99	86.08	81.86	82.47	94.76	81.88	100.33	94.57
11	103.18	93.73	87.68	84.15	81.96	92.07	85.76	97.92	91.97
12.1	102.67	88.79	92.41	92.16	87.48	90.59	89.21	94.17	93.80

9.1.6 MUN/IOT Comparisons

Using the above data from the uncertainty analysis of resistance data from both sets of tests it is possible to make new comparisons of the effective power requirements resulting from both sets of tests. This section will compare the results from both test programs and include the uncertainties in order to determine if the differences in the powering data may be attributed to errors in the test implementation.

The following four plots show the effective power comparisons of each of the four bows tested at both IOT and MUN. The data has been standardized in order to get a better idea of the direct comparison at each half knot of speed. As well, the vertical gridlines have been removed to make the plots clearer for interpretation.

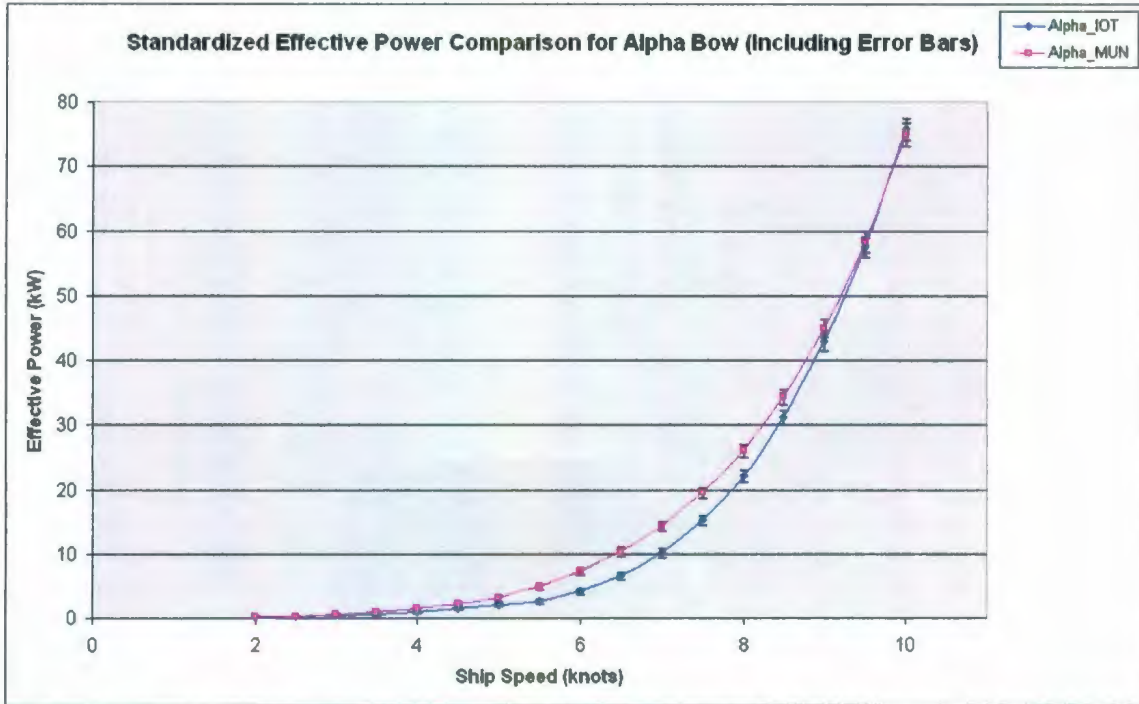


Figure 177: Effective Power Comparison with Error Bars of Alpha Bow Tested at IOT and MUN

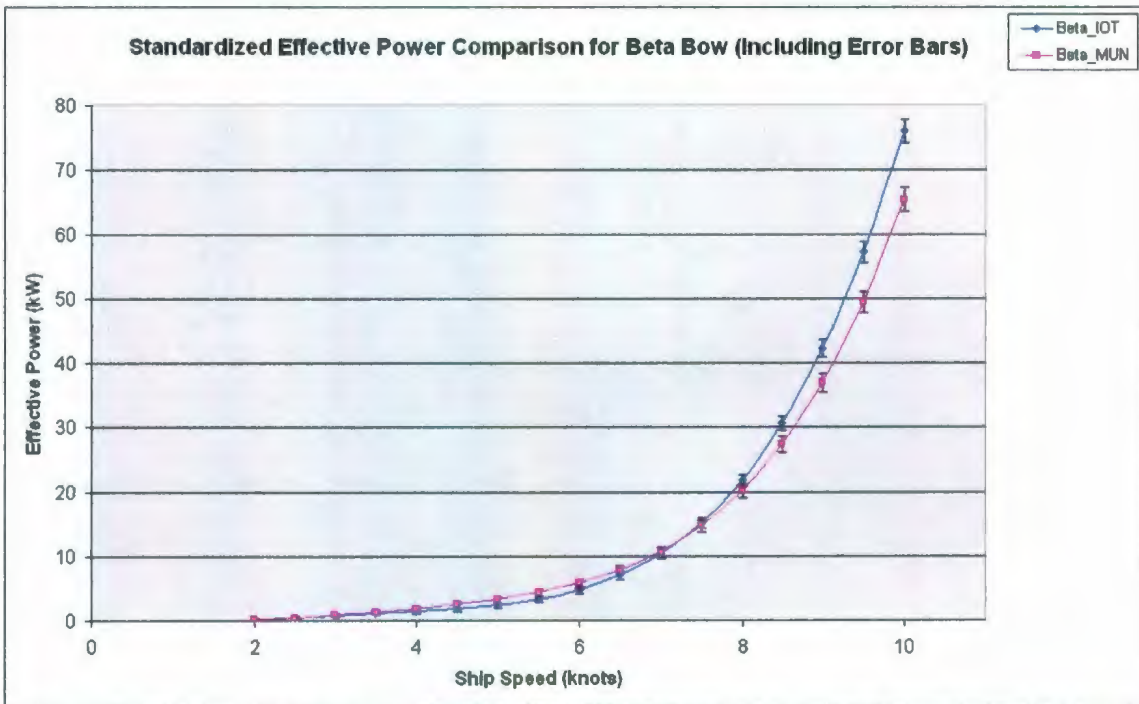


Figure 178: Effective Power Comparison with Error Bars of Beta Bow Tested at IOT and MUN

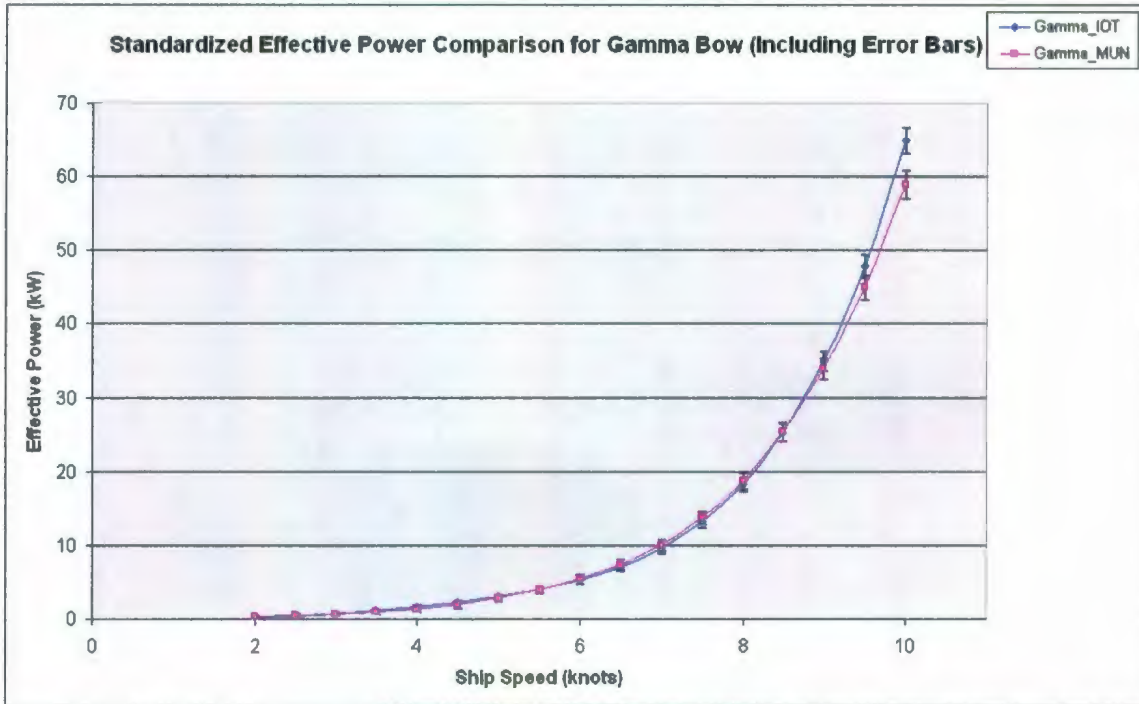


Figure 179: Effective Power Comparison with Error Bars of Gamma Bow Tested at IOT and MUN

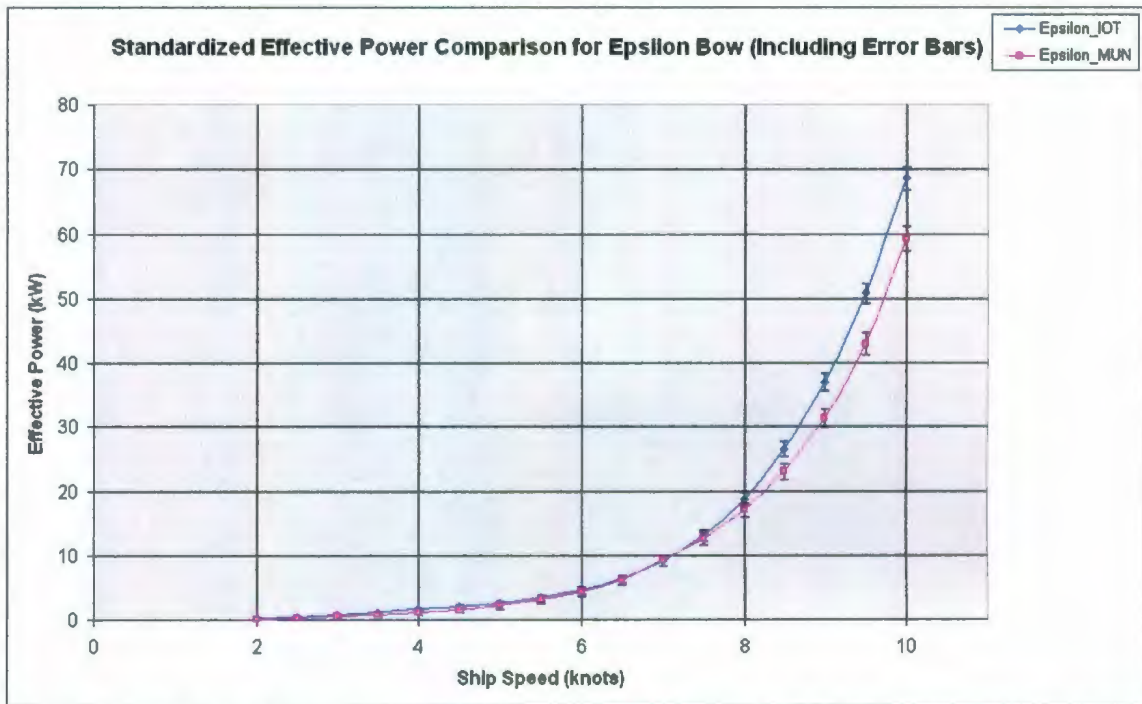


Figure 180: Effective Power Comparison with Error Bars of Epsilon Bow Tested at IOT and MUN

All of the above four plots suggest that the uncertainties due to errors in the experimental procedure do not significantly change the general trends shown in the data. The general trend of the IOT resistance data increasing at a faster rate than the MUN data with

increasing speed is still prominent. The reasons for differences in the resistance data between the two test programs that are outlined in Section 7.3 are still likely the best possible explanations as to why the results have differing trends.

The misalignment issues during the IOT test program is likely the biggest factor in the difference in resistance data between the two sets of data. Unfortunately the magnitude of yaw during any test run was measured, and hence it could not be quantified into an increase in resistance. Because it was not possible to quantify the magnitude of yaw it could not be addressed in the uncertainty analysis for the IOT test program.

Also, the difference in model set-ups between the two test programs caused a different trimming moment for each test program. This will also lead to differing resistance measurements between the two test programs, as the trim angle has a significant influence on the hull resistance.

9.2 Self-Propulsion Tests

Unfortunately a full uncertainty analysis could not be completed for the self-propulsion tests as the calibration data for both thrust and torque could not be found. The calibration errors contribute a significant amount to the bias errors; therefore the uncertainties for both the thrust and torque would not be considered accurate without the calibration data. However it may be possible to make a qualitative assessment of the order of magnitude of the overall uncertainties involved with these tests.

During the self-propulsion tests the following propeller data is measured: thrust, torque, and shaft speed. Each of these variables will have an uncertainty associated with them. It is likely that the uncertainty for each of these variables is on the same order as for the resistance coefficients discussed in Section 9.1.

It is known that during the self-propulsion tests at a given speed the model increasingly trims by the head with increasing propeller shaft speed (on the order of 0.25° from slowest to fastest shaft speed). In turn, this results in a small uncertainty in the resistance

coefficient used in the analysis procedure. This means that after the uncertainty from the resistance tests is carried over into these tests it is further increased due to the model trimming with propeller shaft speed.

Finally, the propeller thrust, torque and shaft speed measured in open water have to be known in order to complete the analysis for the self-propulsion tests. Again, it is likely that the uncertainty for each of these variables is on the same order as for the resistance coefficients discussed in Section 9.1.

The above explanation points to the fact that there are more variables measured during the self-propulsion tests and hence more data reduction equations used during the analysis procedure. This means that there is likely a significantly larger total uncertainty for these tests than found for the resistance tests.

To ensure that the data is as accurate as possible and all bow comparisons are as reliable as possible it is important to ensure that the errors associated with the self-propulsion tests are kept as low as practically possible. This generally means keeping the uncertainties associated with calibrations as low as possible. To do so it is best to keep the individual calibrations within reasonable ranges and use a high number of data points.

Chapter 10 - Conclusions and Recommendations

This report details the design and construction of a 6 ft model of a 45 ft trawler yacht hull form. It also discusses the testing procedure and results of the following testing: bare hull resistance tests carried out in the IOT ice tank, bare hull resistance tests carried out in the MUN tow tank, and self-propulsion tests carried out in the MUN tow tank.

10.1 Bare Hull Resistance Tests

Overall the quality of data gathered from both sets of the bare hull resistance tests was adequate. This subsection will review all of the important conclusions obtained from both sets of resistance tests as well as provide recommendations for further reference.

It was found that at speeds above 8 – 9 knots the effective power for the conventional bow tends to increase with increasing static trim by the stern. However, above these speeds the effective power for a bulbous bow generally tends to decrease with increasing static trim by the stern. It was found that with a bulb attached the flow over the top of the bulb tends to smooth out with increasing static trim by the stern, which in turn reduces the bow wave. It is likely that this smoother flow over the bulb counteracts the increased resistance due to an increase in underwater transom (which will occur with a larger static trim by the stern).

At the static level trim condition it was found that the bulbous bows begin to outperform the conventional bow above 6 – 7 knots ($F_n = 0.27 - 0.32$) in the IOT tests and 5 – 6 knots ($F_n = 0.23 - 0.27$) in the MUN tests. This is consistent with what is found in the literature review.

The following bulb parameters were found to be possible factors which influence the reduction in effective power: bulb length (linearly correlated to both the fairing radius of bulb into stem and top bulb angle), front cross-sectional area, and fairing type.

Analysis of the MUN test data has shown that, when all other bulb parameters are the same, a bulb with a longer length generally provides a higher reduction of required effective power than a bulb with a shorter length. It is known that the bulb length is linearly correlated to both the fairing radius of bulb into stem and top bulb angle. Therefore, either of these two parameters could be the factor influencing the reduction in effective power. It may be possible to perform a statistical analysis on the gathered data to determine which of the three parameters has the greatest influence on reducing the required effective power. Further testing on bulbs with varying bulb length, fairing radii, and top bulb angles may be necessary to supplement the data already gathered.

It was found that, with the exception of Iota bow, the bulbs with a front cross-sectional area corresponding to 17.64% of the amidships sectional area are clearly better performers than the bulbs with a front cross-sectional area of 23.48%. The only direct comparison made was between Beta and Eta bows; which have all the same bulb parameters other than the front cross-sectional area. It was found that Beta, with the smaller front cross-sectional area, performed better than Eta, with the larger front cross-sectional area.

Based on both sets of resistance tests it was found that the fairing type seems to also have an influence on the reduction in effective power. From the IOT test program the bulb ranking are generally given as: (1) Gamma (no fairing); (2) Epsilon (s-shaped fairing); (3) Beta (straight line fairing). From the MUN test program it was found that at the static level trim condition the three bulbs with no fairing placed in the top four of the rankings, while the three bulbs with straight line fairing placed in the bottom four.

Further investigation should be completed into why Iota bulb, with a shorter length and larger front cross-sectional area, performs very well in the design speed range. This may be done by constructing additional bulbous bows with varying front cross-sectional areas, fairing radii as well as top profile angles. It could also be possibly completed by use of some Computational Fluid Dynamics (CFD) computer simulations.

It is clear that Iota, Gamma, and Epsilon bows are the best performers from a resistance reduction point of view. Delta bow also performed well in all trim conditions during the MUN test program. Gamma bow generally slightly outperformed Epsilon bow in the IOT test program and vice versa in the MUN test program. The only comparison for Iota bow to the two other bows is during the MUN test program at static level trim condition. In this condition Iota and Epsilon bows perform almost identically in the design speed range and both slightly outperformed Gamma bow. Iota bow generally outperforms all other bows in the 8 – 10 knot range for the resistance tests completed at MUN with the model trimmed 0.75° and 1.5° by the stern.

Therefore, since Iota, Gamma, and Delta bows are all semi-cylindrical bulbs (i.e. no fairing into the hull) it would be reasonable to conclude that this fairing type is likely the most efficient for reducing the bare hull resistance relative to the conventional bow.

It was shown that there were discrepancies between the test data for the IOT and MUN tests. The model in the IOT tests generally provided higher effective powers at speeds above 8 – 9 knots, while the IOT tests for Epsilon bow provided higher effective power throughout the whole speed range. For dynamic trim, the IOT tests generally provided lower dynamic trim by the head at speeds above 8 – 9.5 knots. For model sinkage, the IOT tests generally provided higher model sinkage at speeds above 5 – 6 knots.

The possible reasons for these discrepancies between the two are listed as: different load cells used for each test program, misalignment issues during IOT test program, and different instrumentation set-ups for each test program, resulting in differing tow points for each test program.

An uncertainty analysis was performed on the resistance data for both the IOT and MUN resistance test programs. The uncertainty analysis showed that the initial results obtained for each set of tests provide a good representation of the actual performance of the hull form under the specific test conditions for each set of tests respectively.

The results from the uncertainty analysis were then used to make further comparisons of the IOT and MUN resistance data. The results showed that the uncertainties due to errors in the experimental procedure did not significantly change the general trends shown in the original resistance data. That is, the reasons for the discrepancies in resistance data between the two test programs, as outlined above, are likely the best possible explanations as to why the results have differing trends.

A statistical analysis of the resistance data gathered during the MUN testing is also possible. There are methods available to complete statistical analysis even if the test program was not performed for the purpose of statistical analysis. This type of analysis would allow one to determine exactly which factors (i.e. fairing type, bulb length, front cross-sectional area, etc.) are important in reducing the required effective power. It may also be possible to retest each of the bulbs with the purpose of completing the statistical analysis. This would take a lot of tank time, but would certainly make the analysis less complicated and also reduce the time to complete the analysis.

In order to better understand which bulb parameters are likely the most significant in reducing the required effective power it would be useful to complete resistance tests on Epsilon, Gamma, and Beta bows in the MUN towing tank at 0.75° and 1.5° by the stern conditions. This data could also be used the statistical analysis as discussed above.

From the dynamic trim data it was found that the model will trim by the head up to somewhere between 8.5 – 9 knots ($F_n = 0.38 - 0.41$) in the IOT test program and between 8.75 – 9.65 knots ($F_n = 0.39 - 0.44$) in the MUN test program. After this point the model will begin to drastically trim by the stern with increasing speed. This is consistent with what was found in studies conducted by Johnson (1958) and Friis et al. (2008).

The sinkage data from both sets of tests show that the model will sink at an increasing rate with increasing speed. This is also consistent with what was found in studies conducted by Johnson (1958) and Friis et al. (2008).

It was found that the bulb submergence, top bulb area, and the pressure around the stern section are all likely factors which affect the magnitude of the dynamic trim and model sinkage. It was found that as bulb size (i.e. bulb submergence and top bulb area) is increased then the magnitude of dynamic trim by the head as well as model sinkage is increased. Again, this is also consistent with what was found in studies conducted by Johnson (1958) and Friis et al. (2008).

In order to determine the extent of each of the above phenomenon on the dynamic trim and model sinkage it may be possible to perform further resistance tests with pressure sensors placed around the bow and stern sections. This would then provide details of how the pressure distributions over the bow and stern are changing with increasing speed as well as different initial trim conditions; and how these pressures affect both the dynamic trim and model sinkage.

10.2 Self-Propulsion Tests

Overall the quality of data gathered from the self-propulsion tests was adequate. This subsection will review all of the important conclusions obtained from these tests as well as provide recommendations for further reference.

The wake values for Alpha bow were found to be generally in the same range as for the bulbous bows. This result fall in between the results found in a study by NORDCO (1990) on a 65 ft Newfoundland type and those found in a study by Friis et al. (2008) on a 90 ft fishing vessel. Since this hull form type falls somewhere in between the two aforementioned hulls it is reasonable to conclude that the wake fractions calculated for this hull form are satisfactory.

The thrust deduction values were found to be generally lower for Alpha bow than the bulbs. This is consistent with what was found by Johnson (1958), NORDCO (1990), and Friis et al. (2008).

The hull efficiencies for Alpha bow were found to be generally higher than that of any of the bulbous bows. This is due to the fact that the thrust deduction fractions for the conventional bow are generally lower than for the bulbous bows. This is consistent with what was concluded from tests completed by Johnson (1958), NORDCO (1990), and Friis et al. (2008).

The relative rotative efficiencies for Alpha bow are generally slightly higher than that of any of the bulbous bows. This suggests that the propeller operating behind the model with the conventional bow is likely operating in a more uniform flow, and hence is more efficient.

It was found that the quasi propulsive efficiencies for the conventional bow are generally higher as for the bulbous bows. From this it can be stated that the propeller operating behind the hull outfitted with the conventional bow will perform better than the propeller operating behind the hull outfitted with any of the bulbous bows.

Further self-propulsion tests should be completed on Theta bow. The relative rotative efficiencies for this bow exhibited strange behaviour which wasn't found with any of the other bows. For this reason this particular bow should be retested to ensure that the data used in the analysis is correct.

Ignoring the Theta bow data and it is clear from the self-propulsion testing that Iota, Gamma, and Epsilon provide the highest reductions of required installed power in the design speed range tested. Iota bow was the best overall performer over the speed range tested. Gamma came in second overall; however it was the best performer at 10 knots. Epsilon bow performs well between 8 – 9 knots. Delta bow also performs fairly well between 8 – 9 knots.

Since Iota, Gamma, and Delta bows all have no fairing into the hull it would be reasonable to conclude that this fairing type is likely the most efficient from a powering performance point of view for this hull form.

The self-propulsion tests were carried out using a stock propeller which is not optimized for this particular hull form. This appears to have lead to low relative rotative efficiencies, which in turn lower the quasi-propulsive efficiencies. Therefore, it would be helpful to design a propeller which is optimized for this hull form and complete the self-propulsion tests over again. This would likely lead to higher quasi-propulsive efficiencies for all bows.

Due to a lack of tank time each bow could only be tested at the static level trim condition. It would be a good idea to complete further tests for each bow at one or two further static trim angles to determine its effect on wake and thrust deduction fractions.

During the analysis it was found that the pressure distribution over the stern section of the hull likely plays an important role in determining the hull efficiency of the model outfitted with any of the bows. Thus, it may be possible to complete testing where pressure sensors are placed around the stern section of the model. A test plan could be implemented similar to that of the self-propulsion testing, where the propeller is run behind the hull, and the pressure distribution could be measured via the pressure sensors. This would then allow one to determine how the pressure distribution is changing with speed for each individual bow as well as over the range of bows tested.

References

Lewis, E., (1988), "Principles of Naval Architecture – Volume 2: Resistance, Propulsion and Vibration," Jersey City, NJ, SNAME, 1988.

Yim, B., (1974), "A Simple Design Theory and Method for Bulbous Bows of Ships," *Journal of Ship Research*, Vol. 18, No. 3, September 1974, pp. 141 – 152.

Kracht, A.M., (1978), "Design of Bulbous Bows," *SNAME Transactions*, Vol. 86, 1978, pp. 197 – 217.

Johnson, N.V., (1958), "Tests with Bulbous Bow on Trawlers," *Division of Ship Hydrodynamics*, Chalmers University Gothenburg, 1958.

Doust, D.J., (1960), "Trawler Forms with Bulbous Bows," *Fishing Boats of the World: 2 – Sea Behavior*, Fishing News (Books) Ltd., London, 1960, pp. 445 – 452.

Heliotis, A.D. and Goudey, C.A., (1985), "Tow Tank Results of Bulbous Bow Retrofits on New England Trawler Hulls," *Center for Fisheries Engineering Research*, MIT, September 1985.

Heliotis, A.D. and Goudey, C.A., (1985), "Tow Effect of Bulbous Bow Retrofits on the Resistance and Seakeeping of a 50 meter Freshfish Stern Trawler," *Center for Fisheries Engineering Research*, MIT, April 1985.

NORDCO Ltd., (1990), "An Investigation of the Resistance, Self-Propulsion and Seakeeping Characteristics of a 65' Fishing Vessel," Project #: 212-89, March 1990.

Friis, D., Bose, N., Luznik, L., Olsen, C., (1998), "F/V Newfoundland Tradition – Bulbous Bow Design and Ice Strengthening Project Carried out for Canadian Centre for Fisheries Innovation and A.M.P. Fisheries Ltd.," OERC, Faculty of Engineering and Applied Science, MUN, 1998.

Friis, D., Bass, D., Gardner, A., Lane, S., (2007), "Design of Two Multi-Species Fishing Vessel, Phase 2, Interim Report to March 31, 2007," OERC, Faculty of Engineering and Applied Science, MUN, 2007.

Friis, D., Bass, D., McGrath, B., Knapp, C., Lane, S., Harris, T., (2008), "Phase 3 of a Multi-species Fishing Vessel Project - Design of a Fishing Vessel for Operation in the Newfoundland and Labrador Fishery and Restricted by the new DFO Vessel Length Restriction of 89'-11"," OERC, Faculty of Engineering and Applied Science, MUN, 2008.

http://iot-ito.nrc-cnrc.gc.ca/facilities/it_e.html

IOT Standard Test Method, (2007), "Construction of Models of ships, offshore structures and propellers," V10.0, 42-8595-S/GM-1, October 18, 2007.

Miles, M.D., (1996), "Test Data File for New GDAC Software," NRC Institute for Marine Dynamics Software Design Specification, Version 3.0, January 2, 1996.

Miles, M.D., (1996), "DACON Configuration File for New GDAC Software," NRC Institute for Marine Dynamics Software Design Specification, Version 3.2, August 14, 1996.

Miles, M.D., (1990), "The GEDAP Data Analysis Software Package," NRC Institute for Mechanical Engineering, Hydraulics Technical Report #TR-HY-030, August 11, 1990.

Proceedings of 8th ITTC, (1957), Madrid, Spain, 1957.

Scott, J.R., (1976), "Blockage Correction at Sub-Critical Speeds," Trans. RINA, 1976, p. 169.

IOT Standard Test Method, (2006), "Resistance in Open Water," V7.0, 42-8595-S/TM-1, December 12, 2006.

<http://www.engr.mun.ca/oerc/towtank.php>

IOT Standard Test Method, (2006), "Model Propulsion in Open Water," V6.0, 42-8595-S/TM-3, December 12, 2006.

IOT Standard Test Method, (2006), "Prediction of Ship Powering," V4.0, 42-8595-S/TM-4, December 12, 2006.

Harvald, S.A., (1983), "Resistance and Propulsion of Ships," New York, Wiley, 1983.

ITTC Recommended Procedures and Guidelines, (1999), "Uncertainty Analysis in EFD – Uncertainty Assessment Methodology," 7.5-02-01-01, 1999.

ITTC Recommended Procedures and Guidelines, (2002), "Uncertainty Analysis – Example for Resistance Test," 7.5-02-02-02, 2002.

Coleman, H.W., Steele, W.G., (1999), "Experimentation and Uncertainty Analysis for Engineers," 2nd Edition, John Wiley & Sons Inc., New York, USA, 1999.

Appendix A: Model Characteristics

Model Particulars							
Bow (w/stern)	L _{wl} (m)	B _{wl} (m)	T _{mid} (m)	T _{max} (m)	∇ (m ³)	Δ (kg)	C _b
Alpha	1.733	0.551	0.188	0.24	0.06775	67.75	0.3774
Beta	1.91	0.551	0.188	0.24	0.07450	74.50	0.3765
Delta	1.862	0.551	0.188	0.24	0.07013	70.13	0.3636
Gamma	1.91	0.551	0.188	0.24	0.07067	70.67	0.3572
Epsilon	1.91	0.551	0.188	0.24	0.07292	72.92	0.3686
Eta	1.91	0.551	0.188	0.24	0.07563	75.63	0.3823
Iota	1.862	0.551	0.188	0.24	0.07214	72.14	0.3740
Theta	1.862	0.551	0.188	0.24	0.07426	74.26	0.3850
Zeta	1.862	0.551	0.188	0.24	0.07226	72.26	0.3747

Table A1: Model Particulars

Model Bulbous Bow Characteristics								
Bow	Beta	Delta	Gamma	Epsilon	Eta	Iota	Theta	Zeta
Fairing Type (-)	Straight Line	None	None	S-Shaped	Straight Line	None	Straight Line	S-Shaped
Length (in)	7.08	5.10	7.08	7.08	7.08	5.10	5.10	5.10
Front Area (in ²)	14.90	14.90	14.90	14.90	19.85	24.91	19.85	14.90
% Amid (%)	17.64	17.64	17.64	17.64	23.48	29.47	23.48	17.64
Max Bulb Width (in)	4.10	4.10	4.10	4.10	5.38	6.52	5.38	4.10
Bulb Width on WL (in)	2.40	2.40	2.40	2.40	3.33	4.49	3.33	2.40
Top Bulb Area (in ²)	62.51	15.25	20.53	39.50	75.03	30.68	62.02	33.88
Underwater Volume (in ³)	1029.9	764.2	786.1	927.5	1099.1	887.1	1016.2	892.3
Fairing Radius(in)	3.71	2.83	3.71	3.71	3.71	2.83	2.83	2.83
Top Profile Angle (deg)	13.0	16.7	13.0	13.0	13.0	16.7	16.7	16.7

Table A2: Model Bulbous Bow Characteristics

		Section Area (in ²)								
		Alpha	Beta	Delta	Gamma	Epsilon	Eta	Iota	Theta	Zeta
AP	0	33.87	33.87	33.87	33.87	33.87	33.87	33.87	33.87	33.87
	0.5	45.48	45.48	45.48	45.48	45.48	45.48	45.48	45.48	45.48
	1	57.27	57.27	57.27	57.27	57.27	57.27	57.27	57.27	57.27
	1.5	64.37	64.37	64.37	64.37	64.37	64.37	64.37	64.37	64.37
	2	69.76	69.76	69.76	69.76	69.76	69.76	69.76	69.76	69.76
	2.5	74.19	74.19	74.19	74.19	74.19	74.19	74.19	74.19	74.19
	3	77.92	77.92	77.92	77.92	77.92	77.92	77.92	77.92	77.92
	3.5	80.96	80.96	80.96	80.96	80.96	80.96	80.96	80.96	80.96
	4	83.33	83.33	83.33	83.33	83.33	83.33	83.33	83.33	83.33
	4.5	84.53	84.53	84.53	84.53	84.53	84.53	84.53	84.53	84.53
	5	84.53	84.53	84.53	84.53	84.53	84.53	84.53	84.53	84.53
	5.5	84.00	84.00	84.00	84.00	84.00	84.00	84.00	84.00	84.00
	6	82.51	82.51	82.51	82.51	82.51	82.51	82.51	82.51	82.51
	6.5	78.23	78.23	78.23	78.23	78.23	78.23	78.23	78.23	78.23
	7	72.15	72.15	72.15	72.15	72.15	72.15	72.15	72.15	72.15
7.5	62.83	65.51	64.04	64.07	64.33	65.76	64.11	65.38	64.38	
8	50.27	57.54	51.36	51.48	55.37	58.56	51.52	57.69	55.29	
8.5	36.60	49.46	37.54	37.72	44.95	51.45	38.11	49.92	44.63	
9	21.58	41.46	22.98	23.07	34.74	44.09	29.41	42.08	34.58	
9.5	7.34	33.92	16.07	16.32	26.75	37.21	26.33	34.79	26.51	
FP	10	0.00	26.34	14.97	15.27	20.48	30.36	25.04	27.31	20.77

Table A3: Model Sectional Areas

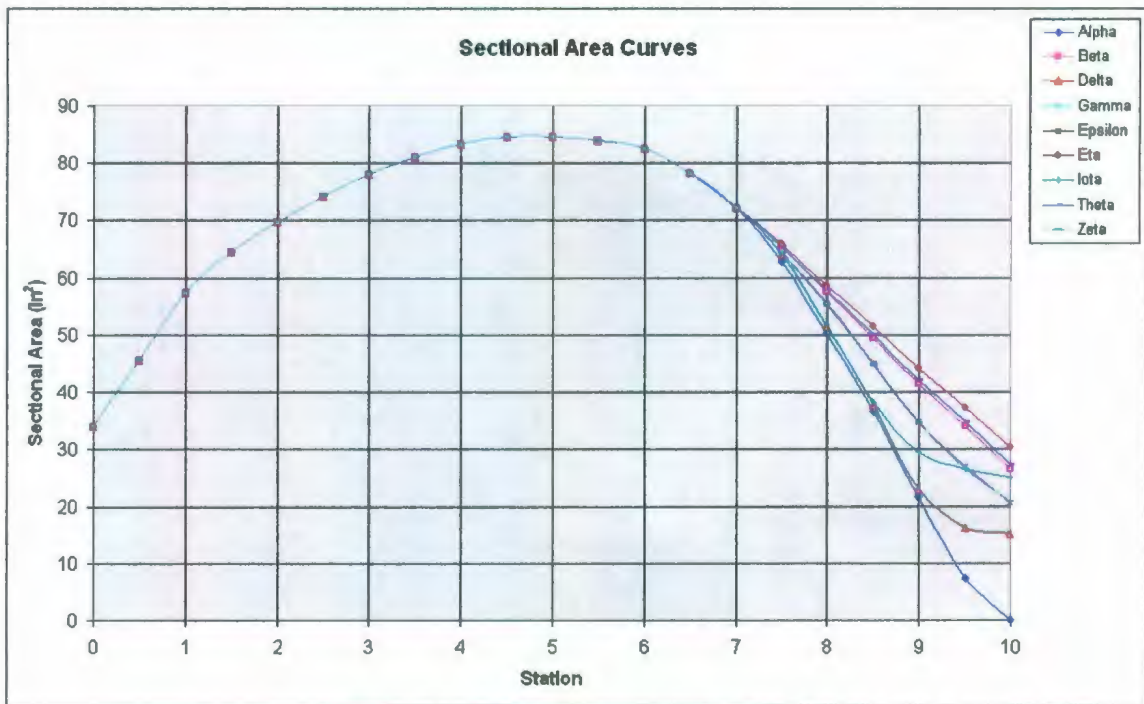


Figure A1: Model Sectional Area Curves

Appendix B: Tabular Data for IOT Bare Hull Resistance Tests

Appendix B-1: Resistance and Powering Data

Lm	1.829	m
Ls	14.00	m
Lwls	13.25	m
Lwlm	1.731	m
Scale	7.654	-
g	9.81	m/s ²
water temp	1.8	°C
v(visc)m	1.68E-06	m ² /s
v(visc)s	1.19E-06	m ² /s
pm	999.8	kg/m ³
ps	1025.9	kg/m ³
Sm	1.138	m ²
Ss	66.68	m ²

Resistance Data for Alpha Bow @ Static Level Trim										
Ship Speed	Fn	CTM	CFM	RnM	CR	RnS	CFS	CTS	RTS	PE
(knots)	(-)	(-)	(-)	(-)	(-)	(-)	(-)	(-)	(N)	(W)
1.00	0.045	0.011972	0.006959	1.92E+05	0.005014	5.73E+06	0.003313	0.008726	78.69	40.38
2.00	0.090	0.007270	0.005833	3.85E+05	0.001437	1.15E+07	0.002928	0.004765	173.30	178.60
3.01	0.136	0.006089	0.005298	5.79E+05	0.000791	1.73E+07	0.002734	0.003925	322.06	498.54
4.01	0.181	0.006104	0.004962	7.72E+05	0.001142	2.31E+07	0.002608	0.004150	606.17	1251.99
5.02	0.226	0.006606	0.004723	9.66E+05	0.001883	2.89E+07	0.002516	0.004798	1096.03	2830.85
6.03	0.272	0.007367	0.004541	1.16E+06	0.002847	3.46E+07	0.002444	0.005691	1872.94	5806.57
7.03	0.317	0.009646	0.004395	1.35E+06	0.005252	4.04E+07	0.002386	0.008038	3601.92	13030.55
8.04	0.363	0.012826	0.004274	1.55E+06	0.008552	4.62E+07	0.002337	0.011290	6609.93	27332.60
8.98	0.405	0.015402	0.004177	1.73E+06	0.011225	5.16E+07	0.002298	0.013923	10176.66	47017.83
10.05	0.453	0.019698	0.004082	1.93E+06	0.015615	5.77E+07	0.002259	0.018275	16725.15	86467.66
10.99	0.496	0.023664	0.004009	2.11E+06	0.019655	6.32E+07	0.002229	0.022284	24400.79	137986.44
12.00	0.541	0.027395	0.003940	2.31E+06	0.023456	6.89E+07	0.002200	0.026056	33991.30	209808.41

Table B1: Resistance Data for Alpha Bow at Static Level Trim

Resistance Data for Alpha Bow @ 1.5° by the Stern										
Ship Speed	Fn	CTM	CFM	RnM	CR	RnS	CFS	CTS	RTS	PE
(knots)	(-)	(-)	(-)	(-)	(-)	(-)	(-)	(-)	(N)	(W)
1.00	0.045	0.013879	0.006954	1.92E+05	0.006925	5.73E+06	0.003313	0.010638	95.89	49.20
2.03	0.092	0.006234	0.005808	3.92E+05	0.000425	1.17E+07	0.002921	0.003746	140.35	146.81
3.02	0.136	0.006212	0.005290	5.82E+05	0.000921	1.74E+07	0.002732	0.004053	335.04	520.55
4.01	0.181	0.006429	0.004962	7.73E+05	0.001467	2.30E+07	0.002608	0.004475	651.14	1342.20
4.99	0.225	0.007599	0.004726	9.63E+05	0.002873	2.87E+07	0.002518	0.005791	1308.52	3361.50
6.03	0.272	0.008327	0.004538	1.16E+06	0.003789	3.46E+07	0.002444	0.006633	2185.29	6778.60
7.02	0.317	0.010948	0.004394	1.35E+06	0.006554	4.03E+07	0.002387	0.009341	4167.08	15041.25
8.00	0.361	0.013269	0.004275	1.54E+06	0.008994	4.60E+07	0.002339	0.011733	6810.20	28038.70
8.99	0.406	0.015725	0.004174	1.73E+06	0.011551	5.17E+07	0.002298	0.014249	10435.36	48261.25
10.03	0.452	0.019008	0.004082	1.93E+06	0.014925	5.76E+07	0.002260	0.017586	16018.89	82621.91
11.01	0.497	0.023469	0.004006	2.12E+06	0.019463	6.33E+07	0.002229	0.022092	24279.49	137552.97
12.00	0.541	0.027652	0.003938	2.31E+06	0.023714	6.90E+07	0.002200	0.026315	34335.56	211953.94

Table B2: Resistance Data for Alpha Bow at 1.5° by the Stern

Resistance Data for Alpha Bow @ 3.0° by the Stern										
Ship Speed	Fn	CTM	CFM	RnM	CR	RnS	CFS	CTS	RTS	PE
(knots)	(-)	(-)	(-)	(-)	(-)	(-)	(-)	(-)	(N)	(W)
0.99	0.045	0.026302	0.006961	1.92E+05	0.019340	5.71E+06	0.003315	0.023055	206.24	105.42
2.03	0.092	0.010553	0.005811	3.91E+05	0.004742	1.17E+07	0.002921	0.008063	301.15	314.52
3.02	0.136	0.009065	0.005292	5.82E+05	0.003774	1.73E+07	0.002733	0.006906	569.81	884.50
4.00	0.181	0.008708	0.004962	7.72E+05	0.003746	2.30E+07	0.002609	0.006754	981.57	2022.16
4.99	0.225	0.010128	0.004727	9.63E+05	0.005402	2.87E+07	0.002518	0.008320	1878.65	4824.35
6.03	0.272	0.009871	0.004538	1.16E+06	0.005333	3.46E+07	0.002444	0.008177	2693.01	8351.68
7.02	0.316	0.013222	0.004394	1.35E+06	0.008827	4.03E+07	0.002387	0.011614	5180.22	18695.98
8.00	0.361	0.014161	0.004275	1.54E+06	0.009886	4.60E+07	0.002339	0.012625	7327.06	30165.32
8.99	0.406	0.016845	0.004174	1.73E+06	0.012671	5.17E+07	0.002298	0.015369	11256.27	52058.41
10.03	0.452	0.020287	0.004082	1.93E+06	0.016205	5.76E+07	0.002260	0.018865	17186.40	86649.07
11.01	0.497	0.024416	0.004006	2.12E+06	0.020410	6.33E+07	0.002229	0.023039	25325.57	143493.61
12.00	0.541	0.028500	0.003938	2.31E+06	0.024563	6.90E+07	0.002200	0.027163	35451.88	218873.52

Table B3: Resistance Data for Alpha Bow at 3.0° by the Stern

Lm	1.829	m
Ls	14.00	m
Lwls	13.25	m
Lwlm	1.731	m
Scale	7.654	-
g	9.81	m/s ²
water temp	3.1	°C
v(visc)m	1.61E-06	m ² /s
v(visc)s	1.19E-06	m ² /s
ρm	999.9	kg/m ³
ρs	1025.9	kg/m ³
Sm	1.138	m ²
Ss	66.68	m ²

Resistance Data for Retests of Alpha Bow @ Static Level Trim										
Ship Speed	Fn	CTM	CFM	RnM	CR	RnS	CFS	CTS	RTS	PE
(knots)	(-)	(-)	(-)	(-)	(-)	(-)	(-)	(-)	(N)	(W)
1.00	0.045	0.031503	0.006885	2.00E+05	0.024619	5.72E+06	0.003314	0.028332	254.35	130.24
2.01	0.091	0.003954	0.005770	4.03E+05	-0.001816	1.15E+07	0.002927	0.001511	55.21	57.04
3.02	0.136	0.005226	0.005241	6.06E+05	-0.000016	1.74E+07	0.002732	0.003116	257.72	400.52
3.99	0.180	0.005243	0.004923	8.00E+05	0.000320	2.29E+07	0.002610	0.003330	479.93	984.54
5.00	0.226	0.005297	0.004684	1.00E+06	0.000614	2.87E+07	0.002517	0.003531	800.06	2058.14
6.01	0.271	0.005765	0.004502	1.21E+06	0.001263	3.46E+07	0.002445	0.004108	1346.15	4164.33
7.03	0.317	0.008124	0.004356	1.41E+06	0.003768	4.04E+07	0.002386	0.006554	2931.95	10597.65
7.99	0.361	0.010875	0.004241	1.60E+06	0.006634	4.59E+07	0.002339	0.009374	5426.79	22314.34
9.01	0.406	0.013668	0.004138	1.81E+06	0.009529	5.18E+07	0.002297	0.012227	8985.96	41631.23
10.02	0.452	0.017661	0.004050	2.01E+06	0.013611	5.76E+07	0.002260	0.016272	14800.29	76279.99
10.99	0.496	0.021871	0.003976	2.21E+06	0.017896	6.31E+07	0.002229	0.020525	22445.66	126847.23
12.00	0.541	0.025317	0.003906	2.41E+06	0.021411	6.89E+07	0.002200	0.024011	31322.74	193334.27

Table B4: Resistance Data for Retests of Alpha Bow at Static Level Trim

Resistance Data for Retests of Alpha Bow @ 0.75° by the Stern										
Ship Speed	F _n	CTM	CFM	RnM	CR	RnS	CFS	CTS	RTS	PE
(knots)	(-)	(-)	(-)	(-)	(-)	(-)	(-)	(-)	(N)	(W)
0.99	0.045	0.008380	0.006891	1.99E+05	0.001489	5.70E+06	0.003316	0.005205	46.42	23.69
1.99	0.090	0.005158	0.005780	4.00E+05	-0.000622	1.15E+07	0.002931	0.002708	97.52	100.00
2.99	0.135	0.004741	0.005252	6.01E+05	-0.000510	1.72E+07	0.002736	0.002625	213.36	328.69
4.00	0.180	0.005308	0.004920	8.02E+05	0.000388	2.30E+07	0.002610	0.003397	491.58	1010.53
5.00	0.225	0.005423	0.004684	1.00E+06	0.000739	2.87E+07	0.002518	0.003657	827.45	2127.18
6.00	0.271	0.006513	0.004504	1.20E+06	0.002009	3.45E+07	0.002446	0.004855	1583.09	4885.18
7.00	0.316	0.008861	0.004360	1.41E+06	0.004501	4.02E+07	0.002388	0.007289	3236.21	11653.47
8.00	0.361	0.011756	0.004240	1.61E+06	0.007516	4.60E+07	0.002339	0.010255	5949.20	24487.27
9.00	0.406	0.013711	0.004139	1.81E+06	0.009573	5.17E+07	0.002297	0.012270	9011.04	41731.59
10.00	0.451	0.017427	0.004051	2.01E+06	0.013376	5.75E+07	0.002261	0.016037	14543.15	74842.91

Table B5: Resistance Data for Retests of Alpha Bow at 0.75° by the Stern

Resistance Data for Retests of Alpha Bow @ 1.5° by the Stern										
Ship Speed	F _n	CTM	CFM	RnM	CR	RnS	CFS	CTS	RTS	PE
(knots)	(-)	(-)	(-)	(-)	(-)	(-)	(-)	(-)	(N)	(W)
0.99	0.045	0.001703	0.006888	1.99E+05	-0.005185	5.71E+06	0.003315	-0.001470	-13.14	-6.72
1.99	0.090	0.005417	0.005780	4.00E+05	-0.000363	1.15E+07	0.002930	0.002968	106.92	109.67
2.99	0.135	0.005192	0.005252	6.01E+05	-0.000060	1.72E+07	0.002736	0.003076	249.96	385.07
4.00	0.180	0.005871	0.004921	8.02E+05	0.000951	2.30E+07	0.002610	0.003960	572.84	1177.33
5.00	0.225	0.006239	0.004685	1.00E+06	0.001554	2.87E+07	0.002518	0.004472	1011.35	2599.18
6.00	0.271	0.007016	0.004504	1.20E+06	0.002512	3.45E+07	0.002446	0.005358	1745.74	5385.19
7.00	0.316	0.009238	0.004360	1.40E+06	0.004878	4.02E+07	0.002388	0.007666	3401.15	12242.47
8.00	0.361	0.011943	0.004240	1.61E+06	0.007703	4.60E+07	0.002339	0.010442	6052.28	24900.63
9.00	0.406	0.013996	0.004139	1.81E+06	0.009857	5.17E+07	0.002298	0.012554	9211.19	42638.59
10.00	0.451	0.017523	0.004051	2.01E+06	0.013472	5.75E+07	0.002261	0.016133	14615.95	75180.75

Table B6: Resistance Data for Retests of Alpha Bow at 1.5° by the Stern

Lm	1.829	m
Ls	14.00	m
Lwls	14.62	m
Lwlm	1.91	m
Scale	7.654	-
g	9.81	m/s ²
water temp	2.1	°C
v(visc)m	1.66E-06	m ² /s
v(visc)s	1.19E-06	m ² /s
ρm	999.9	kg/m ³
ρs	1025.9	kg/m ³
Sm	1.237	m ²
Ss	72.47	m ²

Resistance Data for Beta Bow @ Static Level Trim										
Ship Speed	Fn	CTM	CFM	RnM	CR	RnS	CFS	CTS	RTS	PE
(knots)	(-)	(-)	(-)	(-)	(-)	(-)	(-)	(-)	(N)	(W)
1.00	0.045	0.006445	0.006936	1.94E+05	-0.000491	5.74E+06	0.003312	0.003221	31.65	16.26
2.04	0.092	0.005721	0.005789	3.98E+05	-0.000069	1.17E+07	0.002918	0.003250	133.67	140.50
3.03	0.137	0.005784	0.005274	5.90E+05	0.000509	1.74E+07	0.002730	0.003640	329.86	514.64
4.02	0.181	0.005948	0.004947	7.83E+05	0.001001	2.31E+07	0.002607	0.004007	638.91	1322.11
5.01	0.226	0.005840	0.004713	9.75E+05	0.001127	2.88E+07	0.002516	0.004043	1000.88	2580.68
6.00	0.271	0.006340	0.004534	1.17E+06	0.001806	3.45E+07	0.002446	0.004652	1651.08	5097.79
6.99	0.315	0.007319	0.004389	1.36E+06	0.002930	4.02E+07	0.002388	0.005718	2754.00	9905.19
8.04	0.363	0.010095	0.004264	1.56E+06	0.005832	4.62E+07	0.002338	0.008569	5452.76	22541.96
9.03	0.407	0.012685	0.004163	1.76E+06	0.008522	5.19E+07	0.002296	0.011218	9005.11	41812.20
10.02	0.452	0.016542	0.004076	1.95E+06	0.012467	5.76E+07	0.002261	0.015127	14951.50	77034.20
11.00	0.496	0.020439	0.003999	2.14E+06	0.016440	6.32E+07	0.002229	0.019068	22755.75	128829.12
11.50	0.519	0.022311	0.003964	2.24E+06	0.018347	6.61E+07	0.002214	0.020961	27314.37	161590.25

Table B7: Resistance Data for Beta Bow at Static Level Trim

Resistance Data for Beta Bow @ 1.5° by the Stern										
Ship Speed	Fn	CTM	CFM	RnM	CR	RnS	CFS	CTS	RTS	PE
(knots)	(-)	(-)	(-)	(-)	(-)	(-)	(-)	(-)	(N)	(W)
1.00	0.045	0.009739	0.006938	1.94E+05	0.002800	5.73E+06	0.003313	0.006513	63.79	32.72
2.00	0.090	0.006860	0.005816	3.90E+05	0.001044	1.15E+07	0.002928	0.004371	173.05	178.43
3.01	0.136	0.006936	0.005283	5.86E+05	0.001653	1.73E+07	0.002733	0.004787	427.81	662.83
4.02	0.181	0.007359	0.004948	7.82E+05	0.002411	2.31E+07	0.002607	0.005418	862.37	1783.03
5.00	0.225	0.007544	0.004717	9.72E+05	0.002828	2.87E+07	0.002518	0.005745	1413.02	3631.63
6.00	0.271	0.007853	0.004533	1.17E+06	0.003320	3.45E+07	0.002446	0.006165	2189.49	6761.94
7.01	0.316	0.008214	0.004387	1.36E+06	0.003827	4.03E+07	0.002387	0.006614	3203.43	11553.46
8.02	0.362	0.009645	0.004266	1.56E+06	0.005379	4.61E+07	0.002338	0.008117	5142.18	21210.62
8.99	0.406	0.010884	0.004166	1.75E+06	0.006718	5.17E+07	0.002298	0.009415	7506.46	34735.07
10.00	0.451	0.013522	0.004077	1.95E+06	0.009446	5.75E+07	0.002261	0.012107	11934.88	61412.00

Table B8: Resistance Data for Beta Bow at 1.5° by the Stern

Resistance Data for Beta Bow @ 3.0° by the Stern										
Ship Speed	Fn	CTM	CFM	RnM	CR	RnS	CFS	CTS	RTS	PE
(knots)	(-)	(-)	(-)	(-)	(-)	(-)	(-)	(-)	(N)	(W)
1.00	0.045	0.011507	0.006940	1.94E+05	0.004567	5.73E+06	0.003313	0.008280	80.99	41.51
2.03	0.092	0.006687	0.005798	3.95E+05	0.000889	1.17E+07	0.002921	0.004210	170.92	178.48
3.01	0.136	0.008220	0.005282	5.86E+05	0.002938	1.73E+07	0.002733	0.006071	543.48	842.70
4.00	0.180	0.008227	0.004954	7.78E+05	0.003273	2.30E+07	0.002609	0.006282	989.58	2035.46
4.98	0.225	0.008689	0.004719	9.69E+05	0.003970	2.86E+07	0.002519	0.006889	1685.25	4319.71
6.02	0.271	0.009564	0.004531	1.17E+06	0.005033	3.46E+07	0.002445	0.007878	2809.54	8695.29
7.00	0.316	0.010471	0.004388	1.36E+06	0.006083	4.02E+07	0.002388	0.008870	4283.28	15425.22
7.98	0.360	0.011043	0.004269	1.55E+06	0.006773	4.59E+07	0.002340	0.009513	5976.22	24548.01
9.02	0.407	0.012182	0.004164	1.75E+06	0.008018	5.18E+07	0.002297	0.010715	8586.41	39834.74
10.00	0.451	0.014724	0.004077	1.95E+06	0.010647	5.75E+07	0.002261	0.013308	13119.83	67509.76

Table B9: Resistance Data for Beta Bow at 3.0° by the Stern

Lm	1.829	m
Ls	14.00	m
Lwls	14.62	m
Lwlm	1.91	m
Scale	7.654	-
g	9.81	m/s ²
water temp	2.9	°C
v(visc)m	1.62E-06	m ² /s
v(visc)s	1.19E-06	m ² /s
pm	999.9	kg/m ³
ps	1025.9	kg/m ³
Sm	1.22	m ²
Ss	71.42	m ²

Resistance Data for Gamma Bow @ Static Level Trim										
Ship Speed	Fn	CTM	CFM	RnM	CR	RnS	CFS	CTS	RTS	PE
(knots)	(-)	(-)	(-)	(-)	(-)	(-)	(-)	(-)	(N)	(W)
0.99	0.045	0.011481	0.006901	1.98E+05	0.004580	5.71E+06	0.003314	0.008295	79.65	40.75
2.02	0.091	0.007368	0.005770	4.03E+05	0.001618	1.16E+07	0.002923	0.004941	196.48	204.55
3.00	0.135	0.007044	0.005259	5.98E+05	0.001785	1.72E+07	0.002735	0.004920	430.40	664.57
4.03	0.182	0.007019	0.004920	8.03E+05	0.002099	2.32E+07	0.002606	0.005105	805.41	1670.08
5.01	0.226	0.006720	0.004690	9.97E+05	0.002030	2.88E+07	0.002517	0.004947	1204.98	3104.75
5.99	0.270	0.006551	0.004514	1.19E+06	0.002038	3.44E+07	0.002447	0.004884	1699.68	5234.32
7.02	0.316	0.006963	0.004365	1.40E+06	0.002598	4.03E+07	0.002387	0.005385	2573.54	9288.14
7.99	0.361	0.008656	0.004248	1.59E+06	0.004408	4.59E+07	0.002339	0.007148	4434.69	18235.89
9.02	0.407	0.011038	0.004144	1.80E+06	0.006895	5.18E+07	0.002297	0.009591	7581.62	35190.72
10.00	0.451	0.014404	0.004058	1.99E+06	0.010346	5.75E+07	0.002261	0.013007	12631.02	64981.48

Table B10: Resistance Data for Gamma Bow at Static Level Trim

Resistance Data for Gamma Bow @ 0.75° by the Stern										
Ship Speed	Fn	CTM	CFM	RnM	CR	RnS	CFS	CTS	RTS	PE
(knots)	(-)	(-)	(-)	(-)	(-)	(-)	(-)	(-)	(N)	(W)
1.00	0.045	0.008305	0.006895	1.99E+05	0.001410	5.73E+06	0.003312	0.005123	49.51	25.41
2.02	0.091	0.007326	0.005771	4.03E+05	0.001554	1.16E+07	0.002923	0.004878	193.62	201.40
2.99	0.135	0.007601	0.005263	5.96E+05	0.002339	1.72E+07	0.002736	0.005475	476.00	732.73
4.02	0.181	0.008185	0.004923	8.00E+05	0.003262	2.31E+07	0.002607	0.006269	982.11	2029.29
4.99	0.225	0.008228	0.004695	9.93E+05	0.003533	2.87E+07	0.002518	0.006452	1557.93	3996.79
6.01	0.271	0.007734	0.004510	1.20E+06	0.003225	3.45E+07	0.002445	0.006070	2129.65	6585.65
6.98	0.315	0.007914	0.004369	1.39E+06	0.003544	4.01E+07	0.002389	0.006333	2997.32	10765.02
8.01	0.361	0.008907	0.004247	1.59E+06	0.004660	4.60E+07	0.002339	0.007399	4604.74	18964.45
9.03	0.407	0.010753	0.004143	1.80E+06	0.006610	5.19E+07	0.002296	0.009306	7368.31	34228.59
10.00	0.451	0.013999	0.004058	1.99E+06	0.009942	5.75E+07	0.002261	0.012603	12238.36	62961.04

Table B11: Resistance Data for Gamma Bow at 0.75° by the Stern

Resistance Data for Gamma Bow @ 1.5° by the Stern										
Ship Speed	Fn	CTM	CFM	RnM	CR	RnS	CFS	CTS	RTS	PE
(knots)	(-)	(-)	(-)	(-)	(-)	(-)	(-)	(-)	(N)	(W)
1.00	0.045	0.017040	0.006884	2.00E+05	0.010156	5.72E+06	0.003314	0.013869	133.55	68.41
1.99	0.090	0.006855	0.005781	4.00E+05	0.001074	1.14E+07	0.002931	0.004405	169.63	173.78
2.99	0.135	0.007549	0.005255	6.00E+05	0.002294	1.72E+07	0.002737	0.005431	470.54	723.07
3.98	0.180	0.008482	0.004924	7.99E+05	0.003558	2.29E+07	0.002611	0.006569	1011.76	2073.00
5.02	0.227	0.009260	0.004679	1.01E+06	0.004581	2.89E+07	0.002515	0.007496	1837.02	4747.58
6.02	0.272	0.009404	0.004501	1.21E+06	0.004903	3.46E+07	0.002445	0.007748	2725.86	8440.91
7.01	0.316	0.008999	0.004358	1.41E+06	0.004641	4.03E+07	0.002387	0.007428	3549.42	12809.21
8.01	0.361	0.009348	0.004239	1.61E+06	0.005109	4.60E+07	0.002339	0.007848	4890.11	20152.27
9.01	0.406	0.010852	0.004138	1.81E+06	0.006714	5.18E+07	0.002297	0.009411	7412.62	34344.42
10.00	0.451	0.014197	0.004051	2.01E+06	0.010145	5.75E+07	0.002261	0.012806	12440.48	64011.79

Table B12: Resistance Data for Gamma Bow at 1.5° by the Stern

Lm	1.829	m
Ls	14.00	m
Lwls	14.62	m
Lwlm	1.91	m
Scale	7.654	-
g	9.81	m/s ²
water temp	2.8	°C
v(visc)m	1.63E-06	m ² /s
v(visc)s	1.19E-06	m ² /s
pm	999.9	kg/m ³
ps	1025.9	kg/m ³
Sm	1.227	m ²
Ss	71.89	m ²

Resistance Data for Epsilon Bow @ Static Level Trim										
Ship Speed	Fn	CTM	CFM	RnM	CR	RnS	CFS	CTS	RTS	PE
(knots)	(-)	(-)	(-)	(-)	(-)	(-)	(-)	(-)	(N)	(W)
1.00	0.045	0.012968	0.006899	1.98E+05	0.006069	5.72E+06	0.003314	0.009782	94.74	48.51
1.99	0.090	0.007785	0.005797	3.95E+05	0.001989	1.14E+07	0.002932	0.005321	205.03	209.42
3.02	0.136	0.006339	0.005250	6.02E+05	0.001089	1.74E+07	0.002732	0.004220	376.91	586.10
4.01	0.181	0.006470	0.004924	7.99E+05	0.001546	2.31E+07	0.002608	0.004554	716.74	1479.65
5.00	0.226	0.006404	0.004691	9.96E+05	0.001713	2.87E+07	0.002517	0.004630	1132.73	2915.36
5.99	0.270	0.005692	0.004513	1.19E+06	0.001179	3.44E+07	0.002446	0.004026	1413.23	4357.14
6.98	0.315	0.006580	0.004369	1.39E+06	0.002211	4.01E+07	0.002389	0.004999	2382.79	8560.11
8.02	0.362	0.008900	0.004245	1.60E+06	0.004656	4.61E+07	0.002338	0.007394	4648.80	19181.29
9.01	0.406	0.011567	0.004145	1.79E+06	0.007423	5.18E+07	0.002297	0.010120	8030.53	37224.99
10.00	0.451	0.015082	0.004058	1.99E+06	0.011024	5.75E+07	0.002261	0.013685	13378.21	68828.02

Table B13: Resistance Data for Epsilon Bow at Static Level Trim

Resistance Data for Epsilon Bow @ 0.75° by the Stern										
Ship Speed	Fn	CTM	CFM	RnM	CR	RnS	CFS	CTS	RTS	PE
(knots)	(-)	(-)	(-)	(-)	(-)	(-)	(-)	(-)	(N)	(W)
1.00	0.045	0.008130	0.006895	1.99E+05	0.001235	5.73E+06	0.003312	0.004947	48.14	24.71
2.00	0.090	0.006231	0.005785	3.99E+05	0.000446	1.15E+07	0.002928	0.003774	147.78	152.16
3.01	0.136	0.006565	0.005257	5.98E+05	0.001308	1.73E+07	0.002734	0.004443	392.19	606.36
4.01	0.181	0.007109	0.004925	7.98E+05	0.002184	2.30E+07	0.002608	0.005192	815.71	1682.40
5.01	0.226	0.007594	0.004689	9.98E+05	0.002905	2.88E+07	0.002516	0.005821	1429.88	3687.50
6.02	0.271	0.007092	0.004509	1.20E+06	0.002583	3.46E+07	0.002445	0.005428	1920.58	5944.77
7.02	0.317	0.007223	0.004364	1.40E+06	0.002859	4.03E+07	0.002387	0.005646	2719.85	9823.32
7.99	0.361	0.008930	0.004248	1.59E+06	0.004682	4.59E+07	0.002339	0.007421	4634.20	19055.73
9.00	0.406	0.010850	0.004146	1.79E+06	0.006704	5.17E+07	0.002298	0.009401	7438.02	34426.00
10.00	0.451	0.014169	0.004058	1.99E+06	0.010111	5.75E+07	0.002261	0.012772	12485.53	64235.40

Table B14: Resistance Data for Epsilon Bow at 0.75° by the Stern

Resistance Data for Epsilon Bow @ 1.5° by the Stern										
Ship Speed	Fn	CTM	CFM	RnM	CR	RnS	CFS	CTS	RTS	PE
(knots)	(-)	(-)	(-)	(-)	(-)	(-)	(-)	(-)	(N)	(W)
0.99	0.045	0.007270	0.006901	1.98E+05	0.000369	5.71E+06	0.003315	0.004083	39.44	20.17
1.99	0.090	0.005553	0.005796	3.96E+05	-0.000242	1.14E+07	0.002932	0.003090	119.24	121.90
3.01	0.136	0.005796	0.005254	6.00E+05	0.000543	1.73E+07	0.002733	0.003676	326.45	506.24
4.01	0.181	0.007066	0.004926	7.98E+05	0.002140	2.30E+07	0.002608	0.005149	808.18	1666.14
5.00	0.226	0.007989	0.004692	9.96E+05	0.003297	2.87E+07	0.002517	0.006214	1518.73	3906.86
5.99	0.270	0.008004	0.004513	1.19E+06	0.003492	3.44E+07	0.002446	0.006338	2225.22	6861.04
7.02	0.317	0.007942	0.004364	1.40E+06	0.003578	4.03E+07	0.002387	0.006365	3066.45	11075.34
8.01	0.362	0.009014	0.004246	1.60E+06	0.004768	4.61E+07	0.002339	0.007506	4711.79	19424.97
9.01	0.406	0.010435	0.004145	1.79E+06	0.006290	5.18E+07	0.002297	0.008987	7125.96	33018.07
10.00	0.451	0.013985	0.004058	1.99E+06	0.009927	5.75E+07	0.002261	0.012588	12303.38	63292.89

Table B15: Resistance Data for Epsilon Bow at 1.5° by the Stern

Resistance Data for Epsilon Bow @ 3.0° by the Stern										
Ship Speed	Fn	CTM	CFM	RnM	CR	RnS	CFS	CTS	RTS	PE
(knots)	(-)	(-)	(-)	(-)	(-)	(-)	(-)	(-)	(N)	(W)
0.99	0.045	0.007893	0.006903	1.98E+05	0.000990	5.71E+06	0.003315	0.004705	45.38	23.19
2.00	0.090	0.007280	0.005787	3.98E+05	0.001493	1.15E+07	0.002929	0.004822	188.30	193.63
3.00	0.136	0.007349	0.005258	5.98E+05	0.002091	1.73E+07	0.002735	0.005226	461.00	712.51
4.01	0.181	0.008081	0.004925	7.98E+05	0.003156	2.30E+07	0.002608	0.006164	968.73	1998.30
5.02	0.226	0.008596	0.004689	9.99E+05	0.003907	2.88E+07	0.002516	0.006823	1677.35	4327.64
6.02	0.272	0.009396	0.004508	1.20E+06	0.004888	3.46E+07	0.002445	0.007732	2739.45	8484.90
7.03	0.317	0.010163	0.004363	1.40E+06	0.005800	4.04E+07	0.002386	0.008586	4143.03	14975.16
7.99	0.360	0.011014	0.004248	1.59E+06	0.006766	4.59E+07	0.002340	0.009506	5930.93	24377.56
9.00	0.406	0.011902	0.004146	1.79E+06	0.007756	5.17E+07	0.002298	0.010453	8266.88	38254.90
10.00	0.451	0.015251	0.004058	1.99E+06	0.011193	5.75E+07	0.002261	0.013854	13542.99	69675.18

Table B16: Resistance Data for Epsilon Bow at 3.0° by the Stern

Appendix B-2: Sinkage and Dynamic Trim Data

Sinkage and Trim Data for Alpha Bow @ Static Level Trim			
Ship Speed	Froude Number	Sinkage	Dynamic Trim
(knots)	(-)	(cm)	(degrees)
1.00	0.045	-0.042	-0.002
2.00	0.090	-0.124	-0.017
3.01	0.136	-0.251	-0.041
4.00	0.181	-0.258	-0.070
5.00	0.226	-0.430	-0.112
6.01	0.271	-0.784	-0.161
7.01	0.316	-1.122	-0.179
8.01	0.361	-1.368	-0.298
9.00	0.406	-1.888	-0.215
10.00	0.451	-2.525	0.790
11.00	0.496	-2.921	2.508
12.00	0.541	-2.829	4.474

Table B17: Sinkage and Trim Data for Alpha Bow at Static Level Trim

Sinkage and Trim Data for Alpha Bow @ 1.5° by the Stern			
Ship Speed	Froude Number	Sinkage	Dynamic Trim
(knots)	(-)	(cm)	(degrees)
1.00	0.045	-0.050	0.003
2.00	0.090	-0.135	-0.001
3.01	0.136	-0.216	0.002
4.00	0.181	-0.252	0.003
5.00	0.226	-0.406	0.009
6.00	0.271	-0.750	0.020
7.01	0.316	-1.050	0.078
8.01	0.361	-1.256	0.089
9.00	0.406	-1.729	0.435
10.01	0.451	-2.158	1.524
11.00	0.496	-2.320	3.164
12.00	0.541	-2.056	5.041

Table B18: Sinkage and Trim Data for Alpha Bow at 1.5° by the Stern

Sinkage and Trim Data for Alpha Bow @ 3.0° by the Stern			
Ship Speed	Froude Number	Sinkage	Dynamic Trim
(knots)	(-)	(cm)	(degrees)
0.99	0.045	-0.023	0.009
2.00	0.090	-0.124	0.023
3.01	0.136	-0.186	0.048
4.00	0.180	-0.218	0.078
5.00	0.226	-0.365	0.136
6.00	0.271	-0.688	0.214
7.01	0.316	-0.969	0.350
8.00	0.361	-1.128	0.494
9.00	0.406	-1.504	1.070
10.00	0.451	-1.767	2.271
11.00	0.496	-1.705	3.788
12.00	0.541	-1.385	5.119

Table B19: Sinkage and Trim Data for Alpha Bow at 3.0° by the Stern

Sinkage and Trim Data for Retests of Alpha Bow @ Static Level Trim			
Ship Speed	Froude Number	Sinkage	Dynamic Trim
(knots)	(-)	(cm)	(degrees)
1.00	0.045	0.000	0.002
2.00	0.090	-0.109	-0.018
3.01	0.136	-0.216	-0.042
4.00	0.181	-0.241	-0.081
5.00	0.226	-0.352	-0.127
6.00	0.271	-0.774	-0.190
7.01	0.316	-1.048	-0.212
8.01	0.361	-1.307	-0.366
9.00	0.406	-1.806	-0.344
10.00	0.451	-2.461	0.624
12.00	0.541	-2.888	4.316

Table B20: Sinkage and Trim Data for Retests of Alpha Bow at Static Level Trim

Sinkage and Trim Data for Retests of Alpha Bow @ 0.75° by the Stern			
Ship Speed	Froude Number	Sinkage	Dynamic Trim
(knots)	(-)	(cm)	(degrees)
0.99	0.045	-0.012	0.000
2.00	0.090	-0.118	-0.006
3.00	0.135	-0.178	-0.019
4.00	0.180	-0.230	-0.036
5.00	0.225	-0.401	-0.057
6.00	0.271	-0.724	-0.075
7.01	0.316	-1.034	-0.055
8.00	0.361	-1.258	-0.122
9.00	0.406	-1.742	0.052
10.00	0.451	-2.311	1.086

Table B21: Sinkage and Trim Data for Retests of Alpha Bow at 0.75° by the Stern

Sinkage and Trim Data for Retests of Alpha Bow @ 1.5° by the Stern			
Ship Speed	Froude Number	Sinkage	Dynamic Trim
(knots)	(-)	(cm)	(degrees)
0.99	0.045	-0.053	-0.001
2.00	0.090	-0.109	0.005
3.00	0.135	-0.196	0.000
4.00	0.180	-0.248	-0.001
5.00	0.225	-0.377	0.006
6.00	0.271	-0.724	0.016
7.01	0.316	-0.997	0.075
8.00	0.361	-1.217	0.076
9.00	0.406	-1.668	0.393
10.00	0.451	-2.106	1.473

Table B22: Sinkage and Trim Data for Retests of Alpha Bow at 1.5° by the Stern

Sinkage and Trim Data for Beta Bow @ Static Level Trim			
Ship Speed	Froude Number	Sinkage	Dynamic Trim
(knots)	(-)	(cm)	(degrees)
1.00	0.045	-0.037	-0.007
2.01	0.091	-0.112	-0.018
3.01	0.136	-0.190	-0.042
4.00	0.181	-0.207	-0.091
5.00	0.226	-0.395	-0.198
6.01	0.271	-0.756	-0.374
7.01	0.316	-1.157	-0.614
8.01	0.361	-1.472	-1.009
9.00	0.406	-2.058	-1.506
10.01	0.451	-2.893	-0.969
11.50	0.519	-3.667	1.766

Table B23: Sinkage and Trim Data for Beta Bow at Static Level Trim

Sinkage and Trim Data for Beta Bow @ 1.5° by the Stern			
Ship Speed	Froude Number	Sinkage	Dynamic Trim
(knots)	(-)	(cm)	(degrees)
1.00	0.045	-0.038	0.005
2.01	0.090	-0.125	0.011
3.01	0.136	-0.193	0.019
4.00	0.181	-0.215	0.027
5.00	0.226	-0.363	0.035
6.01	0.271	-0.668	0.022
7.01	0.316	-0.950	-0.005
8.01	0.361	-1.219	-0.104
9.00	0.406	-1.722	-0.091
10.00	0.451	-2.339	0.694

Table B24: Sinkage and Trim Data for Beta Bow at 1.5° by the Stern

Sinkage and Trim Data for Beta Bow @ 3.0° by the Stern			
Ship Speed	Froude Number	Sinkage	Dynamic Trim
(knots)	(-)	(cm)	(degrees)
1.00	0.045	-0.047	0.011
2.00	0.090	-0.146	0.028
3.01	0.136	-0.188	0.067
4.00	0.181	-0.201	0.119
5.00	0.226	-0.296	0.190
6.01	0.271	-0.560	0.299
7.01	0.316	-0.852	0.452
8.01	0.361	-0.986	0.609
9.00	0.406	-1.385	0.999
10.00	0.451	-1.792	1.842

Table B25: Sinkage and Trim Data for Beta Bow at 3.0° by the Stern

Sinkage and Trim Data for Gamma Bow @ Static Level Trim			
Ship Speed	Froude Number	Sinkage	Dynamic Trim
(knots)	(-)	(cm)	(degrees)
0.99	0.045	-0.029	-0.001
2.00	0.090	-0.104	-0.007
3.01	0.136	-0.193	-0.024
4.00	0.180	-0.214	-0.048
5.00	0.226	-0.393	-0.096
6.00	0.271	-0.687	-0.154
7.01	0.316	-1.059	-0.233
8.01	0.361	-1.285	-0.406
9.00	0.406	-1.854	-0.381
10.00	0.451	-2.531	0.484

Table B26: Sinkage and Trim Data for Gamma Bow at Static Level Trim

Sinkage and Trim Data for Gamma Bow @ 0.75° by the Stern			
Ship Speed	Froude Number	Sinkage	Dynamic Trim
(knots)	(-)	(cm)	(degrees)
1.00	0.045	-0.037	0.001
2.00	0.090	-0.107	-0.001
3.01	0.136	-0.200	-0.004
4.00	0.180	-0.199	-0.009
5.00	0.226	-0.376	-0.018
6.00	0.271	-0.681	-0.022
7.01	0.316	-1.011	-0.042
8.00	0.361	-1.242	-0.148
9.00	0.406	-1.764	0.038
10.00	0.451	-2.373	0.920

Table B27: Sinkage and Trim Data for Gamma Bow at 0.75° by the Stern

Sinkage and Trim Data for Gamma Bow @ 1.5° by the Stern			
Ship Speed	Froude Number	Sinkage	Dynamic Trim
(knots)	(-)	(cm)	(degrees)
1.00	0.045	-0.007	0.006
2.00	0.090	-0.124	0.006
3.00	0.136	-0.203	0.017
4.00	0.180	-0.220	0.030
5.00	0.226	-0.321	0.054
6.00	0.271	-0.655	0.119
7.01	0.316	-0.917	0.163
8.01	0.361	-1.167	0.146
9.00	0.406	-1.633	0.435
10.00	0.451	-2.147	1.335

Table B28: Sinkage and Trim Data for Gamma Bow at 1.5° by the Stern

Sinkage and Trim Data for Epsilon Bow @ Static Level Trim			
Ship Speed	Froude Number	Sinkage	Dynamic Trim
(knots)	(-)	(cm)	(degrees)
1.00	0.045	-0.033	0.000
2.00	0.090	-0.107	-0.008
3.01	0.136	-0.187	-0.027
4.00	0.180	-0.207	-0.060
5.00	0.226	-0.356	-0.122
6.00	0.271	-0.706	-0.249
7.01	0.316	-1.064	-0.416
8.01	0.361	-1.360	-0.704
9.00	0.406	-1.936	-0.929
10.00	0.451	-2.687	-0.201

Table B29: Sinkage and Trim Data for Epsilon Bow at Static Level Trim

Sinkage and Trim Data for Epsilon Bow @ 0.75° by the Stern			
Ship Speed	Froude Number	Sinkage	Dynamic Trim
(knots)	(-)	(cm)	(degrees)
1.00	0.045	-0.031	0.003
2.00	0.090	-0.111	-0.002
3.01	0.136	-0.186	-0.004
4.00	0.181	-0.206	-0.010
5.00	0.226	-0.338	-0.026
6.01	0.271	-0.652	-0.052
7.01	0.316	-0.981	-0.127
8.01	0.361	-1.258	-0.310
9.00	0.406	-1.798	-0.318
10.00	0.451	-2.450	0.529

Table B30: Sinkage and Trim Data for Epsilon Bow at 0.75° by the Stern

Sinkage and Trim Data for Epsilon Bow @ 1.5° by the Stern			
Ship Speed	Froude Number	Sinkage	Dynamic Trim
(knots)	(-)	(cm)	(degrees)
0.99	0.045	-0.040	0.011
2.00	0.090	-0.115	0.018
3.01	0.136	-0.180	0.028
4.00	0.180	-0.202	0.042
5.00	0.226	-0.311	0.056
6.00	0.271	-0.623	0.101
7.01	0.316	-0.864	0.129
8.00	0.361	-1.134	0.088
9.00	0.406	-1.621	0.255
10.00	0.451	-2.229	1.136

Table B31: Sinkage and Trim Data for Epsilon Bow at 1.5° by the Stern

Sinkage and Trim Data for Epsilon Bow @ 3.0° by the Stern			
Ship Speed	Froude Number	Sinkage	Dynamic Trim
(knots)	(-)	(cm)	(degrees)
0.99	0.045	-0.062	0.007
2.00	0.090	-0.125	0.032
3.01	0.136	-0.195	0.068
4.00	0.180	-0.213	0.122
5.00	0.226	-0.311	0.203
6.00	0.271	-0.577	0.323
7.01	0.316	-0.774	0.497
8.01	0.361	-0.962	0.694
9.00	0.406	-1.329	1.121
10.00	0.451	-1.739	2.022

Table B32: Sinkage and Trim Data for Epsilon Bow at 3.0° by the Stern

Appendix C: Tabular Data for MUN Bare Hull Resistance Tests

Appendix C-1: Resistance and Powering Data

Lm= 1.829 m
 Ls= 14.00 m
 Lwls= 13.25 m
 Lwlm= 1.731 m
 Scale= 7.654 -
 g= 9.81 m/s²
 water temp 12.4 °C
 v(visc)m= 1.2214E-06 m²/s
 v(visc)m15= 1.1390E-06 m²/s
 v(visc)s= 1.1883E-06 m²/s
 ρm= 999.4 kg/m³
 ρm15= 999 kg/m³
 ps= 1025.9 kg/m³
 Sm= 1.138 m²
 Ss= 66.68 m²

Resistance Data for Alpha Bow @ Static Level Trim										
Ship Speed	F _n	CTM15	CFM15	RnM15	CR	RnS	CFS	CTS	RTS	PE
(knots)	(-)	(-)	(-)	(-)	(-)	(-)	(-)	(-)	(N)	(W)
1.57	0.071	0.014811	0.005641	4.43E+05	0.009170	8.99E+06	0.003056	0.012626	280.80	226
3.66	0.165	0.006299	0.004652	1.04E+06	0.001646	2.10E+07	0.002647	0.004694	570.33	1075
4.72	0.213	0.006254	0.004408	1.33E+06	0.001846	2.71E+07	0.002541	0.004788	964.57	2341
5.77	0.260	0.008172	0.004227	1.63E+06	0.003945	3.31E+07	0.002461	0.006807	2052.98	6096
6.82	0.308	0.009614	0.004085	1.93E+06	0.005528	3.91E+07	0.002398	0.008326	3500.79	12274
7.88	0.355	0.012162	0.003968	2.23E+06	0.008194	4.52E+07	0.002345	0.010939	6144.27	24899
8.92	0.403	0.014100	0.003871	2.52E+06	0.010229	5.12E+07	0.002301	0.012930	9320.26	42788
9.98	0.450	0.017173	0.003787	2.82E+06	0.013386	5.72E+07	0.002262	0.016048	14468.37	74284
11.02	0.497	0.021232	0.003715	3.11E+06	0.017517	6.32E+07	0.002229	0.020146	22139.08	125493
12.07	0.545	0.024818	0.003650	3.41E+06	0.021167	6.92E+07	0.002199	0.023766	31338.14	194584

Table C1: Resistance Data for Alpha Bow at Static Level Trim

Lm= 1.829 m
 Ls= 14.00 m
 Lwls= 14.62 m
 Lwlm= 1.91 m
 Scale= 7.654 -
 g= 9.81 m/s²
 water temp 12.8 °C
 v(visc)m= 1.2082E-06 m²/s
 v(visc)m15= 1.1390E-06 m²/s
 v(visc)s= 1.1883E-06 m²/s
 ρm= 999.4 kg/m³
 ρm15= 999 kg/m³
 ps= 1025.9 kg/m³
 Sm= 1.237 m²
 Ss= 72.47 m²

Resistance Data for Beta Bow @ Static Level Trim										
Ship Speed	Fn	CTM15	CFM15	RnM15	CR	RnS	CFS	CTS	RTS	PE
(knots)	(-)	(-)	(-)	(-)	(-)	(-)	(-)	(-)	(N)	(W)
1.57	0.071	0.007936	0.005641	4.43E+05	0.002295	8.99E+06	0.003056	0.005751	139.02	112
3.67	0.165	0.007505	0.004652	1.04E+06	0.002852	2.10E+07	0.002647	0.005900	779.17	1469
5.77	0.260	0.006392	0.004227	1.63E+06	0.002165	3.31E+07	0.002461	0.005027	1647.82	4893
7.88	0.355	0.008786	0.003968	2.23E+06	0.004817	4.52E+07	0.002345	0.007563	4616.82	18709
8.93	0.403	0.010952	0.003871	2.52E+06	0.007081	5.12E+07	0.002301	0.009782	7664.06	35185
9.98	0.450	0.013993	0.003787	2.82E+06	0.010206	5.72E+07	0.002262	0.012868	12609.82	64742
11.02	0.497	0.017902	0.003715	3.11E+06	0.014187	6.32E+07	0.002229	0.016816	20084.80	113848
12.07	0.545	0.019931	0.003650	3.41E+06	0.016281	6.92E+07	0.002199	0.018880	27058.33	168010

Table C2: Resistance Data for Beta Bow at Static Level Trim

Lm=	1.829	m
Ls=	14.00	m
Lws=	14.25	m
Lwm=	1.862	m
Scale=	7.654	-
g=	9.81	m/s ²
water temp	16.33	°C
v(visc)m=	1.0983E-06	m ² /s
v(visc)m15=	1.1390E-06	m ² /s
v(visc)s=	1.1883E-06	m ² /s
pm=	998.9	kg/m ³
pm15=	999	kg/m ³
ps=	1025.9	kg/m ³
Sm=	1.194	m ²
Ss=	69.96	m ²

Resistance Data for Delta Bow @ Static Level Trim										
Ship Speed	Fn	CTM15	CFM15	RnM15	CR	RnS	CFS	CTS	RTS	PE
(knots)	(-)	(-)	(-)	(-)	(-)	(-)	(-)	(-)	(N)	(W)
1.56	0.070	0.005637	0.005641	4.43E+05	-0.000004	8.99E+06	0.003056	0.003452	80.55	65
3.66	0.165	0.006493	0.004652	1.04E+06	0.001840	2.10E+07	0.002647	0.004888	623.11	1174
4.72	0.213	0.006556	0.004408	1.33E+06	0.002148	2.71E+07	0.002541	0.005089	1075.70	2611
5.77	0.260	0.006436	0.004227	1.63E+06	0.002209	3.31E+07	0.002461	0.005070	1604.44	4765
6.82	0.308	0.006084	0.004085	1.93E+06	0.001999	3.91E+07	0.002398	0.004797	2116.25	7420
7.88	0.355	0.008327	0.003968	2.23E+06	0.004442	4.52E+07	0.002345	0.007187	4235.45	17164
8.93	0.403	0.010020	0.003871	2.52E+06	0.006149	5.12E+07	0.002301	0.008850	6693.33	30728
9.99	0.451	0.013731	0.003787	2.82E+06	0.009944	5.72E+07	0.002262	0.012607	11925.13	61227
11.03	0.498	0.017374	0.003715	3.11E+06	0.013659	6.32E+07	0.002229	0.016288	18779.91	106452
12.08	0.545	0.021427	0.003650	3.41E+06	0.017777	6.92E+07	0.002199	0.020376	28189.80	175036

Table C3: Resistance Data for Delta Bow at Static Level Trim

Resistance Data for Delta Bow @ 0.75° by the Stern										
Ship Speed	Fn	CTM15	CFM15	RnM15	CR	RnS	CFS	CTS	RTS	PE
(knots)	(-)	(-)	(-)	(-)	(-)	(-)	(-)	(-)	(N)	(W)
1.56	0.070	0.005704	0.005641	4.43E+05	0.000063	8.99E+06	0.003056	0.003519	82.11	66
3.67	0.165	0.007606	0.004652	1.04E+06	0.002954	2.10E+07	0.002647	0.006001	765.11	1442
4.71	0.213	0.007417	0.004408	1.33E+06	0.003009	2.71E+07	0.002541	0.005951	1257.81	3053
5.76	0.260	0.007240	0.004227	1.63E+06	0.003013	3.31E+07	0.002461	0.005874	1858.85	5520
6.82	0.308	0.007072	0.004085	1.93E+06	0.002986	3.91E+07	0.002398	0.005785	2551.79	8947
7.88	0.355	0.008798	0.003968	2.23E+06	0.004830	4.52E+07	0.002345	0.007575	4464.20	18091
8.93	0.403	0.010726	0.003871	2.52E+06	0.006855	5.12E+07	0.002301	0.009556	7227.62	33181
9.98	0.450	0.013048	0.003787	2.82E+06	0.009261	5.72E+07	0.002262	0.011923	11278.57	57907
11.03	0.498	0.016628	0.003715	3.11E+06	0.012913	6.32E+07	0.002229	0.015542	17920.04	101578
12.08	0.545	0.021499	0.003650	3.41E+06	0.017849	6.92E+07	0.002199	0.020448	28289.47	175654

Table C4: Resistance Data for Delta Bow at 0.75° by the Stern

Resistance Data for Delta Bow @ 1.5° by the Stern										
Ship Speed	Fn	CTM15	CFM15	RnM15	CR	RnS	CFS	CTS	RTS	PE
(knots)	(-)	(-)	(-)	(-)	(-)	(-)	(-)	(-)	(N)	(W)
1.56	0.071	0.007547	0.005641	4.43E+05	0.001906	8.99E+06	0.003056	0.005363	125.13	101
3.67	0.165	0.007374	0.004652	1.04E+06	0.002722	2.10E+07	0.002647	0.005769	735.51	1386
4.71	0.213	0.008159	0.004408	1.33E+06	0.003751	2.71E+07	0.002541	0.006693	1414.65	3433
5.77	0.260	0.008931	0.004227	1.63E+06	0.004704	3.31E+07	0.002461	0.007566	2394.14	7110
6.83	0.308	0.008063	0.004085	1.93E+06	0.003978	3.91E+07	0.002398	0.006776	2989.21	10481
7.88	0.355	0.009310	0.003968	2.23E+06	0.005341	4.52E+07	0.002345	0.008087	4765.55	19312
8.93	0.403	0.010261	0.003871	2.52E+06	0.006390	5.12E+07	0.002301	0.009091	6875.57	31565
9.97	0.450	0.012860	0.003787	2.82E+06	0.009073	5.72E+07	0.002262	0.011735	11101.01	56995
11.02	0.497	0.016746	0.003715	3.11E+06	0.013031	6.32E+07	0.002229	0.015660	18055.62	102346
12.08	0.545	0.021678	0.003650	3.41E+06	0.018028	6.92E+07	0.002199	0.020626	28536.42	177188

Table C5: Resistance Data for Delta Bow at 1.5° by the Stern

Lm=	1.829	m
Ls=	14.00	m
Lwis=	14.62	m
Lwlm=	1.91	m
Scale=	7.654	-
g=	9.81	m/s ²
water temp	13.2	°C
v(visc)m=	1.1951E-06	m ² /s
v(visc)m15=	1.1390E-06	m ² /s
v(visc)s=	1.1883E-06	m ² /s
pm=	999.3	kg/m ³
pm15=	999	kg/m ³
ps=	1025.9	kg/m ³
Sm=	1.219	m ²
Ss=	71.42	m ²

Resistance Data for Gamma Bow @ Static Level Trim										
Ship Speed	Fn	CTM15	CFM15	RnM15	CR	RnS	CFS	CTS	RTS	PE
(knots)	(-)	(-)	(-)	(-)	(-)	(-)	(-)	(-)	(N)	(W)
1.57	0.071	0.011011	0.005641	4.43E+05	0.005370	8.99E+06	0.003056	0.008826	210.26	170
3.67	0.166	0.005597	0.004652	1.04E+06	0.000945	2.10E+07	0.002647	0.003992	519.62	979
5.77	0.260	0.006811	0.004227	1.63E+06	0.002584	3.31E+07	0.002461	0.005445	1759.23	5224
6.83	0.308	0.006795	0.004085	1.93E+06	0.002709	3.91E+07	0.002398	0.005508	2480.50	8697
7.88	0.356	0.008143	0.003968	2.23E+06	0.004175	4.52E+07	0.002345	0.006920	4163.60	16873
8.93	0.403	0.010466	0.003871	2.52E+06	0.006595	5.12E+07	0.002301	0.009296	7177.79	32952
9.98	0.450	0.012848	0.003787	2.82E+06	0.009061	5.72E+07	0.002262	0.011723	11321.34	58127
11.02	0.497	0.016380	0.003715	3.11E+06	0.012665	6.32E+07	0.002229	0.015294	18003.50	102051
12.07	0.545	0.020949	0.003650	3.41E+06	0.017298	6.92E+07	0.002199	0.019897	28103.88	174502

Table C6: Resistance Data for Gamma Bow at Static Level Trim

Lm= 1.829 m
 Ls= 14.00 m
 Lwls= 14.62 m
 Lwlm= 1.91 m
 Scale= 7.654 -
 g= 9.81 m/s²
 water temp 13.2 °C
 v(visc)m= 1.1951E-06 m²/s
 v(visc)m15= 1.1390E-06 m²/s
 v(visc)s= 1.1883E-06 m²/s
 pm= 999.3 kg/m³
 pm15= 999 kg/m³
 ps= 1025.9 kg/m³
 Sm= 1.227 m²
 Ss= 71.89 m²

Resistance Data for Epsilon Bow @ Static Level Trim										
Ship Speed	Fn	CTM15	CFM15	RnM15	CR	RnS	CFS	CTS	RTS	PE
(knots)	(-)	(-)	(-)	(-)	(-)	(-)	(-)	(-)	(N)	(W)
1.56	0.070	0.000587	0.005641	4.43E+05	-0.005054	8.99E+06	0.003056	-0.001598	-38.32	-31
3.67	0.166	0.004979	0.004652	1.04E+06	0.000327	2.10E+07	0.002647	0.003374	442.08	833
5.77	0.261	0.005162	0.004227	1.63E+06	0.000935	3.31E+07	0.002461	0.003797	1234.72	3667
7.88	0.355	0.007837	0.003968	2.23E+06	0.003869	4.52E+07	0.002345	0.006615	4005.74	16233
8.93	0.403	0.009452	0.003871	2.52E+06	0.005581	5.12E+07	0.002301	0.008282	6437.14	29552
9.98	0.451	0.012858	0.003787	2.82E+06	0.009071	5.72E+07	0.002262	0.011734	11405.92	58561
12.09	0.545	0.019802	0.003650	3.41E+06	0.016152	6.92E+07	0.002199	0.018751	26658.17	165525

Table C7: Resistance Data for Epsilon Bow at Static Level Trim

Lm= 1.829 m
 Ls= 14.00 m
 Lwls= 14.62 m
 Lwlm= 1.91 m
 Scale= 7.654 -
 g= 9.81 m/s²
 water temp 16.67 °C
 v(visc)m= 1.0927E-06 m²/s
 v(visc)m15= 1.1390E-06 m²/s
 v(visc)s= 1.1883E-06 m²/s
 pm= 998.9 kg/m³
 pm15= 999 kg/m³
 ps= 1025.9 kg/m³
 Sm= 1.242 m²
 Ss= 72.77 m²

Resistance Data for Eta Bow @ Static Level Trim										
Ship Speed	Fn	CTM15	CFM15	RnM15	CR	RnS	CFS	CTS	RTS	PE
(knots)	(-)	(-)	(-)	(-)	(-)	(-)	(-)	(-)	(N)	(W)
1.56	0.071	0.005210	0.005641	4.43E+05	-0.000431	8.99E+06	0.003056	0.003025	73.42	59
3.66	0.165	0.005567	0.004652	1.04E+06	0.000914	2.10E+07	0.002647	0.003962	525.34	990
4.71	0.213	0.005660	0.004408	1.33E+06	0.001252	2.71E+07	0.002541	0.004194	922.04	2238
5.77	0.260	0.006817	0.004227	1.63E+06	0.002590	3.31E+07	0.002461	0.005452	1794.50	5329
6.82	0.308	0.007505	0.004085	1.93E+06	0.003420	3.91E+07	0.002398	0.006218	2853.33	10004
7.87	0.355	0.009120	0.003968	2.23E+06	0.005152	4.52E+07	0.002345	0.007897	4840.83	19617
8.93	0.403	0.010883	0.003871	2.52E+06	0.007012	5.12E+07	0.002301	0.009713	7641.64	35082
9.98	0.450	0.014483	0.003787	2.82E+06	0.010696	5.72E+07	0.002262	0.013358	13143.73	67483
11.03	0.497	0.017530	0.003715	3.11E+06	0.013815	6.32E+07	0.002229	0.016444	19722.11	111792
12.08	0.545	0.020239	0.003650	3.41E+06	0.016589	6.92E+07	0.002199	0.019188	27612.96	171454

Table C8: Resistance Data for Eta Bow at Static Level Trim

Resistance Data for Eta Bow @ 0.75° by the Stern										
Ship Speed	Fn	CTM15	CFM15	RnM15	CR	RnS	CFS	CTS	RTS	PE
(knots)	(-)	(-)	(-)	(-)	(-)	(-)	(-)	(-)	(N)	(W)
1.57	0.071	0.007304	0.005641	4.43E+05	0.001663	8.99E+06	0.003056	0.005119	124.26	100
3.67	0.165	0.006958	0.004652	1.04E+06	0.002305	2.10E+07	0.002647	0.005353	709.83	1338
4.72	0.213	0.006453	0.004408	1.33E+06	0.002045	2.71E+07	0.002541	0.004987	1096.40	2661
5.77	0.261	0.007439	0.004227	1.63E+06	0.003213	3.31E+07	0.002461	0.006074	1999.37	5937
6.82	0.308	0.008014	0.004085	1.93E+06	0.003928	3.91E+07	0.002398	0.006726	3086.52	10822
7.87	0.355	0.009174	0.003968	2.23E+06	0.005206	4.52E+07	0.002345	0.007951	4873.85	19751
8.93	0.403	0.010779	0.003871	2.52E+06	0.006908	5.12E+07	0.002301	0.009609	7559.74	34706
9.98	0.450	0.012897	0.003787	2.82E+06	0.009110	5.72E+07	0.002262	0.011772	11583.63	59473
11.04	0.498	0.015570	0.003715	3.11E+06	0.011855	6.32E+07	0.002229	0.014484	17371.48	98468
12.07	0.545	0.018901	0.003650	3.41E+06	0.015250	6.92E+07	0.002199	0.017849	25686.70	159493

Table C9: Resistance Data for Eta Bow at 0.75° by the Stern

Resistance Data for Eta Bow @ 1.5° by the Stern										
Ship Speed	Fn	CTM15	CFM15	RnM15	CR	RnS	CFS	CTS	RTS	PE
(knots)	(-)	(-)	(-)	(-)	(-)	(-)	(-)	(-)	(N)	(W)
1.58	0.071	0.007576	0.005641	4.43E+05	0.001935	8.99E+06	0.003056	0.005391	130.84	106
3.67	0.165	0.006734	0.004652	1.04E+06	0.002082	2.10E+07	0.002647	0.005129	680.22	1282
4.72	0.213	0.007629	0.004408	1.33E+06	0.003221	2.71E+07	0.002541	0.006162	1354.95	3288
5.77	0.260	0.008287	0.004227	1.63E+06	0.004060	3.31E+07	0.002461	0.006922	2278.39	6766
6.82	0.308	0.008984	0.004085	1.93E+06	0.004898	3.91E+07	0.002398	0.007697	3531.69	12383
7.87	0.355	0.009629	0.003968	2.23E+06	0.005661	4.52E+07	0.002345	0.008406	5152.85	20862
8.93	0.403	0.010385	0.003871	2.52E+06	0.006514	5.12E+07	0.002301	0.009215	7249.56	33282
9.98	0.450	0.011848	0.003787	2.82E+06	0.008061	5.72E+07	0.002262	0.010723	10551.35	54173
11.02	0.497	0.014574	0.003715	3.11E+06	0.010860	6.32E+07	0.002229	0.013488	16177.26	91699
12.07	0.544	0.018365	0.003650	3.41E+06	0.014715	6.92E+07	0.002199	0.017314	24916.19	154709

Table C10: Resistance Data for Eta Bow at 1.5° by the Stern

Lm=	1.829	m
Ls=	14.00	m
Lwis=	14.25	m
Lwlm=	1.862	m
Scale=	7.654	-
g=	9.81	m/s ²
water temp	16.4	°C
v(visc)m=	1.0983E-06	m ² /s
v(visc)m15=	1.1390E-06	m ² /s
v(visc)s=	1.1883E-06	m ² /s
pm=	998.9	kg/m ³
pm15=	999	kg/m ³
ps=	1025.9	kg/m ³
Sm=	1.214	m ²
Ss=	71.13	m ²

Resistance Data for Iota Bow @ Static Level Trim										
Ship Speed	Fn	CTM15	CFM15	RnM15	CR	RnS	CFS	CTS	RTS	PE
(knots)	(-)	(-)	(-)	(-)	(-)	(-)	(-)	(-)	(N)	(W)
1.57	0.071	0.009596	0.005641	4.43E+05	0.003955	8.99E+06	0.003056	0.007411	175.82	142
3.67	0.165	0.006481	0.004652	1.04E+06	0.001829	2.10E+07	0.002647	0.004876	632.05	1191
4.71	0.213	0.007213	0.004408	1.33E+06	0.002805	2.71E+07	0.002541	0.005746	1234.98	2997
5.77	0.260	0.007687	0.004227	1.63E+06	0.003460	3.31E+07	0.002461	0.006321	2033.86	6040
6.83	0.308	0.006630	0.004085	1.93E+06	0.002544	3.91E+07	0.002398	0.005343	2396.28	8402
7.87	0.355	0.007952	0.003968	2.23E+06	0.003983	4.52E+07	0.002345	0.006729	4031.70	16338
8.93	0.403	0.009533	0.003871	2.52E+06	0.005662	5.12E+07	0.002301	0.008363	6430.67	29522
9.98	0.450	0.012899	0.003787	2.82E+06	0.009112	5.72E+07	0.002262	0.011774	11324.34	58142
11.03	0.498	0.016743	0.003715	3.11E+06	0.013028	6.32E+07	0.002229	0.015657	18354.59	104041
12.08	0.545	0.020384	0.003650	3.41E+06	0.016734	6.92E+07	0.002199	0.019333	27194.74	168857

Table C11: Resistance Data for Iota Bow at Static Level Trim

Resistance Data for Iota Bow @ 0.75° by the Stern										
Ship Speed	F _n	CTM15	CFM15	RnM15	CR	RnS	CFS	CTS	RTS	PE
(knots)	(-)	(-)	(-)	(-)	(-)	(-)	(-)	(-)	(N)	(W)
1.56	0.070	0.004804	0.005641	4.43E+05	-0.000837	8.99E+06	0.003056	0.002619	62.13	50
3.66	0.165	0.008392	0.004652	1.04E+06	0.003739	2.10E+07	0.002647	0.006787	879.68	1658
4.72	0.213	0.008422	0.004408	1.33E+06	0.004013	2.71E+07	0.002541	0.006955	1494.73	3628
5.77	0.260	0.008702	0.004227	1.63E+06	0.004475	3.31E+07	0.002461	0.007337	2360.49	7010
6.83	0.308	0.007988	0.004085	1.93E+06	0.003903	3.91E+07	0.002398	0.006701	3005.47	10538
7.87	0.355	0.008353	0.003968	2.23E+06	0.004385	4.52E+07	0.002345	0.007130	4272.34	17313
8.92	0.403	0.009622	0.003871	2.52E+06	0.005751	5.12E+07	0.002301	0.008452	6499.43	29838
9.98	0.450	0.012375	0.003787	2.82E+06	0.008588	5.72E+07	0.002262	0.011251	10820.62	55556
11.02	0.497	0.015835	0.003715	3.11E+06	0.012120	6.32E+07	0.002229	0.014749	17290.65	98010
12.08	0.545	0.020384	0.003650	3.41E+06	0.016734	6.92E+07	0.002199	0.019332	27194.27	168854

Table C12: Resistance Data for Iota Bow at 0.75° by the Stern

Resistance Data for Iota Bow @ 1.5° by the Stern										
Ship Speed	F _n	CTM15	CFM15	RnM15	CR	RnS	CFS	CTS	RTS	PE
(knots)	(-)	(-)	(-)	(-)	(-)	(-)	(-)	(-)	(N)	(W)
1.57	0.071	0.005042	0.005641	4.43E+05	-0.000599	8.99E+06	0.003056	0.002857	67.78	55
3.66	0.165	0.007935	0.004652	1.04E+06	0.003283	2.10E+07	0.002647	0.006330	820.54	1547
4.72	0.213	0.009671	0.004408	1.33E+06	0.005263	2.71E+07	0.002541	0.008205	1763.30	4280
5.77	0.260	0.010431	0.004227	1.63E+06	0.006204	3.31E+07	0.002461	0.009066	2916.82	8662
6.81	0.307	0.009676	0.004085	1.93E+06	0.005590	3.91E+07	0.002398	0.008389	3762.54	13192
7.87	0.355	0.009351	0.003968	2.23E+06	0.005383	4.52E+07	0.002345	0.008128	4870.27	19736
8.93	0.403	0.009495	0.003871	2.52E+06	0.005624	5.12E+07	0.002301	0.008325	6401.43	29388
9.98	0.450	0.011828	0.003787	2.82E+06	0.008041	5.72E+07	0.002262	0.010704	10294.44	52854
11.03	0.498	0.015626	0.003715	3.11E+06	0.011911	6.32E+07	0.002229	0.014540	17045.08	96618
12.08	0.545	0.020564	0.003650	3.41E+06	0.016913	6.92E+07	0.002199	0.019512	27447.23	170425

Table C13: Resistance Data for Iota Bow at 1.5° by the Stern

Lm=	1.829	m
Ls=	14.00	m
Lwls=	14.25	m
Lwlm=	1.862	m
Scale=	7.654	-
g=	9.81	m/s ²
water temp	16.57	°C
v(visc)m=	1.0927E-06	m ² /s
v(visc)m15=	1.1390E-06	m ² /s
v(visc)s=	1.1883E-06	m ² /s
pm=	998.9	kg/m ³
pm15=	999	kg/m ³
ps=	1025.9	kg/m ³
Sm=	1.220	m ²
Ss=	71.48	m ²

Resistance Data for Theta Bow @ Static Level Trim										
Ship Speed	Fn	CTM15	CFM15	RnM15	CR	RnS	CFS	CTS	RTS	PE
(knots)	(-)	(-)	(-)	(-)	(-)	(-)	(-)	(-)	(N)	(W)
1.57	0.071	0.006362	0.005641	4.43E+05	0.000721	8.99E+06	0.003056	0.004177	99.59	80
3.67	0.165	0.007638	0.004652	1.04E+06	0.002985	2.10E+07	0.002647	0.006033	785.81	1481
4.72	0.213	0.006288	0.004408	1.33E+06	0.001880	2.71E+07	0.002541	0.004821	1041.23	2527
5.77	0.260	0.007313	0.004227	1.63E+06	0.003086	3.31E+07	0.002461	0.005947	1922.98	5710
6.82	0.308	0.007854	0.004085	1.93E+06	0.003768	3.91E+07	0.002398	0.006567	2959.79	10377
7.88	0.355	0.009815	0.003968	2.23E+06	0.005846	4.52E+07	0.002345	0.008592	5173.39	20965
8.92	0.403	0.011790	0.003871	2.52E+06	0.007919	5.12E+07	0.002301	0.010620	8206.53	37675
9.98	0.450	0.015545	0.003787	2.82E+06	0.011758	5.72E+07	0.002262	0.014420	13937.81	71560
11.03	0.498	0.018912	0.003715	3.11E+06	0.015197	6.32E+07	0.002229	0.017826	21000.86	119041
12.08	0.545	0.021373	0.003650	3.41E+06	0.017723	6.92E+07	0.002199	0.020322	28727.13	178372

Table C14: Resistance Data for Theta Bow at Static Level Trim

Resistance Data for Theta Bow @ 0.75° by the Stern										
Ship Speed	Fn	CTM15	CFM15	RnM15	CR	RnS	CFS	CTS	RTS	PE
(knots)	(-)	(-)	(-)	(-)	(-)	(-)	(-)	(-)	(N)	(W)
1.57	0.071	0.007330	0.005641	4.43E+05	0.001689	8.99E+06	0.003056	0.005146	122.68	99
3.67	0.165	0.007013	0.004652	1.04E+06	0.002361	2.10E+07	0.002647	0.005408	704.47	1328
4.71	0.213	0.007294	0.004408	1.33E+06	0.002886	2.71E+07	0.002541	0.005827	1258.58	3055
5.77	0.260	0.007668	0.004227	1.63E+06	0.003441	3.31E+07	0.002461	0.006303	2037.87	6052
6.82	0.308	0.008323	0.004085	1.93E+06	0.004237	3.91E+07	0.002398	0.007036	3171.24	11119
7.88	0.355	0.009793	0.003968	2.23E+06	0.005825	4.52E+07	0.002345	0.008570	5160.40	20912
8.93	0.403	0.011829	0.003871	2.52E+06	0.007958	5.12E+07	0.002301	0.010659	8236.72	37814
9.98	0.450	0.014025	0.003787	2.82E+06	0.010238	5.72E+07	0.002262	0.012900	12468.22	64015
11.02	0.497	0.017058	0.003715	3.11E+06	0.013343	6.32E+07	0.002229	0.015972	18816.27	106658
12.08	0.545	0.020436	0.003650	3.41E+06	0.016786	6.92E+07	0.002199	0.019384	27402.17	170145

Table C15: Resistance Data for Theta Bow at 0.75° by the Stern

Resistance Data for Theta Bow @ 1.5° by the Stern										
Ship Speed	Fn	CTM15	CFM15	RnM15	CR	RnS	CFS	CTS	RTS	PE
(knots)	(-)	(-)	(-)	(-)	(-)	(-)	(-)	(-)	(N)	(W)
1.56	0.070	0.005382	0.005641	4.43E+05	-0.000259	8.99E+06	0.003056	0.003197	76.23	61
3.66	0.165	0.006810	0.004652	1.04E+06	0.002158	2.10E+07	0.002647	0.005205	678.05	1278
4.71	0.213	0.007416	0.004408	1.33E+06	0.003008	2.71E+07	0.002541	0.005950	1285.02	3119
5.77	0.260	0.008101	0.004227	1.63E+06	0.003874	3.31E+07	0.002461	0.006736	2177.88	6467
6.82	0.308	0.009011	0.004085	1.93E+06	0.004925	3.91E+07	0.002398	0.007724	3481.35	12206
7.87	0.355	0.010215	0.003968	2.23E+06	0.006247	4.52E+07	0.002345	0.008992	5414.40	21942
8.93	0.403	0.011627	0.003871	2.52E+06	0.007756	5.12E+07	0.002301	0.010457	8080.69	37097
9.97	0.450	0.013153	0.003787	2.82E+06	0.009366	5.72E+07	0.002262	0.012028	11625.94	59690
11.02	0.497	0.016034	0.003715	3.11E+06	0.012319	6.32E+07	0.002229	0.014948	17609.86	99819
12.08	0.545	0.020040	0.003650	3.41E+06	0.016390	6.92E+07	0.002199	0.018989	26843.06	166673

Table C16: Resistance Data for Theta Bow at 1.5° by the Stern

Lm= 1.829 m
 Ls= 14.00 m
 Lwls= 14.25 m
 Lwlm= 1.862 m
 Scale= 7.654 -
 g= 9.81 m/s²
 water temp 16.9 °C
 v(visc)m= 1.0871E-06 m²/s
 v(visc)m15= 1.1390E-06 m²/s
 v(visc)s= 1.1883E-06 m²/s
 pm= 998.9 kg/m³
 pm15= 999 kg/m³
 ps= 1025.9 kg/m³
 Sm= 1.202 m²
 Ss= 70.43 m²

Resistance Data for Zeta Bow @ Static Level Trim										
Ship Speed	Fn	CTM15	CFM15	RnM15	CR	RnS	CFS	CTS	RTS	PE
(knots)	(-)	(-)	(-)	(-)	(-)	(-)	(-)	(-)	(N)	(W)
1.56	0.071	0.007967	0.005641	4.43E+05	0.002326	8.99E+06	0.003056	0.005783	135.83	110
3.66	0.165	0.005194	0.004652	1.04E+06	0.000541	2.10E+07	0.002647	0.003589	460.59	868
4.71	0.213	0.006141	0.004408	1.33E+06	0.001733	2.71E+07	0.002541	0.004674	994.60	2414
5.77	0.260	0.006354	0.004227	1.63E+06	0.002127	3.31E+07	0.002461	0.004989	1589.27	4719
6.82	0.308	0.006858	0.004085	1.93E+06	0.002773	3.91E+07	0.002398	0.005571	2473.96	8674
7.86	0.355	0.009001	0.003968	2.23E+06	0.005033	4.52E+07	0.002345	0.007778	4614.38	18700
8.92	0.403	0.011413	0.003871	2.52E+06	0.007542	5.12E+07	0.002301	0.010243	7798.69	35803
9.98	0.450	0.014907	0.003787	2.82E+06	0.011120	5.72E+07	0.002262	0.013783	13124.80	67386
11.02	0.497	0.018067	0.003715	3.11E+06	0.014353	6.32E+07	0.002229	0.016981	19710.68	111728
12.08	0.545	0.021598	0.003650	3.41E+06	0.017948	6.92E+07	0.002199	0.020547	28616.83	177687

Table C17: Resistance Data for Zeta Bow at Static Level Trim

Resistance Data for Zeta Bow @ 0.75° by the Stern										
Ship Speed	Fn	CTM15	CFM15	RnM15	CR	RnS	CFS	CTS	RTS	PE
(knots)	(-)	(-)	(-)	(-)	(-)	(-)	(-)	(-)	(N)	(W)
1.56	0.071	0.006909	0.005641	4.43E+05	0.001268	8.99E+06	0.003056	0.004724	110.96	89
3.66	0.165	0.006205	0.004652	1.04E+06	0.001553	2.10E+07	0.002647	0.004600	590.36	1113
4.71	0.213	0.006531	0.004408	1.33E+06	0.002123	2.71E+07	0.002541	0.005064	1077.59	2615
5.76	0.260	0.007015	0.004227	1.63E+06	0.002788	3.31E+07	0.002461	0.005649	1799.63	5344
6.82	0.308	0.006759	0.004085	1.93E+06	0.002674	3.91E+07	0.002398	0.005472	2430.15	8520
7.87	0.355	0.008886	0.003968	2.23E+06	0.004918	4.52E+07	0.002345	0.007663	4546.17	18423
8.93	0.403	0.010835	0.003871	2.52E+06	0.006964	5.12E+07	0.002301	0.009665	7358.31	33781
9.98	0.450	0.013322	0.003787	2.82E+06	0.009535	5.72E+07	0.002262	0.012197	11614.82	59633
11.02	0.497	0.016559	0.003715	3.11E+06	0.012844	6.32E+07	0.002229	0.015473	17959.68	101802
12.06	0.544	0.020743	0.003650	3.41E+06	0.017092	6.92E+07	0.002199	0.019691	27425.18	170288

Table C18: Resistance Data for Zeta Bow at 0.75° by the Stern

Resistance Data for Zeta Bow @ 1.5° by the Stern										
Ship Speed	Fn	CTM15	CFM15	RnM15	CR	RnS	CFS	CTS	RTS	PE
(knots)	(-)	(-)	(-)	(-)	(-)	(-)	(-)	(-)	(N)	(W)
1.57	0.071	0.006952	0.005641	4.43E+05	0.001311	8.99E+06	0.003056	0.004767	111.98	90
3.66	0.165	0.006730	0.004652	1.04E+06	0.002077	2.10E+07	0.002647	0.005124	657.68	1240
4.72	0.213	0.007694	0.004408	1.33E+06	0.003286	2.71E+07	0.002541	0.006227	1325.16	3216
5.77	0.260	0.007821	0.004227	1.63E+06	0.003595	3.31E+07	0.002461	0.006456	2056.67	6107
6.81	0.307	0.007588	0.004085	1.93E+06	0.003502	3.91E+07	0.002398	0.006301	2798.09	9810
7.87	0.355	0.008999	0.003968	2.23E+06	0.005031	4.52E+07	0.002345	0.007776	4613.37	18695
8.92	0.403	0.010799	0.003871	2.52E+06	0.006928	5.12E+07	0.002301	0.009629	7331.02	33656
9.98	0.450	0.012993	0.003787	2.82E+06	0.009206	5.72E+07	0.002262	0.011869	11302.13	58028
11.03	0.498	0.016075	0.003715	3.11E+06	0.012360	6.32E+07	0.002229	0.014989	17397.53	98616
12.05	0.544	0.020474	0.003650	3.41E+06	0.016823	6.92E+07	0.002199	0.019422	27050.40	167961

Table C19: Resistance Data for Zeta Bow at 1.5° by the Stern

Appendix C-2: Sinkage and Dynamic Trim Data

Sinkage and Trim Data for Alpha Bow @ Static Level Trim			
Ship Speed	Froude Number	Sinkage	Dynamic Trim
(knots)	(-)	(cm)	(degrees)
1.57	0.071	-0.082	0.006
3.66	0.165	-0.296	0.064
4.72	0.213	-0.460	0.103
5.77	0.260	-0.668	0.151
6.82	0.308	-0.924	0.199
7.88	0.355	-1.218	0.260
8.92	0.403	-1.682	0.393
9.98	0.450	-2.176	-0.143
11.02	0.497	-2.778	-1.708
12.07	0.545	-2.919	-3.738

Table C20: Sinkage and Trim Data for Alpha Bow at Static Level Trim

Sinkage and Trim Data for Beta Bow @ Static Level Trim			
Ship Speed	Froude Number	Sinkage	Dynamic Trim
(knots)	(-)	(cm)	(degrees)
1.57	0.067	-0.045	0.009
3.67	0.157	-0.256	0.062
4.72	0.202	0.062	0.006
5.77	0.248	-0.585	0.286
6.82	0.293	0.062	0.006
7.88	0.338	-1.276	0.807
8.93	0.383	-1.775	1.360
9.98	0.429	-2.356	1.321
11.02	0.474	-3.118	-0.113
12.07	0.519	-3.417	-2.317

Table C21: Sinkage and Trim Data for Beta Bow at Static Level Trim

Sinkage and Trim Data for Delta Bow @ Static Level Trim			
Ship Speed	Froude Number	Sinkage	Dynamic Trim
(knots)	(-)	(cm)	(degrees)
1.56	0.068	-0.071	-0.006
3.66	0.159	-0.236	-0.054
4.72	0.205	-0.413	-0.100
5.77	0.251	-0.633	-0.172
6.82	0.297	-0.898	-0.268
7.88	0.343	-1.310	-0.404
8.93	0.388	-1.724	-0.571
9.99	0.434	-2.451	0.009
11.03	0.480	-2.935	1.600
12.08	0.526	-3.117	3.677

Table C22: Sinkage and Trim Data for Delta Bow at Static Level Trim

Sinkage and Trim Data for Delta Bow @ 0.75° by the Stern			
Ship Speed	Froude Number	Sinkage	Dynamic Trim
(knots)	(-)	(cm)	(degrees)
1.56	0.068	-0.034	0.001
3.67	0.159	-0.262	-0.015
4.71	0.205	-0.406	-0.035
5.76	0.251	-0.612	-0.055
6.82	0.297	-0.908	-0.093
7.88	0.343	-1.288	-0.178
8.93	0.388	-1.759	-0.196
9.98	0.434	-2.297	0.515
11.03	0.480	-2.667	2.030
12.08	0.525	-2.908	3.941

Table C23: Sinkage and Trim Data for Delta Bow at 0.75° by the Stern

Sinkage and Trim Data for Delta Bow @ 1.5° by the Stern			
Ship Speed	Froude Number	Sinkage	Dynamic Trim
(knots)	(-)	(cm)	(degrees)
1.56	0.068	-0.079	0.005
3.67	0.159	-0.259	0.015
4.71	0.205	-0.396	0.032
5.77	0.251	-0.596	0.062
6.83	0.297	-0.862	0.086
7.88	0.343	-1.238	0.064
8.93	0.388	-1.605	0.149
9.97	0.434	-2.172	0.950
11.02	0.479	-2.468	2.351
12.08	0.525	-2.617	4.153

Table C24: Sinkage and Trim Data for Delta Bow at 1.5° by the Stern

Sinkage and Trim Data for Gamma Bow @ Static Level Trim			
Ship Speed	Froude Number	Sinkage	Dynamic Trim
(knots)	(-)	(cm)	(degrees)
1.57	0.067	-0.060	0.001
3.67	0.158	-0.245	0.034
4.72	0.202	0.015	-0.030
5.78	0.248	-0.600	0.138
6.83	0.293	-0.902	0.213
7.88	0.338	-1.249	0.361
8.93	0.383	-1.671	0.492
9.98	0.429	-2.254	-0.042
11.02	0.473	-2.775	-1.451
12.07	0.519	-3.083	-3.354

Table C25: Sinkage and Trim Data for Gamma Bow at Static Level Trim

Sinkage and Trim Data for Epsilon Bow @ Static Level Trim			
Ship Speed	Froude Number	Sinkage	Dynamic Trim
(knots)	(-)	(cm)	(degrees)
1.56	0.067	-0.082	0.006
3.67	0.158	-0.241	0.053
4.72	0.202	-0.021	-0.019
5.76	0.248	-0.609	0.205
6.82	0.293	-0.025	-0.017
7.88	0.338	-1.346	0.577
8.93	0.383	-1.713	0.943
9.98	0.429	-2.305	0.636
11.02	0.473	-0.103	-0.972
12.09	0.519	-3.264	-2.793

Table C26: Sinkage and Trim Data for Epsilon Bow at Static Level Trim

Sinkage and Trim Data for Eta Bow @ Static Level Trim			
Ship Speed	Froude Number	Sinkage	Dynamic Trim
(knots)	(-)	(cm)	(degrees)
1.56	0.067	-0.065	-0.010
3.66	0.157	-0.273	-0.082
4.71	0.202	-0.411	-0.167
5.77	0.248	-0.611	-0.364
6.82	0.293	-0.912	-0.647
7.87	0.338	-1.351	-0.972
8.93	0.383	-1.878	-1.618
9.98	0.429	-2.664	-1.713
11.03	0.474	-3.332	-0.300
12.08	0.519	-3.790	2.075

Table C27: Sinkage and Trim Data for Eta Bow at Static Level Trim

Sinkage and Trim Data for Eta Bow @ 0.75° by the Stern			
Ship Speed	Froude Number	Sinkage	Dynamic Trim
(knots)	(-)	(cm)	(degrees)
1.57	0.067	-0.052	-0.003
3.67	0.158	-0.245	-0.032
4.72	0.203	-0.406	-0.079
5.77	0.248	-0.586	-0.177
6.82	0.293	-0.901	-0.349
7.87	0.338	-1.301	-0.547
8.93	0.384	-1.839	-0.947
9.98	0.429	-2.488	-0.802
11.04	0.474	-3.060	0.660
12.07	0.518	-3.445	2.750

Table C28: Sinkage and Trim Data for Eta Bow at 0.75° by the Stern

Sinkage and Trim Data for Eta Bow @ 1.5° by the Stern			
Ship Speed	Froude Number	Sinkage	Dynamic Trim
(knots)	(-)	(cm)	(degrees)
1.58	0.068	-0.034	0.007
3.67	0.158	-0.266	0.014
4.72	0.203	-0.419	0.007
5.77	0.248	-0.568	-0.043
6.82	0.293	-0.811	-0.099
7.87	0.338	-1.137	-0.148
8.93	0.384	-1.666	-0.297
9.98	0.429	-2.294	0.099
11.02	0.474	-2.678	1.470
12.07	0.518	-2.928	3.216

Table C29: Sinkage and Trim Data for Eta Bow at 1.5° by the Stern

Sinkage and Trim Data for Iota Bow @ Static Level Trim			
Ship Speed	Froude Number	Sinkage	Dynamic Trim
(knots)	(-)	(cm)	(degrees)
1.57	0.068	-0.065	-0.011
3.67	0.159	-0.274	-0.096
4.71	0.205	-0.416	-0.155
5.77	0.251	-0.629	-0.292
6.83	0.297	-0.944	-0.451
7.33	0.319	-1.132	-0.530
7.87	0.343	-1.350	-0.641
8.93	0.388	-1.831	-0.934
9.98	0.434	-2.486	-0.508
11.03	0.480	-3.121	1.094
12.08	0.525	-3.447	3.153

Table C30: Sinkage and Trim Data for Iota Bow at Static Level Trim

Sinkage and Trim Data for Iota Bow @ 0.75° by the Stern			
Ship Speed	Froude Number	Sinkage	Dynamic Trim
(knots)	(-)	(cm)	(degrees)
1.56	0.068	-0.042	-0.004
3.66	0.159	-0.280	-0.049
4.72	0.205	-0.419	-0.095
5.77	0.251	-0.604	-0.152
6.83	0.297	-0.868	-0.230
7.87	0.342	-1.278	-0.350
8.92	0.388	-1.794	-0.456
9.98	0.434	-2.383	0.131
11.02	0.479	-2.840	1.564
12.08	0.526	-3.032	3.496

Table C31: Sinkage and Trim Data for Iota Bow at 0.75° by the Stern

Sinkage and Trim Data for Iota Bow @ 1.5° by the Stern			
Ship Speed	Froude Number	Sinkage	Dynamic Trim
(knots)	(-)	(cm)	(degrees)
1.57	0.068	0.010	-0.001
3.66	0.159	-0.279	-0.007
4.72	0.205	-0.352	-0.029
5.77	0.251	-0.596	-0.037
6.81	0.296	-0.818	-0.024
7.87	0.342	-1.198	-0.046
8.93	0.388	-1.681	-0.011
9.98	0.434	-2.298	0.663
11.03	0.480	-2.682	2.025
12.08	0.525	-2.786	3.773

Table C32: Sinkage and Trim Data for Iota Bow at 1.5° by the Stern

Sinkage and Trim Data for Theta Bow @ Static Level Trim			
Ship Speed	Froude Number	Sinkage	Dynamic Trim
(knots)	(-)	(cm)	(degrees)
1.57	0.068	-0.041	-0.018
3.67	0.159	-0.296	-0.096
4.72	0.205	-0.444	-0.216
5.77	0.251	-0.657	-0.411
6.82	0.297	-1.005	-0.716
7.86	0.342	-1.407	-1.037
8.92	0.388	-1.942	-1.619
9.98	0.434	-2.670	-1.691
11.03	0.480	-3.422	-0.175
12.08	0.525	-3.767	2.292

Table C33: Sinkage and Trim Data for Theta Bow at Static Level Trim

Sinkage and Trim Data for Theta Bow @ 0.75° by the Stern			
Ship Speed	Froude Number	Sinkage	Dynamic Trim
(knots)	(-)	(cm)	(degrees)
1.57	0.068	-0.058	-0.002
3.67	0.159	-0.266	-0.040
4.71	0.205	-0.422	-0.102
5.77	0.251	-0.647	-0.239
6.82	0.297	-0.960	-0.448
7.88	0.343	-1.348	-0.665
8.93	0.388	-1.833	-1.086
9.98	0.434	-2.500	-0.901
11.02	0.480	-3.047	0.687
12.08	0.525	-3.386	2.960

Table C34: Sinkage and Trim Data for Theta Bow at 0.75° by the Stern

Sinkage and Trim Data for Theta Bow @ 1.5° by the Stern			
Ship Speed	Froude Number	Sinkage	Dynamic Trim
(knots)	(-)	(cm)	(degrees)
1.57	0.068	-0.050	0.000
3.66	0.159	-0.261	0.000
4.71	0.205	-0.385	-0.011
5.77	0.251	-0.611	-0.072
6.82	0.297	-0.880	-0.175
7.87	0.342	-1.267	-0.278
8.93	0.388	-1.745	-0.477
9.97	0.434	-2.275	-0.028
11.02	0.479	-2.787	1.579
12.08	0.525	-2.904	3.511

Table C35: Sinkage and Trim Data for Theta Bow at 1.5° by the Stern

Sinkage and Trim Data for Zeta Bow @ Static Level Trim			
Ship Speed	Froude Number	Sinkage	Dynamic Trim
(knots)	(-)	(cm)	(degrees)
1.56	0.068	-0.057	-0.006
3.66	0.159	-0.285	-0.072
4.71	0.205	-0.440	-0.140
5.77	0.251	-0.643	-0.279
6.82	0.297	-0.989	-0.480
7.86	0.342	-1.356	-0.706
8.92	0.388	-1.944	-1.146
9.98	0.434	-2.562	-0.872
11.02	0.479	-3.234	0.620
12.08	0.525	-3.451	2.973

Table C36: Sinkage and Trim Data for Zeta Bow at Static Level Trim

Sinkage and Trim Data for Zeta Bow @ 0.75° by the Stern			
Ship Speed	Froude Number	Sinkage	Dynamic Trim
(knots)	(-)	(cm)	(degrees)
1.56	0.068	-0.073	0.000
3.66	0.159	-0.280	-0.025
4.71	0.205	-0.402	-0.061
5.76	0.251	-0.651	-0.135
6.82	0.297	-0.885	-0.274
7.87	0.342	-1.307	-0.423
8.93	0.388	-1.880	-0.708
9.98	0.434	-2.429	-0.284
11.02	0.480	-2.619	1.168
12.06	0.525	-3.575	3.368

Table C37: Sinkage and Trim Data for Zeta Bow at 0.75° by the Stern

Sinkage and Trim Data for Zeta Bow @ 1.5° by the Stern			
Ship Speed	Froude Number	Sinkage	Dynamic Trim
(knots)	(-)	(cm)	(degrees)
1.57	0.068	-0.045	0.003
3.66	0.159	-0.270	0.014
4.72	0.205	-0.349	0.010
5.77	0.251	-0.496	-0.011
6.81	0.296	-0.792	-0.030
7.87	0.342	-1.208	-0.113
8.92	0.388	-1.591	-0.221
9.98	0.434	-2.271	0.406
11.03	0.480	-2.739	1.866
12.05	0.524	-2.730	3.695

Table C38: Sinkage and Trim Data for Zeta Bow at 1.5° by the Stern

Appendix D: Experimental Results for Self-Propulsion Tests

Lm	1.829	m
Ls	14.00	m
Lwls	13.25	m
Lwlm	1.731	m
Scale	7.654	-
g	9.81	m/s ²
water temp	16.2	°C
v(visc)m	1.104E-06	m ² /s
v(visc)s	1.188E-06	m ² /s
Ss	66.68	m ²
Dm	0.1205	m
c0.75	0.054	m
Ds	0.9223	m

Self Propulsion Data for Alpha Bow										
Ship Speed	np	Jp	Tp	Qp	KTp	10KQp	CTS	Jo	w	t
(knots)	(rps)	(-)	(N)	(N-m)	(-)	(-)	(-)	(-)	(-)	(-)
7.86	15.947	0.761	16.259	0.391	0.304	0.606	0.01071	0.691	0.093	0.182
8.92	19.269	0.715	24.907	0.629	0.319	0.667	0.01286	0.662	0.073	0.184
9.98	22.873	0.673	34.766	0.860	0.316	0.648	0.01604	0.668	0.007	0.098

Table D1: Self-Propulsion Data for Alpha Bow

Lm	1.829	m
Ls	14.00	m
Lwls	14.62	m
Lwlm	1.912	m
Scale	7.654	-
g	9.81	m/s ²
water temp	16.2	°C
v(visc)m	1.104E-06	m ² /s
v(visc)s	1.188E-06	m ² /s
Ss	72.47	m ²
Dm	0.1205	m
c0.75	0.054	m
Ds	0.9223	m

Self Propulsion Data for Beta Bow										
Ship Speed	np	Jp	Tp	Qp	KTp	10KQp	CTS	Jo	w	t
(knots)	(rps)	(-)	(N)	(N-m)	(-)	(-)	(-)	(-)	(-)	(-)
7.86	15.418	0.788	13.690	0.369	0.273	0.612	0.00744	0.748	0.051	0.257
8.92	18.684	0.737	22.820	0.589	0.310	0.665	0.00977	0.678	0.081	0.262
9.98	22.455	0.686	34.561	0.853	0.325	0.667	0.01299	0.649	0.053	0.202

Table D2: Self-Propulsion Data for Beta Bow

Lm	1.829	m
Ls	14.00	m
Lwls	14.25	m
Lwlm	1.862	m
Scale	7.654	-
g	9.81	m/s ²
water temp	16.5	°C
v(visc)m	1.104E-06	m ² /s
v(visc)s	1.188E-06	m ² /s
Ss	69.96	m ²
Dm	0.1205	m
c0.75	0.054	m
Ds	0.9223	m

Self Propulsion Data for Delta Bow										
Ship Speed	np	Jp	Tp	Qp	KTp	10KQp	CTS	Jo	w	t
(knots)	(rps)	(-)	(N)	(N-m)	(-)	(-)	(-)	(-)	(-)	(-)
7.86	14.912	0.815	13.688	0.340	0.292	0.603	0.00703	0.712	0.126	0.368
8.92	18.199	0.757	22.215	0.575	0.318	0.684	0.00880	0.662	0.125	0.311
9.98	21.614	0.712	32.738	0.898	0.333	0.758	0.01264	0.635	0.108	0.221

Table D3: Self-Propulsion Data for Delta Bow

Lm	1.829	m
Ls	14.00	m
Lwls	14.62	m
Lwlm	1.912	m
Scale	7.654	-
g	9.81	m/s ²
water temp	16.2	°C
v(visc)m	1.104E-06	m ² /s
v(visc)s	1.188E-06	m ² /s
Ss	71.42	m ²
Dm	0.1205	m
c0.75	0.054	m
Ds	0.9223	m

Self Propulsion Data for Gamma Bow										
Ship Speed	np	Jp	Tp	Qp	KTp	10KQp	CTS	Jo	w	t
(knots)	(rps)	(-)	(N)	(N-m)	(-)	(-)	(-)	(-)	(-)	(-)
7.86	15.071	0.806	12.401	0.353	0.259	0.613	0.00679	0.774	0.039	0.261
8.92	17.719	0.777	18.346	0.504	0.277	0.633	0.00927	0.740	0.047	0.167
9.98	21.420	0.718	31.725	0.777	0.328	0.668	0.01175	0.644	0.104	0.211

Table D4: Self-Propulsion Data for Gamma Bow

Lm	1.829	M
Ls	14.00	m
Lwls	14.62	m
Lwlm	1.912	m
Scale	7.654	-
g	9.81	m/s ²
water temp	16.2	°C
v(visc)m	1.104E-06	m ² /s
v(visc)s	1.188E-06	m ² /s
Ss	71.89	m ²
Dm	0.1205	m
c0.75	0.054	m
Ds	0.9223	m

Self Propulsion Data for Epsilon Bow										
Ship Speed	np	Jp	TP	Qp	KTp	10KQp	CTS	Jo	w	t
(knots)	(rps)	(-)	(N)	(N-m)	(-)	(-)	(-)	(-)	(-)	(-)
7.86	15.053	0.807	13.520	0.354	0.283	0.615	0.00649	0.729	0.096	0.342
8.92	18.010	0.765	21.251	0.554	0.311	0.673	0.00823	0.676	0.115	0.286
9.98	21.893	0.703	34.265	0.848	0.339	0.697	0.01186	0.622	0.115	0.279

Table D5: Self-Propulsion Data for Epsilon Bow

Lm	1.829	m
Ls	14.00	m
Lwls	14.62	m
Lwlm	1.912	m
Scale	7.654	-
g	9.81	m/s ²
water temp	16.7	°C
v(visc)m	1.104E-06	m ² /s
v(visc)s	1.188E-06	m ² /s
Ss	72.77	m ²
Dm	0.1205	m
c0.75	0.054	m
Ds	0.9223	m

Self Propulsion Data for Eta Bow										
Ship Speed	np	Jp	TP	Qp	KTp	10KQp	CTS	Jo	w	t
(knots)	(rps)	(-)	(N)	(N-m)	(-)	(-)	(-)	(-)	(-)	(-)
7.86	15.480	0.785	16.883	0.419	0.335	0.689	0.00781	0.632	0.195	0.342
8.92	18.434	0.747	23.880	0.595	0.334	0.690	0.00967	0.633	0.152	0.230
9.98	22.312	0.690	37.342	0.900	0.356	0.712	0.01353	0.590	0.145	0.232

Table D6: Self-Propulsion Data for Eta Bow

Lm	1.829	m
Ls	14.00	m
Lwls	14.25	m
Lwlm	1.862	m
Scale	7.654	-
g	9.81	m/s ²
water temp	16.4	°C
v(visc)m	1.104E-06	m ² /s
v(visc)s	1.188E-06	m ² /s
Ss	71.13	m ²
Dm	0.1205	m
c0.75	0.054	m
Ds	0.9223	m

Self Propulsion Data for Iota Bow										
Ship Speed	np	Jp	Tp	Qp	KTp	10KQp	CTS	Jo	w	t
(knots)	(rps)	(-)	(N)	(N-m)	(-)	(-)	(-)	(-)	(-)	(-)
7.86	14.651	0.829	12.421	0.320	0.275	0.587	0.00664	0.745	0.101	0.272
8.92	17.746	0.776	20.528	0.516	0.310	0.645	0.00823	0.679	0.124	0.255
9.98	21.422	0.719	32.310	0.833	0.334	0.715	0.01188	0.632	0.120	0.225

Table D7: Self-Propulsion Data for Iota Bow

Lm	1.829	m
Ls	14.00	m
Lwls	14.25	m
Lwlm	1.862	m
Scale	7.654	-
g	9.81	m/s ²
water temp	16.2	°C
v(visc)m	1.104E-06	m ² /s
v(visc)s	1.188E-06	m ² /s
Ss	71.48	m ²
Dm	0.1205	m
c0.75	0.054	m
Ds	0.9223	m

Self Propulsion Data for Theta Bow										
Ship Speed	np	Jp	Tp	Qp	KTp	10KQp	CTS	Jo	w	t
(knots)	(rps)	(-)	(N)	(N-m)	(-)	(-)	(-)	(-)	(-)	(-)
7.86	15.887	0.765	14.765	0.441	0.278	0.688	0.00848	0.740	0.033	0.187
8.92	19.076	0.723	25.097	0.716	0.327	0.776	0.01085	0.645	0.107	0.204
9.98	22.839	0.674	39.296	1.305	0.358	0.986	0.01459	0.587	0.130	0.217

Table D8: Self-Propulsion Data for Theta Bow

Lm	1.829	m
Ls	14.00	m
Lwls	14.25	m
Lwlm	1.862	m
Scale	7.654	-
g	9.81	m/s ²
water temp	16.2	°C
v(visc)m	1.104E-06	m ² /s
v(visc)s	1.188E-06	m ² /s
Ss	70.43	m ²
Dm	0.1205	m
c0.75	0.054	m
Ds	0.9223	m

Self Propulsion Data for Zeta Bow										
Ship Speed	np	Jp	Tp	Qp	KTp	10KQp	CTS	Jo	w	t
(knots)	(rps)	(-)	(N)	(N-m)	(-)	(-)	(-)	(-)	(-)	(-)
7.86	15.796	0.769	14.237	0.417	0.271	0.659	0.00772	0.752	0.021	0.273
8.92	18.705	0.736	21.645	0.572	0.294	0.644	0.01024	0.709	0.036	0.177
9.98	22.568	0.682	34.083	0.911	0.318	0.705	0.01391	0.664	0.026	0.167

Table D9: Self-Propulsion Data for Zeta Bow

Appendix E: Uncertainty Analysis for Bare Bull Resistance Tests

Appendix E-1: IOT Test Program

Bias Limit - Model Length

Data Acquisition: Model accuracy of ± 1 mm in all coordinates.

$B_L = 0.002 \text{ m} \rightarrow$ Model length bias

Bias Limit - Wetted Surface Area

Data Acquisition: Error due to manufacturing error of ± 1 mm in all coordinates.
 Length will increase by 2 mm, beam by 2 mm, draft by 1 mm.
 Assume block coefficient remains constant.
 (Assume the error for Alpha bow is fine for all bows)

$\nabla =$	67.75	kg	
$S =$	1.138	m^2	
$LWL' =$	1.733	m	
$B' =$	0.553	m	
$T' =$	0.19	m	
$C_B =$	0.3774	-	
$\nabla' =$	68.71937	kg	
$\nabla' - \nabla =$	0.969373	kg	
$C_S =$	0.105024	-	Where: $C_S = S / \sqrt{\nabla LWL}$
$S' =$	1.146112	m^2	
$S' - S =$	0.008112	m^2	
AWP	0.8054	m^2	

\rightarrow An increase of 0.9694 kg gives a decreased draft of: (using $\rho = 1000 \text{ kg/m}^3$)

$T'' = 0.001204 \text{ m}$

\rightarrow The smaller draft decreases the wetted surface by: $S'' = 3.462 * 0.001204$

*(using a total waterline length of $2 * LWL = 3.462 \text{ m}$)*

$S'' - S = 0.004167 \text{ m}^2$

$B_{WSI} = 0.003946 \text{ m}^2 \rightarrow$ Hull form bias

Calibration: Error due to measurement of model weight is $\pm 0.2 \text{ kg}$.

\rightarrow An increase in model weight of 0.2 kg gives a additional draft of: (using $\rho = 1000 \text{ kg/m}^3$)

$$T''' = 0.000248 \quad \text{m}$$

→ The increased draft increases the wetted surface by: $S'' = 3.462 * 0.000248$
 *(using a total waterline length of $2 * LWL = 3.462 \text{ m}$)*

$$S''' - S = 0.00086 \quad \text{m}^2$$

$$B_{ws2} = 0.00086 \quad \text{m}^2 \quad \rightarrow \text{Displacement bias}$$

Total: The wetted surface bias is obtained by the RSS of the 2 components above

$$B_{ws} = 0.004038 \quad \text{m}^2 \quad \rightarrow \text{Total bias limit for wetted surface area}$$

Bias Limit - Speed

The required info to determine the error for speed was not available for the MUN tests.
 The bias limit is based on information gathered from the IOT resistance tests.
 It is assumed that the bias limit will be similar during the MUN resistance tests.

Required test set-up information:

Resolution	10000 pulse/m
Diameter of wheel	0.5 m
Max pulse duration	0.0000002 s
Min pulse duration	0.00000012 s
Max output signal	5 volts
Circuit speed	100 ms
AD/DA card	16 bits
Number of windows	6366 pulses/rev

The output from the encoder is calculated with the following equation:

$$V = \frac{c\pi D}{6366\Delta t}$$

→ **Pulse Count** (denoted as 'C')

Calibration: Assumed accuracy of optical encoder of ± 1 pulse on every update.

$$B_{C1} = 1 \quad \text{pulse} \quad \rightarrow \text{Encoder calibration bias}$$

Data Acquisition: The AD boards are assumed to be accurate to 1.5 bits or pulses.

$B_{C2} =$ 1.5 pulses → AD conversion bias

$B_{C3} =$ 1.5 pulses → DA conversion bias

Data Reduction: Occurs when converting analogue voltage to a frequency that Represents the pulse count over 10 time bases, or one second. This bias limit is introduced by the linear curve fit obtained from a set of calibration data that is applied to the measured data to allow this conversion.

→ Curve fit bias limit determined previously to be 2.5 Hz

$B_{C4} =$ 0.25 pulses

→ The total bias limit for pulse count is obtained by the RSS of the components above

$$(B_C)^2 = (B_{C1})^2 + (B_{C2})^2 + (B_{C3})^2 + (B_{C4})^2$$

$B_C =$ 2.358495 pulses → Total bias limit for pulse count

→ Wheel Diameter (denoted as 'D')

Calibration: The wheel diameter is considered accurate within 0.000115 m

$B_D =$ 0.000115 m → Wheel diameter bias

→ Time Base (denoted as ' Δt ')

Calibration: Rated accuracy, based on ITTC procedure 7.5-02-02-02, is 1.025×10^{-5} s

$B_{\Delta t} =$ 0.00001025 m

→ The error in speed is obtained by using the equation given below:

$$(B_v)^2 = \left(\frac{\partial V}{\partial c} B_C \right)^2 + \left(\frac{\partial V}{\partial D} B_D \right)^2 + \left(\frac{\partial V}{\partial \Delta t} B_{\Delta t} \right)^2$$

Where:

$$\frac{\partial V}{\partial c} = \frac{\pi D}{6366 \Delta t} \quad \rightarrow \text{Calculated to be equal to } 0.00247$$

$$\frac{\partial V}{\partial D} = \frac{c\pi}{6366\Delta t}$$

$$\frac{\partial V}{\partial \Delta t} = \frac{c\pi D}{6366} \left(-\frac{1}{\Delta t^2} \right)$$

→ Table for tested speeds:

V_M (m/s)	c	$\partial V/\partial D$	$\partial V/\partial \Delta t$
0.185	75.07666525	0.3705	-1.8525
0.372	150.8625568	0.7445	-3.7225
0.559	226.4458122	1.1175	-5.5875
0.744	301.5224774	1.488	-7.44
0.930	376.7004607	1.859	-9.295
1.116	452.2837162	2.232	-11.16
1.303	527.8669716	2.605	-13.025
1.488	603.0449549	2.976	-14.88
1.672	677.716348	3.3445	-16.7225
1.859	753.4009214	3.718	-18.59

Total:

The error in speed is then calculated to be:

V_M (m/s)	B_V (m)
0.185	0.005826
0.372	0.005826
0.559	0.005827
0.744	0.005828
0.930	0.005830
1.116	0.005832
1.303	0.005835
1.488	0.005838
1.672	0.005841
1.859	0.005844

→ **Total bias limit for speed**

Bias Limit - Resistance

The horizontal x-force is to be measured for the model when towed through the water.

The measured x-force for each bow during the IOT tests are given in the table below:

	Alpha	Beta	Gamma	Epsilon
V_M (m/s)	R_x (N)	R_x (N)	R_x (N)	R_x (N)
0.185	0.62	0.14	0.24	0.27
0.372	0.3	0.50	0.63	0.66
0.559	0.95	1.12	1.35	1.21
0.744	1.69	2.06	2.38	2.19
0.930	2.61	3.13	3.55	3.41
1.116	4.02	4.89	4.97	4.32
1.303	7.83	7.61	7.17	6.89
1.488	13.82	13.80	11.76	12.09
1.672	21.79	21.83	18.71	19.78
1.859	34.78	35.47	30.50	32.15

Calibration: Assumed tolerance for individual weights of 0.005%.

The bias limit due to errors in calibration weights is calculated by multiplying the accuracy of the weights by the measured resistance.

$$B_{R_{x1}} = (\text{accuracy_of_weights})(R_x)$$

$$B_{R_{x1}} = (0.00005)(R_x)$$

The measured resistances used in this spreadsheet are the actual model resistances measured during the tests in the IOT tank.

→ Resistance calibration bias

	Alpha	Beta	Gamma	Epsilon
V_M (m/s)	$B_{R_{x1}}$ (N)	$B_{R_{x1}}$ (N)	$B_{R_{x1}}$ (N)	$B_{R_{x1}}$ (N)
0.185	0.000031	0.000007	0.000012	0.000014
0.372	0.000015	0.000025	0.000032	0.000033
0.559	0.000048	0.000056	0.000068	0.000061
0.744	0.000085	0.000103	0.000119	0.000110
0.930	0.000131	0.000157	0.000178	0.000171
1.116	0.000201	0.000245	0.000249	0.000216
1.303	0.000392	0.000381	0.000359	0.000345
1.488	0.000691	0.000690	0.000588	0.000605
1.672	0.001090	0.001092	0.000936	0.000989
1.859	0.001739	0.001774	0.001525	0.001608

Data Acquisition: Data from the calibration (table below) shows the mass/volt relationship

Weight (kg)	Actual (N)	Predicted (N)	$(Y_i - (axi-b))^2$
0.0	0	0.132	0.017424
2.0	19.613	19.538	0.005625
4.0	39.227	39.181	0.002116

→ IOT calibration data

6.0	58.84	58.742	0.009604
8.0	78.453	78.43	0.000529
10.0	98.066	98.117	0.002601

From these values the SEE can be calculated using the following equation:

$$SEE = \sqrt{\frac{\sum_{i=1}^N (Y_i - (aX_i + b))^2}{N - 2}}$$

Where: N = 6

$$SEE = 0.0973383$$

The curve fit bias is then calculated as twice the SEE:

$$B_{Rx2} = 2SEE$$

B_{Rx2} 0.1946767 N → Resistance curve fit bias

There is also a possible error due to misalignment of the load cell (i.e. difference in orientation between calibration and test condition)

→ This is estimated to be ± 0.25°, and will effect the measured resistance as:

$$B_{Rx3} = R_x - (\cos 0.25^\circ R_x)$$

$$B_{Rx3} = R_x (1 - \cos 0.25^\circ)$$

→ Load cell misalignment bias

	Alpha	Beta	Gamma	Epsilon
V _M (m/s)	B _{Rx3} (N)	B _{Rx3} (N)	B _{Rx3} (N)	B _{Rx3} (N)
0.185	0.000006	0.000001	0.000002	0.000003
0.372	0.000003	0.000005	0.000006	0.000006
0.559	0.000009	0.000011	0.000013	0.000012
0.744	0.000016	0.000020	0.000023	0.000021
0.930	0.000025	0.000030	0.000034	0.000032
1.116	0.000038	0.000047	0.000047	0.000041
1.303	0.000075	0.000072	0.000068	0.000066
1.488	0.000132	0.000131	0.000112	0.000115
1.672	0.000207	0.000208	0.000178	0.000188
1.859	0.000331	0.000338	0.000290	0.000306

Resistance data is acquired by an AD converter, which normally has an error of 1 bit out of an AD accuracy of 16 bits.

→ The following table gives the necessary converter data:

AD card resolution	16 bits
AD card voltage range	10 volts
AD card error	1 bit

This voltage can be translated into Newton by using the slope value of the calibration (30.2283). AD conversion bias shall be given by AD converter error in bit multiplied by AD range divided by AD accuracy:

$$B_{Rx4} = 0.0092249 \text{ N} \rightarrow \text{AD conversion bias}$$

Total: The error in resistance is then calculated to be:

→ **Total bias limit for resistance**

	Alpha	Beta	Gamma	Epsilon
V_M (m/s)	B_{Rx} (N)	B_{Rx} (N)	B_{Rx} (N)	B_{Rx} (N)
1.000	0.194895	0.194895	0.194895	0.194895
0.372	0.194895	0.194895	0.194895	0.194895
0.559	0.194895	0.194895	0.194895	0.194895
0.744	0.194895	0.194895	0.194895	0.194895
0.930	0.194895	0.194895	0.194895	0.194895
1.116	0.194895	0.194895	0.194895	0.194895
1.303	0.194896	0.194895	0.194895	0.194895
1.488	0.194896	0.194896	0.194896	0.194896
1.672	0.194898	0.194898	0.194897	0.194898
1.859	0.194903	0.194903	0.194901	0.194902

Bias Limit - Temperature

Calibration: The thermometer used has been calibrated by the manufacturer. It has a guaranteed accuracy of $\pm 0.5^\circ\text{C}$.

$$B_{tw1} = 0.5 \text{ } ^\circ\text{C} \rightarrow \text{Temperature calibration bias}$$

Data Acquisition: The range of test temperatures observed during testing for any bow was in the range of $\pm 0.2^\circ\text{C}$.

$$B_{tw2} = 0.1 \text{ } ^\circ\text{C} \rightarrow \text{Temperature measurement bias}$$

Total: The error in temperature is obtained by the RSS of the 2 components above

$$(B_{tw})^2 = (B_{tw1})^2 + (B_{tw2})^2$$

$$B_{tw} = 0.509902 \text{ } ^\circ\text{C} \rightarrow \text{Total bias limit for water temperature}$$

Bias Limit - Density

Calibration: The density-temperature relationship according to the ITTC Procedure 7.5-02-01-03 for $g = 9.81 \text{ m/s}^2$ can be expressed as:

$$\rho = 1000.1 + 0.0552t_w - 0.0077t_w^2 + 0.00004t_w^3$$

→ Derivation gives:

$$\left| \frac{\partial \rho}{\partial t_w} \right| = \left| 0.0552 - 0.0154t_w + 0.00012t_w^2 \right|$$

→ Using a temperature, t_w , of 15°C and $B_{tw} = 0.510^\circ\text{C}$, $B_{\rho 1}$ can be calculated using:

$$B_{\rho 1} = \left| \frac{\partial \rho}{\partial t_w} \right| B_{tw}$$

$B_{\rho 1} = 0.075873 \text{ kg/m}^3$ → Density calibration bias

Data Reduction: There is an error associated with converting the temperature to a density (i.e. table lookup). It is calculated as twice the SEE of the curve fit to the density/temperature values for the whole temperature range.

→ According to the ITTC Procedure 7.2-02-02-02 this bias error is given as:

$B_{\rho 2} = 0.07 \text{ kg/m}^3$ → Density data reduction bias

Conceptual: Since the temperature/density used in the analysis is the actual test temperature/density, there is no bias error here.

$B_{\rho 3} = 0 \text{ kg/m}^3$ → Density conceptual bias

Total: The error in density is obtained by the RSS of the 2 components above

$$(B_{\rho})^2 = (B_{\rho 1})^2 + (B_{\rho 2})^2$$

$B_{\rho} = 0.103232 \text{ kg/m}^3$ → Total bias limit for density

Bias Limit - Viscosity

Calibration: The viscosity-temperature relationship for freshwater adopted by the ITTC Procedure 7.5-02-01-03 can be calculated by:

$$\nu = ((0.000585(t_w - 12) - 0.03361)(t_w - 12) + 1.2350) * 10^{-6}$$

$$\nu = (0.000585t_w^2 - 0.04765t_w + 1.72256) * 10^{-6}$$

→ Partial derivation gives:

$$\frac{\partial \nu}{\partial t_w} = (0.00117t_w - 0.04765) * 10^{-6}$$

→ Using a temperature, t_w , of 15°C and $B_{tw} = 0.510^\circ\text{C}$, $B_{\nu 1}$ can be calculated using:

$$B_{\nu 1} = \left| \frac{\partial \nu}{\partial t_w} \right| B_{tw}$$

$B_{\nu 1} =$ **1.5348E-08** m^2/s → Viscosity calibration bias

Data Reduction: Since the above expression is representative of a curve fit to a table of data, there is an inherent error that may be estimated by taking the difference of the viscosity value calculated using this expression and the viscosity value given in the ITTC Procedure 7.5-02-01-03 ($\nu = 1.13902 * 10^{-6} \text{ m}^2/\text{s}$).

→ This bias error may be estimated by:

$$B_{\nu 2} = 1.13902 * 10^{-6} - 1.139435 * 10^{-6}$$

$B_{\nu 2} =$ **-4.15E-10** m^2/s → Viscosity data reduction bias

Total: The error in viscosity is obtained by the RSS of the 2 components above

$$(B_\nu)^2 = (B_{\nu 1})^2 + (B_{\nu 2})^2$$

$B_\nu =$ **1.53537E-08** m^2/s → Total bias limit for viscosity

Total Bias Limit - Total Model Resistance Coefficient

The bias limit associated with C_T can be found using:

$$(B_{CT})^2 = \left(\frac{\partial C_T}{\partial S} B_{WS} \right)^2 + \left(\frac{\partial C_T}{\partial V} B_V \right)^2 + \left(\frac{\partial C_T}{\partial R_x} B_{R_x} \right)^2 + \left(\frac{\partial C_T}{\partial \rho} B_\rho \right)^2$$

→ Where the partial derivatives are:

$$\frac{\partial C_T}{\partial WS} = \frac{R_x}{0.5\rho V^2} \left(\frac{-1}{S^2} \right)$$

$$\frac{\partial C_T}{\partial V} = \frac{R_x}{0.5\rho S} \left(\frac{-2}{V^3} \right)$$

$$\frac{\partial C_T}{\partial R_x} = \frac{1}{0.5\rho V^2 S}$$

$$\frac{\partial C_T}{\partial \rho} = \frac{R_x}{0.5V^2 S} \left(\frac{-1}{\rho^2} \right)$$

Where: $\rho = 999.9 \text{ kg/m}^3$ → Average density during IOT tests
 $S = 1.138 \text{ m}^2$ → Alpha bow

→ Tables for tested speeds:

Alpha

V_M (m/s)	R_x (N)	$\partial C_T / \partial WS$	$\partial C_T / \partial V$	$\partial C_T / \partial R_x$	$\partial C_T / \partial \rho$
0.185	0.62	-0.0279	-0.34283	0.051217	-3.1758E-05
0.372	0.3	-0.00334	-0.02044	0.012684	-3.8056E-06
0.559	0.95	-0.0047	-0.01914	0.00563	-5.3489E-06
0.744	1.69	-0.00472	-0.01443	0.003175	-5.3668E-06
0.930	2.61	-0.00467	-0.01142	0.002034	-5.3103E-06
1.116	4.02	-0.00499	-0.01017	0.001411	-5.6738E-06
1.303	7.83	-0.00713	-0.01246	0.001036	-8.113E-06
1.488	13.82	-0.00964	-0.01475	0.000794	-1.0972E-05
1.672	21.79	-0.01203	-0.01638	0.000629	-1.3697E-05
1.859	34.78	-0.01554	-0.01903	0.000509	-1.7691E-05

Beta

V_M (m/s)	R_x (N)	$\partial C_T / \partial WS$	$\partial C_T / \partial V$	$\partial C_T / \partial R_x$	$\partial C_T / \partial \rho$
0.185	0.14	-0.0063	-0.07741	0.051217	-7.1711E-06
0.372	0.50	-0.00557	-0.03407	0.012684	-6.3427E-06

0.559	1.12	-0.00554	-0.02257	0.00563	-6.3061E-06
0.744	2.06	-0.00575	-0.01758	0.003175	-6.5418E-06
0.930	3.13	-0.0056	-0.0137	0.002034	-6.3683E-06
1.116	4.89	-0.00606	-0.01237	0.001411	-6.9017E-06
1.303	7.61	-0.00693	-0.01211	0.001036	-7.885E-06
1.488	13.80	-0.00963	-0.01472	0.000794	-1.0956E-05
1.672	21.83	-0.01206	-0.01641	0.000629	-1.3722E-05
1.859	35.47	-0.01585	-0.01941	0.000509	-1.8042E-05

Gamma

V_M (m/s)	R_x (N)	$\partial C_T/\partial WS$	$\partial C_T/\partial V$	$\partial C_T/\partial R_x$	$\partial C_T/\partial p$
0.185	0.24	-0.0108	-0.13271	0.051217	-1.2293E-05
0.372	0.63	-0.00702	-0.04293	0.012684	-7.9918E-06
0.559	1.35	-0.00668	-0.0272	0.00563	-7.601E-06
0.744	2.38	-0.00664	-0.02032	0.003175	-7.558E-06
0.930	3.55	-0.00635	-0.01554	0.002034	-7.2228E-06
1.116	4.97	-0.00616	-0.01257	0.001411	-7.0146E-06
1.303	7.17	-0.00653	-0.01141	0.001036	-7.4291E-06
1.488	11.76	-0.0082	-0.01255	0.000794	-9.3363E-06
1.672	18.71	-0.01033	-0.01406	0.000629	-1.1761E-05
1.859	30.50	-0.01363	-0.01669	0.000509	-1.5514E-05

Epsilon

V_M (m/s)	R_x (N)	$\partial C_T/\partial WS$	$\partial C_T/\partial V$	$\partial C_T/\partial R_x$	$\partial C_T/\partial p$
0.185	0.27	-0.01215	-0.1493	0.051217	-1.383E-05
0.372	0.66	-0.00736	-0.04498	0.012684	-8.3724E-06
0.559	1.21	-0.00599	-0.02438	0.00563	-6.8128E-06
0.744	2.19	-0.00611	-0.01869	0.003175	-6.9546E-06
0.930	3.41	-0.0061	-0.01493	0.002034	-6.9379E-06
1.116	4.32	-0.00536	-0.01093	0.001411	-6.0972E-06
1.303	6.89	-0.00627	-0.01096	0.001036	-7.139E-06
1.488	12.09	-0.00843	-0.0129	0.000794	-9.5983E-06
1.672	19.78	-0.01092	-0.01487	0.000629	-1.2434E-05
1.859	32.15	-0.01437	-0.01759	0.000509	-1.6353E-05

Total: The error in total resistance coefficient is then calculated to be:

→ **Total bias limit for total resistance coefficient**

	Alpha	Beta	Gamma	Epsilon
V_M (m/s)	B_{CT}	B_{CT}	B_{CT}	B_{CT}
0.185	0.01018	0.009982	0.009982	0.009982
0.372	0.002475	0.002472	0.002472	0.002472
0.559	0.001103	0.001097	0.001098	0.001097
0.744	0.000625	0.000619	0.000619	0.000619
0.930	0.000402	0.000397	0.000397	0.000397
1.116	0.000282	0.000276	0.000276	0.000276
1.303	0.000217	0.000204	0.000204	0.000204

1.488	0.000181	0.00016	0.000158	0.000158
1.672	0.000163	0.000132	0.000129	0.00013
1.859	0.000162	0.000118	0.000113	0.000115

Total Bias Limit - Residual Resistance Coefficient

Residuary resistance can be obtained from ITTC-57 as:

$$C_R = C_T - C_F$$

→ The bias limit associated with C_R can be found using:

$$(B_{CR})^2 = \left(\frac{\partial C_R}{\partial C_T} B_{CT} \right)^2 + \left(\frac{\partial C_R}{\partial C_F} B_{CF} \right)^2$$

→ Where the partial derivatives are:

$$\frac{\partial C_R}{\partial C_T} = 1$$

$$\frac{\partial C_R}{\partial C_F} = -1$$

Total: The error in residual resistance coefficient is then calculated to be:

→ **Total bias limit for residual resistance coefficient**

	Alpha	Beta	Gamma	Epsilon
V_M (m/s)	B_{CR}	B_{CR}	B_{CR}	B_{CR}
0.185	0.010181	0.009982	0.009982	0.009982
0.372	0.002475	0.002472	0.002472	0.002472
0.559	0.001103	0.001098	0.001098	0.001098
0.744	0.000625	0.000619	0.00062	0.00062
0.930	0.000403	0.000397	0.000398	0.000397
1.116	0.000282	0.000276	0.000276	0.000276
1.303	0.000217	0.000204	0.000204	0.000204
1.488	0.000182	0.00016	0.000159	0.000159
1.672	0.000163	0.000132	0.00013	0.000131
1.859	0.000162	0.000118	0.000114	0.000115

Bias Limit - Model Skin Frictional Resistance Coefficient

The skin frictional resistance coefficient is calculated through the ITTC-57 skin friction line as:

$$C_F = \frac{0.075}{(\log_{10} VL / \nu - 2)^2}$$

→ Bias errors in skin friction may be tracked back to errors in model length, speed, and viscosity.

→ The bias limit associated with C_F can be found using:

$$(B_{CF})^2 = \left(\frac{\partial C_F}{\partial V} B_V \right)^2 + \left(\frac{\partial C_F}{\partial L} B_L \right)^2 + \left(\frac{\partial C_F}{\partial \nu} B_\nu \right)^2$$

→ Where the partial derivatives are:

$$\frac{\partial C_F}{\partial V} = 0.075 \left(\frac{-2}{(\log VL / \nu - 2)^3} \right) \left(\frac{1}{V \ln 10} \right)$$

$$\frac{\partial C_F}{\partial L} = 0.075 \left(\frac{-2}{(\log VL / \nu - 2)^3} \right) \left(\frac{1}{L \ln 10} \right)$$

$$\frac{\partial C_F}{\partial \nu} = 0.075 \left(\frac{-2}{(\log VL / \nu - 2)^3} \right) \left(\frac{-1}{\nu \ln 10} \right)$$

→ Table for tested speeds:

V_M (m/s)	$\partial C_F / \partial V$	$\partial C_F / \partial L$	$\partial C_F / \partial \nu$
0.185	-0.008567219	-0.00092	1393.371
0.372	-0.003311646	-0.00071	1082.299
0.559	-0.001922284	-0.00062	942.9826
0.744	-0.001314813	-0.00057	858.8267
0.930	-0.000980567	-0.00053	800.1938
1.116	-0.000771553	-0.0005	755.9598
1.303	-0.00063058	-0.00047	721.0852
1.488	-0.00053027	-0.00046	692.7374
1.672	-0.00045574	-0.00044	669.0933
1.859	-0.000397384	-0.00043	648.5721

Total: The error in frictional resistance coefficient is then calculated to be:

V_M (m/s)	B_{CF}
0.185	5.43325E-05
0.372	2.55037E-05
0.559	1.83476E-05
0.744	1.52931E-05
0.930	1.35917E-05
1.116	1.24882E-05
1.303	1.17052E-05
1.488	1.11148E-05
1.672	1.06487E-05
1.859	1.02607E-05

→ Total bias limit for frictional resistance coefficient

Precision Limits

The SDev. for C_{TM} , C_R , and C_F were based on the small number of repeated tests carried out for each bow in the MUN towing tank. The SDev. was calculated for each bow/speed combination and an average taken.

The following numbers were calculated for the SDev. for C_{TM} , C_R , and C_F :

	C_{TM}	C_R	C_F
SDev.	0.00016	0.000165	5.1874E-07

→ The precision limits for a single run is calculated as:

$$P_{CT} = \frac{K \cdot SDev_{CT}}{\sqrt{M}} \quad P_{CR} = \frac{K \cdot SDev_{CR}}{\sqrt{M}} \quad P_{CF} = \frac{K \cdot SDev_{CF}}{\sqrt{M}}$$

$P_{CT} = 0.0002263$ → Precision limit for total resistance coefficient

$P_{CR} = 0.0002333$ → Precision limit for residual resistance coefficient

$P_{CF} = 7.3360E-07$ → Precision limit for frictional resistance coefficient

Total Uncertainties

Total Resistance Coefficient:

The total uncertainty for C_T can be calculated as:

$$(U_{CT})^2 = (B_{CT})^2 + (P_{CT})^2$$

→ Total uncertainty for total model resistance coefficient

V_M (m/s)	Alpha	Beta	Gamma	Epsilon
	U_{CT}	U_{CT}	U_{CT}	U_{CT}
0.185	0.010183	0.009985	0.009985	0.009985
0.372	0.002485	0.002483	0.002483	0.002483
0.559	0.001126	0.001121	0.001121	0.001121
0.744	0.000665	0.000659	0.000659	0.000659
0.930	0.000462	0.000457	0.000457	0.000457
1.116	0.000362	0.000357	0.000357	0.000357
1.303	0.000313	0.000305	0.000304	0.000304
1.488	0.00029	0.000277	0.000276	0.000276
1.672	0.000279	0.000262	0.000261	0.000261
1.859	0.000278	0.000255	0.000253	0.000254

The total uncertainty for C_R can be calculated as:

Residual Resistance Coefficient:

$$(U_{CR})^2 = (B_{CR})^2 + (P_{CR})^2$$

→ Total uncertainty for residual resistance coefficient

V_M (m/s)	Alpha	Beta	Gamma	Epsilon
	U_{CR}	U_{CR}	U_{CR}	U_{CR}
0.185	0.010183	0.009985	0.009985	0.009985
0.372	0.002486	0.002483	0.002483	0.002483
0.559	0.001128	0.001122	0.001122	0.001122
0.744	0.000667	0.000662	0.000662	0.000662
0.930	0.000465	0.000461	0.000461	0.000461
1.116	0.000366	0.000362	0.000362	0.000362
1.303	0.000319	0.00031	0.00031	0.00031
1.488	0.000296	0.000283	0.000282	0.000282
1.672	0.000285	0.000268	0.000267	0.000267
1.859	0.000284	0.000262	0.00026	0.00026

The total uncertainty for C_F can be calculated as:

Frictional Resistance Coefficient:

$$(U_{CF})^2 = (B_{CF})^2 + (P_{CF})^2$$

→ Total uncertainty for frictional resistance coefficient

V_M (m/s)	U_{CF}
0.185	5.434E-05
0.372	2.551E-05
0.559	1.836E-05
0.744	1.531E-05
0.930	1.361E-05
1.116	1.251E-05
1.303	1.173E-05
1.488	1.114E-05
1.672	1.067E-05
1.859	1.029E-05

Appendix E-2: MUN Test Program

Bias Limit - Model Length

Data Acquisition: Model accuracy of ± 1 mm in all coordinates.

$B_L = 0.002 \text{ m} \rightarrow$ Model length bias

Bias Limit - Wetted Surface Area

Data Acquisition: Error due to manufacturing error of ± 1 mm in all coordinates.
 Length will increase by 2 mm, beam by 2 mm, draft by 1 mm.
 Assume block coefficient remains constant.
 (Assume the error for Alpha bow is fine for all bows)

$\nabla = 67.75 \text{ kg}$
 $S = 1.138 \text{ m}^2$
 $LWL' = 1.733 \text{ m}$
 $B' = 0.553 \text{ m}$
 $T' = 0.19 \text{ m}$
 $C_B = 0.3774$
 $\nabla' = 68.71937 \text{ kg}$

$\nabla' - \nabla = 0.969373 \text{ kg}$

$C_S = 0.105024$ - Where: $C_S = S / \sqrt{\nabla LWL}$

$S' = 1.146112 \text{ m}^2$

$S' - S = 0.008112 \text{ m}^2$

$AWP = 0.8054 \text{ m}^2$

\rightarrow An increase of 0.9694 kg gives a decreased draft of: (using $\rho = 1000 \text{ kg/m}^3$)

$T'' = 0.001204 \text{ m}$

\rightarrow The smaller draft decreases the wetted surface by: $S'' = 3.462 * 0.001204$

*(using a total waterline length of $2 * LWL = 3.462 \text{ m}$)*

$S'' - S = 0.004167 \text{ m}^2$

$B_{WS1} = 0.003946 \text{ m}^2 \rightarrow$ Hull form bias

Calibration: Error due to measurement of model weight is $\pm 0.2 \text{ kg}$.

\rightarrow An increase in model weight of 0.2 kg gives a additional draft of: (using $\rho = 1000 \text{ kg/m}^3$)

$$T''' = 0.000248 \quad \text{m}$$

→ The increased draft increases the wetted surface by: $S'' = 3.462 * 0.000248$
 *(using a total waterline length of $2 * LWL = 3.462 \text{ m}$)*

$$S''' - S = 0.00086 \quad \text{m}^2$$

$$B_{ws2} = 0.00086 \quad \text{m}^2 \quad \rightarrow \text{Displacement bias}$$

Total: The wetted surface bias is obtained by the RSS of the 2 components above

$$B_{ws} = 0.004038 \quad \text{m}^2 \quad \rightarrow \text{Total bias limit for wetted surface area}$$

Bias Limit - Speed

The required info to determine the error for speed was not available for the MUN tests.
 The bias limit is based on information gathered from the IOT resistance tests.
 It is assumed that the bias limit will be similar during the MUN resistance tests.

Required test set-up information:

Resolution	10000 pulse/m
Dia of wheel	0.5 m
Max pulse duration	0.0000002 s
Min pulse duration	0.00000012 s
Max output signal	5 volts
Circuit speed	100 ms
AD/DA card	16 bits
Number of windows	6366 pulses/rev

The output from the encoder is calculated with the following equation:

$$V = \frac{c\pi D}{6366\Delta t}$$

→ **Pulse Count** (denoted as 'C')

Calibration: Assumed accuracy of optical encoder of ± 1 pulse on every update.

$$B_{C1} = 1 \quad \text{pulse} \quad \rightarrow \text{Encoder calibration bias}$$

Data Acquisition: The AD boards are assumed to be accurate to 1.5 bits or pulses.

$B_{C2} =$ 1.5 pulses → AD conversion bias

$B_{C3} =$ 1.5 pulses → DA conversion bias

Data Reduction: Occurs when converting analogue voltage to a frequency that Represents the pulse count over 10 time bases, or one second. This bias limit is introduced by the linear curve fit obtained from a set of calibration data that is applied to the measured data to allow this conversion.

→ Curve fit bias limit determined previously to be 2.5 Hz

$B_{C4} =$ 0.25 pulses

→ The total bias limit for pulse count is obtained by the RSS of the components above

$$(B_C)^2 = (B_{C1})^2 + (B_{C2})^2 + (B_{C3})^2 + (B_{C4})^2$$

$B_C =$ 2.358495 pulses → Total bias limit for pulse count

→ Wheel Diameter (denoted as 'D')

Calibration: The wheel diameter is considered accurate within 0.000115 m

$B_D =$ 0.000115 m → Wheel diameter bias

→ Time Base (denoted as ' Δt ')

Calibration: Rated accuracy, based on ITTC procedure 7.5-02-02-02, is 1.025×10^{-5} s

$B_{\Delta t} =$ 0.00001025 m

→ The error in speed is obtained by using the equation given below:

$$(B_V)^2 = \left(\frac{\partial V}{\partial c} B_C \right)^2 + \left(\frac{\partial V}{\partial D} B_D \right)^2 + \left(\frac{\partial V}{\partial \Delta t} B_{\Delta t} \right)^2$$

Where:

$$\frac{\partial V}{\partial c} = \frac{\pi D}{6366 \Delta t} \quad \rightarrow \text{Calculated to be equal to } 0.00247$$

$$\frac{\partial V}{\partial D} = \frac{c\pi}{6366\Delta t}$$

$$\frac{\partial V}{\partial \Delta t} = \frac{c\pi D}{6366} \left(-\frac{1}{\Delta t^2} \right)$$

→ Table for tested speeds:

V_M (m/s)	c	$\partial V/\partial D$	$\partial V/\partial \Delta t$
0.185	75.07666525	0.3705	-1.8525
0.372	150.8625568	0.7445	-3.7225
0.559	226.4458122	1.1175	-5.5875
0.744	301.5224774	1.488	-7.44
0.930	376.7004607	1.859	-9.295
1.116	452.2837162	2.232	-11.16
1.303	527.8669716	2.605	-13.025
1.488	603.0449549	2.976	-14.88
1.672	677.716348	3.3445	-16.7225
1.859	753.4009214	3.718	-18.59

Total:

The error in speed is then calculated to be:

V_M (m/s)	B_V (m)
0.185	0.005826
0.372	0.005826
0.559	0.005827
0.744	0.005828
0.930	0.005830
1.116	0.005832
1.303	0.005835
1.488	0.005838
1.672	0.005841
1.859	0.005844

→ Total bias limit for speed

Bias Limit - Resistance

The horizontal x-force is to be measured for the model when towed through the water.

The measured x-force for each bow during the MUN tests are given in the table below:

	Alpha	Beta	Delta	Gamma
V_M (m/s)	R_x (N)	R_x (N)	R_x (N)	R_x (N)
0.291	0.73	0.43	0.29	0.58
0.681	1.68	2.19	1.81	1.60
0.877	2.79	3.06	3.02	2.73
1.073	5.40	4.63	4.44	4.87
1.267	8.96	7.28	5.86	6.73
1.465	15.18	11.92	10.97	10.91
1.659	22.57	19.19	16.79	18.06
1.856	34.51	30.76	28.94	27.73
2.049	52.11	48.13	44.88	43.31
2.244	72.90	63.79	66.47	66.58

	Epsilon	Eta	Iota	Theta	Zeta
V_M (m/s)	R_x (N)				
0.291	0.03	0.27	0.50	0.33	0.41
0.681	1.46	1.61	1.83	2.18	1.44
0.877	2.27	2.71	3.39	2.94	2.85
1.073	3.72	4.92	5.41	5.18	4.42
1.267	6.37	7.57	6.48	7.76	6.67
1.465	10.57	12.33	10.54	13.05	11.77
1.659	16.44	18.97	16.15	20.21	19.27
1.856	28.19	31.85	27.70	33.52	31.65
2.049	42.84	46.99	43.99	49.76	46.78
2.244	63.45	65.08	64.11	67.25	67.17

Calibration: Assumed tolerance for individual weights of 0.005%.

The bias limit due to errors in calibration weights is calculated by multiplying the accuracy of the weights by the measured resistance.

$$B_{Rx1} = (\text{accuracy_of_weights})(R_x)$$

$$B_{Rx1} = (0.00005)(R_x)$$

The measured resistances used in this spreadsheet are the actual model resistances measured during the tests in the MUN towing tank.

→ Resistance calibration bias

	Alpha	Beta	Delta	Gamma
V_M (m/s)	B_{Rx1} (N)	B_{Rx1} (N)	B_{Rx1} (N)	B_{Rx1} (N)
0.291	3.65E-05	2.14E-05	1.43E-05	2.92E-05
0.681	8.39E-05	1.10E-04	9.04E-05	8.02E-05
0.877	0.00014	0.000153	0.0001511	0.000137
1.073	0.00027	0.000231	0.0002219	0.000244
1.267	0.000448	0.000364	0.0002932	0.000336

1.465	0.000759	0.000596	0.0005485	0.000545
1.659	0.001128	0.00096	0.0008395	0.000903
1.856	0.001726	0.001538	0.0014472	0.001387
2.049	0.002606	0.002407	0.002244	0.002165
2.244	0.003645	0.003189	0.0033234	0.003329

	Epsilon	Eta	Iota	Theta	Zeta
V_M (m/s)	B_{Rx1} (N)				
0.291	1.71E-06	1.37E-05	2.50E-05	1.65E-05	2.03E-05
0.681	7.32E-05	8.04E-05	9.13E-05	1.09E-04	7.20E-05
0.877	0.000114	0.000135	0.0001695	0.000147	0.000143
1.073	0.000186	0.000246	0.0002704	0.000259	0.000221
1.267	0.000319	0.000378	0.0003239	0.000388	0.000334
1.465	0.000529	0.000617	0.000527	0.000653	0.000588
1.659	0.000822	0.000948	0.0008073	0.001011	0.000964
1.856	0.001409	0.001593	0.0013852	0.001676	0.001583
2.049	0.002142	0.002349	0.0021993	0.002488	0.002339
2.244	0.003172	0.003254	0.0032054	0.003362	0.003358

Data Acquisition: Data from the calibration shows the mass/volt relationship

Weight (kg)	Actual (N)	Predicted (N)	$(Y_i - (aX_i + b))^2$
0.0	0.00	0.02	0.000549
0.2	1.96	2.09	0.016051
2.2	21.55	21.62	0.004843
4.7	46.17	46.00	0.028136
7.2	70.80	70.77	0.001034
9.2	90.48	90.49	0.000082
11.5	112.76	112.64	0.012409
13.8	135.03	134.95	0.007030
16.0	157.29	157.30	0.000007
18.3	179.61	179.70	0.008321
20.3	199.27	199.34	0.005269

From these values the SEE can be calculated using the following equation:

$$SEE = \sqrt{\frac{\sum_{i=1}^N (Y_i - (aX_i + b))^2}{N - 2}}$$

Where: N = 11

SEE = 0.09645

The curve fit bias is then calculated as twice the SEE:

$$B_{Rx2} = 2SEE$$

B_{Rx2} 0.19291 N → Resistance curve fit bias

There is also a possible error due to misalignment of the load cell (i.e. difference in orientation between calibration and test condition)

→ This is estimated to be $\pm 0.25^\circ$, and will effect the measured resistance as:

$$B_{Rx3} = R_x - (\cos 0.25^\circ R_x)$$

$$B_{Rx3} = R_x (1 - \cos 0.25^\circ)$$

→ Load cell misalignment bias

	Alpha	Beta	Delta	Gamma
V _M (m/s)	B _{Rx3} (N)	B _{Rx3} (N)	B _{Rx3} (N)	B _{Rx3} (N)
0.291	6.95E-06	4.08E-06	2.71E-06	5.57E-06
0.681	1.60E-05	2.09E-05	1.72E-05	1.53E-05
0.877	2.66E-05	2.92E-05	2.88E-05	2.60E-05
1.073	5.14E-05	4.40E-05	4.22E-05	4.64E-05
1.267	8.53E-05	6.93E-05	5.58E-05	6.40E-05
1.465	0.000145	0.000113	0.0001044	0.000104
1.659	0.000215	0.000183	0.0001598	0.000172
1.856	0.000329	0.000293	0.0002755	0.000264
2.049	0.000496	0.000458	0.0004272	0.000412
2.244	0.000694	0.000607	0.0006327	0.000634

	Epsilon	Eta	Iota	Theta	Zeta
V _M (m/s)	B _{Rx3} (N)				
0.291	3.25E-07	2.62E-06	4.75E-06	3.15E-06	3.87E-06
0.681	1.39E-05	1.53E-05	1.74E-05	2.07E-05	1.37E-05
0.877	2.17E-05	2.58E-05	3.23E-05	2.80E-05	2.71E-05
1.073	3.54E-05	4.69E-05	5.15E-05	4.93E-05	4.20E-05
1.267	6.06E-05	7.20E-05	6.17E-05	7.39E-05	6.35E-05
1.465	0.000101	0.000117	0.0001003	0.000124	0.000112
1.659	0.000156	0.000181	0.0001537	0.000192	0.000183
1.856	0.000268	0.000303	0.0002637	0.000319	0.000301
2.049	0.000408	0.000447	0.0004187	0.000474	0.000445
2.244	0.000604	0.00062	0.0006103	0.00064	0.000639

Resistance data is acquired by an AD converter, which normally has an error of 1 bit out of an AD accuracy of 16 bits.

AD card resolution	16 bits
AD card volt range	10 volts
AD card error	1 bit

This voltage can be translated into Newton by using the slope value of the calibration (796.18194). AD conversion bias shall be given by AD converter error in bit multiplied by AD range divided by AD accuracy:

$$B_{Rx4} \quad 0.24298 \quad N \quad \rightarrow \text{AD conversion bias}$$

Total: The error in resistance is then calculated to be:

→ Total bias limit for resistance

	Alpha	Beta	Delta	Gamma
V_M (m/s)	B_{Rx} (N)	B_{Rx} (N)	B_{Rx} (N)	B_{Rx} (N)
0.291	0.310243	0.310243	0.3102427	0.310243
0.681	0.310243	0.310243	0.3102428	0.310243
0.877	0.310243	0.310243	0.3102428	0.310243
1.073	0.310243	0.310243	0.3102428	0.310243
1.267	0.310243	0.310243	0.3102429	0.310243
1.465	0.310244	0.310243	0.3102433	0.310243
1.659	0.310245	0.310244	0.3102439	0.310244
1.856	0.310248	0.310247	0.3102462	0.310246
2.049	0.310254	0.310252	0.3102512	0.310251
2.244	0.310265	0.31026	0.3102612	0.310261

	Epsilon	Eta	Iota	Theta	Zeta
V_M (m/s)	B_{Rx} (N)				
0.291	0.310243	0.310243	0.3102427	0.310243	0.310243
0.681	0.310243	0.310243	0.3102428	0.310243	0.310243
0.877	0.310243	0.310243	0.3102428	0.310243	0.310243
1.073	0.310243	0.310243	0.3102429	0.310243	0.310243
1.267	0.310243	0.310243	0.3102429	0.310243	0.310243
1.465	0.310243	0.310243	0.3102432	0.310243	0.310243
1.659	0.310244	0.310244	0.3102438	0.310244	0.310244
1.856	0.310246	0.310247	0.310246	0.310247	0.310247
2.049	0.31025	0.310252	0.3102508	0.310253	0.310252
2.244	0.31026	0.31026	0.3102599	0.310262	0.310262

Bias Limit - Density

Calibration: The density-temperature relationship according to the ITTC Procedure 7.5-02-01-03 for $g = 9.81 \text{ m/s}^2$ can be expressed as:

$$\rho = 1000.1 + 0.0552t_w - 0.0077t_w^2 + 0.00004t_w^3$$

→ Derivation gives:

$$\left| \frac{\partial \rho}{\partial t_w} \right| = \left| 0.0552 - 0.0154t_w + 0.00012t_w^2 \right|$$

→ Using a temperature, t_w , of 15°C and $B_{tw} = 0.510^\circ\text{C}$, $B_{\rho 1}$ can be calculated using:

$$B_{\rho 1} = \left| \frac{\partial \rho}{\partial t_w} \right| B_{tw}$$

$$B_{\rho 1} = \quad \quad \quad 0.075873 \quad \text{kg/m}^3 \quad \rightarrow \text{Density calibration bias}$$

Data Reduction: There is an error associated with converting the temperature to a density (i.e. table lookup). It is calculated as twice the SEE of the curve fit to the density/temperature values for the whole temperature range.

→ According to the ITTC Procedure 7.2-02-02-02 this bias error is given as:

$$B_{\rho 2} = \quad \quad \quad 0.07 \quad \text{kg/m}^3 \quad \rightarrow \text{Density data reduction bias}$$

Conceptual: Since the temperature/density used in the analysis is the actual test temperature/density, there is no bias error here.

$$B_{\rho 3} = \quad \quad \quad 0 \quad \text{kg/m}^3 \quad \rightarrow \text{Density conceptual bias}$$

Total: The error in density is obtained by the RSS of the 2 components above

$$(B_{\rho})^2 = (B_{\rho 1})^2 + (B_{\rho 2})^2$$

$$B_{\rho} = \quad \quad \quad 0.103232 \quad \text{kg/m}^3 \quad \rightarrow \text{Total bias limit for density}$$

Bias Limit - Temperature

Calibration: The thermometer used has been calibrated by the manufacturer. It has a guaranteed accuracy of $\pm 0.5^\circ\text{C}$.

$$B_{tw1} = \quad \quad \quad 0.5 \quad \quad \quad ^\circ\text{C} \quad \rightarrow \text{Temperature calibration bias}$$

Data Acquisition: The range of test temperatures observed during testing for any bow was in the range of $\pm 0.2^\circ\text{C}$.

$B_{tw2} = 0.1 \text{ } ^\circ\text{C} \rightarrow \text{Temperature measurement bias}$

Total: The error in temperature is obtained by the RSS of the 2 components above

$$(B_{tw})^2 = (B_{tw1})^2 + (B_{tw2})^2$$

$B_{tw} = 0.509902 \text{ } ^\circ\text{C} \rightarrow \text{Total bias limit for water temperature}$

Bias Limit - Viscosity

Calibration: The viscosity-temperature relationship for freshwater adopted by the ITTC Procedure 7.5-02-01-03 can be calculated by:

$$\nu = ((0.000585(t_w - 12) - 0.03361)(t_w - 12) + 1.2350) * 10^{-6}$$

$$\nu = (0.000585t_w^2 - 0.04765t_w + 1.72256) * 10^{-6}$$

\rightarrow Partial derivation gives:

$$\frac{\partial \nu}{\partial t_w} = (0.00117t_w - 0.04765) * 10^{-6}$$

\rightarrow Using a temperature, t_w , of 15°C and $B_{tw} = 0.510^\circ\text{C}$, $B_{\nu1}$ can be calculated using:

$$B_{\nu1} = \left| \frac{\partial \nu}{\partial t_w} \right| B_{tw}$$

$B_{\nu1} = 1.5348\text{E-}08 \text{ } \text{m}^2/\text{s} \rightarrow \text{Viscosity calibration bias}$

Data Reduction: Since the above expression is representative of a curve fit to a table of data, there is an inherent error that may be estimated by taking the difference of the viscosity value calculated using this expression and the viscosity value given in the ITTC Procedure 7.5-02-01-03 ($\nu = 1.13902 * 10^{-6} \text{ m}^2/\text{s}$).

\rightarrow This bias error may be estimated by:

$$B_{\nu2} = 1.13902 * 10^{-6} - 1.139435 * 10^{-6}$$

$B_{\nu2} = -4.15\text{E-}10 \text{ } \text{m}^2/\text{s} \rightarrow \text{Viscosity data reduction bias}$

Total: The error in viscosity is obtained by the RSS of the 2 components above

$$(B_v)^2 = (B_{v1})^2 + (B_{v2})^2$$

$B_v =$ 1.53537E-08 m²/s → Total bias limit for viscosity

Total Bias Limit - Total Resistance Coefficient

The bias limit associated with C_T can be found using:

$$(B_{CT})^2 = \left(\frac{\partial C_T}{\partial S} B_{WS} \right)^2 + \left(\frac{\partial C_T}{\partial V} B_V \right)^2 + \left(\frac{\partial C_T}{\partial R_x} B_{R_x} \right)^2 + \left(\frac{\partial C_T}{\partial \rho} B_\rho \right)^2$$

→ Where the partial derivatives are:

$$\frac{\partial C_T}{\partial WS} = \frac{R_x}{0.5 \rho V^2} \left(\frac{-1}{S^2} \right)$$

$$\frac{\partial C_T}{\partial V} = \frac{R_x}{0.5 \rho S} \left(\frac{-2}{V^3} \right)$$

$$\frac{\partial C_T}{\partial R_x} = \frac{1}{0.5 \rho V^2 S}$$

$$\frac{\partial C_T}{\partial \rho} = \frac{R_x}{0.5 V^2 S} \left(\frac{-1}{\rho^2} \right)$$

Where: $\rho =$ 999.4 kg/m³ → Alpha bow tests at MUN
 $S =$ 1.138 m² → Alpha bow

→ Tables for tested speeds:

Alpha					
V_M (m/s)	R_x (N)	$\partial C_T / \partial WS$	$\partial C_T / \partial V$	$\partial C_T / \partial R_x$	$\partial C_T / \partial \rho$
0.291	0.73	-0.0133	-0.1037	0.0207	-1.51E-05
0.681	1.68	-0.0056	-0.0187	0.00379	-6.36E-06
0.877	2.79	-0.0056	-0.0145	0.00229	-6.38E-06
1.073	5.40	-0.0072	-0.0154	0.00153	-8.25E-06

1.267	8.96	-0.0086	-0.0155	0.0011	-9.82E-06
1.465	15.18	-0.0109	-0.017	0.00082	-1.25E-05
1.659	22.57	-0.0127	-0.0174	0.00064	-1.44E-05
1.856	34.51	-0.0155	-0.019	0.00051	-1.76E-05
2.049	52.11	-0.0192	-0.0213	0.00042	-2.18E-05
2.244	72.90	-0.0224	-0.0227	0.00035	-2.55E-05

Beta

V_M (m/s)	R_x (N)	$\partial C_T / \partial WS$	$\partial C_T / \partial V$	$\partial C_T / \partial R_x$	$\partial C_T / \partial \rho$
0.291	0.43	-0.0078	-0.0609	0.0207	-8.87E-06
0.681	2.19	-0.0073	-0.0244	0.00379	-8.32E-06
0.877	3.06	-0.0062	-0.016	0.00229	-7.01E-06
1.073	4.63	-0.0062	-0.0132	0.00153	-7.07E-06
1.267	7.28	-0.007	-0.0126	0.0011	-7.97E-06
1.465	11.92	-0.0086	-0.0133	0.00082	-9.78E-06
1.659	19.19	-0.0108	-0.0148	0.00064	-1.23E-05
1.856	30.76	-0.0138	-0.0169	0.00051	-1.57E-05
2.049	48.13	-0.0177	-0.0197	0.00042	-2.02E-05
2.244	63.79	-0.0196	-0.0199	0.00035	-2.23E-05

Delta

V_M (m/s)	R_x (N)	$\partial C_T / \partial WS$	$\partial C_T / \partial V$	$\partial C_T / \partial R_x$	$\partial C_T / \partial \rho$
0.291	0.29	-0.0052	-0.0405	0.0207	-5.91E-06
0.681	1.81	-0.006	-0.0201	0.00379	-6.85E-06
0.877	3.02	-0.0061	-0.0158	0.00229	-6.91E-06
1.073	4.44	-0.006	-0.0126	0.00153	-6.78E-06
1.267	5.86	-0.0056	-0.0101	0.0011	-6.43E-06
1.465	10.97	-0.0079	-0.0123	0.00082	-9E-06
1.659	16.79	-0.0094	-0.0129	0.00064	-1.07E-05
1.856	28.94	-0.013	-0.0159	0.00051	-1.48E-05
2.049	44.88	-0.0165	-0.0184	0.00042	-1.88E-05
2.244	66.47	-0.0204	-0.0207	0.00035	-2.32E-05

Gamma

V_M (m/s)	R_x (N)	$\partial C_T / \partial WS$	$\partial C_T / \partial V$	$\partial C_T / \partial R_x$	$\partial C_T / \partial \rho$
0.291	0.58	-0.0106	-0.0831	0.0207	-1.21E-05
0.681	1.60	-0.0053	-0.0179	0.00379	-6.08E-06
0.877	2.73	-0.0055	-0.0142	0.00229	-6.25E-06
1.073	4.87	-0.0065	-0.0139	0.00153	-7.45E-06
1.267	6.73	-0.0065	-0.0116	0.0011	-7.37E-06
1.465	10.91	-0.0079	-0.0122	0.00082	-8.95E-06
1.659	18.06	-0.0101	-0.0139	0.00064	-1.15E-05
1.856	27.73	-0.0124	-0.0153	0.00051	-1.42E-05
2.049	43.31	-0.0159	-0.0177	0.00042	-1.82E-05
2.244	66.58	-0.0204	-0.0207	0.00035	-2.33E-05

Epsilon

V_M (m/s)	R_x (N)	$\partial C_T / \partial WS$	$\partial C_T / \partial V$	$\partial C_T / \partial R_x$	$\partial C_T / \partial p$
0.291	0.03	-0.0006	-0.0049	0.0207	-7.08E-07
0.681	1.46	-0.0049	-0.0163	0.00379	-5.55E-06
0.877	2.27	-0.0046	-0.0119	0.00229	-5.2E-06
1.073	3.72	-0.005	-0.0106	0.00153	-5.69E-06
1.267	6.37	-0.0061	-0.011	0.0011	-6.98E-06
1.465	10.57	-0.0076	-0.0118	0.00082	-8.67E-06
1.659	16.44	-0.0092	-0.0127	0.00064	-1.05E-05
1.856	28.19	-0.0126	-0.0155	0.00051	-1.44E-05
2.049	42.84	-0.0158	-0.0175	0.00042	-1.8E-05
2.244	63.45	-0.0195	-0.0197	0.00035	-2.22E-05

Eta

V_M (m/s)	R_x (N)	$\partial C_T / \partial WS$	$\partial C_T / \partial V$	$\partial C_T / \partial R_x$	$\partial C_T / \partial p$
0.291	0.27	-0.005	-0.039	0.0207	-5.69E-06
0.681	1.61	-0.0054	-0.0179	0.00379	-6.09E-06
0.877	2.71	-0.0054	-0.0141	0.00229	-6.19E-06
1.073	4.92	-0.0066	-0.014	0.00153	-7.52E-06
1.267	7.57	-0.0073	-0.0131	0.0011	-8.29E-06
1.465	12.33	-0.0089	-0.0138	0.00082	-1.01E-05
1.659	18.97	-0.0106	-0.0146	0.00064	-1.21E-05
1.856	31.85	-0.0143	-0.0175	0.00051	-1.63E-05
2.049	46.99	-0.0173	-0.0192	0.00042	-1.97E-05
2.244	65.08	-0.02	-0.0203	0.00035	-2.27E-05

Iota

V_M (m/s)	R_x (N)	$\partial C_T / \partial WS$	$\partial C_T / \partial V$	$\partial C_T / \partial R_x$	$\partial C_T / \partial p$
0.291	0.50	-0.0091	-0.0709	0.0207	-1.03E-05
0.681	1.83	-0.0061	-0.0203	0.00379	-6.93E-06
0.877	3.39	-0.0068	-0.0177	0.00229	-7.75E-06
1.073	5.41	-0.0073	-0.0154	0.00153	-8.27E-06
1.267	6.48	-0.0062	-0.0112	0.0011	-7.1E-06
1.465	10.54	-0.0076	-0.0118	0.00082	-8.65E-06
1.659	16.15	-0.0091	-0.0124	0.00064	-1.03E-05
1.856	27.70	-0.0124	-0.0153	0.00051	-1.42E-05
2.049	43.99	-0.0162	-0.018	0.00042	-1.84E-05
2.244	64.11	-0.0197	-0.02	0.00035	-2.24E-05

Theta

V_M (m/s)	R_x (N)	$\partial C_T / \partial WS$	$\partial C_T / \partial V$	$\partial C_T / \partial R_x$	$\partial C_T / \partial p$
0.291	0.33	-0.006	-0.047	0.0207	-6.85E-06
0.681	2.18	-0.0072	-0.0242	0.00379	-8.25E-06
0.877	2.94	-0.0059	-0.0153	0.00229	-6.73E-06
1.073	5.18	-0.007	-0.0148	0.00153	-7.92E-06
1.267	7.76	-0.0075	-0.0134	0.0011	-8.51E-06
1.465	13.05	-0.0094	-0.0146	0.00082	-1.07E-05
1.659	20.21	-0.0113	-0.0156	0.00064	-1.29E-05

1.856	33.52	-0.015	-0.0184	0.00051	-1.71E-05
2.049	49.76	-0.0183	-0.0204	0.00042	-2.09E-05
2.244	67.25	-0.0206	-0.0209	0.00035	-2.35E-05

Zeta

V_M (m/s)	R_x (N)	$\partial C_T / \partial WS$	$\partial C_T / \partial V$	$\partial C_T / \partial R_x$	$\partial C_T / \partial \rho$
0.291	0.41	-0.0074	-0.0578	0.0207	-8.43E-06
0.681	1.44	-0.0048	-0.016	0.00379	-5.46E-06
0.877	2.85	-0.0057	-0.0149	0.00229	-6.52E-06
1.073	4.42	-0.0059	-0.0126	0.00153	-6.75E-06
1.267	6.67	-0.0064	-0.0115	0.0011	-7.31E-06
1.465	11.77	-0.0085	-0.0132	0.00082	-9.65E-06
1.659	19.27	-0.0108	-0.0148	0.00064	-1.23E-05
1.856	31.65	-0.0142	-0.0174	0.00051	-1.62E-05
2.049	46.78	-0.0172	-0.0191	0.00042	-1.96E-05
2.244	67.17	-0.0206	-0.0209	0.00035	-2.35E-05

Total: The error in total resistance coefficient is then calculated to be:

→ Total bias limit for total resistance coefficient

	Alpha	Beta	Delta	Gamma
V_M (m/s)	B_{CT}	B_{CT}	B_{CT}	B_{CT}
0.291	0.006452	0.006424	0.006423	0.006424
0.681	0.001181	0.001176	0.001176	0.001176
0.877	0.000714	0.00071	0.00071	0.000709
1.073	0.000483	0.000475	0.000475	0.000475
1.267	0.000353	0.000341	0.000341	0.000341
1.465	0.000277	0.000257	0.000256	0.000256
1.659	0.000228	0.000203	0.000202	0.000202
1.856	0.000203	0.000168	0.000167	0.000166
2.049	0.000196	0.000148	0.000146	0.000145
2.244	0.000194	0.000134	0.000136	0.000136

	Epsilon	Eta	Iota	Theta	Zeta
V_M (m/s)	B_{CT}	B_{CT}	B_{CT}	B_{CT}	B_{CT}
0.291	0.006423	0.006423	0.006424	0.006423	0.0064235
0.681	0.001176	0.001176	0.001176	0.001176	0.00117583
0.877	0.000709	0.000709	0.00071	0.000709	0.00070945
1.073	0.000474	0.000475	0.000475	0.000475	0.00047451
1.267	0.000341	0.000341	0.000341	0.000341	0.00034073
1.465	0.000256	0.000257	0.000256	0.000257	0.00025663
1.659	0.000202	0.000203	0.000202	0.000203	0.00020294
1.856	0.000166	0.000169	0.000166	0.00017	0.00016852
2.049	0.000145	0.000148	0.000146	0.00015	0.00014745
2.244	0.000134	0.000135	0.000134	0.000137	0.00013664

Total Bias Limit - Residual Resistance Coefficient

Residuary resistance can be obtained from ITTC-57 as:

$$C_R = C_T - C_F$$

→ The bias limit associated with C_R can be found using:

$$(B_{CR})^2 = \left(\frac{\partial C_R}{\partial C_T} B_{CT} \right)^2 + \left(\frac{\partial C_R}{\partial C_F} B_{CF} \right)^2$$

→ Where the partial derivatives are:

$$\frac{\partial C_R}{\partial C_T} = 1$$

$$\frac{\partial C_R}{\partial C_F} = -1$$

Total: The error in residual resistance coefficient is then calculated to be:

→ **Total bias limit for residual resistance coefficient**

	Alpha	Beta	Delta	Gamma
V_M (m/s)	B_{CR}	B_{CR}	B_{CR}	B_{CR}
0.291	0.006452	0.006424	0.006424	0.006424
0.681	0.001181	0.001176	0.001176	0.001176
0.877	0.000715	0.00071	0.00071	0.00071
1.073	0.000483	0.000475	0.000475	0.000475
1.267	0.000353	0.000341	0.000341	0.000341
1.465	0.000277	0.000257	0.000257	0.000257
1.659	0.000229	0.000203	0.000202	0.000203
1.856	0.000204	0.000168	0.000167	0.000167
2.049	0.000196	0.000149	0.000146	0.000145
2.244	0.000194	0.000134	0.000136	0.000137

	Epsilon	Eta	Iota	Theta	Zeta
V_M (m/s)	B_{CR}	B_{CR}	B_{CR}	B_{CR}	B_{CR}
0.291	0.006424	0.006424	0.006424	0.006424	0.006424
0.681	0.001176	0.001176	0.001176	0.001176	0.001176
0.877	0.000709	0.00071	0.00071	0.00071	0.00071
1.073	0.000475	0.000475	0.000475	0.000475	0.000475

1.267	0.000341	0.000341	0.000341	0.000341	0.000341
1.465	0.000256	0.000257	0.000256	0.000257	0.000257
1.659	0.000202	0.000203	0.000202	0.000204	0.000203
1.856	0.000167	0.000169	0.000167	0.00017	0.000169
2.049	0.000145	0.000148	0.000146	0.00015	0.000148
2.244	0.000134	0.000135	0.000135	0.000137	0.000137

Bias Limit - Skin Frictional Resistance Coefficient

The skin frictional resistance coefficient is calculated through the ITTC-57 skin friction line as:

$$C_F = \frac{0.075}{(\log_{10} VL / \nu - 2)^2}$$

→ Bias errors in skin friction may be tracked back to errors in model length, speed, and viscosity.

→ The bias limit associated with C_F can be found using:

$$(B_{CF})^2 = \left(\frac{\partial C_F}{\partial V} B_V \right)^2 + \left(\frac{\partial C_F}{\partial L} B_L \right)^2 + \left(\frac{\partial C_F}{\partial \nu} B_\nu \right)^2$$

→ Where the partial derivatives are:

$$\frac{\partial C_F}{\partial V} = 0.075 \left(\frac{-2}{(\log VL / \nu - 2)^3} \right) \left(\frac{1}{V \ln 10} \right)$$

$$\frac{\partial C_F}{\partial L} = 0.075 \left(\frac{-2}{(\log VL / \nu - 2)^3} \right) \left(\frac{1}{L \ln 10} \right)$$

$$\frac{\partial C_F}{\partial \nu} = 0.075 \left(\frac{-2}{(\log VL / \nu - 2)^3} \right) \left(\frac{-1}{\nu \ln 10} \right)$$

→ Table for tested speeds:

V_M (m/s)	$\partial C_F / \partial V$	$\partial C_F / \partial L$	$\partial C_F / \partial v$
0.291	-0.004610781	-0.00078	1179.735
0.681	-0.001477475	-0.00058	883.6326
0.877	-0.001058216	-0.00054	814.9324
1.073	-0.000812313	-0.0005	765.195
1.267	-0.000653568	-0.00048	727.1245
1.465	-0.000541301	-0.00046	696.0319
1.659	-0.000460388	-0.00044	670.6455
1.856	-0.000398328	-0.00043	648.9206
2.049	-0.000350538	-0.00041	630.4756
2.244	-0.000311699	-0.0004	614.1056

Total: The error in frictional resistance coefficient is then calculated to be:

V_M (m/s)	B_{CF}
0.291	3.24357E-05
0.681	1.61109E-05
0.877	1.39915E-05
1.073	1.27076E-05
1.267	1.1836E-05
1.465	1.11815E-05
1.659	1.06787E-05
1.856	1.02672E-05
2.049	9.92953E-06
2.244	9.63758E-06

→ Total bias limit for frictional resistance coefficient

Precision Limits

The SDev. for C_{TM} , C_R , and C_F were based on the small number of repeated tests carried out for each bow in the MUN towing tank. The SDev. was calculated for each bow/speed combination and an average taken.

The following numbers were calculated for the SDev. for C_{TM} , C_R , and C_F :

	C_{TM}	C_R	C_F
SDev.	0.00016	0.000165	5.1874E-07

→ The precision limits for a single run is calculated as:

$$P_{CT} = \frac{K \cdot SDev_{CT}}{\sqrt{M}} \quad P_{CR} = \frac{K \cdot SDev_{CR}}{\sqrt{M}} \quad P_{CF} = \frac{K \cdot SDev_{CF}}{\sqrt{M}}$$

$P_{CT} = 0.0002263 \rightarrow$ Precision limit for total resistance coefficient
 $P_{CR} = 0.0002333 \rightarrow$ Precision limit for residual resistance coefficient
 $P_{CF} = 7.3360E-07 \rightarrow$ Precision limit for frictional resistance coefficient

Total Uncertainties

Total Resistance Coefficient:

The total uncertainty for C_T can be calculated as:

$$(U_{CT})^2 = (B_{CT})^2 + (P_{CT})^2$$

\rightarrow Total uncertainty for total resistance coefficient

	Alpha	Beta	Delta	Gamma
V_M (m/s)	U_{CT}	U_{CT}	U_{CT}	U_{CT}
0.291	0.006456	0.006427	0.006427	0.006428
0.681	0.001202	0.001198	0.001197	0.001197
0.877	0.000749	0.000745	0.000745	0.000745
1.073	0.000534	0.000526	0.000526	0.000526
1.267	0.00042	0.000409	0.000409	0.000409
1.465	0.000357	0.000342	0.000342	0.000342
1.659	0.000322	0.000304	0.000303	0.000304
1.856	0.000304	0.000282	0.000281	0.000281
2.049	0.000299	0.000271	0.000269	0.000269
2.244	0.000298	0.000263	0.000264	0.000264

	Epsilon	Eta	Iota	Theta	Zeta
V_M (m/s)	U_{CT}	U_{CT}	U_{CT}	U_{CT}	U_{CT}
0.291	0.006427	0.006427	0.006428	0.006427	0.006427
0.681	0.001197	0.001197	0.001197	0.001198	0.001197
0.877	0.000745	0.000745	0.000745	0.000745	0.000745
1.073	0.000526	0.000526	0.000526	0.000526	0.000526
1.267	0.000409	0.000409	0.000409	0.000409	0.000409
1.465	0.000342	0.000342	0.000342	0.000343	0.000342
1.659	0.000303	0.000304	0.000303	0.000304	0.000304
1.856	0.000281	0.000282	0.000281	0.000283	0.000282
2.049	0.000269	0.00027	0.000269	0.000271	0.00027
2.244	0.000263	0.000264	0.000263	0.000264	0.000264

Residual Resistance Coefficient:

The total uncertainty for C_R can be calculated as:

$$(U_{CR})^2 = (B_{CR})^2 + (P_{CR})^2$$

→ Total uncertainty for residual resistance coefficient

	Alpha	Beta	Delta	Gamma
V_M (m/s)	U_{CR}	U_{CR}	U_{CR}	U_{CR}
0.291	0.006456	0.006428	0.006428	0.006428
0.681	0.001204	0.001199	0.001199	0.001199
0.877	0.000752	0.000747	0.000747	0.000747
1.073	0.000537	0.000529	0.000529	0.000529
1.267	0.000424	0.000413	0.000413	0.000413
1.465	0.000362	0.000347	0.000347	0.000347
1.659	0.000327	0.000309	0.000309	0.000309
1.856	0.00031	0.000288	0.000287	0.000287
2.049	0.000305	0.000277	0.000276	0.000275
2.244	0.000303	0.000269	0.00027	0.00027

	Epsilon	Eta	Iota	Theta	Zeta
V_M (m/s)	U_{CR}	U_{CR}	U_{CR}	U_{CR}	U_{CR}
0.291	0.006428	0.006428	0.006428	0.006428	0.006428
0.681	0.001199	0.001199	0.001199	0.001199	0.001199
0.877	0.000747	0.000747	0.000747	0.000747	0.000747
1.073	0.000529	0.000529	0.000529	0.000529	0.000529
1.267	0.000413	0.000413	0.000413	0.000413	0.000413
1.465	0.000347	0.000347	0.000347	0.000347	0.000347
1.659	0.000309	0.000309	0.000309	0.00031	0.000309
1.856	0.000287	0.000288	0.000287	0.000289	0.000288
2.049	0.000275	0.000276	0.000275	0.000277	0.000276
2.244	0.000269	0.00027	0.000269	0.000271	0.000271

Frictional Resistance Coefficient:

The total uncertainty for C_F can be calculated as:

$$(U_{CF})^2 = (B_{CF})^2 + (P_{CF})^2$$

→ Total uncertainty for frictional resistance coefficient

V_M (m/s)	U_{CF}
0.291	3.244E-05
0.681	1.613E-05
0.877	1.401E-05
1.073	1.273E-05
1.267	1.186E-05
1.465	1.121E-05
1.659	1.070E-05
1.856	1.029E-05
2.049	9.957E-06
2.244	9.665E-06



